Universitat Autònoma de Barcelona

Analysis of the genetic basis of porcine meat quality and coat color by using genomic and transcriptomic tools

Tainã Figueiredo Cardoso

UNIVERSITAT AUTÒNOMA DE BARCELONA

Departament de Ciència Animal i dels Aliments, Facultat de Veterinària

CENTRE DE RECERCA EN AGRIGENÒMICA

Departament de Genètica Animal

Analysis of the genetic basis of porcine meat quality and coat color by using genomic and transcriptomic tools

Tainã Figueiredo Cardoso

Doctoral thesis to obtain the Ph.D degree in Animal Production of the Universitat Autònoma de Barcelona, April 2018

Supervisors

Dr. Marcel Amills Eras

Dra. Angela Canovas Tienda

El Dr Marcel Amills Eras, professor agregat del Departament de Ciència Animal i dels Aliments de la Universitat Autònoma de Barcelona, i la Dra. Angela Canovas Tienda, professora assistent de la Universitat de Guelph,

fan constar

que el treball de recerca i la redacció de la memòria de la tesi doctoral titulada "**Analysis of the genetic basis of porcine meat and color phenotypes by using genomic and transcriptomic tools**" han estat realitzats sota la seva direcció per

Tainã Figueiredo Cardoso

I certifiquen

que aquest treball s'ha dut a terme al Departament de Ciència Animal i del Aliments de la Facultat de Veterinària de la Universitat Autònoma de Barcelona i al Departament de Genètica Animal del Centre de Recerca en Agrigenòmica,

considerant

que la memòria resultant es apta per optar al grau de Doctor en Producció Animal per la Universitat Autònoma de Barcelona.

I perqué quedi constància, signen aquest document al març del 2018.

Dr. Marcel Amills Eras Dra. Angela Canovas Tienda Tainã Figueiredo Cardoso

Cover design by Renata Benites, 2018

This work was funded by the Spanish Ministry of Economy and Competitiveness (grant numbers: AGL2010-22208-C02-02 and AGL2013-48742-C2-1-R). We acknowledge the support of the Spanish Ministry of Economy and Competitiveness for the *Centre of Excellence Severo Ochoa 2016–2019* (SEV-2015-0533) grant awarded to the Centre for Research in Agricultural Genomics.

Tainã Figueiredo Cardoso was funded by the program "*Science without Borders*" fellowship provided by the "Coordenação de Aperfeiçoamento de Pessoal de Nível Superior (CAPES)" from Brazilian Federal Government (2014-2018).

Aos meus pais, Jorge Tomás e Denize,

e a minha irmã Thaís.

Porque não importa a distância que nos separa,

se há um céu que nos une.

Content

Summary

The main objectives of this Thesis were to investigate the genetic basis of fatness in pigs and to identify the genetic factors involved in the establishment of blond *vs* red pigmentation patterns in Mangalitza pigs by using genomic and transcriptomic tools. In the first study of the Thesis (Chapter 3), we compare the skeletal muscle expression patterns of two groups of Duroc pigs with different growth and fatness profiles (HIGH: high backfat thickness, intramuscular fat, saturated and unsaturated fatty acid content and serum lipids *vs* LOW: opposite phenotypes). By using a RNA-Seq technology, we identified 96 genes differentially expressed. Several of these genes are related to lipid metabolism (*e.g. SLC27A4*, *SFRP5* and *CES1*) and the transcription factor PPARG appears to be a key regulator of porcine fatness. We have also observed that very few non-coding RNAs are differentially expressed in these two groups of pigs, suggesting that the non-coding transcriptome has a limited effect on the establishment of the HIGH and LOW phenotypes. In the second study of the Thesis, we demonstrate the differential expression of specific mRNA isoforms of four genes with a known role in obesity (*ITGA5*, *LITAF*, *TIMP1* and *ANXA2*) in HIGH *vs* LOW pigs. The differential expression of these isoforms may have effects on transcript structure as well as on the protein sequence. In the third study, we aimed to investigate the differential expression of mRNA encoding genes in response to food ingestion. This goal has been achieved by comparing the muscle mRNA expression patterns of Duroc sows before feeding (T0) and 5 h. (T1) and 7 h. (T2) after feeding. Besides genes with a well-known role in energy homeostasis (*e.g. PFKFB3* and *G0S2*), we have identified several genes with a plausible but poorly characterized role in metabolism (*e.g. MIGA2*, *SDC4*, and *CSRNP1*). We have also observed that the set of genes differentially expressed before and after feeding is enriched in transcription factors and pathways related to oxidative stress, angiogenesis, and circadian rhythms. Considering these results, in the fourth study we use quantitative RT-qPCR technique to find out how the expression of 8 circadian genes (*ARNTL, BHLHE40, CRY2, NPAS2, NR1D1, PER1, PER2* and *SIK1*) changes in response to food ingestion in five porcine tissues *i.e.* skeletal muscle, hypothalamus, liver, intestine and dorsal fat. Our results indicate that the expression of the Clock genes does not change in the hypothalamus, the tissue containing the central clock entrained by light, but in contrast, it is strongly modified in the other four tissues. This finding demonstrates that nutrition changes the expression of circadian genes integrated in peripheral clocks. Finally, in the fifth study, we have analysed, in

collaboration with researchers of the Research Institute for Animal Breeding and Nutrition (Hungary) and the University of Cluj-Napoca (Romania), the genetic basis of coat color (red *vs* blond) of Mangalitza pigs. By combining a selection scan and a genome-wide association study, we have found that the *SLC45A2* gene is probably involved in the genetic determination of pigmentation in Mangalitza pigs, a result that agrees well with previous studies demonstrating the implication of this *locus* on the color patterns of multiple mammalian species including humans. More specifically, two missense SNPs c.806G>A (p.Gly269Glu) and c.956G>A (p.Arg319His) in the *SLC45A2* locus appear to be strongly but not fully associated with the red and blond coat colors of Mangalitza pigs. This finding suggests the existence of addiitonal genetic factors regulating the pigmentation of Mangalitza pigs.

Resumen

Los principales objetivos de esta Tesis fueron investigar la base genética de la composición y deposito de la grasa en cerdos, e identificar los factores genéticos involucrados en el establecimiento de los patrones de pigmentación rubia *vs* roja en cerdos Mangalitza, mediante el uso de herramientas genómicas y transcriptómicas. En el primer estudio comparamos los patrones de expresión del músculo esquelético en dos grupos de cerdos Duroc, con diferentes perfiles de crecimiento y engrasamiento (HIGH: elevado espesor del tocino dorsal, grasa intramuscular, contenido de ácidos grasos saturados e insaturados y lípidos séricos *vs* LOW: fenotipos opuestos). Mediante el uso de la técnica *RNA-Seq*, hemos encontrado que 96 genes se expresan diferencialmente en el músculo gluteus medius de cerdos HIGH y LOW. Varios de estos genes están relacionados con el metabolismo lipídico (*p.ej, SLC27A4, SFRP5, y CES1*) y el factor de transcripción PPARG parece ser un regulador clave del engrasamiento en porcino. También hemos observado que muy pocos *RNAs* no codificantes se expresan diferencialmente en estos dos grupos de cerdos, lo que sugiere que el transcriptoma no codificante tiene un efecto limitado sobre el establecimiento de los fenotipos HIGH y LOW. En el segundo estudio, analizamos la expresión de isoformas de *mRNA* en cerdos HIGH y LOW y demostramos la expresión diferencial de isoformas específicas de cuatro genes muy relacionados con la obesidad (*ITGA5*, *LITAF*, *TIMP1* y *ANXA2*). La expresión diferencial de estas isoformas podría tener efectos sobre la estructura del transcrito, así como sobre la secuencia de la proteína. En el tercer estudio, hemos analizado la expresión diferencial de genes que codifican *mRNA* en respuesta a la ingestión de alimentos. Este objetivo se ha logrado al comparar los patrones de expresión muscular de cerdas Duroc antes de comer (T0), 5 h. (T1) y 7 h. (T2) después de comer. Además de los genes con un papel bien conocido en la homeostasis energética (*p.ej, PFKFB3* y *G0S2*), hemos identificado varios genes con un rol plausible pero mal caracterizado en el metabolismo (*p.ej, MIGA2, SDC4* y *CSRNP1*). También hemos observado un enriquecimiento de un conjunto de genes expresados diferencialmente antes y después de comer que engloba diversos factores de transcripción así como genes implicados en el estrés oxidativo, la angiogénesis y los ritmos circadianos. Teniendo en cuenta estos resultados, en el cuarto estudio hemos desarrollado un experimento basado en RT-qPCR para descubrir cómo la expresión de 8 genes circadianos (*ARNTL, BHLHE40, CRY2, NPAS2, NR1D1, PER1, PER2* y *SIK1*) se modifica en respuesta a la ingestión de alimentos en cinco tejidos porcinos (músculo esquelético, hipotálamo, hígado, intestino y

grasa dorsal). Nuestros resultados indican que la expresión de los genes circadianos no cambia en el hipotálamo, el tejido que contiene el reloj central influenciado por la luz. Por el contrario, dicha expresión sí que presenta fuertes variaciones en los otros cuatro tejidos. Este hallazgo demuestra que la nutrición cambia la expresión de los genes circadianos integrados en los relojes periféricos. Finalmente, en el quinto estudio, hemos analizado, en colaboración con investigadores del Research Institute for Animal Breeding and Nutrition (Hungría) y la Universidad de Cluj-Napoca (Rumanía), la base genética del color de la capa (rojo *vs* rubio) en cerdos Mangalitza. Combinando un barrido de selección y un estudio de asociación del genoma completo, hemos encontrado que el gen *SLC45A2* probablemente esté involucrado en la determinación genética de la pigmentación roja y rubia de los cerdos Mangalitza, un resultado que concuerda bien con estudios previos que demuestran la implicación de este *locus* en los patrones de color de múltiples especies de mamíferos, incluyendo la especie humana. Más específicamente, dos SNP con efecto no-sinónimo, c.806G>A (p.Gly269Glu) y c.956G>A (p.Arg319His), situados en el *gen* S*LC45A*2, están fuertemente asociados con los colores rojo y rubio, no obstante dicha asociación no es completa por lo que cabe deducir la existencia de factores genéticos adicionales en la pigmentación de los cerdos Mangalitza.

Resumo

Os principais objetivos desta tese foram investigar a base genética do depósito de gordura em suínos e identificar os fatores genéticos envolvidos no estabelecimento de padrões de pigmentação loiro *vs* vermelho em suínos Mangalitza utilizando ferramentas genômicas e transcriptômicas. No primeiro estudo, comparamos os padrões de expressão em músculo esquelético de dois grupos de suínos Duroc (*HIGH*: alta espessura de gordura, gordura intramuscular, conteúdo de ácidos graxos saturados e insaturados e lipídios séricos *vs LOW*: fenótipos opostos) com diferentes perfis de crescimento e gordura. Usando uma abordagem de *RNA-Seq*, mostramos que 96 genes são diferencialmente expressos. Vários destes genes estão relacionados com o metabolismo lipídico (p. ex. *SLC27A4*, *SFRP5* e *CES1*) e o fator de transcrição PPARG parece ser um regulador chave da gordura suína. Também observamos que poucos *RNA* não-codificantes são diferencialmente expressos nesses dois grupos de suínos, sugerindo que o transcriptoma não-codificante tem um efeito limitado sobre o estabelecimento dos fenótipos *HIGH* e *LOW*. No segundo estudo, analisamos a expressão de isoformas de *mRNA* comparando os mesmos animais *HIGH* e *LOW*, e demonstramos uma expressão diferencial de isoformas específicas de quatro genes com papel conhecido na obesidade (*ITGA5*, *LITAF*, *TIMP1* e *ANXA2*). A expressão diferencial destas isoformas pode ter efeitos na estrutura do transcrito, bem como na sequência da proteína. No terceiro estudo, analisamos a expressão diferencial de *mRNA* codificando genes em resposta à ingestão de alimentos, através da comparação dos padrões de expressão de *mRNA* musculares de suínos Duroc antes da alimentação (T0) e 5 h (T1) e 7 h (T2) após a alimentação. Identificamos genes diferencialmente expressos entre os grupos com um papel bem conhecido na homeostase energética (p. ex., *PFKFB3* e *G0S2*), além de vários genes com um papel plausível, mas pouco caracterizado no metabolismo (p. ex., *MIGA2*, *SDC4* e *CSRNP1*). Também observamos um enriquecimento de genes relacionados a fatores de transcrição e vias metabólicas relacionadas ao estresse oxidativo, angiogênese e ritmos circadianos diferencialmente expressados antes e após a alimentação. Considerando estes resultados, no quarto estudo usamos uma técnica quantitativa de RT-qPCR para descobrir como a expressão de oito genes circadianos (*ARNTL*, *BHLHE40*, *CRY2*, *NPAS2*, *NR1D1*, *PER1*, *PER2* e *SIK1*) muda em resposta à ingestão de alimentos em cinco tecidos suínos (músculo esquelético, hipotálamo, fígado, intestino e gordura dorsal). Nossos resultados indicam que a expressão dos genes *Clock* não se altera no hipotálamo (tecido contendo o relógio central e estimulado pela luz), mas em contraste, é

fortemente modificado nos outros quatro tecidos. Estes resultados demonstram que a nutrição altera a expressão de genes circadianos de forma integrada nos relógios periféricos. Finalmente, no quinto estudo, analisamos, em colaboração com pesquisadores do *Research Institute for Animal Breeding and Nutrition* (Hungria) e da Universidade de *Cluj-Napoca* (Romênia), a base genética da cor da pelagem (vermelho *vs* loiro) de suínos Mangalitza. Ao combinar uma varredura de seleção e um estudo de associação genômica, encontramos que o gene *SLC45A2* está provavelmente envolvido na determinação genética da pigmentação, um resultado em concordância com estudos prévios que demonstram a participação desse *locus* nos padrões de cor de múltiplas espécies de mamíferos, incluindo em seres humanos. Mais especificamente, dois *Single Nucleotide Polimorfism* (*SNP)* com efeitos não sinônimos, c.806G> A (p.Gly269Glu) e c.956G> A (p.Arg319His) no gene *SLC45A2* parecem estar fortemente, mas não totalmente, associados às cores vermelho e louro da pelagem dos suínos Mangalitza.

List of Tables

General introduction

Paper I

Paper II

Paper III

Paper IV

Paper V

General discussion

List of Figures

General introduction

Paper I

Paper II

Paper III

Paper IV

Paper V

General discussion

List of annexes

Annexes Paper 1

Annexes Paper 2

Annexes Paper 3

Annexes Paper 4

Annexes Paper 5

List of publications

The present thesis is based on the work contained in the list of articles below:

- Paper I: **Cardoso TF**, Cánovas A, Canela-Xandri O, González-Prendes R, Amills M, Quintanilla R. RNA-Seq based detection of differentially expressed genes in the skeletal muscle of Duroc pigs with distinct lipid profiles. *Scientific Reports*. 2017 Feb 14;7:40005. doi: 10.1038/srep40005.
- Paper II: **Cardoso TF**, Quintanilla R, Castelló A, González-Prendes R, Amills M, Cánovas Á. Differential expression of mRNA isoforms in the skeletal muscle of pigs with distinct growth and fatness profiles. *BMC Genomics.* 2018 Feb 14;19(1):145. doi: 10.1186/s12864-018-4515-2.
- Paper III: **Cardoso TF**, Quintanilla R, Tibau J, Gil M, Mármol-Sánchez E, González-Rodríguez O, González-Prendes R, Amills M. Nutrient supply affects the mRNA expression profile of the porcine skeletal muscle. *BMC Genomics.* 2017 Aug 10;18(1):603. doi: 10.1186/s12864-017-3986-x.
- Paper IV: **Cardoso TF**, Quintanilla R, Castelló A, Mármol-Sánchez E, Ballester M, Jordana J, Amills, M. The ingestion of food promotes changes in the expression of genes regulating circadian rhythms in four porcine tissues containing peripheral clocks (*Submitted to Frontiers in Genetics*).
- Paper V: Balteanu VA, **Cardoso TF**, Amills M, Egerszegi I, Anton I, Beja-Pereira A, Zsolnai A. The red and blond pigmentation of Mangalitza pigs is strongly associated with the polymorphism of the Solute Carrier Family 45 Member 2 (*SLC45A2*) gene (*Manuscript in preparation*).

Other publications from the author

(Not included in the thesis)

- Mentzel CMJ, **Cardoso TF**, Pipper CB, Jacobsen MJ, Jørgensen CB, Cirera S, Fredholm M. Deregulation of obesity-relevant genes is associated with progression in BMI and the amount of adipose tissue in pigs. *Molecular Genetics and Genomics*. 2018 Feb;293(1):129-136. doi: 10.1007/s00438-017-1369-2.
- Mentzel CMJ, **Cardoso TF**, Lex AMJ, Sørensen DB, Fredholm M, Cirera S. Fat and carbohydrate content in the diet induces drastic changes in gene expression in young Göttingen minipigs. *Mammalian Genome*. 2017 Jun;28(5-6):166-175. doi: 10.1007/s00335-017-9690-y.
- Eusebi PG, González-Prendes R, Quintanilla R, Tibau J, **Cardoso TF**, Clop A, Amills M. A genome-wide association analysis for carcass traits in a commercial Duroc pig population. *Animal Genetics.* 2017 Aug;48(4):466-469. doi: 10.1111/age.12545.
- Gonzalez-Prendes R, Quintanilla R, Canovas A, Manunza A, **Cardoso TF**, Jordana J, Noguera JL, Pena RN, Amills M. Joint QTL mapping and gene expression analysis identify positional candidate genes influencing pork quality traits. *Scientific Reports*, v. 7, p. 39830, 2017. doi:10.1038/srep39830.
- Manunza A, **Cardoso TF**, Noce A, Martínez A, Pons A, Bermejo LA, Landi V, Sànchez A, Jordana J, Delgado JV, Adán S, Capote J, Vidal O, Ugarte E, Arranz JJ, Calvo JH, Casellas J, Amills M. Population structure of eleven Spanish ovine breeds and detection of selective sweeps with BayeScan and hapFLK. *Scientific Reports*, v. 6, 27296. 10.1038/srep27296
- **Cardoso TF**, Amills M, Bertolini F, Rothschild M, Marras G, Boink G, Jordana J, Capote J, Carolan S, Hallsson JH, Kantanen J, Pons A, Lenstra JA, ADAPTmap Consortium. Patterns of homozygosity in insular and continental goat breeds. (*Submitted to Genetics Selection Evolution*)

General introduction

Chapter 1

1.1 A brief history of pig breeds

Pigs were independently domesticated in the Near East and China approximately 10,000 years ago (Larson et al., 2007; Larson et al., 2005). From these two primary domestication sites, pigs spread across Europe, North Africa, and Asia (revised in Amills et al., 2010). The concept of breed is relatively recent because they were created around 150-200 years ago in the United Kingdom. However, local types with specific morphological and productive features were developed in much more ancient times, being Europe and China the two main pig breeding centers in the Old World (Larson et al. 2005). The first herd book of the Large White breed was published in the United Kingdom in the end of the 19th century and the first association of Duroc pig breeders (Duroc or Jersey Red Swine Club) was founded in the United States also in the end of the 19th century (Jones, 1998). It is difficult to estimate the current number of pig breeds might, but it might range between 200–300 (Jones, 1998; Porter, 1993).

Many studies have aimed to reconstruct the history of pig breeds by using microsatellite and mitochondrial markers. By using such approaches, it has been established the existence of a strong genetic divergence between Western and Asian pigs, giving support to the existence of two primary domestication sites in the Near East and China (Giuffra et al., 2000; Larson et al., 2005). It was also revealed that certain European breeds, that now have a cosmopolite distribution (*e.g.* Large White, Landrace, and Piétrain), carry Asian alleles at significant frequencies due to an introgression event that took place in the United Kingdom during the 18th-19th centuries (Fang & Andersson, 2006). Moreover, it has been shown that gene flow between domestic and wild pigs has been relatively frequent (Scandura et al., 2008). Ancient DNA studies also provided proof of the entry of Near Eastern pigs into Europe (Larson et al., 2007). In 2017, it was published a comprehensive study reporting the diversity of pig breeds around the world (Yang et al., 2017). Genome-wide single nucleotide polymorphism (SNP) data from more than 3,400 pigs were analyzed confirming that many breeds have mixed Western and Asian ancestries and that breeds from Southern Europe are genetically distinct from those of Middle and North Europe. Evidence was also provided that breeds from Africa and America have basically a European ancestry, a finding that is consistent with the process of colonization of these two continents. Moreover, Yang et al. (2017) studied the abundance and frequency of runs of homozygosity (ROH) (*i.e.* genomic regions displaying a series of consecutive homozygous genotypes) in pig breeds. Their results showed that 40 native pig

breeds have a large fraction of the genome (> 200 Mb) covered by ROH, indicating that they have undergone a history of intensive inbreeding. Such pattern was especially evident in Mangalitza and Romagnola pigs, implying that appropriate genetic conservation measures should be implemented in order to prevent a further loss of diversity.

1.2 The search for causal mutations in pigs associated with economical traits

Porcine meat production

Pork is the most widely consumed meat around the world, representing 36.4% of total meat intake (Food and Agriculture Organization of the United Nations - FAO, 2013 - http://faostat3.fao.org/). In recent decades, improvement of the pig breeding technologies (modern production systems and genetic upgrading) made possible to raise worldwide 1 billion pigs by 2014, more than 2-fold the number in the mid-1960s (FAO, 2013 - http://faostat3.fao.org/). Pig breeding is one of the fastest growing livestock subsectors (Figure 1.1) and the main producers are China, United States of America, Germany, Spain and Brazil (FAO, 2016 - http://faostat3.fao.org/).

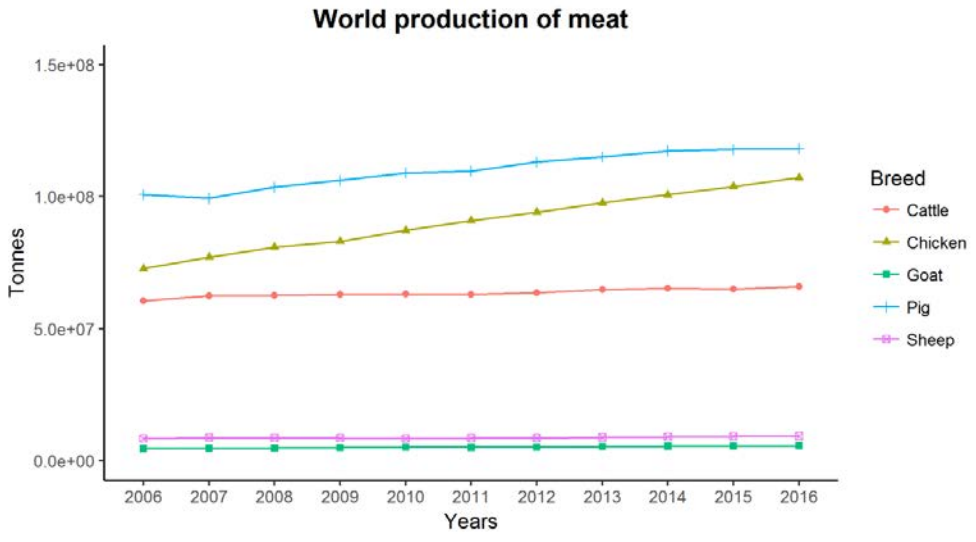

Figure 1.1 - World production of cattle, chicken goat, pig and sheep meat. Production of meat in the world from 2004 to 2016 (FAO, 2016 - http://faostat3.fao.org/).

However, the FAO predicts that the rate of meat consumption in the world will decelerate in the years to come, principally due to a slower population growth (Alexandratos & Bruinsma, 2012). Furthermore, environmental and health concerns may affect the consumption of meat. In recent years, an increased evidence for a positive association between red meat consumption and several chronic diseases, *e.g.* colorectal cancer, coronary heart disease and type 2 diabetes, has been reported in the media (De Smet & Vossen, 2016). Nevertheless, meat and its processed products contribute significantly to the intake of energy, protein and important micronutrients that support human growth and development (Leroy & Praet, 2015). Dickenson & Bailey (2002) and Lyford et al. (2010) reported that consumers are willing to pay more for high-quality meat. Thus, the pork industry should make an effort towards fulfilling consumer expectations in terms of healthier nutritional value with better eating quality.

Relevant traits in the porcine industry

Meat production and quality traits are complex phenotypes of considerable importance to the producers, consumers, and processing industry because they strongly influence meat acceptance and commercial safety (Listrat et al., 2016). The main determinants of meat quality, such as intramuscular fat (IMF), marbling, loin eye area, water-holding capacity, pH, glycolytic potential, color, tenderness, juiciness, and flavor (Davoli & Braglia, 2008), are influenced by a large number of interacting factors, *e.g.* environmental conditions, animal genetics and tissue characteristics (Figure 1.2). Importantly, these traits can be improved by traditional selection, management practices, and also by genomic selection.

In the pork industry, ultimate pH and meat color are the most important indices of meat quality and they are significantly affected by pre and post-slaughter factors. Stress and excessive energy expenditure in the pre-slaughter period cause the depletion of muscle glycogen stores and, the acidification of the pH, resulting in adverse changes of color, structure, taste, and tenderness of meat (Adzitey & Nurul, 2011). Pale Soft Exudative (PSE) and Dark Firm Dry (DFD) meats are two of the major meat quality defects and they have a strong impact on the pig industry. The PSE condition is characterized by a pale, soft and exudative meat, while DFD is the opposite condition, being characterized by a dark, firm and dry meat (Adzitey & Nurul, 2011). These two types of defective meat are produced by an excessively low (PSE) or high (DFD) ultimate pH after slaughter (Adzitey & Nurul, 2011). Acute or short-term stress just before slaughtering leads to PSE,

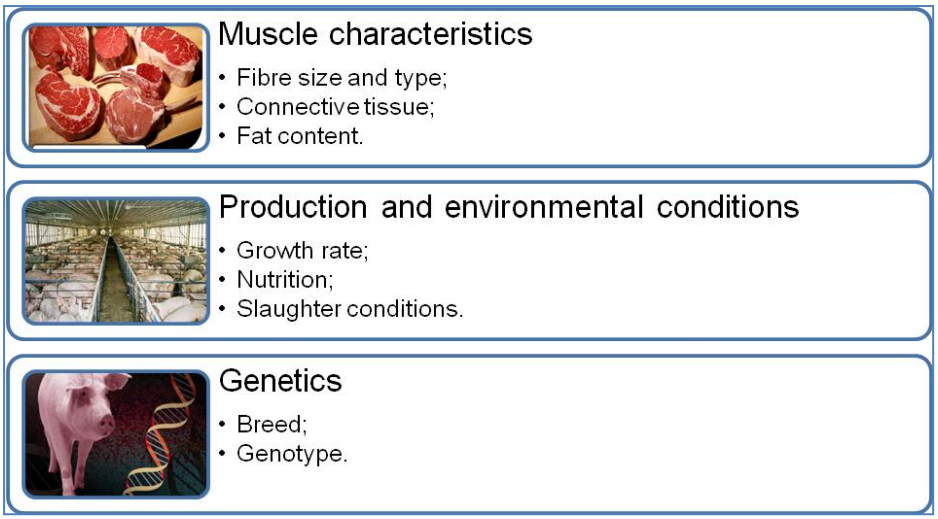

Figure 1. 2 - Schematic representation of the main factors that affect relevant meat traits in pigs.

stimulated by a rate of acidification faster than normal and lower ultimate pH values (< 6 at 45 minutes after slaughter). This acidification combined with a raised carcass temperature (Przybylski & Hopkins, 2015) provokes protein denaturation and an increase in the extracellular space, thus causing a poor water holding capacity and a lighter color (Przybylski & Hopkins, 2015; Warriss, 2000). With regard to DFD meat, it occurs when animals are exposed to chronic or long-term stress before slaughtering, leading to the depletion of stored glycogen and an increase in the postmortem pH (measured 12 – 48 hours after slaughter), which reaches values higher than 6 (Adzitey & Nurul, 2011). High pH results in a relatively little denaturation of proteins, as indicated by low solubility of sarcoplasmic and myofibrillar proteins, retaining more water during storage and darkening the color of meat (Warriss, 2000).

Furthermore, IMF content and composition also affect the technological and nutritional properties of meat. It is generally accepted that IMF positively influences the overall consumer acceptability of meat by increasing flavor, juiciness, and tenderness (Hocquette et al., 2010). Fernandez et al. (1999) reported that flavor and juiciness were significantly enhanced when IMF levels increased above 2.5% in pig meat. However, during many years the pig industry devoted its efforts to improve leanness, which has an unfavorable correlated effect on IMF by decreasing it (Ciobanu et al., 2011). This unfavorable correlated response has led to the development of genetic lines with an IMF content that does not match the requirements of specialized markets (Hocquette et al., 2010; Wood et al., 2008). Another important aspect determining meat quality is IMF composition (Wood

et al., 2008) *i.e.* polyunsaturated fatty acids (FAs) are prone to become oxidized, worsening fat firmness and oiliness and leading to the development of rancidity as shelf-time increases. Moreover, FA composition affects meat flavor due to the production of volatile and odorous compounds during cooking (Hausman et al., 2009; Wood et al., 2008).

Heritability values for IMF content and composition are moderate (from 0.27 to 0.47, Casellas et al., 2010; Torres-Vázquez & Spangler, 2016), while, meat quality traits, such as pH, cooking loss and color display a broad range of heritabilities going from 0.19 to 0.79 (Cabling et al., 2015). This important genetic determinism demonstrates that these traits can be successfully modified by selection (Casellas et al., 2010; Hernandez-Sanchez et al., 2013). The development of molecular markers and genome maps, together with advances in molecular genetics and computational biology, enhanced by the recent availability of the swine genome sequence, has paved the way to increase the rate of genetic gain by identifying the genetic factors that modulate the variation of traits of economic interest.

Performance of Genome-Wide Association Studies and Selection Scans in pigs

The quest to identify genes and quantitative trait locus (QTLs) associated with traits of economic importance in pigs began several decades ago. Up to the first decade of the 21th century, the search of QTL involved the genotyping of microsatellite markers in resource populations with available phenotypic records (Dekkers, 2004). The advent of whole-genome sequencing technologies and the availability of affordable genome-wide SNPs panels made possible to explore the genetic architecture of complex traits with a much higher resolution. In humans, the first successful genome-wide association study (GWAS) was published in 2005 by Klein et al., (2005). These authors made a genome-wide scan of polymorphisms associated with the age-related macular degeneration and found two SNPs which displayed altered allele frequencies when patients were compared with healthy controls. In pigs, the first GWAS for meat traits was published by Duijvesteijn et al. (2010), who identified 37 SNPs on pig chromosomes SSC1 and SSC6 related to androstenone levels in a commercial Duroc-based sire line. Since then, many GWAS have been carried out to identify causal mutations in pigs (see Sharma et al. 2015 for a thorough review). Moreover, Ma et al. (2014) demonstrated that a point mutation in a splice site modifies the expression of the *PHKG1* gene, thus producing an increase of 43% of the glycolytic potential and a negative effect on a broad array of pig meat quality traits. The

GWAS approach has also been used to elucidate the genetic basis of simple phenotypes such as coat color. For instance, Ren et al. (2011) performed a GWAS and identified a single locus variant (c.1484_1489del) in the *TYRP1* gene as the causative mutation for the brown coloration in Chinese indigenous pigs. This information complements previous data indicating that the polymorphism of the *KIT* (Giuffra et al., 2002) and *MC1R* (Fang et al., 2009) genes has a crucial role in the determination of pig pigmentation.

On the other hand, the combination of gene expression data obtained with microarrays with high throughput SNP genotypic information has provided valuable options for identifying causal mutations. Expression QTL (eQTL) are polymorphisms associated with the transcript levels of one or more genes. Obviously, eQTL can have perceptible consequences on complex phenotypes, so their detection can be crucial in elucidating the genetic basis of complex traits. Ponsuksili et al. (2010) investigated the genome-wide transcriptional profiles of the *longissimus dorsi* muscle and detected 653 putative *cis*-eQTL. Moreover, the mRNA levels of 262 transcripts encoded by the *cis*-regulated genes showed significant correlations with at least one meat quality trait. In this study, it was also observed that *cis*-eQTL were more consistently detected than trans-eQTL, possibly because they have larger effects and the correction for multiple testing is less stringent. These findings demonstrate that global microarray eQTL analysis can be used for exploring functional and regulatory gene networks and scanning *cis*-eQTL. Further studies have reported several candidate genes for muscle traits based on GWAS supported by eQTL-analysis (Cinar et al., 2012; Ponsuksili et al., 2014; González-Prendes et al., 2017).

Genome-wide SNP data have also been used to detect the footprint of selection in the porcine genome (Vitti et al., 2013). Here, the basic assumption is that such footprint can be detected because positive selection sweeps beneficial alleles towards high frequencies or fixation. This causes a reduction in diversity around the selected locus and an increase in the magnitude of linkage disequilibrium because the frequencies of the variants near the selected allele are modified due to a hitchhiking effect (Vitti et al., 2013). Many studies have been carried out to detect the footprint of selective processes related to domestication (Rubin et al., 2012; Zhu et al., 2017), litter size (Trenhaile et al., 2016), and adaptation to high altitudes (Burgos-Paz et al., 2013), to mention a few. Recently, a selection scan investigating the genetic basis of the six-white-point pigmentation pattern of Diannan small-ear pigs showed that this color coat is strongly determined by three loci *i.e. EDNRB*, *CNTLN*, and *PINK1* (Lü et al., 2016).

1.3 The generation of biological information is essential to identify potencial causal mutations

One of the main drawbacks of GWAS studies is that genomic regions displaying significant associations with phenotypes may contain hundreds of genes and thousands of polymorphisms. In the absence of biological information, it is very difficult to distinguish the causal mutation from the set of "innocent bystander" polymorphisms linked with it. Indeed, the vast majority of genetic variants (> 80%) detected by GWAS lie in intronic or intergenic regions of unknown function, and it is unclear how these non-coding variants affect traits and diseases (Hindorff et al., 2009) This is why it is so important to characterize with enough detail and resolution the functional elements of the whole porcine genome or, at least, of regions displaying significant associations with quantitative traits.

In human and mouse, a coordinated genome-wide effort towards the identification of functional elements has enabled to gain new insights into the molecular basis of gene expression and its potential phenotypic consequences (The ENCODE Project Consortium, 2012; The GTEx Consortium, 2015). Compared to human and mouse, the functional complexity of the transcriptomes in domesticated animals has been poorly characterized so far. Whilst approximately 70% to 90% of the coding elements can be readily identified, little information about non-coding genes and regulatory sequences underlying complex traits is available (Andersson et al., 2015). Recently, a Functional Annotation of ANimal Genomes (FAANG) international project began to be developed in order to produce comprehensive maps of functional elements in the genomes of domesticated animal species (Andersson et al., 2015). The results of this project should start to be published in the next few years, yielding valuable biological data about the genomic architecture of gene expression and production phenotypes, domestication, and evolution. Such information will be essential to interpret the results of GWAS and selection scans, making possible to identify which functional elements are present in genomic regions involved in the variation of phenotypic traits (Figure 1.3). Currently, many methodological approaches are being developed to identify functional elements (*e.g.* transcription factor binding sites and chromatin modifications) as well as the three-dimensional organization of the genome and other aspects that are essential to improve our understanding of the genomic architecture of complex traits - Figure 1.3 (Ritchie et al., 2015).

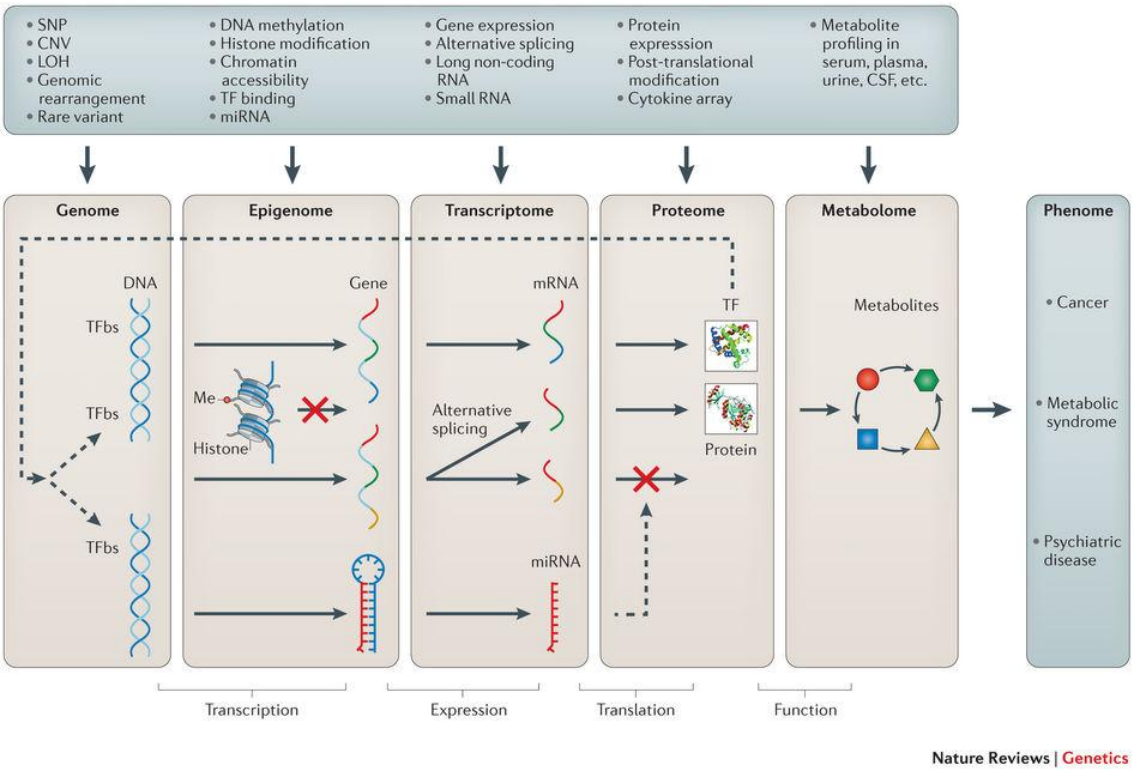

Figure 1.3 - Biological systems multi-omics from the genome, epigenome, transcriptome, proteome, and metabolome to the phenome (Ritchie et al., 2015)**.**

Transcriptomics analysis

In eukaryotes, cell-cell differences are determined by the expression of different sets of genes. It is now clear that processing of primary transcripts as well as translational control opens a myriad of opportunities for regulating gene expression (Day & Tuite, 1998). Transcriptomic studies attempt to catalog and quantify the RNA content of a cell, tissue or an organism. In some cases, the goal is to target all transcripts, regardless of their complexity. Many transcripts can be generated from a single gene by alternative splicing (AS) and by the use of alternative promoters or polyadenylation sites. The GTEx Consortium (2015) described the landscape of gene expression across tissue in humans, demonstrating a similar number of expressed mRNA genes for most tissues (average of 20,940). Moreover, they showed that tissue-specific transcription is typically dominated by a few highly expressed genes which vary from tissue to tissue *e.g.* casein genes in the mammary gland, loci encoding myofibrillar proteins in the skeletal muscle and heart etc. (Mele et al., 2015). Ferraz et al. (2008) and Freeman et al. (2012) made pioneering studies

about the pig transcriptome. In this way, Ferraz et al. (2008) conducted a microarray expression profiling of 16 different tissues from two males and two females from two pig breeds, Large White and Iberian, with highly divergent growth and fatness profiles. They found that tissue type accounted for ~11 times more variability than sex or breed. On the other hand, Freeman et al. (2012) built a gene expression atlas of the domestic pig and identified multiple large clusters of genes showing a tissue-restricted pattern of expression. Moreover, the analysis of genes expressed in the gastrointestinal tract showed marked regional differences. For instance, the *SLC40A1* gene, which is involved in the export of iron, was only expressed in the duodenum, while *SLC26A3* expression was restricted to the large bowel (Freeman et al. 2012). Many tissues were analyzed looking for candidate genes and metabolic routes related to complex characters, thus providing new clues about the molecular mechanisms that determine distinct phenotypes. In liver, genes associated with cholesterol metabolism, oxidation and reduction processes (*e.g. CYP2E1*, *CYP2C9*, and *HPGD*) were differentially expressed between animals displaying divergent fatness profiles (Ramayo-Caldas et al., 2012; Sodhi et al., 2014). In the porcine adipose tissue and skeletal muscle, individuals with higher polyunsaturated fatty acids (PUFAs) content showed a lower expression of lipogenic genes (Cánovas et al., 2010; Corominas et al., 2013; Puig-Oliveras et al., 2014). Indeed, a higher PUFA content may enhance fatty acid oxidation, thus decreasing the intracellular accumulation of triglycerides.

Transcriptome analysis has also revealed that genes producing non-coding RNAs can be involved in skeletal muscle growth and development in pigs. Zou et al. (2017) identified 323 large intergenic non-coding RNAs (lincRNAs) that are expressed in the porcine leg muscle and they found that lincRNA gene expression is correlated with the methylation status of the respective promoters. In addition, lincRNA genes produced shorter transcripts with lower levels of expression than protein-coding genes. In another study, Jing et al. (2015) detected 15 differentially expressed microRNAs (miRNAs) when studying pigs with different residual feed intakes. Through a miRNA-targeted pathway analysis, 55 KEGG pathways comprised genes potentially targeted by up or down-regulated miRNAs *e.g.* the *TGF-beta* signaling pathway, PI3K-Akt signaling pathway, mTOR signaling pathway and GnRH signaling pathway (Jing et al., 2015).

Epigenetics

Initially, the term “epigenetics” defined changes in the phenotype without changes in the genotype (Triantaphyllopoulos et al., 2016) but the molecular basis of such phenomenon was poorly understood. Currently, we know that epigenetic mechanisms transduce the inheritance of gene expression patterns without altering the underlying DNA sequence but by modifying chromatin (Allis & Jenuwein, 2016). These chromatin changes are achieved through a broad variety of chemical modifications including DNA methylation as well as histone acetylation, methylation, sumoylation, phosphorylation, and ubiquitination. Technologies for epigenetics research such as ChIP–seq, MNase-seq, FAIRE–seq, DNase-seq, Hi-C, ChIA-PET and ATAC-seq (Meyer & Liu, 2014) can reveal different aspects of chromatin structure and are vital for deciphering interactions between specific proteins and DNA as well as for mapping transcription-factor binding sites and histone/chromatin modifications (Farnham, 2009). Recent studies suggest that the interplay between chromatin and transcriptional activity is dynamic, very complex and species-specific (Schmidt et al., 2010). Indeed, a variety of phenotypic changes important for the normal development as well as for the progression of diseases are temporally and spatially controlled by chromatin-coordinated gene expression programs (Robertson et al., 2007; Zhao et al., 2016).

Epigenetic studies in pigs are scarce. Fan et al. (2012) investigated the epigenetic effects of sulforaphane, a histone deacetylase inhibitor, in myostatin satellite cells. They demonstrated that the supplementation of sulforaphane not only acts as a histone deacetylase inhibitor but also as a DNA methyltransferase inhibitor in porcine satellite cells. Braunschweig et al. (2012) examined the transgenerational epigenetic effects of dietary methylating micronutrients on gene expression and DNA methylation in three generations of Large White pigs offspring. The boars which received a hypermethylating diet had a higher percentage of shoulder and were leaner compared to the offspring of the control group fed with a standard diet.

DNA methylation is a common heritable epigenetic mark that cells use to lock genes in the "off" position, thus regulating gene expression (Jin et al., 2011). DNA methylation is essential for normal development, and it plays a very important role in numerous cellular processes, including embryonic development, genomic imprinting, X-chromosome inactivation, and preservation of chromosome stability. Differential methylation profiles can be associated with diseases (Toyota et al., 1999) and distinct phenotypes (Yoon et al.,

2017; Zhang et al., 2016). Li et al. (2012) generated a landscape of the DNA methylome of adipose and muscle tissues in three pig breeds differing in their fatness levels. They found that differentially methylated regions in promoters are highly associated with obesity development via expression-repression of known obesity-related genes and novel genes. Zhang et al. (2016) performed a DNA methylation analysis of adipose tissue and showed evidence of functionally relevant methylation differences in the backfat tissue of obese *vs* lean pigs. A total of 483 differentially methylated regions were located in promoter regions for genes involved in lipid transport and localization (*e.g. PLIN1*, *BDKRB2*, *NSDHL*, *APOL1*, and *APOL4*).

1.4 The landscape of mammalian transcriptomes

Understanding the biological significance of the genome sequence involves the functional characterization of its RNA products. The Encyclopedia of the DNA element (ENCODE) pilot project (The ENCODE Project Consortium, 2012) demonstrated that up to 80% of the human genome has some type of biological function, with just 2.9% of the genome covered by protein-coding genes. In the mouse, at least 46% of the genome is capable of producing polyadenylated messenger RNAs (mRNA) and the vast majority (87–93%) of exonic nucleotides are transcribed (Yue et al., 2014). These studies provide evidence that the genome is largely transcribed, but a relevant fraction of the produced RNAs do not encode proteins (Carninci et al., 2005; Derrien et al., 2012; The ENCODE Project Consortium, 2012; Yue et al., 2014).

The mammalian transcriptome mainly comprises ribosomal RNA (~80-90%, rRNA), transfer RNA (~10-15%, tRNA), mRNA (~3–7%) and a small proportion of non-coding RNA (< 0.2%, ncRNA) with regulatory functions (Palazzo & Lee, 2015). In recent years, the analysis of expression data sets from tissues and primary cells made possible to gather a huge amount of information about the nature and function of coding and non-coding transcripts and their isoforms. Such effort has been particularly fruitful in humans (Lappalainen et al., 2013; Mele et al., 2015; The GTEx Consortium, 2015, Iyer et al., 2015) and mice (Barak et al., 2013; Russ et al., 2013; Li et al., 2016). In this way, the Genotype-Tissue Expression (GTEx) project (The GTEx Consortium, 2015) has collected and analyzed samples from 175 postmortem human donors, retrieving an average of 43 tissue samples per donor, in order to examine the patterns of expression of transcribed

genes across tissues. An average of 20,940 genes are expressed in the majority of analyzed tissues (The GTEx Consortium, 2015). Moreover, between 919 (heart) and 2,244 (thyroid gland) were regulated by *cis*-eQTL, and more than 50% of all QTL were shared across the nine tissues under analysis. Mele et al. (2015) showed that tissue-specific transcription is typically dominated by a small number of genes that vary from tissue to tissue. In the case of skeletal muscle, genes related to actin and other myofibrillar proteins were the main contributors to the overall transcriptome. Though there are thousands of genes that are differentially expressed across tissues, a few hundreds are exclusively expressed in a single tissue (Mele et al., 2015). The majority of such genes are expressed in the testis and encoded by lncRNAs. Moreover, variation of gene expression is much higher amongst tissues than amongst individuals, and a number of genes show sex-, population- or age-biased patterns of expression (Mele et al., 2015).

Transcripts from ncRNA genes are not translated into proteins and they are loosely grouped into classes based on transcript size and/or characteristics (Table 1.1). There are strong evidences that ncRNAs are key elements of cellular homeostasis by interacting with chromatin complexes, working as RNA enhancers, recruiting or assembling certain proteins and interacting with other RNAs at the post-transcriptional level (Beltrami et al., 2014; Huarte & Marín-Béjar, 2015). Moreover, there are several ncRNAs with key roles in the maintenance of muscle function (Table 1.2).

Due to their poor evolutionary conservation, it is unclear how many ncRNA genes are present in a typical mammalian genome (Palazzo & Lee, 2015). Currently, 22,521 and 15,074 ncRNA genes have been annotated in the human (assembly GRCh38.p7) and mice (assembly GRCh38.p5) genomes. Mirbase (http://www.mirbase.org) encompasses a total of 1,881 miRNA precursor genes that are processed into 2,588 mature miRNA sequences in human, and 1,193 precursors and 1,915 mature miRNA sequences in mouse. Recently, Iyer et al. (2015) curated 7,256 RNA-Seq libraries from normal tissues, cell lines and different types of tumors, identifying 58,648 lncRNA-encoding loci, of which 79% were previously unannotated. They observed that only 1% (597) of the lncRNAs harbored ultraconserved elements, whilst miRNAs are evolutionarily conserved from plants to mammals (Nie et al., 2015). However, the majority of these ncRNAs have yet to be biochemically characterized for clarifying their biological functions (Palazzo & Lee, 2015).

Table 1.1 -Regulatory non-coding RNA types (adapted from Byron et al., 2016).

RNA types	Associated name	Length (nt)	Description
miRNA	Micro RNA	~ 18–24	Represent the most extensively characterized group of small ncRNAs and they are mainly involved in gene repression.
piRNA	PIWI-interacting RNA	~ 26–32	Functions in transposon repression and maintenance of germline genome integrity.
snRNA	Small nuclear RNA	~ 100–300	Localized to the nucleus, with functions in RNA processing and splicing.
snoRNA	Small nucleolar RNAs	~ 60–140	snoRNAs play a key role in ribosome biogenesis and rRNA modifications.
lncRNA	Long ncRNA	> 200	Regulating gene expression through a broad variety of mechanisms.
circRNA	Circular RNA	~ 100–500	Contain a covalent bond between the 5' and 3' ends, resulting in a continuous circular loop. CircRNAs can act as miRNA sponges and regulators of splicing and transcription.
tRNA	Transfer RNA	~ 75–90	Help with translation of mRNA to protein. tRNAs are highly structured and have many modifications to bases, making them difficult to sequence through.

Nt = nucleotide.

Table 1.2 - miRNAs and lncRNAs implicated in the development of skeletal muscle (revised by Neguembor et al., 2014; Nie et al., 2015)**.**

		Function	Effector molecule	References
miRNA	*miR-1*	Promotes differentiation	*HDAC4*	Chen et al. (2006)
		Inhibits proliferation	*PAX7*	Chen et al. (2010)
	miR-199a-3p	Inhibits differentiation	*IGF-1*, *MTOR*, and *RPS6KA6*	Jia et al. (2013)
	miR-31	Maintenance of quiescence/stemness	*MYF5*	Crist et al. (2012)
lncRNA	*Malat1*	Epigenetic repression, pre-mRNA splicing	*CBX4* and SR family of splicing factors	Watts et al. (2013)
	Neat1	Structural integrity of nuclear paraspeckles	Various RNA-binding proteins	Sunwoo et al. (2009)
	l2/Meg3	Epigenetic repression	*PRC2*	Zhou et al. (2015)

***miRNA**= microRNA; **lnRNA** = long non-coding RNA.

Alternative mRNA splicing takes place when a primary transcript is processed in different ways, during the mRNA maturation process, thus yielding multiple mRNA isoforms. A global survey of mRNA splicing events showed that a total of 62.1% of the human genome is covered by processed transcripts (Djebali et al., 2012). The relative location of strong and weak splice sites may result, depending on the cellular context, in different AS events, as shown in Figure 1.4**.** Deep sequencing of 15 human tissues and cell lines was consistent with these findings, thus demonstrating that exon skipping was the most frequent AS event, followed by alternative 3' splice site, alternative 5' splice site and alternative first exon (Wang et al., 2008). Exon skipping accounts for nearly 40% of AS events in higher eukaryotes, while intron retention, in which an intron remains in the mature mRNA transcript, is the rarest AS event in vertebrates and invertebrates, accounting for less than 5% of known events (Alekseyenko et al., 2007).

The GTEx Pilot project has revealed the existence of splicing QTL for 1,900 human genes and only 7-21% of them happened to be tissue-specific (The GTEx Consortium, 2015). Moreover, a large fraction of splicing QTLs (20 - 48%) associated with changes in gene transcript isoforms was identified as eQTL. In mice, Giudice et al. (2016) suggested that AS in trafficking and membrane dynamics genes (*SNAP23, TRIP10, CLTC*, and *TMED2*) is involved in T-tubule maturation and possibly in mitochondria positioning during the postnatal phase of striated muscle development. Interestingly, a *MICU1.1* splice variant confers high sensitivity to the mitochondrial Ca^{2+} uptake, a process required to increase ATP supply for skeletal muscle contraction (Reane et al., 2016). Another important source of transcript variation involves the alternative usage of promoters and polyadenylation sites. In a recent study, Reyes & Huber et al. (2017) investigated the cell type-dependent differences in exon usage of over 18,000 protein-coding genes in 23 cell types and found that alternative transcription start and termination sites, instead of AS, accounted for most of tissue-dependent exon usage. Their results also indicated that AS mostly affects untranslated exons and thus it has a limited impact on proteome complexity. In the light of this, alternative transcription start and termination sites would be the main drivers of transcript isoform diversity across tissues. Natural variation in gene expression is extensive in humans and other organisms, and variation in the baseline expression level of many genes has a heritable component (Cheung et al., 2003a; Cheung et al., 2003b). The tissue-specificity of eQTLs across different tissues and cell types is relevant to identify putative regulatory variants and linking them with phenotypes or diseases.

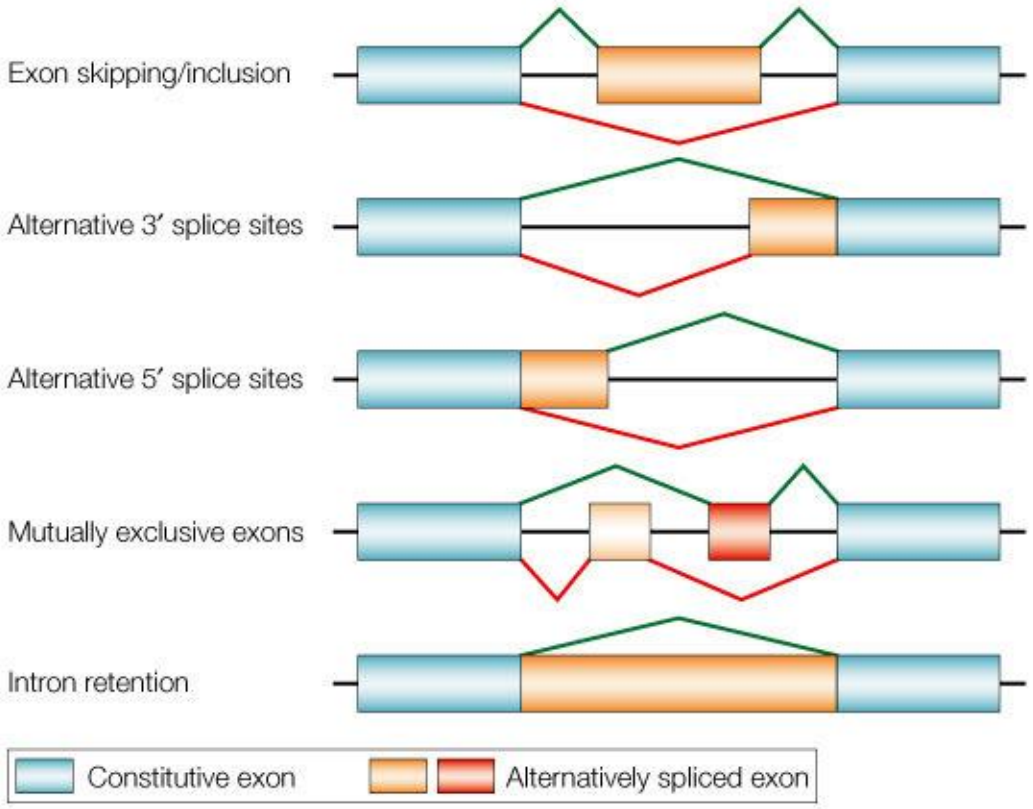

Figure 1.4 -Schematic representation of different types of alternative splicing events (Cartegni et al., 2002)**.** The figure illustrates different types of alternative splicing events: exon inclusion or skipping, alternative splice-site selection, mutually exclusive exons, and intron retention for an individual pre-mRNA.

Nica et al. (2011) explored in-depth the role of *cis*-regulatory variation in three human tissues: lymphoblastoid cell lines, skin, and fat. In doing so, they discovered that 4.7% of genes in each tissue are regulated by *cis*-eQTLs, whilst 29% of eQTLs happen to be tissue-specific. Grundberg et al. (2012) showed that at least 40% of the total heritable *cis* effect on expression cannot be accounted for by common *cis* variants in twins, highlighting the importance of characterizing low frequency/rare regulatory variants which may have large effects. The GTEx project (The GTEx Consortium, 2013) investigated the patterns of eQTLs sharing across tissues by using a data set of 22,286 genes expressed in nine tissues. They observed that 50% of all detected eQTL were common to all nine tissues. The majority of the significant *cis*-eQTL clustered around the transcription start site of target genes. As a complementary approach, the GTEx project (The GTEx Consortium, 2015) investigated the allele-specific expression of genes in order to estimate the overall effect of *cis*-regulatory variants on the expression of nearby genes. Allele-specific expression ratios

and gene expression levels were highly correlated (r = 0.77), indicating that tissues with similar gene expression profiles share similar regulatory mechanisms.

1.4 Methods to characterize the transcriptome

The generation of global gene expression profiles is a common approach in basic and translational research. Different methods to comprehensively and systematically interrogate gene expression have been developed. The choice of the technology depends on the number of genes to be analyzed. Quantitative PCR is best suited for the analysis of limited numbers of genes; while microarrays and RNA-Seq make possible to characterize the transcript levels of thousands of genes in a single experiment. The microarray technology (Figure 1.5) has been extensively used in porcine transcriptomic studies but in the last five years, it has been progressively replaced by next-generation sequencing methods.

While microarrays have been incredibly useful in a wide variety of applications, they have a number of limitations. First, arrays provide an indirect measure of relative transcript concentrations and the intensity of fluorescence is not linearly proportional to the concentration of the species hybridizing to the array. For example, the signal may become saturated in the case of highly expressed transcripts and, the sensitivity threshold is probably lower for cell types with a more-limited concentration range of transcripts (Bumgarner, 2013). Second, there is a cross-hybridization of sequences with high identity, a feature that is specially relevant for complex mammalian transcriptomes and can be particularly problematic for gene families and for genes with multiple splice variants (Koltai & Weingarten-Baror, 2008). Third, a DNA array can only detect probed transcripts. Finally, many problems related to chip to chip variation (*e.g.* unequal dye incorporation, sample preparation, hybridization conditions) and analysis and interpretation of data (image capture and processing) may influence the accuracy, sensitivity, and reproducibility of results (Daly et al., 2005; Koltai & Weingarten-Baror, 2008).

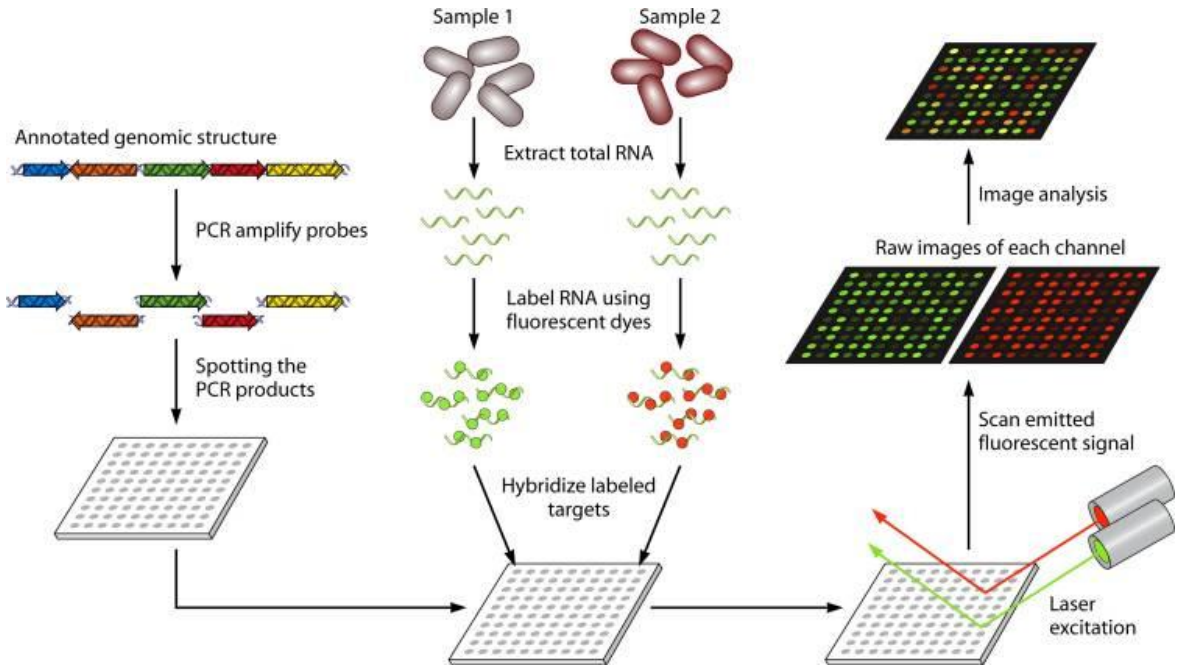

Figure 1.5 -Workflow summary of printed microarrays (Miller & Tang, 2009). Probes are usually oligonucleotides that are spotted onto a solid surface. In this example, RNA from two samples representing different conditions is used as template to synthesize cDNA which is differentially labeled. This cDNA is hybridized to the arrayed probes and fluorescent signals are recorded by confocal microscopy, providing information about which genes are expressed in each sample as well as their levels of expression.

RNA-Seq, a sequencing technology to investigate gene expression

RNA-Seq involves the sequencing of the whole transcriptome of a sample, thus making possible to characterize not only transcript abundance but also RNA splice events and edited RNAs (Piskol et al., 2013; Wolf, 2013; Korir & Seoighe, 2014). This technological development eliminated many challenges posed by microarrays (hybridization-based) and Sanger (sequencing-based) approaches that were previously used for measuring gene expression (Table 1.3). A typical RNA-Seq experiment implies purification of RNA, synthesis of cDNA, preparation of the library and its sequencing in a next-generation sequencing (NGS) platform. However, many experimental issues should be carefully considered before performing an RNA-Seq experiment (Kukurba & Montgomery, 2015). For example, the RNA extraction protocol needs to be adjusted having in mind the targeted RNA-species *i.e.* all RNAs, small or large RNAs etc. (Wolf, 2013). Another key consideration, concerning library construction, is whether or not to prepare strand-specific libraries. Strand-specific information about the orientation of transcripts is valuable for transcriptome annotation, especially for regions with overlapping transcription from

opposite directions (Borodina et al., 2011). Moreover, the amplified fragments can be sequenced either from one end (single-end) or from both ends (paired-end). Paired reads allow more accurate alignment to a reference genome, facilitating the discovery of novel transcripts, splice isoforms and the *de novo* assembly of the transcriptome (Berglund et al., 2011).

Several NGS platforms are commercially available and many more are under active development (Table 1.4)**.** Each commercially available platform has similarities and differences relative to the others depending on the chemistries and detection methods used. Sequencing platforms can be generally classified on the basis of three features (Berglund et al., 2011; van Dijk et al., 2014; Levy & Myers, 2016). First, they may detect single molecules (Pacific Biosciences and Oxford Nanopore) or clonally amplified DNAs (Illumina, Ion Torrent, and Roche 454). Second, detection can be optical, *e.g.* fluorescence (Illumina and Pacific Biosciences) or light (Roche 454), or non-optical, *e.g.* IonTorrent (detection of the release of H^+ during a polymerization reaction via a solid-state sensor) and Oxford Nanopore (measurement of the translocation of DNA through a nanopore sensor) platforms. Finally, the majority of sequencing technologies are based on sequencing-by-synthesis reactions, as performed by Illumina, Ion Torrent, Pacific Biosciences, and Roche 454 platforms, whereas the Applied Biosystems SOLiD and the Polonator platforms use a ligation-mediated synthesis approach. Direct analysis of DNA sequences is performed by the Oxford Nanopore platform (Berglund et al., 2011; Levy & Myers, 2016; van Dijk et al., 2014). A comparison of the different sequencing platforms in terms of read length, output and runtime can be found in Figure 1.6. The majority of platforms can generate reads of one or few hundreds of bp (Figure 1.6A). PacBio (Pacific Biosciences) can produce long reads, with maximum read lengths over 20 kb, making this technology an ideal tool to finish genome assemblies. Illumina currently offers the highest throughput per run and the lowest per-base cost (Figure 1.6B). These improvements have resulted in a substantial decrease in the costs of sequencing genomes (Figure 1.6C). Ion Torrent PGM and PACBio are the fastest bench-top NGS platforms (Figure 1.6D). Nowadays, Illumina produces the most widely used family of sequencing platforms (GA/HiSeq/MiSeq/NextSeq) (Hodkinson & Grice, 2015) and, by this reason, a schematic presentation of the library preparation and sequencing processes is provided in Figure 1.7**.**

Table 1.3 - Advantages of RNA-Seq techonology compared with other transcriptomics methods (Wang et al., 2009)**.**

Technology	Microarray	cDNA or EST sequencing	RNA-Seq
Technology specifications			
Principle	Hybridization	Sanger sequencing	High-throughput sequencing
Resolution	From several to 100 bp	Single base	Single base
Throughput	High	Low	High
Reliance on genomic sequence	Yes	No	In some cases
Background noise	High	Low	Low
Application			
Simultaneously map transcribed regions and gene expression	Yes	Limited for gene expression	Yes
Dynamic range to quantify gene expression level	Up to a few-hundredfold	Not practical	> 8,000-fold
Ability to distinguish different isoforms	Limited	Yes	Yes
Ability to distinguish allelic expression	Limited	Yes	Yes
Practical issues			
Required amount of RNA	High	High	Low
Cost for mapping transcriptomes of large genomes	High	High	Relatively low

Table 1.4 - Summary of next generation sequencing (NGS) technologies (adapted from Levy & Myers, 2016)**.**

Manufacturer	Amplification	Detection	Chemistry	URL
Commercial				
Illumina	Clonal	Optical	Sequencing by synthesis	http://www.illumina.com
Oxford Nanopore	Single molecule	Nanopore	Nanopore	http://www.nanoporetech.com
Pacific Biosciences	Single molecule	Optical	Sequencing by synthesis	http://www.pacb.com
ThermoFisher Ion Torrent	Clonal	Solid state	Sequencing by synthesis	http://www.thermofisher.com/us/ en/home/brands/ion-torrent.html
QIAGEN (GeneReader)	Clonal	Optical	Sequencing by synthesis	http://www.qiagen.com
Pre-commercial				
Quantum Biosystems	Single molecule	Nanogate	Nanogate	http://www.quantumbiosystems.com
Base4	Single molecule	Optical	Pyrophosphorolysis	http://base4.co.uk
GenapSys (GENIUS)	Clonal	Solid state	Sequencing by synthesis	http://www.genapsys.com
Roche Genia	Single molecule	Solid state	Nanopore	http://geniachip.com
Post-commercial				
Roche 454 (GS FLX)	Clonal	Optical	Sequencing by synthesis	http://www.454.com
Helicos BioSciences (Heliscope)	Single molecule	Optical	Sequencing by synthesis	—
Dover (Polonator)	Clonal	Optical	Sequencing by ligation	—
ThermoFisher Applied Biosystems (SOLiD)	Clonal	Optical	Sequencing by ligation	http://www.thermofisher.com/us/en/ home/brands/applied-biosystems. html
Complete Genomics	Clonal	Optical	Sequencing by ligation	http://www.completegenomics.com

*Dashes indicate that no URL or reference is available. Platforms listed as precommercial have been announced but at the time of writing have not been formally launched; platforms listed as post-commercial are no longer commercially available as new instrument sales.

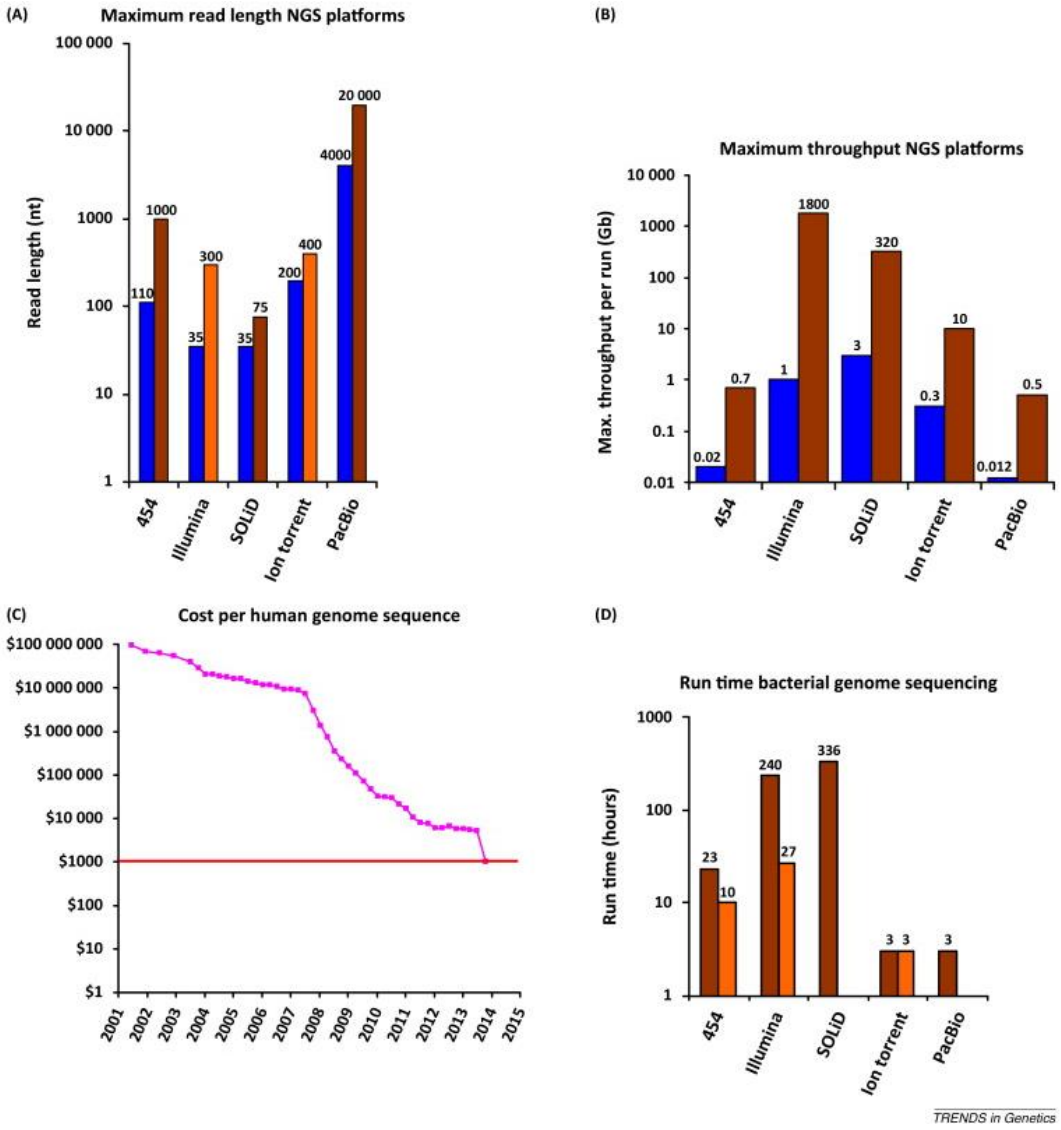

Figure 1.6 -Evolution of high-throughput sequencing platforms (van Dijk et al., 2014) (A) Blue bars: maximum read length of the first commercially available sequencing instruments. Orange bars: maximum read length obtained today on the bench-top versions; brown bars: maximum read length obtained today for the large instruments. (B) Blue bars Maximum throughput of the first commercially available sequencing instruments. Brown bars: current maximum throughput. (C) Evolution of the cost of sequencing a human genome from 2001-2015. (D) Run times to complete a bacterial genome sequence using the sequencing platforms of various manufacturers. Brown: large instruments. Orange: bench-top machines

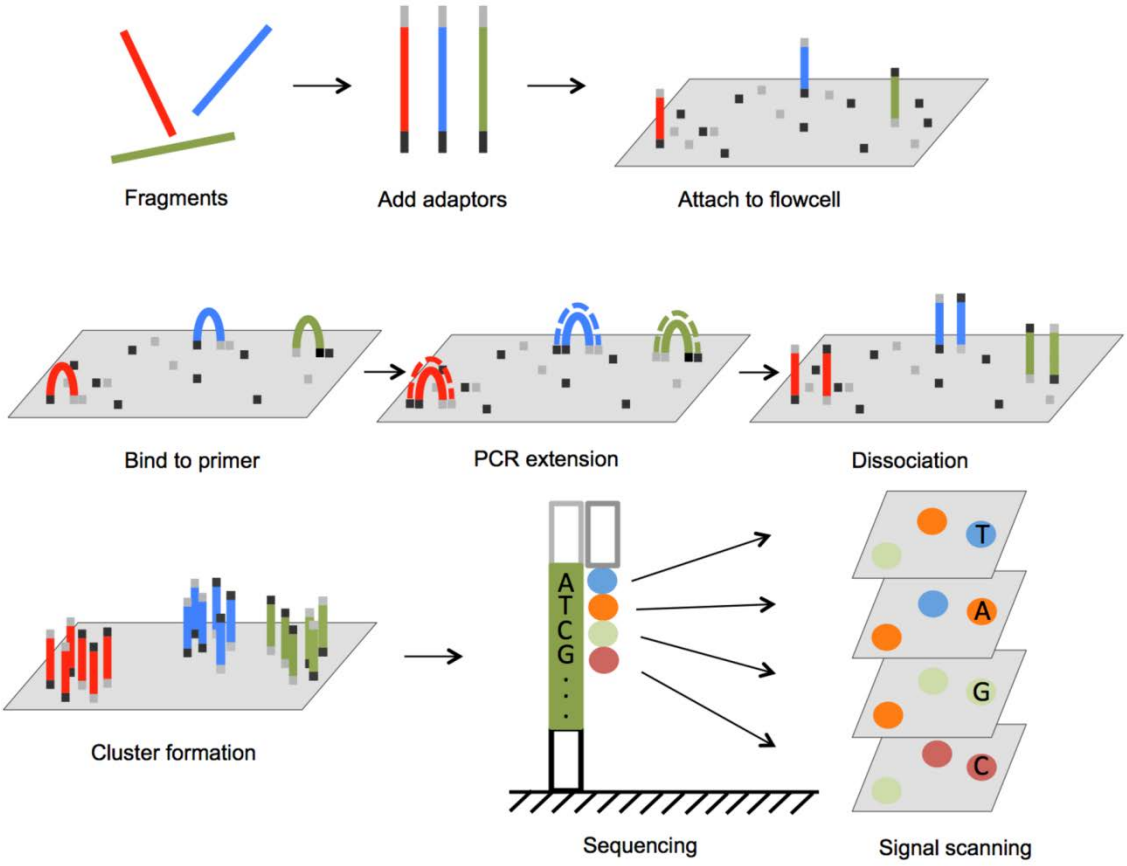

Figure 1.7 - Schematic presentation of the library preparation and sequencing processes associated with the Illumina Sequencing Platform. (http://www.3402bioinformaticsgroup.com/service/; accessed in October 2017). Outline of Illumina genome analyzer sequencing process. (1) Adaptors are annealed to the ends of sequence fragments. (2) Fragments bind to primer-loaded flow cells and bridge PCR reactions amplify each bound fragment to produce clusters of fragments. (3) During each sequencing cycle, one fluorescent nucleotide is added to the growing strands. Laser excites the fluorophores in all the fragments that are being sequenced and an optic scanner collects the signals from each fragment cluster. Then the sequencing terminator is removed and the next sequencing cycle starts.

Bioinformatic data processing

A single run of any sequencing platform generates an appreciable amount of sequencing data, quickly reaching hundreds of gigabytes. Like other high-throughput sequencing technologies, RNA-Seq faces several informatics challenges. Different tools have been developed by bioinformaticians, using different algorithms and models, to analyze the data flood in order to make biological inferences. Routine RNA-Seq data analysis is shown in Figure 1.8, and consists of the following five steps: 1 - raw data quality control and processing; 2 - alignment of the reads and visualization of data; 3-

transcriptome reconstruction; 4 - expression quantification, and 5 - differential expression analysis. Some bioinformatic tools for NGS data processing are shown in Table 1.5.

As an initial step, RNA-Seq data should be subjected to the quality control of the raw data, and an additional quality control procedure can be performed to evaluate the quality of the aligned reads after read alignment (Conesa et al., 2016). Depending on the RNA-Seq library construction strategy, it is recommended some form of read trimming prior to aligning the RNA-Seq data. Adapter and quality trimming aim to remove adapter sequences used during library construction and to eliminate poor quality bases (Conesa et al., 2016). When a reference sequence is available, two strategies can be used to align reads *i.e.* mapping to the genome or mapping to the annotated transcriptome (Yang & Kim, 2015). If a transcriptome is used as a reference, only known exons and junctions are mapped. However, when the reference is the genome, spliced aligners should be employed because they allow a spliced-read placement and make possible the filling of a wide range of gaps. This approach facilitates the identification of novel transcripts generated by AS (Yang & Kim, 2015). Transcriptome reconstruction is based on two strategies *e.g.* the reference-guided approach and the reference-independent approach. Reference-guided approach is advantageous when reference annotation information is complete and thorough. However, when a reference genome is not available or its annotation is deficient, RNA-Seq reads can be assembled *de novo* by building consensus transcripts from short reads with bioinformatic packages such as Trinity (Haas et al., 2013).

The most common application of RNA-Seq is to estimate gene and transcript expression levels. This application is primarily based on inferring the number of reads that map to each transcript sequence. The simplest approach to quantification is to aggregate raw counts of mapped gene reads by using programs such as HTSeq-count (Anders et al., 2014) or FeatureCounts (Liao et al., 2014). Algorithms that quantify expression from transcriptome mappings include RSEM (Li & Dewey, 2011), Cufflinks (Trapnell et al., 2012), Sailfish (Patro et al., 2014) and Kallisto (Bray et al., 2016). Sequencing depths and/or library sizes may diverge across samples (implying that the observed counts are not directly comparable between samples). Complex normalization schemes have been proposed and are used by different softwares for quantification of transcripts, such as total counts (Vêncio et al., 2004); trimmed mean of M-values - TMM (Robinson et al., 2010), counts normalization (Anders & Huber, 2010) and quantile normalization - Reads Per Kilobase Million (RPKM) (Mortazavi et al., 2008). Differential expression analysis takes

as input normalized read count data and performs statistical analysis to detect differences in the expression of loci across different treatments or conditions (Conesa et al., 2016). An extensive number of software packages and pipelines have been developed with such purpose (Table 1.5). In the methods explicitly developed for the analysis of differential expression based on count data, the Poisson [employed by DEGseq2 - Love et al. (2014)] and the Negative Binomial [adopted by edgeR - Robinson et al. (2010) and DESeq - Anders & Huber (2010)] distributions are the two most commonly used approaches to model RNA-Seq data. Alternatively, user-friendly tools such as CLC Bio (http://www.clcbio.com; CLC inc, Aarhus, Denmark), Galaxy (Blankenberg et al., 2010; http://g2.bx.psu.edu), GeneSpring (http://genespring-support.com/; Silicon Genetics, Redwood, CA), BaseSpace Apps (https:// basespace.illumina.com/home/index***;*** Illumina Inc., CA, USA) and Partek (http://www.partek.com; Partek Inc, St Louis, MO, USA) can be employed to carry out all the analysis detailed above in a single dedicated platform.

There is not a broad consensus on how to approach an optimal study design in order to ensure the validity of the results in terms of reproducibility, accuracy, and robustness. Zhang et al. (2014) and Schurch et al. (2016) affirmed that each method has its own particular strengths and pitfalls making them suitable for specific RNA-Seq datasets. Therefore, a crucial prerequisite for a successful RNA-Seq study is a good experimental design and the selection of an appropriate bioinformatic pipeline. Other important decisions are the choice of library sizes, sequencing depth and the number of replicates under study. Moreover, it is also very important to take into account the heterogeneity of the samples in order to eliminate potential biases.

The last step in a standard transcriptomics study is the characterization of the molecular functions or metabolic pathways in which differentially expressed (DE) genes are involved. A commonly used approach includes Gene Ontology (GO) and pathways enrichment analysis with the aim of determining if DE genes are associated with a certain biological process or molecular function. Popular softwares for gene set enrichment and metabolic pathway analysis are Panther, DAVID, STRING, Cytoscape and Reactome among others (Table 1.5). However, very little functional information is available for ncRNAs such as lncRNAs or miRNAs (Conesa et al., 2016). In some cases, functional annotation of predicted unknown genes and transcripts can be done by assessing their sequence similarity across orthologs, *e.g.* using approaches based on BLAST, with a success rate of 50-80% (Conesa et al., 2016).

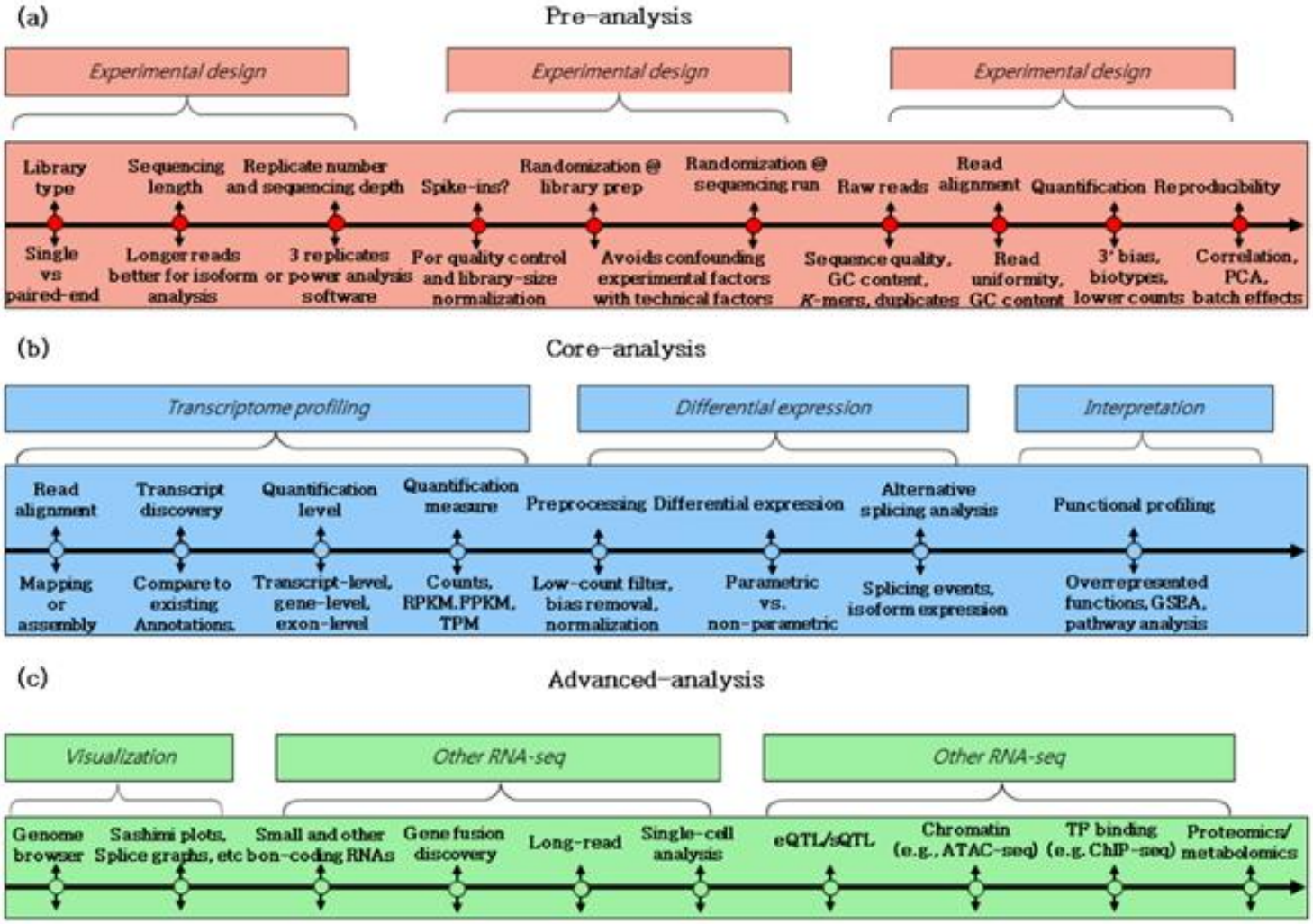

Figure 1.8 - Typical workflow for RNA sequencing (RNA-Seq) data analysis (Conesa et al., 2016)**.**

Table 1.5 - Summary of selected bioinformatics tools for NGS data processing.

Workflow	Package	Reference
Quality control and read processing	FastQC, Qualimap 2, HTSeq	Andrews (2010), García-Alcalde et al. (2012), Anders et al. (2014)
Read alignment	Bowtie, BWA, SOAP, Tophat2, STAR	Down et al. (2008), Li et al. (2008), Li & Durbin (2009), Kim et al. (2013), Dobin et al. (2013)
Transcriptome reconstruction	Cufflinks, Trinity	Trapnell et al. (2010), Grabherr et al. (2011)
Expression quantification	ALEXA-seq, Cufflinks, RSEM, FeatureCounts, HTSeq-count, Sailfish, Kallisto.	Griffith et al. (2010), Trapnell et al. (2010), Li & Dewey (2011), Liao et al. (2014), Anders et al. (2014), Patro et al. (2015), Bray et al. (2016)
Differential expression	Limma, EdgeR, RSEM, Cuffdiff, DESeq2, Sailfish, NOIseq	Smyth (2004), Robinson et al. (2010), Li & Dewey (2011), Trapnell et al. (2012), Love et al. (2014), Patro et al. (2014), Tarazona et al. (2015)
Genomic variants	Samtools mpileup, SOAPsnp, Comrad, FusionHunter, GATK	Li et al. (2009b), Li et al. (2009a), DePristo et al. (2011), Li et al., 2011), McPherson et al. (2011)
Gene function and interaction	Cytoscape, KEGG, DAVID, GOSeq, STRING	Shannon et al. (2003), Kanehisa & Goto (2000), Huang et al. (2007), Young et al. (2010), Szklarczyk et al. (2015)

1.5 Transcriptomic studies in pigs

The characterization of the pig transcriptome is an essential step towards identifying the functional elements of the porcine genome and understanding the genetic architecture of complex traits such as fat deposition, metabolism, and growth. So far, the functional annotation of the pig genome is quite poor, particularly for lncRNAs displaying a limited evolutionary conservation. High-throughput techniques, such as cDNA, oligo-based arrays or RNA-Seq approaches, represent valuable tools to study the transcriptome and its regulatory mechanisms. Numerous cDNA-microarray (revised by Pena et al., 2014) and RNA-Seq studies aiming to characterize the expression of key tissues (*e.g.* liver, fat and skeletal muscle) in pigs with divergent phenotypes or subject to different experimental conditions have been reported. Published RNA-Seq experiments investigating gene expression in the porcine skeletal muscle are shown in Table 1.6.

Differences in gene expression across different muscles

Ayuso et al. (2016) investigated the differences in gene expression in two distinct skeletal muscles (*longissimus dors*i and *biceps femoris*). *Biceps femoris* has a higher PUFA content than the *longissimus dors*i muscle, and the set of DE genes showed an enrichment of pathways related with adipocyte differentiation and lipid metabolism (LXR/RXR activation, FXR/RXR activation, and biosynthesis of retinoids). These results suggest a more active lipid metabolism in *biceps femoris* than in *longissimus dors*i. In contrast, growth and proliferative processes were more prevalent in genes overexpressed in *longissimus dors*i, with an enrichment of biological functions related to cell proliferation and body size. Zhu et al. (2016) compared differences in the transcriptome between *extensor digitorum longus* (white fiber) and *soleus* (red fiber) muscles of Large White pigs and identified a large number of DE genes and pathways implicated in muscle fiber type determination. Myofibril was the most significant gene ontology term in the muscle fiber type determination process. Moreover, several collagen encoding genes (*COL12A1*, *COL11A2*, *COL11A1*, and *COL13A1*) display a higher expression in the *soleus* muscle suggesting differences in collagen composition between different types of myofibers.

Table 1.6 - Published RNA-Seq experiments interrogating pig muscle phenotypes or subject to different experimental conditions.

Breed/phenotype of comparison	Replicates	Thresholds of significance	Number of DEGs*	Reference
Differences in gene expression across tissues				
*Longissimus dors*i and *Biceps femoris*	24	p < 0.01 and FC > 1.5	135	Ayuso et al. (2016)
Extensor digitorum longus and *soleus*	3	FDR < 0.001 and FC > 2	561	Zhu et al. (2016)
Differences in gene expression amongst porcine breeds				
Indigenous Chinese pig and introduced pig breeds	8	p < 0.05 and FC > 2	315	Wang et al. (2015)
Purebred and Duroc-crossbred Iberian pigs	9-10	p < 0.01 and FC > 1. 5	149	Ayuso et al. (2015)
Jeju native pig and Berkshire piglets	5	FDR < 0.001 and FC > 2	56	Ghosh et al. (2015)
Differences in gene expression amongst pigs with highly divergent phenotypes				
Intramuscular fat content and composition	6	p < 0.01 and FC > 1.2	131	Puig-Oliveras et al. (2014)
Postweaning growth rates	9	p < 0.01	768	Pilcher et al. (2015)
Drip loss	2 (pool)	FDR < 0.005 and FC > 2	150	Li et al. (2016a)
Developmental stage				
Eleven developmental stages in Tongcheng and Yorkshire pigs.	~35	FC > 2 and prob >0.7	8,289	Zhao et al. (2015)
Birth and growth	5-6	p < 0.01 and FC > 1.5	5.812	Ayuso et al. (2016)
Four developmental stages in Laiwu pigs	3	FDR < 0.01 and FC > 4	-	Wang et al. (2017)
Diet induced differences in gene expression				
Fed with a supplemented diet	2 (pool)	FDR < 0.001 and FC > 2	749	Ogłuszka et al. (2017)
Expression of mRNA isoforms				
Global view of porcine transcriptome	2	-	-	Chen et al. (2011)
Biceps femoris and *Soleus*.	3	-	-	Li et al. (2016b)
Expression of non-coding RNA				
Domesticated pigs and wild boars	93	FDR < 0,01	30	Zhou et al. (2014)
Global view of porcine transcriptome	2	-	-	Chen et al. (2011)
Indigenous Chinese pig and introduced pig breeds	8	p < 0.05 and FC > 2	30	Wang et al. (2015b)
Four developmental stages	6	p < 0.01 and FC > 1.2	8	Wang et al. (2017a)

***DEGs** = differentially expressed genes; **FDR** = false discovery rate; **FC** = fold-change

Differences in gene expression amongst porcine breeds

When comparing the muscle expression profiles of Chinese pigs *vs* introduced (European) swine, Wang et al. (2015b) identified 315 DE genes. The ryanodine receptor 3 (*RYR3*) and mannose receptor C type 2 (*MRC2*) genes were 30-fold overexpressed in Chinese breeds when compared with the European ones, a finding that is relevant because these two genes have important roles in muscle growth. Moreover, several genes related to lipid deposition (*e.g. ESR1, SCD, FASN,* and *LDLR*) were overexpressed in Chinese pigs explaining their increased fatness. In another study, Ayuso et al. (2015) investigated gene expression differences between Iberian purebred and Duroc x Iberian crossbred pigs. They detected 149 DE genes and demonstrated an enrichment of genes involved in cellular and muscle growth in lean Duroc x Iberian crossbred pigs in contrast with Iberian purebred pigs. Genes overexpressed in Iberian purebred pigs showed an enrichment of functions and pathways related to lipid and glucose metabolism in accordance with the greater adipose accretion of this breed. Ghosh et al. (2015) carried out a study to investigate DE genes between Jeju native pigs (better taste, tenderness and marbling quality than from Western breeds) and Berkshire swine (better growth rate and meat palatability traits than do Jeju pigs). In doing so, they observed that 65% of genes in muscle had a higher expression in Jeju than in Berkshire pigs. However, an upregulation of DE genes related with body growth and skeletal system development (*COL21A1, COL2A1,* and *POSTN*) and immunity (*IL7R, CRP,* and *CD*) was detected in the Berkshire breed.

Differences in gene expression amongst pigs with divergent phenotypes

Puig-Oliveras et al. (2014) compared the muscle expression profile of sows from an Iberian x Landrace backcross displaying extreme phenotypes for fatty acid composition and found 131 DE genes, and an enrichment of genes related with lipid metabolism. Puig-Oliveras et al. (2014) proposed that a high intramuscular PUFA content may influence FA metabolism and glucose uptake resulting in an inhibition of the lipogenesis and in the increase of the rate of FA oxidation. This interpretation agrees well with previous microarray studies (Cánovas et al., 2010; Corominas et al., 2013; Pena et al., 2013) suggesting that a higher PUFA content would enhance fatty acid oxidation and decrease the intracellular accumulation of triglycerides through the establishment of a cycle where triacylglycerols are synthesized and degraded continuously. In another study, Pilcher et al.

(2015) characterized gene expression in the skeletal muscle to investigate the metabolic basis of poor weaned-pig transition. The group of DE genes with decreased expression in the *longissimus dorsi* muscle of pigs with a poor transition was enriched in loci with functions related to muscle contraction, glucose metabolism, cytoskeleton organization, muscle development, and response to hormone stimulus, while genes related with protein catabolism displayed an increased expression. Li et al. (2016a) used a commercial pig population to perform a transcriptional study contrasting animals with high and low drip loss values. Drip loss is defined as weight loss (mainly consisting of water and proteins) of a fresh meat under gravity at 0–4 °C for 24 h and it has a low heritability (van Wijk et al., 2005). This comparative analysis of gene expression levels made possible to detect 150 DE genes in the High group relative to the Low group. The authors also reported that the *TRDN* gene, which is involved in muscle contraction and fat deposition, and the *MSTN* gene, which has a role in muscle growth, can be critical candidate genes responsible for drip loss.

Developmental stage

Zhao et al. (2015a) analyzed the muscle transcriptome profiles across 11 developmental stages for Yorkshire and Tongcheng pigs. Yorkshire pigs are characterized by fast growth, low backfat and a high lean meat percentage. Several genes with a key position in the muscle regulatory networks were overexpressed in the Yorkshire pigs, *e.g. SGCD*, *ENG*, *THBD*, *AQP*, and *BTG2*, whereas *CXCL10*, *EIF2B5*, *PSMA6*, *FBXO32*, and *LOC100622249* were overexpressed in the Tongcheng breed. These genes showed breed-specific and development-dependent differential expression patterns. Ayuso et al. (2016), analyzed ten litters at birth and 12 at growing stage and observed more than 5,800 DE genes between the two ages under comparison. Several genes overexpressed in newborn piglets were involved in the synthesis of cholesterol, triglycerides and other metabolites (*e.g. ELOVL1*, *LSS* and *NSDHL*). In growing pigs, an overexpression of genes associated with the immune response and related to catabolic processes (*e.g. PGK1*, *GAPDH*, *PFKM*, and *ME1*) was reported. Wang et al. (2017a) analyzed the evolution of IMF content in four developmental stages in the porcine *longissimus dorsi* muscle. They found three temporal expression profiles correlated with IMF variation, *i.e.* 15 DE genes with known functions in lipid metabolism (*e.g. ACACA*, *SCD*, *ACLY*, *ELOVL1* and *FAS)*, 4 DE genes encoding

desaturases (*SCD*, *FADS1*, *FADS2*, and *FADS3*) and 6 DE genes involved in the steroid biosynthesis pathway (*CYP51*, *DHCR24*, *EBP*, *HSD17B7*, *SOAT1*, and *SQLE*) .

Diet induced differences in gene expression

Next-generation sequencing was used by Ogłuszka et al. (2017) to compare animals subjected to either a control diet or a diet supplemented with linseed and rapeseed oil to increase polyunsaturated fatty acid content. In the group of pigs supplemented with omega-3 and omega-6 fatty acids, the expression of 219 and 530 genes was upregulated and downregulated, respectively. In the light of these results, the authors proposed a role of fatty acids in the regulation of the expression of genes which are essential for muscle tissue development and functioning. Interestingly, the identified genes were important for diverse biological processes related to the inflammatory response, signaling, lipid metabolism, and homeostasis.

Expression of mRNA isoforms

Chen et al. (2011) used RNA-Seq to generate a high-resolution map of the porcine mRNA and miRNA transcriptome in liver, *longissimus dorsi* and abdominal fat from White Duroc × Erhualian pigs with divergent phenotypes for growth and fat deposition. They found that about 18.8% of the annotated genes showed AS isoforms, and alternative 3' splicing was the most common type of AS events in pigs. In addition, they demonstrated that the majority of AS events showed a clear pattern of tissue specificity. These results highlighted the importance of AS in tissue-specific programs of gene expression and its major role in expanding functional complexity. Interestingly, the *RYR1* gene presented the largest number of *longissimus dorsi*-specific AS events. According to Li et al., (2016b), exon skipping was the most common AS event and, accounted for more than 85% of all AS events in *biceps femoris* and *soleus muscle*. These results suggest that the frequencies of AS type events may vary across and even within tissues.

Reyer et al. (2013) explored the structural diversity of the *NR3C1* gene in pigs. This gene encodes the glucocorticoid receptor, and showed the highest proportion of transcripts containing the predominant exon 1C variant and only minor variability in the usage of other alternative first exons in tissues related to metabolism (skeletal muscle and fat), suggesting a major role of the promoter region of exon 1C in driving constitutive

expression and, at the same time, limited plasticity in the regulation of *NR3C1* in metabolic tissues. In another study, five different isoforms of the glycogen synthase kinase 3 (*GSK3β*) gene were identified in different porcine tissues (Wang et al., 2012). Interestingly, the *GSK3β* isoforms have different effects on glycogen synthase activity. In this way, an overexpression of *GSK3b1, GSK3b2,* and *GSK3b3* isoforms, but not *GSK3b5*, decreased significantly glycogen synthase enzyme activity in PK-15 cells (Wang et al., 2012). These results suggest that different *GSK3β* isoforms may have different roles in the *insulin signaling* pathway in pigs. Ma et al. (2014) described a mutation in a splice acceptor site of intron 9 (g.8283C>A) of the porcine phosphorylase kinase catalytic subunit gamma 1 (*PHKG1)* gene that drives the synthesis of an aberrant transcript subjected to nonsense-mediated decay. This polymorphism has causal effects on glycogen content and meat quality.

Expression of non-coding RNAs

Currently, there are 3,250 annotated porcine ncRNAs in the Ensembl database (http://www.ensembl.org/Sus_scrofa/Info/Annotation; *Sscrofa* v.11.1). The MiRBase database (http://www.mirbase.org) contains 382 miRNA precursor genes that are processed into 411 mature miRNA sequences. Very likely, the catalog of non-coding RNAs in pigs is much larger. Anthon et al. (2014) annotated 3,183 high confidence ncRNAs mapping to the pig genome. Zhou et al. (2014) identified 6,621 lincRNA transcripts from 4,515 genes loci using RNA-Seq data from 93 samples. The domestic-animal lncRNA database (ALDB - Li et al., 2015) currently comprises 12,103 pig lincRNAs. In contrast, the NONCODE database recently made available the information of 17,811 lncRNA genes encoding 29,585 lncRNA transcripts compiled from many different sources (Noncode database; http://www.bioinfo.org/NONCODE2016). Despite these advances, there is a pressing need to improve the genomic annotation of non-coding RNAs. Indeed, in human and mouse 90,062 and 79,940 ncRNAs have been annotated so far, respectively.

Non-coding RNAs carry out a broad variety of biological functions, regulating gene expression at the levels of transcription, RNA processing, and translation (Cech & Steitz, 2014). In consequence, they may play a fundamental role in the metabolism of the porcine skeletal muscle. However, only a few studies have catalogued and investigated muscle

ncRNAs in pigs. Zhou et al. (2014) compared the expression profile of lincRNAs in domesticated pigs and wild boars and found 30 lincRNAs that showed a differential expression between groups. *Linc-sscg2561* displayed 1.4-fold higher expression in domesticated pigs compared with wild boars. Adjacent to this lincRNA, there is the *DNMT3A* gene which displayed a 1.4-fold higher expression in the domesticated pig. The *DNMT3A* gene is a DNA methyltransferase which regulates behavioral plasticity to emotional stimuli (LaPlant et al., 2010). Thus, together *DNMT3A* and *Linc-sscg2561* could contribute to changes in behavior during the domestication of the pig (Zhou et al. 2014).

With regard to miRNAs, Chen et al. (2011) detected increased levels of *miR-1/206* in the porcine muscle *vs* liver. Myostatin gene is a target-gene to *miR-1/206* and can present a mutation that creates an illegitimate binding site for this miRNA leading to efficient translational inhibition of the myostatin gene and an increase in muscularity in Texel sheep (Clop et al., 2006). Wang et al. (2015b) also compared miRNA sequences from *longissimus dorsi* muscle of the two indigenous Chinese pig breeds and two introduced pig breeds. They found 20 upregulated (*e.g. ssc-miR-145-5p, -339* and *133a-5p*) and 10 downregulated (*e.g. ssc-let-7c, ssc-miR-122* and *-4332*) miRNAs in the fat Chinese pig breeds. Through a miRNA target gene prediction and functional analysis, these authors anticipated that these miRNAs might target 2,393 genes, which are mainly involved in pathways associated with lipogenesis, metabolism, and adipocyte lineage commitment (*e.g. insulin- signaling, mitogen-activated protein kinase 1 signaling* and *GnRH signaling* pathways). Recently, Wang et al., (2017a) explored the relationship between the miRNA profile and the development of porcine muscle and adipose tissue. They found 17 core miRNAs that were differentially expressed in adipose tissue *vs* skeletal muscle at three development stages (30, 90, 240 days-old pigs). Amongst them, *ssc-miR-128* and *-133a-5p* and *-489* are muscle-related miRNAs differentially expressed at all four stages and they may have a major role in regulating the muscle differentiation and development of pigs.

Epigenetic differences

Schachtschneider et al. (2015) produced DNA methylome maps and gene transcription profiles of eight tissues, including muscle tissue, from one adult Duroc female. Analysis of over 500,000 CpG sites demonstrated patterns similar to those observed in humans, including a reduction of CpG and an increase of TpG density at transcription start sites of

lowly expressed genes, suggesting that DNA methylation can play a significant role in adaptive evolution by modulating gene expression. CpG methylation levels (defined as the ratio of methylated reads/total reads at a given site) were similar across tissues, with an average of 41.39% (Schachtschneider et al., 2015). Skeletal muscle presents a lower methylation level than other tissues (39.52 %, Schachtschneider et al., 2015). Choi et al. (2015) performed a correlation analysis between the levels of gene expression and tissue-specific differentially methylated CpG sites in diverse pig tissues. In the muscle, 18 tissue-specific differentially methylated CpG sites were associated with 11 genes which promote muscle development. As expected, a negative correlation between gene expression and methylation was observed. Li et al. (2012) analyzed the genome-wide DNA methylation levels of three porcine breeds (Landrace, Rongchang, and Tibetan) which display different obesity and muscle-related phenotypes and two different muscles were analyzed (*longissimus dorsi* and red *psoas* major muscles). A total of 2,510 and 218,623 regions in the genome showed changes in their methylation rate across muscle types and breeds, respectively. Several of these differentially methylated regions (223) comprised genes orthologous to known human obesity-related loci, thus suggesting that changes in the methylation rates can be associated with fatness phenotypes in pigs. Zhou et al. (2015b) analyzed the same dataset used by Li et al. (2012) with the aim of characterizing the DNA methylation patterns of lincRNA genes in adipose and muscle tissues in pigs. They showed that 13.2% and 6.8% of differentially methylated regions overlap with lincRNA genes when comparing muscle types and breeds, respectively.

Objectives

Chapter 2

This Ph.D. thesis was done under the framework of the project *Study of traits related to pigs lipid metabolism and pork quality by means of integral analyses of high density genotyping and gene expression data* (grant number: AGL2010-22208-C02-02) and *Genomic physiology of intramuscular fat storage in pigs* (grant number: AGL2013-48742-C2-1-R) awarded by the Spanish Ministry of Economy, Industry and Competitiveness. The main goal of these projects is to analyze the genetic basis of fatness in pigs by using next-generation sequencing and high throughput genotyping approaches. More specifically, the objectives of the Thesis are:

- To identify differentially expressed mRNA genes (and their isoforms) and non-coding RNA genes in the skeletal muscle of pigs with distinct fatness profiles and to ascertain their potential roles on fat deposition (Chapters 1 and 2).
- To investigate the effects of food ingestion on the mRNA expression patterns of the porcine muscle (Chapter 3) and to evaluate how food intake modulates the expression of eight circadian genes in five porcine tissues (Chapter 4).

In the framework of a collaborative study with the Research Institute for Animal Breeding and Nutrition (Hungary) and the University of Cluj-Napoca (Romania), the following objective was undertaken in the Thesis:

- To identify the genetic factors involved in the segregation of blond *vs* red pigmentation patterns in Mangalitza pigs (Chapter 5).

Papers and Studies

Chapter 3

RNA-Seq based detection of differentially expressed genes in the skeletal muscle of Duroc pigs with distinct lipid profiles

T. F. Cardoso,[1,2] A. Cánovas,[1] O. Canela-Xandri,[3] R. González-Prendes,[1] M. Amills,[a,1,4] and R. Quintanilla[a,3]

[1]Department of Animal Genetics, Center for Research in Agricultural Genomics (CSIC-IRTA-UAB-UB), Universitat Autònoma de Barcelona, Bellaterra, 08193, Spain [2]CAPES Foundation, Ministry of Education of Brazil, Brasilia D. F., Zip Code 70.040-020, Brazil. [3]Animal Breeding and Genetics Program, Institute for Research and Technology in Food and Agriculture (IRTA), Torre Marimon, Caldes de Montbui 08140, Spain [4]Departament de Ciència Animal i dels Aliments, Universitat Autònoma de Barcelona, Bellaterra, 08193, Spain

[a]Corresponding authors: R. Quintanilla and M. Amills

Sci Rep. 2017; 7: 40005.

Published 2017 Feb 14. doi: 10.1038/srep40005

Abstract

We have used a RNA-Seq approach to investigate differential expression in the skeletal muscle of swine (N = 52) with divergent lipid profiles *i.e.* HIGH (increased intramuscular fat and muscle saturated and monounsaturated fatty acid contents, higher serum lipid concentrations and fatness) and LOW pigs (leaner and with an increased muscle polyunsaturated fatty acid content). The number of mRNAs and non-coding RNAs (ncRNAs) expressed in the porcine *gluteus medius* muscle were 18,104 and 1,558, respectively. At the nominal level of significance (P-value ≤ 0.05), we detected 1,430 mRNA and 12 non-coding RNA (ncRNA) transcripts as differentially expressed (DE) in the *gluteus medius* muscle of HIGH *vs* LOW pigs. This smaller contribution of ncRNAs to differential expression may have biological and technical reasons. We performed a second analysis, that was more stringent (P-value $\leq 0.01$and fold-change ≥ 1.5), and only 96 and 0 mRNA-and ncRNA-encoding genes happened to be DE, respectively. The subset of DE mRNA genes was enriched in pathways related with lipid (lipogenesis and triacylglycerol degradation) and glucose metabolism. Moreover, HIGH pigs showed a more lipogenic profile than their LOW counterparts.

Introduction

Several RNA-Seq studies have been carried out on different pig breeds in order to identify genes involved in fat deposition and meat quality[1,2]. Besides analysing gene expression differences, these studies aimed to dissect the complex networks of pathways and genes that determine porcine phenotypes of economic interest. In this way, the expression patterns of porcine liver, *longissimus dorsi* and abdominal fat were examined in two full-sib hybrid pigs with extreme phenotypes for growth and fatness traits[3]. The proportion of tissue-specific mRNA transcripts happened to be quite modest (<10%) and several microRNAs (miRNAs) were differentially expressed (DE) across tissues. Other studies analysing differential gene expression in muscle, fat and liver tissues of Iberian x Landrace pigs with extreme phenotypes for muscle fatty acid (FA) composition revealed that DE loci are inte-grated in common pathways related with LXR/RXR activation, peroxisome proliferator-activated receptors (PPARs) and β-oxidation[1,4,5]. A recent analysis comparing Iberian and Iberian x Duroc pigs also identified LXR/ RXR activation and

cholesterol synthesis as enriched pathways in the set of DE genes[2]. In contrast, the potential role of ncRNAs in muscle fat deposition has been scarcely studied in pigs[4,6].

In a previous experiment, we demonstrated that genes involved in FA uptake, lipogenesis, triacylglycerol syn-thesis, lipolysis and insulin signalling are DE in the skeletal muscle of Duroc pigs with divergent lipid phenotypes[7]. One drawback of this study was that gene expression was measured with microarrays, which have a limited dynamic range, sensitivity (specially for low-abundance transcripts) and specificity. Moreover, the expression of non-coding RNAs could not be measured with Affymetrix porcine microarrays. In the current work, we aimed to circumvent all these limitations by analysing, through a RNA-Seq approach, the muscle transcriptome of a subset of these Duroc pigs. Our goal was to determine the relative contributions of protein-coding and non-coding RNAs to differential expression in the skeletal muscle of pigs with distinct lipid profiles.

Results

The RNA-Seq experiment allowed us generating an average of 133 million paired-end reads per sample and 72.8% of them were successfully mapped to the pig *Sscrofa10.2* genome assembly. The percentages of exonic and intronic reads were 91.4% and 8.6%, respectively. After quality control analysis, four samples were discarded. Thereby, we used a final dataset of 26 animals per group (HIGH and LOW) to identify DE genes.

Differential expression of mRNA encoding genes.

A total of 1,430 mRNA genes happened to be DE when considering exclusively a significance threshold of *P*-value $\leq$ 0.05 (Supplementary Table S1). Only 76 of these 1,430 mRNA-encoding genes were identified as DE by Cánovas *et al.*[7] when they compared the gene expression of HIGH and LOW pigs retrieved from the same population employed by us (Supplementary Figure 1, Supplementary Table S2). When we performed a more stringent analysis (*P*-value $\leq$0.01 and fold-change $\geq$1.5), 96 genes were DE (Supplementary Table S3). Moreover, twenty-one genes remained significant after correction for multiple testing (*q*-value $\leq$0.05 and fold-change $\geq$1.5) as shown in Table 1.

Table 1 - List of the most significant differentially expressed genes in HIGH and LOW pigs after correcting for multiple testing (*q*-value ≤ 0.05 and fold-change ≥ 1.5). A negative FC means that the affected gene is overexpressed in LOW pigs.

Ensembl ID	Gene name	Fold-change	*P*-value	*q*-value
ENSSSCG00000005648	*SLC27A4*	1.66	1.32E-06	4.28E-03
ENSSSCG00000027946	*MVP*	1.78	2.63E-06	5.97E-03
ENSSSCG00000017232	*SLC9A3R1*	1.72	1.26E-05	1.36E-02
ENSSSCG00000005935	*AGO2*	1.59	1.77E-05	1.43E-02
ENSSSCG00000003379	*KLHL21*	1.79	1.61E-05	1.43E-02
ENSSSCG00000011740	*SERPINI1*	−1.81	2.48E-05	1.72E-02
ENSSSCG00000001931	*GRAMD2*	−1.58	2.74E-05	1.76E-02
ENSSSCG00000011444	*NT5DC2*	1.54	3.26E-05	1.76E-02
ENSSSCG00000007574	*SDK1*	1.58	2.97E-05	1.76E-02
ENSSSCG00000007745	*SUMF2*	−1.54	4.21E-05	1.95E-02
ENSSSCG00000000293	*ITGA5*	1.72	4.46E-05	1.96E-02
ENSSSCG00000007133	*ACSS1*	1.51	5.18E-05	2.09E-02
ENSSSCG00000028814	*SOD3*	1.97	5.37E-05	2.09E-02
ENSSSCG00000006277	*SPIDR*	2.04	5.90E-05	2.19E-02
ENSSSCG00000007554	*ZFAND2A*	2.54	1.01E-04	2.88E-02
ENSSSCG00000003105	*SLC1A5*	1.67	1.17E-04	3.07E-02
ENSSSCG00000010529	*SFRP5*	2.03	1.31E-04	3.11E-02
ENSSSCG00000006245	*SDR16C5*	3.02	1.36E-04	3.15E-02
ENSSSCG00000013579	*CD209*	1.95	1.50E-04	3.31E-02
ENSSSCG00000008232	*RNF181*	−2.09	2.05E-04	3.57E-02
ENSSSCG00000030165	*MAFF*	1.67	2.22E-04	3.72E-02

We used the IPA package (QIAGEN Redwood City, www.qiagen.com/ingenuity) to identify pathways to which DE genes belong to as well as to explore the existence of signalling networks connecting DE genes. Forty four pathways were significantly enriched in the dataset of 96 DE genes (Supplementary Table S4). This information should be interpreted with caution because, in general, pathways were represented by a small number of genes and statistical significance was not very high. Amongst the enriched pathways, it is worth to mention TR/RXR activation, synthesis of palmitate and stearate, FA biosynthesis, triacylglycerol degradation, and the conversion of acetate into acetyl-CoA (Table 2, Supplementary Table S4). A complementary analysis with the ReactomeFIViz app[8] revealed 50 significant pathways (Supplementary Table S5). Differentially expressed mRNA genes were also grouped in gene regulatory networks with the IPA software. As shown in Supplementary Table S6, we found eleven regulatory networks related with a variety of functions, and the top-scoring one was that of *Cardiovascular Disease, Cardiovascular System Development and Function, Organismal Injury and Abnormalities* (Fig. 1 and Supplementary Table S6).

The Regulator Effects tool of the IPA package was employed to identify potential transcriptional regulators that may explain the differential patterns of expression observed between HIGH and LOW pigs (Fig. 2). By doing so, two main transcriptional regulators were identified *i.e.* peroxisome proliferator-activated receptor γ (PPARG) and platelet-derived growth factor BB (PDGFB). In the network shown in Fig. 2, these genes appear to be involved in an heterogeneous array of biological functions related with the quantity of carbohydrate, insulin sensitivity, necrosis of prostate cancer cell lines and apoptosis of lymphocytes. Indeed, the *PPARG* gene (*P*-value = 0.02 and FC = 1.36) is depicted as a key regulator of genes related with carbohydrate metabolism (*CEBPA, CES1, CIDEC*) and the inhibition of insulin sensitivity (*CES1, CIDEC, FASN*).

Table 2 - IPA-based pathway analysis of the list of genes that are differentially expressed in HIGH and LOW pigs (*P*-value ≤ 0.01 and fold-change ≥ 1.5). Ratio: number of DE genes in a pathway divided by the number of genes comprised in the same pathway**.**

Ingenuity Canonical Pathways	−log(p-value)	Ratio	Nodes
Acute Myeloid Leukemia Signaling	3.22	4/91	*CEBPA, FLT3, RUNX1, STAT3*
Hematopoiesis from Pluripotent Stem Cells	2.98	3/47	*CD3E, CD8E, CSF1*
Primary Immunodeficiency Signaling	2.96	3/48	*CD3E, CD8E, ZAP70*
Hepatic Fibrosis/Hepatic Stellate Cell Activation	2.12	4/183	*CCR5, CSF1, IGFBP4, TIMP1*
TR/RXR Activation	2.08	3/98	*BCL3, FASN, SYT2*
Palmitate Biosynthesis I (Animals)	2.07	1/2	*FASN*
Fatty Acid Biosynthesis Initiation II	2.07	1/2	*FASN*
CTLA4 Signaling in Cytotoxic T Lymphocytes	2.07	3/99	*CD3E, CD8A, ZAP70*
Retinoate Biosynthesis I	2.04	2/34	*RDH5, SDR16C5*
Stearate Biosynthesis I (Animals)	2.02	2/35	*FASN, SLC27A4*

Differential expression of non-coding RNAs.

We identified 1,558 ncRNA transcripts expressed in the pig *gluteus medius* muscle, with sizes between 53 and 9,032 bp (Supplementary Table S7). Amongst these, 1,354 and 204 transcripts were classified as small (sncRNA) and long (lncRNA) non-coding RNAs, respectively. It is important to emphasize that the annotation of porcine ncRNAs is still very preliminar and it should be taken with caution. In general, sncRNA had orthologous sequences in other mammalian species, while lncRNAs were much less conserved (Table 3). We only detected 12 ncRNAs (11 lncRNAs and 1 sncRNA) that were DE at the

nominal level (*P*- value ≤ 0.05), while none of these ncRNAs remained significant after correction for multiple testing (in all cases the *q*-value was non-significant, Table 4).

In addition, we identified 25 mRNA-encoding genes that mapped near (30 kb or less) to the subset of DE ncRNA loci (Table 5). This observation may have biological implications because ncRNAs often *cis*-regulate the expression of genes located in their vicinity. Within this list of neighbouring genes (Table 5), *CU468594.8* (*P*-value =0.003 and FC =1.26) and *MT-ND6* (*P*-value =0.038 and FC =−1.21) mRNAs are DE in HIGH *vs* LOW pigs (*P*-value < 0.05 and 1.2-fold change in expression).

Discussion

Divergent muscle mRNA expression profiles in pigs with extreme phenotypes for fatness traits.

After correcting for multiple testing, twenty-one genes, displaying a wide array of functional roles, showed a significant DE between HIGH and LOW pigs (Table 1). For instance, *SLC27A4* is involved in the translocation of long-chain fatty acids across the plasma membrane[9] while *SFRP5* plays a role in anti-inflammatory and insulin-sensitizing processes[10] and *AGO2* and *MVP* contribute to RNA interference[11] and signal transduction and transport[12], respectively. Two of the genes listed in Table 1 might be related with meat quality *i.e. RNF181*, which encodes a E3 ubiquitin-protein ligase that participates in the degradation of muscle proteins through the ubiquitin-proteasome system[13], and *SDK1*, which has been associated with intramuscular fat (IMF) content in Large White pigs[14].

The Spearman correlation between the microarray data reported by Canovas *et al.*[7] in 68 HIGH and LOW pigs and RNA-seq data generated in the current study (N = 52) was 0.54. This value is comparable to what has been published in previous studies analysing gene expression in human brain cells (r = 0.61–0.67)[15] and proliferating *vs* quiescent fibroblasts (r =0.18–0.42)[16]. We also compared our dataset of DE genes with those detected by Canovas *et al.*[7]. As shown in Suppl Figure 1 the level of concordance was quite low (only 76 genes were simultaneously identified by both platforms). A modest overlap between microarray and RNA-Seq data has been reported in previous studies. For instance, Trost *et al.*[16] analysed the concordance between both types of data in fibroblasts cultured at two different developmental stages, and they just found an overlap of around 25% in the

two lists of DE genes. This value is higher than the one reported by us, but it is important to highlight that the analysis of Trost *et al.* [16] was based on a set of probes common to both platforms. Moreover, the microarray analysis performed by Canovas *et al.*[7] was based on a dataset of around 68 pigs, while we used a subset of 52 individuals in our RNA-Seq analysis. Trost *et al.*[16] used quantitative real-time PCR as a third approach to validate microarray and RNA-Seq data and they found that RNA-Seq outperforms the microarray technology. However, differences between both methods are not dramatic *i.e.* the Spearman correlations between microarray and RNA-Seq data *vs* qPCR validation results were 0.44 and 0.56, respectively. This means that both technologies detect different sets of DE expressed genes and, in consequence, they are complementary[17]. According to Wang *et al.* [18], the magnitude of the treatment effect has a strong impact on the level of concordance between microarray and RNA-Seq platforms *i.e.* large discrepancies can be anticipated when two similar biological conditions are compared. Low-abundance transcripts are another source of discrepancy between both methodological approaches[18].

We found some evidence that pathways related with lipid synthesis (stearate, palmitate and FA synthesis) and catabolism (triacylglycerol degradation), glucose metabolism (glucose synthesis and degradation) and hormonal response (growth hormone signalling) were enriched in the set of DE genes (Table 2 and Supplementary Table S4). Similar results were obtained by Cánovas *et al.*[7] *i.e*. they detected an overexpression of pathways related with the synthesis of FA and insulin signaling in HIGH pigs. Puig-Oliveras *et al.*[1] compared the muscle mRNA expression of pigs with high saturated (SFA) and monounsaturated (MUFA) FA muscle contents against those with a high polyunsaturated FA (PUFA) content and also observed an enrichment of pathways related with fat deposition (PPAR and insulin signalling) in the set of DE genes. Insulin stimulates the absorption of glucose, which is a lipogenic substrate, and *PPARG* enhances triglyceride storage[19]. By using the same animal material employed by Puig-Oliveras *et al.*[1], Corominas *et al.*[5] observed an overexpression of genes belonging to the LXR/RXR activation pathway in the adipose tissue of pigs with high muscle SFA and MUFA contents. These results, which agree well with ours (Supplementary Table S4), make sense because liver X receptors are sterol-activated transcription factors that enhance lipogenesis[20].

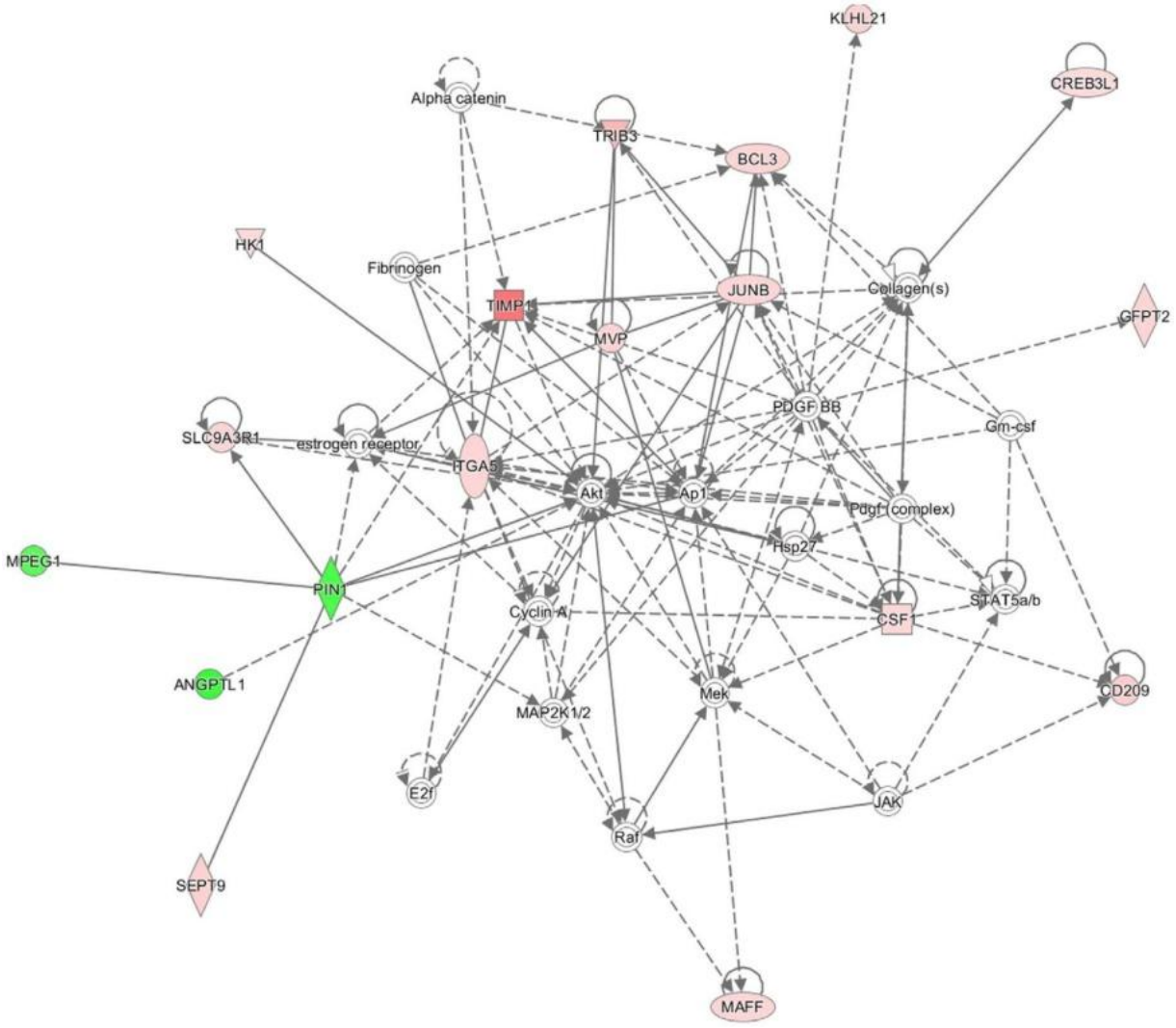

Figure 1 - The top-scoring regulatory network identified with the IPA software corresponded to *Cardiovascular Disease, Cardiovascular System Development and Function, Organismal Injury and Abnormalities.* Genes that are upregulated and downregulated in HIGH pigs (when compared with the LOW ones) are displayed within red and green nodes, respectively. Solid and dashed lines between genes represent known direct and indirect gene interactions, respectively. The shapes of the nodes reflect the functional class of each gene product: transcriptional regulator (horizontal ellipse), transmembrane receptor (vertical ellipse), enzyme (vertical rhombus), cytokine/ growth factor (square), kinase (inverted triangle) and complex/group/other (circle).

Though not all studies comparing pigs with divergent lipid phenotypes identify the same sets of pathways, an outcome that partly depends on the software and databases used as well as on the targeted tissue and phenotype variability, the general trend that emerges is that biochemical routes that promote lipid deposition are overexpressed in the skeletal muscle of fat pigs with high muscle SFA and MUFA contents. In close concordance with a previous study[7], we have also found that one gene that promotes the catabolism of

triglycerides, carboxylesterase 1 (*CES1*), is strongly upregulated in HIGH pigs (*P* -value = 0.0006, FC = 2.4). The CES1 protein has hydrolase activity and its inactivation leads to hyperlipidemia and increased fat deposition in peripheral tissues, obesity, fatty liver, hyperinsulinemia and insulin insensitivity and a decreased energy expenditure[21]. According to Cánovas and coworkers[7], the upregulation of lipolytic genes in HIGH pigs suggests the existence of a cycle where triacylglycerols are continuously synthesized and degraded. However, we have also detected the downregulation of lipolytic genes such as lipase C, hepatic type (*LIPC*, *P*-value =0.002, FC =−1.5)[22], a feature that suggests that the mechanisms that promote an adequate balance between anabolic and catabolic lipid metabolism routes are highly complex.

Analysis of the data with the IPA software (QIAGEN) showed that the top-scoring regulatory network was *Cardiovascular Disease, Cardiovascular System Development and Function, Organismal Injury and Abnormalities*, a result that it is not surprising given the tight relationship between lipoprotein metabolism and cardiovascular risk[23]. In the network shown in Fig. 1, the V-Akt murine thymoma viral oncogene homolog molecule (AKT) occupies a central position, having connections with several DE lipid-related genes (*e.g.*, *TRIB3*, *TIMP1* and *ITGA5*). Interestingly, AKT is one of the main regulators of glucose homeostasis[24], a feature that is consistent with the existence of tight links between lipid and carbohydrate metabolism.

When we used the Regulator Effects tool of IPA, the *PPARG* and *PDGFB* genes were predicted to be major transcriptional regulators of the set of 96 DE loci (Fig. 2). The PPARG transcription factor is critically required for adipogenesis, being a powerful modulator of whole-body lipid homeostasis and insulin sensitivity[25]. Polymorphism in the *PPARG* gene is associated with individual susceptibility to type 2 diabetes, obesity and body mass index[26]. In our study, *PPARG* is upregulated (*P*-value = 0.02 and FC = 1.36) in HIGH pigs and appears to regulate several genes, such as *CEBPA* (*P*-value = 0.009 and FC = 1.64), *CES1* (*P*-value = 0.0004 and FC = 2.03), *CIDEC* (*P*-value = 0.0005 and FC = 2.46) and *FASN* (*P*-value = 0.0009 and FC = 2), that play distinct roles in lipid metabolism (http://www.genome.jp/kegg/pathway.html).

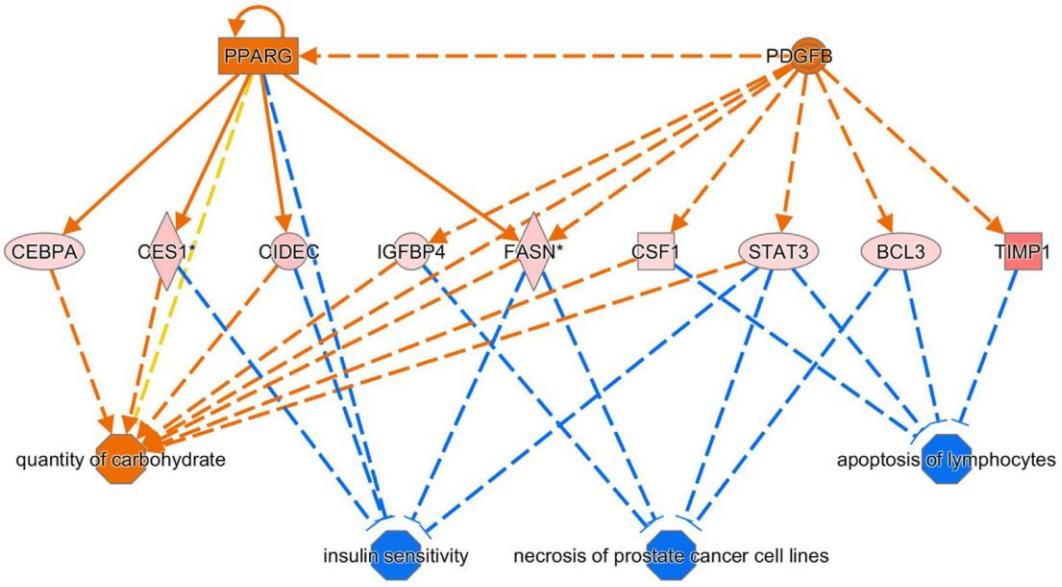

Figure 2 - The Regulator Effects tool of the IPA package was employed to identify two major upstream regulators (*PPARG* and *PDGFB*) of the networks of differentially expressed genes. This tool integrates Upstream Regulator results with Downstream Effects results to build causal hypotheses that help to interpret what may be occurring upstream to cause particular phenotypic or functional outcomes downstream (http://www. ingenuity.com/products/ipa/ipa-spring-release-2014). In the upper tier, there are two upstream regulators (*PPARG* and *PDGFB*) predicted to be activated (orange color). In the middle tier, we can see the genes whose expression changes in response to the activation of upstream regulators (red = upregulation). The shapes of the nodes reflect the functional class of each gene product: enzyme (vertical rhombus), transcription regulator (vertical ellipse), cytokine/growth factor (square), ligand-dependent nuclear receptor (horizontal rectangle) and complex/group/ other (circle). In the lower tier, the expected phenotypic consequences of changes in gene expression are shown by considering the Ingenuity Knowledge Base (absolute z-score > 2 and P-value < 0.05). The octagonal symbol defines Function, while solid and dashed lines between genes represent known direct and indirect gene interactions, respectively. Orange leads to activation, while blue leads to inhibition predicted relationships. Orange (predicted to be activated) and blue (predicted to be inhibited) lines represent relationships with causal consistency.

Table 3 - Evolutionary conservation of non-coding RNAs transcribed in the porcine *gluteus medius* muscle. miRNA =microRNAs; misc_RNA=miscellaneous other RNA; Mt-rRNA =Mitochondrial ribosomal RNA; Mt-tRNA =transfer RNA located in the mitochondrial genome; rRNA =ribosomal RNA; snoRNA =small nucleolar RNA; snRNA =small nuclear RNA; lincRNA =Long intergenic non-coding RNAs.

Transcript	Transcript Type	Number	Conserved ncRNA
Small ncRNA	miRNA	433	137
	misc_RNA	95	82
	Mt-rRNA	2	0
	Mt-tRNA	22	0
	rRNA	57	52
	snoRNA	417	395
	snRNA	328	273
Long ncRNA	Non coding	4	0
	Processed transcript	143	0
	Antisense	15	0
	lincRNA	42	0

Limited contribution of the non-coding RNA transcriptome to differential expression between HIGH and LOW pigs.

Non-coding RNAs have been shown to regulate gene expression by interacting with chromatin complexes, working as RNA enhancers, recruiting or assembling certain proteins and interacting with other RNAs at the post-transcriptional level[27]. In consequence they may play a fundamental role in the metabolism of the porcine skeletal muscle. In our study, we have identified 1,558 muscle-expressed ncRNA transcripts (Supplementary Table S7). The total number of ncRNAs in the pig genome is currently unknown, but Zhou *et al.*[28] highlighted the existence of at least 6,621 long intergenic non-coding RNAs (lincRNA) transcripts encoded by 4,515 gene loci. In humans, 58,648 lncRNA encoding loci have been identified so far[29]. In our dataset (Table 3), the degree of evolutionary conservation of ncRNAs happened to be much higher than that of lncRNAS. Zhou *et al.*[28] characterized the porcine lincRNA transcriptome and found that only 40% of the transcripts had a detectable human lincRNA ortholog. This scarcity of orthologous sequences can be due, in part, to the poor annotation of ncRNAs in all investigated species.

Table 4 - List of non-coding RNAs that are differentially expressed (at the nominal level, *P*-value ≤ 0.05) in the *gluteus medius* muscle of HIGH and LOW pigs. A negative FC means that the affected gene is overexpressed in LOW pigs; lincRNA = Long intergenic non-coding RNAs, Mt-tRNA = transfer RNA located in the mitochondrial genome.

Ensembl ID	Gene ID	Size (bp)	Fold Change	*P*-value	Type of ncRNA
ENSSSCG00000031004	*CH242-227G20.3*	1833	−1.44	0.002	lincRNA
ENSSSCG00000031028	*CH242-15C8.2*	1495	−1.34	0.014	lincRNA
ENSSSCG00000015579	*PTGS2*	3601	−1.47	0.016	Processed transcript
ENSSSCG00000030904	*CU468594.10*	1083	−1.49	0.025	Non coding
ENSSSCG00000001227	*TMP-SLA-3*	1767	−1.31	0.026	Processed transcript
ENSSSCG00000030767	*TMP-SLA-5*	1147	−1.29	0.027	Processed transcript
ENSSSCG00000015549	*RNASEL*	2716	−1.87	0.028	Processed transcript
ENSSSCG00000018090	*Unavailable*	70	−2.05	0.036	Mt-tRNA
ENSSSCG00000001397	*TMP-CH242-74M17.4*	1726	−1.27	0.038	Processed transcript
ENSSSCG00000001227	*TMP-SLA-3*	1700	−1.30	0.043	Processed transcript
ENSSSCG00000004334	*MAP3K7-001*	2818	−1.72	0.044	Processed transcript
ENSSSCG00000015897	*IFIH1*	3720	−1.60	0.046	Processed transcript

Table 5 - Protein-encoding genes that map near (30 kb) to the subset of 12 differentially expressed ncRNAs (HIGH *vs* LOW pigs). Differentially expressed ncRNAs and mRNAs (HIGH *vs* LOW pigs) *P*-value ≤ 0.05, Fold Change ≥ 1.2) are shown in bold. A negative Fold Change means that the affected gene is overexpressed in LOW pigs.

Non-coding RNA	Neighboring mRNA gene	Fold Change	*P*-value	RPKM-means LOW	RPKM-means HIGH
CH242-15C8.2	*USP9X*	−1.02	0.500	10.70	10.50
CH242-227G20.3	*PDK3*	−1.03	0.435	8.97	8.69
	PCYT1B	−1.07	0.461	0.35	0.33
CU468594.10	***CU468594.8***	**1.26**	**0.003**	1.40	1.77
	CPSF1	1.10	0.020	12.60	13.90
	SLC39A4	1.24	0.316	0.09	0.11
	FBXL6	−1.03	0.777	1.88	1.84
	ADCK5	−1.04	0.865	2.82	2.72
	TMEM249	1.07	0.587	0.08	0.08
ENSSSCG00000018090	*MT-ND2*	−1.15	0.024	5019.58	4372.26
	MT-ATP6	−1.13	0.033	25335.60	22504.43
	MT-ND6	**−1.21**	**0.038**	5199.05	4287.84
	MT-COX2	−1.12	0.051	20299.35	18062.05
	MT-ND5	−1.16	0.051	3264.12	2809.24
	MT-COX1	−1.13	0.064	24826.52	21886.25
	MT-ND3	−1.10	0.086	4413.22	4010.71
	MT-CYTB	−1.10	0.123	10033.49	9149.34
	MT-ATP8	−1.07	0.162	6421.54	5974.98
	MT-COX3	−1.08	0.164	31328.03	28896.14
	MT-ND1	−1.06	0.197	8412.34	7957.73
	MT-ND4	−1.04	0.243	5784.35	5564.63
	MT-ND4L	−1.03	0.289	2042.94	1980.50
IFIH1	*FAP*	−1.10	0.665	2.56	2.33
RNASEL	*RGS8*	2.22	0.300	0.11	0.24
TMP-SLA-5 and *TMP-CH242-74M17.4*	*SLA-1*	−1.17	0.123	79.31	67.50

There is growing evidence that there might be a positive correlation between the expression of ncRNAs and nearby mRNA encoding genes, suggesting that the former may regulate the expression of the latter [30]. We investigated this issue by analysing if there are DE protein-coding genes in the vicinity of any of the 12 DE ncRNAs identified in our work (*P*-value ≤ 0.05, Tables 4 and 5). Two protein-coding genes, *i.e.* mitochondrially encoded NADH:ubiquinone oxidoreductase core subunit 6 (*MT-ND6*) and *CU468594.8*, fulfilled this condition (*P*-value ≤ 0.05 and FC ≥ 1.2, Table 5). The *MT-ND6* gene encodes a NADH dehydrogenase that catalyses the oxidation of NADH by ubiquinone, an essential step in the mitochondrial electron transport chain[31]. The *CU468594.8* locus is orthologous to human solute carrier family 52-riboflavin transporter, member 2 (*SLC52A2*). Riboflavin is the precursor of flavin adenine dinucleotide (FAD) and flavin mononucleotide (FMN), two essential cofactors that participate in a wide range of redox reactions[32,33].

We aimed to ascertain if differences amongst HIGH and LOW pigs, in terms of IMF content and composition, are mainly due to the DE of either mRNA or ncRNA encoding genes. When considering a nominal *P*-value of 0.05 as a threshold of significance, the number of DE ncRNAs (12 loci) was much smaller than that of DE mRNAs (1,430 loci), even if we take into account that the number of expressed mRNAs (18,104) was also higher than that of ncRNAs (1,558). Moreover, none of the DE ncRNAs remained significant after correction for multiple testing. In a recent experiment, the transcriptome of pig endometrial samples collected at different pregnancy stages was characterized, and 2,376 transcripts were identified as DE in pairwise comparisons[34]. Only 12% of these transcripts corresponded to lncRNAs indicating that changes in the endometrial transcriptome associated with pregnancy mainly affect the expression of protein-coding genes. However, studies performed in humans indicate a much more balanced contribution of mRNAs and ncRNAs to differential expression. For instance, Wang *et al.*[35] investigated the expression patterns of peripheral leukocytes of healthy and autistic individuals and identified 3,929 and 2,591 DE lncRNAs and mRNAs, respectively. Similarly, Zhou *et al.*[36] identified 891 and 576 DE mRNAs and lncRNAS, respectively, when comparing the expression patterns of ectopic and eutopic endometrial tissue. These differences between humans and pigs are probably the consequence of technical rather than biological causes,

evidencing the pressing need of improving the genomic and functional annotation of porcine ncRNAs.

Conclusions

By comparing the mRNA expression of HIGH and LOW pigs by RNA-Seq, we have identified 96 loci displaying differential expression (*P*- value ≤ 0.01 and FC ≥ 1.5). Many of these loci were not detected in a previous microarray-based experiment, suggesting that distinct platforms detect different sets of DE genes. Lipid biosynthetic pathways were enriched in DE genes and upregulated in HIGH pigs, a result that is consistent with previous reports. We have also undertaken the analysis of non-coding RNAs, a feature that has been neglected in previous studies investigating the differential expression of porcine genes. Our results indicate that the number of DE non-coding RNAs is much lower than that of mRNAs, an outcome that might be partly explained by the poor annotation of porcine ncRNAs.

Material and Methods

Ethics statement.

All experiments were performed in accordance with the ARRIVE guidelines (https://www.nc3rs.org.uk/arrive-guidelines). Animal care and management procedures were approved by the Ethical Committee of the Institut de Recerca i Tecnologia Agroalimentàries, IRTA.

Animal Material.

One population of 350 Duroc barrows belonging to 5 half-sib families, and distributed in 4 fattening batches was generated in 2003. All animals were kept under the same feeding and man-agement conditions[37]. A wide array of growth, fatness, feed efficiency and carcass and meat quality traits were recorded in these animals, including weight, daily

food intake, fat deposition, and IMF content and composition (C:12-C:22 interval) of the *gluteus medius* muscle[7]. By using a principal component analysis based on 13 lipid-related traits, we selected two groups of pigs, *i.e.* HIGH and LOW, displaying distinct phenotypic profiles[7] (Supplementary Table S8). Compared with their LOW counterparts, HIGH pigs were fatter and they had a higher IMF, SFA and MUFA muscle contents as well as elevated serum lipid concentrations[7]. LOW pigs, in contrast, had a higher muscle PUFA content[7].

RNA isolation and library construction and sequencing.

Total RNA was isolated from 56 porcine *gluteus medius* muscle samples (28 HIGH and 28 LOW) by using the acid phenol method implemented in the RiboPure kit (Ambion, Austin, TX). Total RNA was quantified in a Nanodrop ND -1000 spectrophotometer, checked for purity and integrity in a Bioanalyzer-2100 device (Agilent Technologies, Inc., Santa Clara, CA) and submitted to the Centre Nacional d'Anàlisi Genòmica (CNAG, http://www.cnag.cat) for sequencing. Libraries were prepared using the TruSeq RNA Sample Preparation Kit (Illumina Inc) according to the protocols recommended by the manufacturer. Each library was paired-end sequenced (2 × 75 bp) by using the TruSeq SBS Kit v3-HS, in a HiSeq2000 platform.

Bioinformatic analyses.

All bioinformatic analyses were performed with the CLC Bio Workbench software (CLC Bio, Aarhus, Denmark). Quality control was carried out with the NGS Core Tools, considering several parameters based on the FastQC-project (http://www.bioinformatics.babraham.ac.uk/projects/fastqc/). We carried out per-sequence and per-base analyses to filter reads according to the following criteria: sequence-read distribution =75 bp, 100% coverage in all bases, GC -content ~50%, ~25% of A, T, G and C nucleotide contribu-tions, ambiguous base-content <0.1% and a Phred score higher than 30 (*i.e.* base-calling accuracy larger than 99.9%). Short sequence reads were assembled, mapped and annotated by using as template the pig reference genome version 10.2

(*Sscrofa*10.2-http://www.ensembl.org/info/data/ ftp/index.html). For mapping purposes, we just considered alignments with a length fraction of 0.7 and a similarity fraction of 0.8. Besides, two mismatches and three insertions and deletions per read were allowed.

Gene expression data were normalized by calculating the reads per kilobase per million mapped reads (RPKM)[38]. Using scales of abundance estimates by exon length and millions of mapped reads, original expression values were transformed and normalized. More specifically, data were transformed on a decimal logarithmic scale and a scaling algorithm was utilized for the normalization of average scores[39]. For the statistical analysis of differential expression, we used a two- tailed t-test that assumes a Gaussian distribution and homogeneous variances. This statistical test compares the mean expression levels in the two experimental groups (HIGH *vs* LOW) and evaluates the significance of the difference relative to the variance of the data within the groups. Multiple testing correction was performed by using a false-discovery rate approach (cut-off =0.05) implemented in the QVALUE R package[40]. Fold-Change was computed as the ratio of HIGH *vs* LOW gene expressions (a negative FC means that the affected gene is upregulated in LOW pigs).

Ingenuity Pathway Analysis (IPA, QIAGEN Redwood City, www.qiagen.com/ingenuity) was used to identify gene ontologies, pathways, and regulatory networks to which DE genes belong to, as well as upstream regulators. Ingenuity Pathway Analysis can transform a set of genes into a number of relevant networks based on comprehensive records maintained in the Ingenuity Pathways Knowledge Base. Networks are presented as graphs depicting the biological relationships between genes/gene products. Genes are shown as nodes, and the molecular relationship between two nodes is represented with either a solid (direct interactions) or a dashed (indirect interactions) line. The analysis of upstream regulators considers every possible transcription factor and upstream regulator contained in the Ingenuity Knowledge Base repository as well as their predicted effects on gene expression (inferred from the scientific literature). Then, this tool analyses if the patterns of expression observed in the DE genes can be explained by the activation/inhibition of any of these regulators through the calculation of a z-score *i.e.* a statistical measure of the match between expected relationship direction between the regulator and its targets and observed gene expression[41].

A parallel analysis was performed with the Cytoscape software[42] by using the ReactomeFIViz app[8]. IPA and Cytoscape analyses were performed on a subset of DE genes, with *P*-value ≤ 0.01 and a FC ≥ 1.5. Transcript classification and the search of homologs of porcine ncRNAs in other mammalian species were carried out with tools implemented in the BioMart web interface (http://www.ensembl. org/biomart/martview).

References

1. Puig-Oliveras, A. *et al.* Differences in muscle transcriptome among pigs phenotypically extreme for fatty acid composition. *Plos One* **9,** e99720 (2014).
2. Ayuso, M. *et al.* Comparative analysis of muscle transcriptome between pig genotypes identifies genes and regulatory mechanisms associated to growth, fatness and metabolism. *Plos One* **10,** e0145162 (2015).
3. Chen, C. *et al.* A global view of porcine transcriptome in three tissues from a full-sib pair with extreme phenotypes in growth and fat deposition by paired-end RNA sequencing. *BMC Genomics* **12,** 448 (2011).
4. Ramayo-Caldas, Y. *et al.* Liver transcriptome profile in pigs with extreme phenotypes of intramuscular fatty acid composition. *BMC Genomics* **13,** 547 (2012).
5. Corominas, J. *et al.* Analysis of porcine adipose tissue transcriptome reveals differences in *de novo* fatty acid synthesis in pigs with divergent muscle fatty acid composition. *BMC Genomics* **14,** 843 (2013).
6. Ye, R.-S. *et al.* Comparative anterior pituitary miRNA and mRNA expression profiles of Bama minipigs and Landrace pigs reveal potential molecular network involved in animal postnatal growth. *Plos One* **10,** e0131987 (2015).
7. Cánovas, A., Quintanilla, R., Amills, M. & Pena, R. N. Muscle transcriptomic profiles in pigs with divergent phenotypes for fatness traits. *BMC Genomics* **11,** 372 (2010).
8. Wu, G., Dawson, E., Duong, A., Haw, R. & Stein, L. ReactomeFIViz: a Cytoscape app for pathway and network-based data analysis. *F1000Res* **3,** 146 (2014).
9. Jia, Z., Moulson, C. L., Pie, Z., Miner, J. H. & Watkins, P. A. Fatty acid transport protein 4 is the principal very long chain fatty acyl-CoA synthetase in skin fibroblasts. *J. Biol. Chem.* **282,** 20573–83 (2007).
10. Carstensen, M. *et al.* Effect of Sfrp5 on cytokine release and insulin action in primary human adipocytes and skeletal muscle cells. *Plos One* **9,** e85906 (2014).
11. Kalantari, R., Chiang, C. M. & Corey, D. R. Regulation of mammalian transcription and splicing by nuclear RNAi. *Nucl. Acids Res.* **44,** 524–37 (2016).

12. Berger, W., Steiner, E., Grusch, M., Elbling, L. & Micksche, M. Vaults and the major vault protein: novel roles in signal pathway regulation and immunity. *Cell. Mol. Life Sci.* **66,** 43–61 (2009).

13. Cao, P. R., Kim, H. J. & Lecker, S. H. Ubiquitin-protein ligases in muscle wasting. *Int. J. Biochem. Cell Biol.* **37,** 2088–97 (2005).

14. Davoli, R. *et al.* Genome-wide study on intramuscular fat in Italian Large White pig breed using the PorcineSNP60 BeadChip. *J. Anim. Breed. Genet.* **133,** 277–82 (2014).

15. Fu, X. *et al.* Estimating accuracy of RNA-Seq and microarrays with proteomics. *BMC Genomics* **10,** 161 (2009).

16. Trost, B. *et al.* Concordance between RNA-Sequencing data and DNA microarray data in transcriptome analysis of proliferative and quiescent fibroblasts. *R. Soc. Open Sci.* **2** (2015).

17. Kogenaru, S., Qing, Y., Guo, Y. & Wang, N. RNA-Seq and microarray complement each other in transcriptome profiling. *BMC Genomics* **13,** 629 (2012).

18. Wang, C. *et al.* The concordance between RNA-Seq and microarray data depends on chemical treatment and transcript abundance. *Nat. Biotechnol.* **32,** 926–32 (2014).

19. Ferré, P. The biology of peroxisome proliferator-activated receptors: relationship with lipid metabolism and insulin sensitivity. *Diabetes* **53** Suppl 1, S43–50 (2004).

20. Hong, C. & Tontonoz, P. Liver X receptors in lipid metabolism: opportunities for drug discovery. *Nat. Rev. Drug Discov.* **13,** 433–44 (2014).

21. Quiroga, A. D. *et al.* Deficiency of carboxylesterase 1/esterase-x results in obesity, hepatic steatosis, and hyperlipidemia. *Hepatology* **56,** 2188–98 (2012).

22. Perret, B. *et al.* Hepatic lipase: structure/function relationship, synthesis, and regulation. *J. Lipid Res.* **43,** 1163–9 (2002).

23. Millán, J. *et al.* Lipoprotein ratios: Physiological significance and clinical usefulness in cardiovascular prevention. *Vasc. Health Risk Manag.* **5,** 757–65 (2009).

24. Hay, N. Akt isoforms and glucose homeostasis - the leptin connection. *Trends Endocrinol. Metab.* **22,** 66–73 (2011).

25. Ahmadian, M. *et al.* PPARγ signaling and metabolism: the good, the bad and the future. *Nat. Med.* **99,** 557–66 (2013).

26. Masud, S. & Ye, S. Effect of the peroxisome proliferator activated receptor-c gene Pro12Ala variant on body mass index: a meta-analysis. *J. Med. Genet* **40,** 773–80 (2003).

27. Huarte, M. & Marín-Béjar, O. Long noncoding RNAs: from identification to functions and mechanisms. *Adv. Genomics Genet.* **5,** 257 (2015).

28. Zhou, Z.-Y. *et al.* Genome-wide identification of long intergenic noncoding RNA genes and their potential association with domestication in pigs. *Genome Biol. Evol.* **6,** 1387–92 (2014).

29. Iyer, M. K. *et al.* The landscape of long noncoding RNAs in the human transcriptome. *Nat. Genet.* **47,** 199–208 (2015).

30. Guil, S. & Esteller, M. *Cis*-acting noncoding RNAs: friends and foes. *Nat. Struct. Mol. Biol.* **19,** 1068–75 (2012).

31. Vartak, R., Deng, J., Fang, H. & Bai, Y. Redefining the roles of mitochondrial DNA-encoded subunits in respiratory Complex I assembly. *Biochim. Biophys. Acta.* **1852,** 1531–9 (2015).

32. Powers, H. J. Riboflavin (vitamin B-2) and health. *Am. J. Clin. Nutr.* **77,** 1352–60 (2003).

33. Ghisla, S. & Massey, V. Mechanisms of flavoprotein-catalyzed reactions. *Eur. J. Biochem.* **181,** 1–17 (1989).

34. Wang, Y. *et al.* Analyses of long non-coding RNA and mRNA profiling using RNA sequencing during the pre-implantation phases in pig endometrium. *Sci. Rep.* **6,** 20238 (2016).

35. Wang, Y. *et al.* Genome-wide differential expression of synaptic long noncoding RNAs in autism spectrum disorder. *Transl. Psychiatry.* **5,** e660 (2015).

36. Zhou, C. *et al.* The differential expression of mRNAs and long noncoding RNAs between ectopic and eutopic endometria provides new insights into adenomyosis. *Mol. Biosyst.* **12,** 362–70 (2016).

37. Gallardo, D. *et al.* Mapping of quantitative trait loci for cholesterol, LDL, HDL, and triglyceride serum concentrations in pigs. *Physiol. Genomics* **35,** 199–209 (2008).

38. Mortazavi, A., Williams, B. A., McCue, K., Schaeffer, L. & Wold, B. Mapping and quantifying mammalian transcriptomes by RNA-Seq. *Nat. Methods* **5,** 621–8 (2008).

39. Bolstad, B. M., Irizarry, R. A., Astrand, M. & Speed, T. P. A comparison of normalization methods for high density oligonucleotide array data based on variance and bias. *Bioinformatics* **19,** 185–93 (2003).

40. J. D. Storey, A. J. Bass, A. Dabney & D. R. Q-value estimation for false discovery rate control. R package version 2.1.1-http://github. com/jdstor at http://www.bioconductor.org/packages/release/bioc/vignettes/qvalue/inst/doc/qvalue.pdf (2015).

41. Krämer, A., Green, J., Pollard, J. & Tugendreich, S. Causal analysis approaches in Ingenuity Pathway Analysis. *Bioinformatics* **30,** 523–30 (2014).

42. Shannon, P. *et al.* Cytoscape: a software environment for integrated models of biomolecular interaction networks. *Genome Res.* **13,** 2498–504 (2003).

Acknowledgements

Part of the research presented in this publication was funded by grants AGL2013-48742-C2-1-R and AGL2013-48742-C2-2-R awarded by the Spanish Ministry of Economy and Competitivity. We also acknowledge the support of the Spanish Ministry of Economy and Competitivity for the *Center of Excellence Severo Ochoa 2016–2019* (SEV-2015-0533) grant awarded to the Center for Research in Agricultural Genomics. The authors are indebted to Selección Batallé S.A. for providing the animal material. We gratefully acknowledge to J. Reixach (Selección Batallé) and J. Soler (IRTA) for their collaboration in the experimental protocols. Tainã F Cardoso was funded with a fellowship from the CAPES Foundation-Coordination of Improvement of Higher Education, Ministry of Education (MEC) of the Federal Government of Brazil.

Author Contributions

R.Q. and M.A. conceived the study and designed the experiment; R.Q. was responsible for producing the animal material, phenotypic records and RNA-Seq data; T.F.C., A.C. and O.C. did the bioinformatic analyses; R.G.P. helped in the statistical analyses; M.A. and T.F.C. wrote the manuscript. All authors helped to draft the manuscript and read and approved its final version.

Additional Information

Table S1 - Differentially expressed genes in the gluteus medius muscle of HIGH and LOW pigs (*P*-value ≤ 0.05)

Table S2 - List of DE genes (*P*-value ≤ 0.05) detected simultaneously with RNA-Seq (current work) and microarrays (Cánovas et al. 2010. BMC Genomics 11, 372).

Table S3 - Differentially expressed genes in the gluteus medius muscle of HIGH and LOW pigs (*P*-value ≤ 0.01 and fold-change ≥ 1.5)

Table S4 - Enriched pathways identified by IPA when using the data set of 96 differentially expressed genes (*P*-value ≤ 0.01 and fold-change ≥ 1.5).

Table S5 - Pathways identified by Reactome as enriched in differentially expressed genes (*P*-value ≤ 0.01 and fold-change ≥ 1.5)

Table S6 - Regulatory networks of genes that are differentially expressed (*P*-value ≤ 0.01 and fold-change ≥ 1.5) in HIGH and LOW pigs

Table S7 - Non-coding transcripts expressed in the gluteus medius muscle of HIGH and LOW pigs.

Table S8 - HIGH and LOW group mean values ± standard deviation (SD) for 13 lipid-related traits

Differential expression of mRNA isoforms in the skeletal muscle of pigs with distinct growth and fatness profiles.

Cardoso TF[1,2], Quintanilla R[3], Castelló A[1,4], González-Prendes R[1], Amills M[5,6,a], Cánovas A[7,a].

[1]Department of Animal Genetics, Centre for Research in Agricultural Genomics (CRAG), CSIC-IRTA-UAB-UB, Campus de la Universitat Autònoma de Barcelona, Bellaterra, 08193, Barcelona, Spain. [2]CAPES Foundation, Ministry of Education of Brazil, Brasilia D.F, 70.040-020, Brazil. [3]Animal Breeding and Genetics Programme, Institute for Research and Technology in Food and Agriculture (IRTA), Torre Marimon, 08140, Caldes de Montbui, Spain. [4]Departament de Ciència Animal i dels Aliments, Universitat Autònoma de Barcelona, Bellaterra, 08193, Barcelona, Spain. [5]Department of Animal Genetics, Centre for Research in Agricultural Genomics (CRAG), CSIC-IRTA-UAB-UB, Campus de la Universitat Autònoma de Barcelona, Bellaterra, 08193, Barcelona, Spain. marcel.amills@uab.cat. [6]Departament de Ciència Animal i dels Aliments, Universitat Autònoma de Barcelona, Bellaterra, 08193, Barcelona, Spain. [7]Centre for Genetic Improvement of Livestock, Department of Animal Biosciences, University of Guelph, Guelph, ON, Canada.

[a]Corresponding authors: A. Cánovas and M. Amills

BMC Genomics. 2018 Feb 14;19(1):145.

doi: 10.1186/s12864-018-4515-2.

Abstract

The identification of genes differentially expressed in the skeletal muscle of pigs displaying distinct growth and fatness profiles might contribute to identify the genetic factors that influence the phenotypic variation of such traits. So far, the majority of porcine transcriptomic studies have investigated differences in gene expression at a global scale rather than at the mRNA isoform level. In the current work, we have investigated the differential expression of mRNA isoforms in the *gluteus medius* (GM) muscle of 52 Duroc HIGH (increased backfat thickness, intramuscular fat and saturated and monounsaturated fatty acids contents) and LOW pigs (opposite phenotype, with an increased polyunsaturated fatty acids content). Our analysis revealed that 10.9% of genes expressed in the GM muscle generate alternative mRNA isoforms, with an average of 2.9 transcripts per gene. By using two different pipelines, one based on the CLC Genomics Workbench and another one on the STAR, RSEM and DESeq2 softwares, we have identified 10 mRNA isoforms that both pipelines categorize as differentially expressed in HIGH *vs* LOW pigs (*P*-value < 0.01 and ±0.6 $\log_2$fold-change). Only five mRNA isoforms, produced by the *ITGA5*, *SEMA4D*, *LITAF*, *TIMP1* and *ANXA2* genes, remain significant after correction for multiple testing (q-value < 0.05 and ±0.6 $\log_2$fold-change), being upregulated in HIGH pigs. The increased levels of specific *ITGA5*, *LITAF*, *TIMP1* and *ANXA2* mRNA isoforms in HIGH pigs is consistent with reports indicating that the overexpression of these four genes is associated with obesity and metabolic disorders in humans. A broader knowledge about the functional attributes of these mRNA variants would be fundamental to elucidate the consequences of transcript diversity on the determinism of porcine phenotypes of economic interest.

Keywords: Alternative splicing, mRNA isoform, Swine, Differential expression

Background

Recent estimates indicate that in mammals, at least 70% of genes have multiple polyadenylation sites, > 50% of genes have alternative transcription start sites and nearly 95% of genes undergo alternative splicing (AS) yielding multiple messenger ribonucleic acid (mRNA) isoforms [1, 2]. The use of alternative transcriptional initiation and/or termination sites can produce diverse pre-mRNAs, which can further be subjected to AS yielding a broad array of mRNA isoforms that are derived from a single gene. A recent study indicated that alternative transcription start and termination sites, rather than AS, encompasses most of tissue-dependent exon usage [1]. Transcripts produced by any of the mechanisms mentioned above might contribute to differences between tissues or cells by modifying protein structure and expression [3–5]. Indeed, the differential expression of mRNA isoforms has been associated with a broad array of physiological and pathological conditions in humans [3, 4] and domestic species [5, 6].

The important consequences of transcript diversity on porcine phenotypes of economic interest have been recently evidenced in a couple of studies. In White Duroc × Erhualian F_2 intercross pigs, a mutation in a splice acceptor site of intron 9 (g.8283C > A) of the porcine phosphorylase kinase catalytic subunit gamma 1 (*PHKG1*) gene has been shown to drive the synthesis of an aberrant transcript subjected to nonsense-mediated decay [7]. This results in the inactivation of this enzyme, which plays a key role in the degradation of glycogen, and in the production of a low quality meat with a poor water-holding capacity [7]. Moreover, Koltes et al. [8], identified a mutation located in the pig guanylate binding protein 5 (*GBP5*) gene that introduces a new splice acceptor site that results in the insertion of five additional nucleotides, thus altering the open reading frame and introducing a premature stop-codon. This mutation has a major effect on the host response to the porcine respiratory and reproductive syndrome virus [8].

Transcript diversity of the porcine muscle has been poorly characterized so far and the majority of studies comparing the transcriptomes of pigs with distinct phenotypic attributes have just focused on global differences in gene expression, rather than identifying the specific transcripts that are differentially expressed (DE) [9–12]. The goals of the current

experiment were to provide a first picture of transcript diversity in the *gluteus medius* (GM) muscle of pigs as well as to identify mRNA isoforms that are DE in the GM muscle of Duroc swine with distinct growth and fatness profiles.

Methods

Animal material

The muscle transcriptomes of 56 Duroc pigs, retrieved from a population of 350 individuals distributed in 5 half-sib families, were analyzed using RNA-Sequencing (RNA-Seq) (Additional file 1: Table S1). As previously reported by Gallardo et al. [13], barrows were transferred to the IRTA-CCP experimental test station after weaning (3–4 weeks of age) and bred under normal intensive conditions. In the first stage of fattening (up to 90 kg of live weight, around 150 days of age) barrows were fed ad libitum a standard diet with 18% protein, 3.8% fiber, 7.0% fat, 1.0% lysine, and 0.3% methionine (net energy concentration: 2450 kcal/kg). In the last period of fattening (*i.e*. 30–40 days before slaughter) animals were fed ad libitum a standard diet with 15.9% protein, 4.5% fiber, 5.2% fat, 0.7% lysine, and 0.2% methionine (net energy concentration: 2375 kcal/kg). Pigs were slaughtered when they reached ≈ 122 kg live weight (*i.e.* at an age of 180–200 days approximately). Backfat and ham fat thickness were measured with a ruler in the cutting room 24 h after slaughtering. Lean meat content was estimated on the basis of fat and muscle thickness data measured with an Autofom ultrasound device. Samples of the GM muscle were retrieved, snap frozen in liquid nitrogen and stored at − 80 °C. A near infrared transmittance device (NIT, Infratec 1625, Tecator Hoganas, Sweden) was employed to determine intramuscular fat content. The determination of fatty acid composition was achieved with a technique based on the gas chromatography of methyl esters [14]. As reported by Gallardo and coworkers [13], blood samples were obtained at 190 days and a variety of enzymatic methods were used to determine cholesterol (cholesterol oxidase-based method), high-density lipoprotein (immunoinhibition method) and triglyceride concentrations (glycerol kinase reaction). Low density lipoprotein concentration was calculated according to the equation of Friedewald et al. [15].

Principal component analysis based on the 13 traits listed in Table 1 was performed in order to select pigs with distinct growth and fatness phenotypes (HIGH and LOW pigs) [10]. When compared with LOW pigs, the HIGH (n = 28) ones showed a higher live weight, backfat thickness and intramuscular fat content and also displayed increased serum lipid concentrations and muscle saturated (SFA) and monounsaturated (MUFA) fatty acids contents (Table 1). On the other hand, LOW pigs (n = 28), were lighter, leaner and had a higher muscle polyunsaturated fatty acids (PUFA) content than HIGH pigs.

RNA isolation, library construction and sequencing

Each muscle sample (N = 56, 28 HIGH and 28 LOW) was individually submerged in liquid nitrogen and grinded with a mortar and a pestle to produce a homogenous powder. This powder was submerged in TRIzol reagent (Thermo Fisher Scientific, Barcelona, Spain) and homogenized with a Polytron device (IKA, Staufen, Germany). Total RNA was purified with the Ambion RiboPure kit (Thermo Fisher Scientific, Barcelona, Spain) by following the instructions of the manufacturer. RNA samples were resuspended in a buffer solution provided in the kit and kept at − 80 °C until use. RNA quantification and purity were assessed with a Nanodrop ND-1000 spectrophotometer (Thermo Fisher Scientific, Barcelona, Spain), while integrity was checked with a Bioanalyzer-2100 equipment (Agilent Technologies, Santa Clara, CA). All samples showed an RNA integrity number above 7.5. Sequencing libraries were prepared with the TruSeq RNA Sample Preparation Kit (Illumina, San Diego, CA) and sequenced in a paired-end mode (2 × 75 bp), multiplexing two samples in each sequencing lane, on a HiSeq2000 Sequencing System (Illumina, San Diego, CA). Library preparation and sequencing were developed according to the protocols recommended by the manufacturer.

Differential expression analyses of mRNA isoforms between HIGH and LOW pigs

Adaptors and low quality bases were trimmed from sequences by using Trimmomatic [16] with default parameters. Quality control of sequences in FASTQ and BAM format was assessed with the FASTQC software (Babraham Bioinfomatics,

http://www.bioinformatics.-babraham.ac.uk/projects/fastqc/). Sequence quality was measured by taking into account sequence-read lengths and base-coverage (distribution = 75 bp, 100% coverage in all bases), nucleotide contributions and base ambiguities (GC-content ~ 50%, ~ 25% of A, T, G and C nucleotide contributions and an ambiguous base-content < 0.1%) and a Phred score higher than (*i.e.* base-calling accuracy larger than 99.9%). All samples, except four, passed the quality control parameters, so our final data set consisted of 52 animals. With the aim of minimizing the rate of false positives, we used two different pipelines in the analysis of differential expression. In the first pipeline, read mapping and counting were carried out with CLC Genomics Workbench 8.5 (CLC Bio, Aarhus, Denmark, https://www.qiagenbioinformatics.com/). In the second pipeline, reads were mapped with Spliced Transcripts Alignment to a Reference (STAR) v. 2.4 [17], counted with the RNA-Seq by Expectation Maximization (RSEM) software v. 1.3 [18] and differential expression was analysed with DESeq2 [19]. We considered as DE mRNA isoforms those simultaneously identified with the two pipelines.

Pipeline 1 (CLC genomics workbench)

The Large Gap Mapper (LGM) tool of CLC Genomics Workbench 8.5 was used to map the reads. This tool can map sequence reads that span introns without requiring prior transcript annotations. In this way, the LGM tool finds the best match for a given read. If there is an unaligned end which is long enough for the mapper to handle (17 bp for standard mapping) this segment of the read is re-mapped with the standard read mapper of the CLC Genomics Workbench. This process is repeated until no reads have unaligned ends that are longer than 17/18 bp. In our study, short sequence reads were mapped and annotated by using as template the pig reference genome version 10.2 (Sscrofa 10.2 - http:// www.ensembl.org/info/data/ftp/index.html). Additional details can be found in http://resources.qiagenbioinformatics./com/manuals/transcriptdiscovery/208/index.php?manual=-Large_gap_mapper.html. For mapping purposes, we considered alignments with a length fraction of 0.7 and a similarity fraction of 0.8. Two mismatches and three insertions and deletions per read were allowed. The quantification of mRNA isoform levels by the CLC Genomics Workbench follows a count-based model, where reads are counted on

small counting units (exons), instead of the whole transcript unit, and the two possible splicing out-comes (inclusion and/or exclusion) are tested for each counting unit. Normalized count values are transformed on a decimal logarithmic scale. Statistical analysis of differential expression of splicing variants is based on an empirical analysis of digital gene expression [20] that implements an 'Exact Test' for two-group comparisons, assuming a negative binomial distribution and an overdispersion caused by biological variability estimated at 5%.

Table 1 - Mean values ± standard deviation (SD) for 13 phenotypes recorded in HIGH and LOW Duroc pigs

Phenotypes	HIGH group (N=28) Mean ± SD	LOW group (N=28) Mean ± SD
Carcass traits		
LW - Live weight (kg)	130.90 ± 9.46 [a]	110.75 ± 16.62 [b]
BFTiv - Backfat thickness *in vivo* (mm)	28.74 ± 3.47 [a]	18.76 ± 3.90 [b]
BFT - Backfat thickness 3^{rd}-4^{th} ribs (mm)	47.07 ± 11.94 [a]	33.89 ± 10.03 [b]
HFT - Ham fat thickness (mm)	28.02 ± 2.70 [a]	20.97 ± 3.56 [b]
LEAN - Lean content (%)	39.17 ± 5.15 [a]	45.48 ± 4.21 [b]
Meat quality traits (*gluteus medius*)		
IMF - Intramuscular fat content (%)	7.27 ± 1.70 [a]	3.69 ± 0.93 [b]
SFA - Saturated fatty acids content (%)	38.70 ± 1.41 [a]	34.76 ± 1.30 [b]
PUFA - Polyunsaturated fatty acids content (%)	14.71 ± 3.08 [a]	27.82 ± 4.40 [b]
MUFA - Monounsaturated fatty acids content (%)	46.58 ± 2.67 [a]	37.4 ± 4.30 [b]
Serum lipid levels - 190 days		
CHOL - Total cholesterol (mg/dL)	161.11 ± 30.32 [a]	104.17 ± 16.40 [b]
HDL - HDL-cholesterol (mg/dL)	61.12 ± 8.58 [a]	42.92 ± 9.19 [b]
LDL - LDL-cholesterol (mg/dL)	86.34 ± 29.32 [a]	50.57 ± 15.12 [b]
TG - Triacylglycerides (mg/dL)	68.07 ± 26.28 [a]	50.71 ± 29.7 [b]

Means with different letters are significantly different (*P*-value < 0.05), t-test for: LW, IMF, MUFA, CHOL and LDL; Wilcoxon test for: BFTiv, BFT, LEAN, SFA, PUFA, HDL and TG

Pipeline 2 (STAR/RSEM/DESeq2)

The STAR software v. 2.4 [17] was employed to map the reads generated in the RNA-Seq experiment. The STAR algorithm comprises two main steps. First, a sequential maximum mappable seed search is carried out. For instance, if a read contains a single splice junction, a first seed is mapped to a donor splice site and the unmapped portion of the read is mapped again (in this case to an acceptor splice site). Subsequently, STAR builds alignments of the entire read sequence by stitching together all the seeds that were aligned to the genome in the first step [17]. In our study, the parameters employed in STAR mapping were those reported by Zhang et al. [21] and the pig reference genome v. 10.2 (*Sscrofa* 10.2) was used as template.

Once reads were mapped, they were counted with the RSEM v. 1.3 [18] software by using default parameters with the option "–paired-end" and considering the porcine gene annotation file and the pig *Sscrofa* 10.2 genome sequence. RSEM generates a set of reference transcript sequences and subsequently a set of RNA-Seq reads are aligned to these reference transcripts [18]. Alignments generated with this procedure are used to infer transcript abundances by computing maximum likelihood abundance estimates with the Expectation-Maximization algorithm [18]. Credibility intervals at 95% are built with a Bayesian approach implemented in RSEM. Additional details can be found in Li et al. [18]. Read counts associated with each specific mRNA isoform were employed to carry out analysis of differential expression with DESeq2 [19]. DESeq2 assumes that read counts follow a negative binomial distribution, for each gene *i* and for each sample *j*, with a mean μ_{ij} and a dispersion value α_i. Means are proportional to the amounts of complementary deoxyribonucleic acid (cDNA) fragments corresponding to each gene scaled by a normalization factor. Gene-wise dispersion values are calculated with a maximum likelihood approach and subsequently they are shrunk towards a set of predicted dispersion values with an empirical Bayes approach. Subsequently, DESeq2 shrinks $\log_2$ fold-change (FC) estimates, with an empirical Bayes procedure [19], to reduce variance due to noisiness issues of genes that are poorly expressed. Finally, a Wald test is used to infer if shrunk $\log_2$FC estimates (and their standard errors) are significantly different from zero. In

the Wald test, the shrunken estimate of the log_2FC is divided by its standard error, generating a z-statistic that can be compared to a standard normal distribution [19].

Transcript annotation

To classify splicing events with the SUPPA [22] and Splicing Express [23] softwares, genome BAM files were generated with the STAR software [17], by using the same parameters described above. These BAM files were employed to assemble transcripts with Cufflinks [24], taking as a reference the *Sscrofa* 10.2 genome, and a master transcriptome was generated with Cuffmerge. The SUPPA software annotates AS events from a general input annotation file generated with Cuffmerge. The AS event types considered by SUPPA are: exon skipping, alternative 5′ and 3′ splice sites, and intron retention. For each event, SUPPA calculates the inclusion parameter Ψ, which is defined as the ratio of the abundance of transcripts that include one form of the event over the abundance of the transcripts that contain either form of the event. On the other hand, the Splicing Express software uses a well-annotated set of reference sequences to detect different AS events from a transcriptome data (GTF file) input file *i.e.* exon skipping, intron retention and alternative 5′ and 3′ splicing borders. Splicing Express clusters expressed transcripts to identify their gene of origin and identifies AS events by using an algorithm based on the pairwise comparison. Besides, expressed sequences are represented as binary sequences (exons = 1, introns = 0) that are pairwisely compared thus generating numerical patterns which reflect their splicing differences. Finally, a graphic representation of the expression level is created for each gene and for each identified AS event [23].

Transcript type annotation of porcine GM mRNA isoforms was retrieved from the BioMart database, available in the Ensembl database (http://www.ensembl.org/biomart/martview/). Gene Ontology (GO) Enrichment Analysis was performed by using the Panther database v. 12.0 (http://www.pantherdb.org/) with the data set of 87 genes simultaneously detected by both pipelines (*P*-value < 0.05) as producing mRNA isoforms DE in HIGH *vs* LOW pigs.

Validation of differentially expressed mRNA isoforms by RT-qPCR

Differential expression of mRNA isoforms was validated for the MAF BZIP transcription factor F (*MAFF*), stearoyl-CoA desaturase (*SCD*), retinoic acid receptor γ (*RXRG*) and integrin α5 (*ITGA5*) genes by reverse transcription-quantitative polymerase chain reaction (RT-qPCR). Primers spanning exon-exon boundaries, or alternatively binding at different exons (in order to avoid the amplification of residual contaminating genomic DNA), and complementary to exonic regions that define specific isoforms were designed with the Primer Express software (Applied Biosystems) (Additional file 2: Table S2). One μg of total RNA from 14 pigs (7 from each group - HIGH and LOW), selected at random from the global population of 52 pigs, was used as template for cDNA synthesis. The reverse transcription reaction was carried out with the High-Capacity cDNA Reverse Transcription Kit (Applied Biosystems, Foster City, CA) in a final volume of 20 μl. Quantitative PCR reactions included 7.5 μl of SYBR Select Master Mix, 300 nM of each primer and 3.75 μl of a 1:25 dilution of the cDNA in a final volume reaction of 15 μl. Three genes *e.g*. β-actin (*ACTB*), TATA-Box binding protein (*TBP*) and hypoxanthine phosphoribosyltransferase 1 (*HPRT1*) were used as endogenous controls. The PCR thermal cycle involved one denaturing step at 95 °C for 10 min plus 40 cycles of 15 s at 95 °C and 1 min at 60 °C. Reactions were run in a QuantStudio 12 K Flex Real-Time PCR System (Applied Biosystems, Foster City, CA). A melting curve analysis *i.e.* 95 °C for 15 s, 60 °C for 15 s and a gradual increase in temperature, with a ramp rate of 1% up to 95 °C, followed by a final step of 95 °C for 15 s, was performed after the thermal cycling protocol to ensure the specificity of the amplification. We made sure that housekeeping and target genes had comparable amplification efficiencies (90–110%) by performing standard curve assays with serial 1:5 dilutions. Gene expression levels were quantified relative to the expression of endogenous controls by employing an optimized com-parative Ct (2^{-Ct} method) value approach [25] implemented in the Thermo Fisher Cloud (Thermo Fisher Scientific, Barcelona, Spain). Each sample was analysed in triplicate. All results were evaluated using RT-qPCR data analysis software (Thermo Fisher Cloud, Thermo Fisher Scientific, Barcelona, Spain). The sample displaying the lowest expression was used as calibrator. Differential expression was assessed with a Student's t-test.

Results

After quality control analysis, we used a final dataset of 52 GM muscle samples equally distributed between the HIGH (N = 26) and LOW (N = 26) groups. RNA-Sequencing of these samples generated an average of 66 million paired-end reads per sample. The majority of reads (72.8%, CLC Bio; 89% STAR software) were successfully mapped to the pig *Sscrofa* 10.2 genome assembly. The mean mapping proportions obtained with CLC Bio were 91.4% and 8.6% for reads corresponding to exonic and intronic regions, respectively. When using STAR, 79.3% of the mapped reads were located in exons and 6.5% in introns. The remaining (14.2%) reads mapped to intergenic regions.

In the CLC Bio analysis, we found evidence of the existence of alternative transcripts in 2066 genes (11.7% of protein-coding genes expressed in the GM muscle of HIGH and LOW swine) which produced 5835 mRNA isoforms (2.8 transcripts per gene). In contrast, the STAR software detected 1430 genes (10.2% of expressed protein-coding genes) yielding 4391 different transcripts (3.0 transcripts per gene). Only 5.0% of alternative transcript variants were potentially subject to nonsense-mediated decay (Additional file 3: Table S3). Interestingly, 93% of the genes identified by STAR/ RSEM/DESeq2 as displaying alternative transcripts were also detected with CLC Bio. Analysis of transcriptomic data with the SUPPA software [22] evidenced that exon skipping is the most prevalent AS event, while intron retention is the rarest one, *i.e.* they comprise 36.7% and 12.2% of all GM AS events, respectively (Additional file 4: Table S4). Similar results were obtained with the Splicing Express software [23] (Additional file 4: Table S4), *i.e.* exon skipping was the most prevalent AS event (41.1%) and intron retention the least favoured one (12.7%).

We used two different pipelines (CLC Bio and STAR/RSEM/DESeq2) to detect DE mRNA isoforms in HIGH *vs* LOW pigs. Combination of such data sets made possible to identify 104 alternative transcripts and 87 genes that were simultaneously detected by both pipelines (P-value < 0.05) (Additional file 5: Table S5). A more stringent analysis (P-value < 0.01 and ±0.6 $\log_2$FC) ascertained 10 DE transcripts (corresponding to 10 genes) concurrently discovered by both pipelines (Table 2). Five of these transcripts remained

significant after correction for multiple testing (q-value < 0.05 and ±0.6 log_2FC; Table 2). In general, differential expression only affected one isoform and, more particularly, that showing a predominant pattern of expression (Tables 2, 3 and Additional file 6: Table S6). In order to validate the accuracy of our RNA-Seq approach, we measured the expression of four DE mRNA isoforms (*ITGA5, SCD, RXRG* and *MAFF*) by RT-qPCR analysis (Additional file 7: Figure S1). A significant differential expression was confirmed for two splicing variants *e.g. ITGA5* (4445 bp) and *SCD* (5585 bp) genes (*P*-value < 0.04). Besides, a strong statistical tendency was observed for the *RXRG* (544 bp) gene (*P*-value = 0.06). In contrast, the *MAFF* (2145 bp, *P*-value = 0.23) did not show a statistically significant differential expression, though RT-qPCR data reflected the same trends (FC and raw abundance estimates) detected by RNA-Seq. We carried out a GO analysis of the data set of 87 genes producing alternative transcripts (P-value < 0.05). We did not analyse the two other data sets (10 genes, *P*-value < 0.01 and ±0.6 log_2FC; 5 genes, q-value < 0.05 and ±0.6 log_2FC) because they are too small. The main molecular functions identified in the data set of 87 genes were *Binding* and *Catalytic activity* (Fig. 1a). These results are consistent with those of Lindholm et al. [26], who found that the main functions of mRNA encoding genes expressed in the human skeletal muscle are also related with binding and catalytic activity. The top GO terms of the cellular component GO category were *Membrane* and *Cell part* (Fig. 1b), while *Metabolism* and *Cellular process* were the most common biological processes amongst genes producing alternative transcripts (Fig. 1c). These results agree well with previous data obtained in humans, mouse and cow [23]. These functional processes are remarkably unspecific, thus probably reflecting the heterogeneous biological roles of genes expressing alternative transcripts.

Discussion

About 10.9% (average of CLC Bio and STAR results) of pig genes expressed in the GM muscle produced alternative transcripts, as opposed to 95% of genes detected in a broad array of human tissues [2]. Besides, the average number of mRNA isoforms per gene in the porcine skeletal muscle was 2.9 (average of CLC Bio and STAR results). The

analysis of transcript diversity in the human skeletal muscle revealed a similar pattern, with an average of 2 isoforms per gene [26], a figure that is clearly below the average transcript diversity (5.4 isoforms/gene) found in other human tissues [27]. Such feature might be due to the fact that in the skeletal muscle there is a reduced number of transcripts (*e.g.* myofibrillar proteins) that encompass a disproportionate fraction of the total transcriptome [26]. Besides that, Taneri et al. [28] predicted a lower quantity of transcripts per gene in primary tissues *e.g.* skeletal muscle. In cattle, Chacko et al. [29] observed that 21% of genes are alternatively spliced, and similar percentages were observed by Kim et al. [30] in cows (26%) and dogs (14%).

The types of splicing events detected in the porcine muscle have been compiled in Additional file 4: Table S4. Exon skipping was the most frequent AS event predicted by SUPPA and Splicing Express softwares, followed by the use of alternative 5′ splice (SUPPA) and 3′ splice (Splicing Express) sites. Deep sequencing of 15 human tissues and cell lines was consistent with these findings, thus demonstrating that exon skipping was the most frequent AS event, followed by the use of alternative 3′ splice and 5′ splice sites [31]. In accordance with results obtained in humans [31], the less frequent event was intron retention (Additional file 4: Table S4). Besides, only 5.0% of produced transcripts were predicted to undergo nonsense-mediated decay. In humans, nonsense-mediated decay and nuclear sequestration and turnover of intron-retention transcripts have been involved in the downregulation of genes in tissues where they do not have a relevant physiological role [32].

Though SUPPA and Splicing Express yielded consistent results about the relative importance of distinct AS event categories in the porcine skeletal muscle, the sets of genes identified by these two softwares as yielding alternative transcripts were quite different. The proportions of genes overlapping the SUPPA and Splicing Express data sets classified according to the type of AS event were: exon skipping = 27%, alternative 5′ =24%, 3′ splice sites = 20% and intron retention = 14%. Though we do not have a straightforward explanation for these discrepancies, we hypothesize that they might be due to the existence of relevant differences in the assumptions and algorithms on which these two softwares are based.

Estimating isoform mRNA abundance is a challenging task and results may vary depending on the bioinformatics approach employed in differential expression analysis [33]. One of the main factors influencing the outcome of differential mRNA isoform expression is the quality and completeness of the transcript assembly [33]. The mRNA isoform annotation of the pig genome is still incomplete and obviously this might affect the results of our analysis, but we have not attempted to re-construct transcripts because bioinformatic and statistical approaches to do so are not very robust and they may lead to inaccurate transcript quantitations [34].

In order to obtain results as much precise as possible, we have used two different pipelines to identify DE mRNA isoforms and we have considered as genuine differential expression events those identified by both approaches. This combined analysis highlighted the existence of five genes with DE mRNA isoforms that remained significant after correction for multiple testing (q-value < 0.05, ± 0.6 $\log_2$FC). It is worth to highlight that the DE isoform (487 bp) of the pig semaphorin 4D (*SEMA4D*) gene is annotated, in the Ensembl database (*Sscrofa* 10.2 assembly; https://www.ensembl.org), as truncated in its 3'end. In the human *SEMA4D* gene, there are 13 protein-encoding mRNA isoforms and five of them are also truncated in their 3'ends (GRCh38.p10 assembly; https://www.ensembl.org). The existence of truncated transcripts is due to the inability of conventional RNA-Seq experiments to define the ends of genes with high precision [35]. Moreover, automated gene prediction is a difficult task and, in consequence, first-pass annotations can be quite inaccurate [35]. Obviously, the analysis of the differential expression of mRNA isoforms strongly depends on the accuracy of transcript annotation, so the results presented in the current work need to be interpreted with this caveat in mind.

Table 2 - Splicing variants that are differentially expressed (*P*-value < 0.01 and ±0.6 log_2Fold-Change) in the gluteus medius muscle of HIGH (N = 26) vs LOW pigs (N = 26)[1]

Feature ID	Feature transcript ID	Transcript ID	Length (bp)	Relative expression mean (%)	CLC Bio			STAR/RSEM/DESeq2		
					Log_2 (FC)	*P*-value	q-value	Log_2 (FC)	*P*-value	q-value[2]
ENSSSCG00000000293	**ENSSSCT00000000314**	***ITGA5-201***	**4445**	**99.00**	**0.85**	**2.64E-05**	**2.56E-02**	**0.85**	**2.54E-06**	**1.21E-03**
ENSSSCG00000001252	ENSSSCT00000001367	*UBD-201*	1281	75.81	-0.72	1.37E-03	2.29E-01	-0.83	7.73E-04	NA
ENSSSCG00000003079	ENSSSCT00000003416	*PVR-202*	1167	48.41	0.77	7.76E-03	5.94E-01	0.66	9.27E-03	1.27E-01
ENSSSCG00000004578	**ENSSSCT00000005057**	***ANXA2-202***	**1455**	**99.36**	**0.70**	**3.32E-06**	**6.56E-03**	**0.69**	**4.56E-06**	**1.58E-03**
ENSSSCG00000012277	**ENSSSCT00000013426**	***TIMP1-001***	**931**	**97.85**	**2.57**	**4.61E-07**	**1.68E-03**	**0.79**	**2.01E-04**	**1.32E-02**
ENSSSCG00000012653	ENSSSCT00000013834	*ZDHHC9-209*	2967	17.79	0.77	3.29E-03	3.75E-01	0.77	2.56E-03	6.11E-02
ENSSSCG00000013579	ENSSSCT00000014831	*CD209-001*	1042	95.10	1.04	7.84E-05	4.18E-02	1.01	2.09E-05	NA
ENSSSCG00000006328	ENSSSCT00000033501	*RXRG-202*	544	17.68	-0.70	4.09E-04	1.18E-01	-0.76	9.31E-05	8.98E-03
ENSSSCG00000009584	**ENSSSCT00000034286**	***SEMA4D-208***	**487**	**8.57**	**1.40**	**2.75E-06**	**6.53E-03**	**1.09**	**5.87E-05**	**6.59E-03**
ENSSSCG00000024982	**ENSSSCT00000036552**	***LITAF-201***	**2190**	**88.44**	**1.01**	**1.02E-04**	**4.38E-02**	**0.79**	**1.21E-04**	**1.04E-02**

[1]Differentially expressed mRNA isoforms that remained significant after correction for multiple testing (q-value < 0.05 and ±0.6 log_2Fold-Change) are shown in bold. A positive log_2FC means that the gene is upregulated in HIGH pigs.

[2]For multiple testing correction, DESeq2 carries out a filtering step based on the average expression strength of each gene across all samples with the aim of discarding genes which are likely to loose significance after correcting for multiple testing. The purpose of this filtering step is to increase statistical power by reducing the list of candidate genes to be tested. The q-values of the genes which do not pass the filtering step are set to NA.

Table 3 - Relative expression of the set of isoforms of four loci (*TIMP1, ITGA5, ANXA2* and *LITAF*) in HIGH (N=26) *vs* LOW (N=26) pigs[1].

Feature ID	Feature transcript ID	Transcript ID	Length (bp)	Type[2]	Relative expression mean (%)	CLC Bio			STAR/RSEM/DESeq2		
						Log_2 (FC)	*P*-value	q-value	Log_2 (FC)	*P*-value	q-value[3]
ENSSSCG00000004578	ENSSSCT00000034155	*ANXA2-201*	1609	Protein coding	0.64	0.21	6.77E-01	1.00E+00	0.07	9.20E-01	NA
ENSSSCG00000004578	**ENSSSCT00000005057**	***ANXA2-202***	**1455**	**Protein coding**	**99.36**	**0.70**	**3.32E-06**	**7.23E-03**	**0.69**	**4.56E-06**	**1.58E-03**
ENSSSCG00000000293	**ENSSSCT00000000314**	***ITGA5-201***	**4445**	**Protein coding**	**99.00**	**0.85**	**2.64E-05**	**2.82E-02**	**0.85**	**2.54E-06**	**1.21E-03**
ENSSSCG00000000293	ENSSSCT00000035821	*ITGA5-203*	1255	NMD	0.34	-0.03	9.18E-01	1.00E+00	-	-	-
ENSSSCG00000000293	ENSSSCT00000034427	*ITGA5-204*	1013	NMD	0.71	-0.08	1.00E+00	1.00E+00	-	-	-
ENSSSCG00000000293	ENSSSCT00000033141	*ITGA5-205*	766	NMD	0.48	-0.29	1.00E+00	1.00E+00	-0.01	9.97E-01	NA
ENSSSCG00000012277	**ENSSSCT00000013426**	***TIMP1-001***	**931**	**Protein coding**	**97.86**	**2.57**	**4.61E-07**	**1.85E-03**	**0.79**	**2.01E-04**	**1.32E-02**
ENSSSCG00000012277	ENSSSCT00000033796	*TIMP1-002*	598	Protein coding	0.38	1.12	5.56E-01	1.00E+00	0.38	8.98E-01	NA
ENSSSCG00000012277	ENSSSCT00000034602	*TIMP1-003*	641	Protein coding	1.57	1.19	8.47E-01	1.00E+00	-0.19	7.39E-01	NA
ENSSSCG00000012277	ENSSSCT00000036308	*TIMP1-004*	173	Protein coding	0.19	3.05	4.21E-01	1.00E+00	0.18	9.52E-01	NA
ENSSSCG00000024982	**ENSSSCT00000036552**	***LITAF-201***	**2190**	**Protein coding**	88,45	1,01	**1,02E-04**	**4,82E-02**	0,79	1,21E-04	1,04E-02
ENSSSCG00000024982	ENSSSCT00000025103	*LITAF-202*	2370	Protein coding	11,55	-0,04	1,00E+00	1,00E+00	0,49	7,52E-01	NA

[1] Differentially expressed mRNA isoforms that remained significant after correction for multiple testing (q-value < 0.05 and ± 0.6 log_2Fold-Change) are shown in bold. A positive log_2FC means that the gene is upregulated in HIGH pigs.

[2] NMD= Nonsense-mediated mRNA decay.

[3] For multiple testing correction, DESeq2 carries out a filtering step based on the average expression strength of each gene across all samples with the aim of discarding genes which are likely to loose significance after correcting for multiple testing. The purpose of this filtering step is to increase statistical power by reducing the list of candidate genes to be tested. The q-values of the genes which do not pass the filtering step are set to NA.

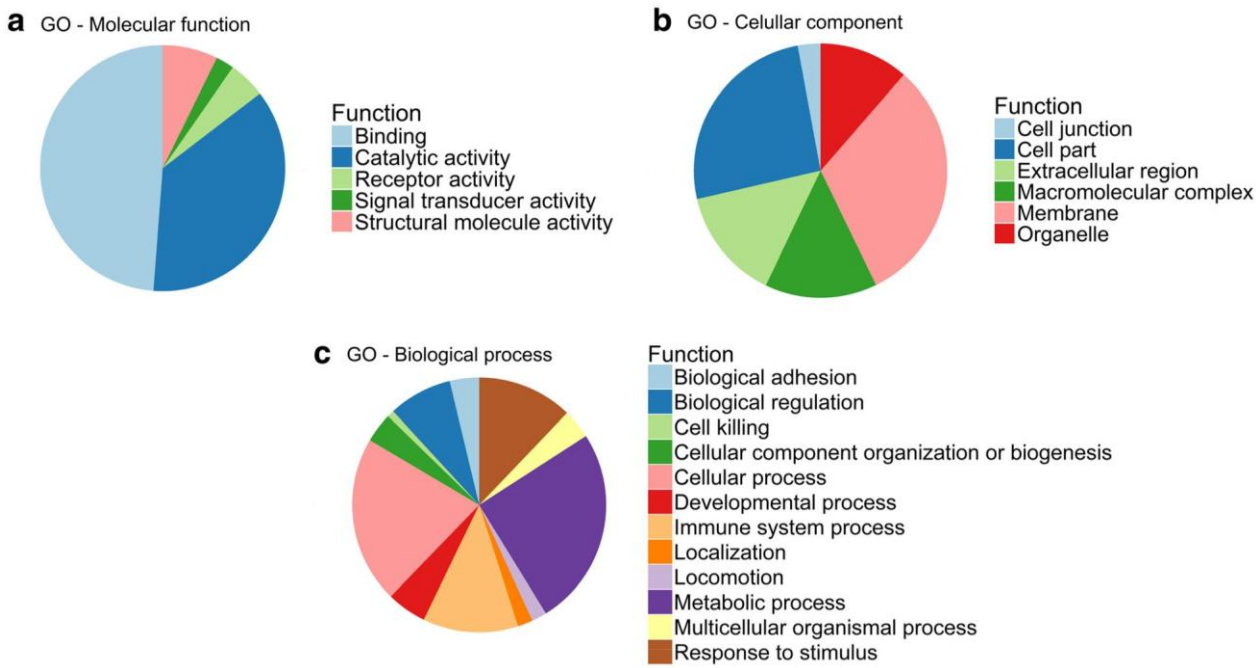

Figure 1 - Functional classification of genes with differentially expressed (*P*-value < 0.05) mRNA isoforms identified with the CLC Genomics Workbench and STAR/RSEM/DESeq2 pipelines in the gluteus medius muscle of HIGH *vs* LOW pigs. a) molecular function, b) cellular components and c) biological processes. Categorizations were based on information provided by the online resource PANTHER classification system (http://www.pantherdb.org).

By examining Tables 2 and 3, we have noticed that the differential expression of mRNA isoforms might have different functional consequences depending on the gene under consideration. For instance, in the case of the *ITGA5* and *TIMP* metallopeptidase inhibitor 1 (*TIMP1*) genes the DE mRNA isoform encodes a protein that is longer than the proteins encoded by the remaining mRNA isoforms recorded in the Ensembl database (*Sscrofa* 10.2 assembly; https://www.ensembl.org). With regard to *ITGA5*, the DE isoform (4445 bp) encodes a full length protein of 1057 amino acids (aa) and it has a predominant pattern of expression (99%), while the remaining porcine *ITGA5* isoforms reported in the Ensembl database correspond to processed transcripts or transcripts subject to nonsense-mediated decay. Similarly, in humans there is one major *ITGA5* isoform (4444 bp), another one that might encode a protein but it is truncated in its 5'end, and eleven isoforms that correspond to processed transcripts, retained introns and transcripts subject to nonsense-

mediated decay (https:// www.ensembl.org). Concerning the *TIMP1* gene, the DE isoform (931 bp) encodes a full length protein of 207 aa that is longer than the proteins encoded by other isoforms (*Sscrofa* 10.2 assembly; https://www.ensembl.org): 195 aa (but incomplete 5'end), 123 aa and 38 aa (but incomplete 3'end). If we compare the 207 aa (931 bp transcript) and the 123 aa (598 bp transcript) *TIMP1* isoforms, the latter lacks a central part of the protein (from aa site 68 to 151), a feature that involves the loss of four of the six disulfide bridges which stabilize the fold of the molecule and of two aa residues (sites 68 and 69) which bind to the catalytic zinc [36, 37]. These observations imply that the two 207 aa and 123 aa porcine protein isoforms are expected to be very different at the functional level.

A different case is represented by the annexin A2 (*ANXA2*) and lipopolysaccharide-induced TNF-alpha factor (*LITAF*) genes in which the DE mRNA isoform (*ANXA2*: 1455 bp, *LITAF*: 2190 bp) is shorter than the longest annotated transcript (*ANXA2*: 1609 bp, *LITAF*: 2370 bp, Table 3) but both encode proteins of identical length (*ANXA2*: 339 aa, *LITAF*: 161 aa, *Sscrofa* 10.2 assembly; https://www.ensembl.org). This situation is comparable to what has been reported in humans for the *ANXA2* (1676 bp, 1444 bp and 1435 bp isoforms encoding a protein of 339 aa) and *LITAF* (six different isoforms *e.g.* 2632 bp, 2467 bp, 2356 bp, 1118 bp, 717 bp and 603 bp mRNAs encoding a protein of 161 aa) genes (GRCh38.p10 assembly; http://www.ensembl.org). Though proteins with an identical length and sequence composition should be functionally equivalent, differences in transcript length might affect mRNA translatability (*e.g.* presence of short upstream open reading frames in the 5'UTR), stability (*e.g.* formation of stable stem-loops, presence of microRNA binding sites and of AU-rich elements) and cell localization [38].

The upregulation of certain mRNA isoforms of the *ITGA5*, *TIMP1*, *ANXA2* and *LITAF* genes in HIGH pigs is relevant because these four genes have been implicated in human obesity and diabetes. For instance, high glucose concentrations induce the overexpression of the fibronectin receptor, an heterodimer whose α-chain is encoded by the *ITGA5* gene [39]. Moreover, *TIMP1* expression is increased in the serum and adipose tissue of obese mouse models [40]. There is also evidence that the knockout of the *ANXA2* gene in mice involves an hypotrophy of the white adipose tissue due to reduced fatty acid uptake [41],

and *LITAF* mRNA is overexpressed in overweight and obese humans [42]. In summary, the upregulation of these four genes in HIGH swine is consistent with the increased fatness and live weight of these pigs and suggests that the differential expression of specific mRNA isoforms might contribute to the phenotypic differences observed in HIGH *vs* LOW pigs.

Finally, we would like to discuss a third case in which DE mRNA isoforms encode proteins that are shorter than the canonical full-length protein. We have observed that a 3155 bp transcript corresponding to the porcine ubiquitin specific peptidase 2 (*USP2*) gene and encoding a 396 aa protein is upregulated in HIGH pigs (Additional file 5: Table S5). In the Ensembl database (http://www.ensembl.org, *Sscrofa* 10.2), a second mRNA isoform that encodes a 606 aa protein has been annotated. In humans, two USP2 protein isoforms of 605 aa (*USP2–69*) and 396 aa (*USP2–45*) have been reported and that there are evidences that both are able to prevent the degradation of the low density lipoprotein (LDL) receptor. The upregulation of the 396 aa *USP2* isoform in HIGH swine might constitute a mechanism to cope with the elevated serum LDL concentrations observed in this group of pigs (Table 1). It is also worth to highlight that the *USP2–69* and *USP2–45* isoforms might not be functionally equivalent. In Xenopus, for instance, *USP2–45* can deubiquitylate epithelial Na^+ channels in oocytes, while *USP2–69* cannot perform such function due to differences in their N-terminal domains. In humans, functional differences have been also observed with regard to the implication of *USP2* isoforms in cell cycle progression and antiviral response [43], but unfortunately no such data are currently available for pigs.

Conclusions

We have demonstrated that around 10.9% of genes expressed in the porcine skeletal muscle produce alternative transcripts, thus generating an average of 2.9 different mRNA isoforms per gene. Exon skipping is the most frequent splicing event, followed by the use of alternative 5′ splice sites (SUPPA) and 3′ splice sites (Splicing Express). By analysing the differential expression of mRNA isoforms in HIGH *vs* LOW pigs, we have demonstrated that in the GM muscle of HIGH pigs, which display an increased fatness,

specific *ITGA5, ANXA2, LITAF* and *TIMP1* mRNA isoforms are upregulated. This finding is biologically meaningful because these four genes have been implicated in human obesity and metabolism [39–42]. A deeper functional characterization of these mRNA isoforms, through initiatives such as the Functional Annotation of Farm Animal Genomes project [44], will be essential to infer the consequences of their differential expression on porcine growth and fatness.

Additional files

Additional file 1: Table S1. Distribution of the 56 animals sequenced by RNA-Seq in the 5 half-sib families reported by Gallardo et al. [13].

Additional file 2: Table S2. Primers employed in the validation of four differentially expressed isoforms by RT-qPCR.

Additional file 3: Table S3. Alternatively spliced mRNA isoforms identified in the porcine gluteus medius muscle of Duroc pigs by CLC Bio and/or STAR/ RSEM/ DESEq2.

Additional file 4: Table S4. Classification of alternative splicing (AS) events detected in the porcine gluteus medius muscle with the SUPPA and Splicing Express softwares.

Additional file 5: Table S5. Differentially expressed (*P*-value < 0.05) mRNA isoforms (HIGH *vs* LOW pigs) found with CLC Bio and STAR/RSEM/ DESeq2 softwares.

Additional file 6: Table S6. Relative transcript levels of a set of isoforms corresponding to five genes expressed in the gluteus medius muscle of HIGH and LOW pigs identified with the CLC Bio and STAR/RSEM/DESeq2 pipelines.

Additional file 7: Figure S1. Validation by RT-qPCR of the differential expression of mRNA isoforms corresponding to the *RXRG, SCD*, *MAFF* and *ITGA5* genes in HIGH *vs* LOW pigs.

Acknowledgements

The authors are indebted to Selección Batallé S.A. for providing the animal material. We gratefully acknowledge to J. Reixach (Selecció Batallé), J. Soler (IRTA), C. Millan (IRTA), A. Quintana (IRTA) and A. Rossell (IRTA) for their collaboration in the experimental protocols and pig management.

Funding

Part of the research presented in this publication was funded by grants AGL2013–48742-C2–1-R and AGL2013–48742-C2–2-R awarded by the Spanish Ministry of Economy and Competitivity and grant 2014 SGR 1528 from the Agency for Management of University and Research Grants of the Generalitat de Catalunya. We also acknowledge the support of the Spanish Ministry of Economy and Competitivity for the Center of Excellence Severo Ochoa 2016–2019 (SEV-2015-0533) grant awarded to the Centre for Research in Agricultural Genomics (CRAG). Tainã Figueiredo Cardoso was funded with a fellowship from the CAPES Foundation-Coordination of Improvement of Higher Education, Ministry of Education of the Federal Government of Brazil. Rayner Gonzalez-Prendes was funded with a FPU Ph.D. grant from the Spanish Ministry of Education (FPU12/00860). Thanks also to the CERCA Programme of the Generalitat de Catalunya. The funders had no role in study design, data collection and analysis, decision to publish or preparation of the manuscript.

Availability of data and materials

Data have been deposited in the Figshare database (https://doi.org/10.6084/m9.figshare.5831235.v1).

Authors' contributions

MA, ACan and RQ designed the experiment; RQ was responsible for the experimental protocols and generation of animal material; all authors contributed to the obtaining of biological samples; TFC and RGP performed RNA extractions; TFC analysed the RNA-Sequencing data; ACas designed the RT-qPCR experiments; TFC carried out the RT-qPCR validation experiments; TFC and ACas analysed the RT-qPCR data; MA, ACan and TFC wrote the paper. All authors read and approved the manuscript.

Ethics approval and consent to participate

Animal care, management procedures and blood sampling were performed following national guidelines for the Good Experimental Practices and they were approved by the Ethical Committee of the Institut de Recerca i Tecnologia Agroalimentàries (IRTA).

Consent for publication

Not applicable.

Competing interests

The authors declare no competing interests.

References

1. Reyes A, Huber W. Alternative start and termination sites of transcription drive most transcript isoform differences across human tissues. Nucleic Acids Res. 2017;46:582–92.
2. Barash Y, Calarco JA, Gao W, Pan Q, Wang X, Shai O, et al. Deciphering the splicing code. Nature. 2010;465:53–9.
3. Eswaran J, Horvath A, Godbole S, Reddy SD, Mudvari P, Ohshiro K, et al. RNA sequencing of cancer reveals novel splicing alterations. Sci Rep. 2013;3:93–7.

4. Yao Y, Shang J, Song W, Deng Q, Liu H, Zhou Y. Global profiling of the gene expression and alternative splicing events during hypoxia-regulated chondrogenic differentiation in human cartilage endplate-derived stem cells. Genomics. 2016;107:170–7.

5. Zhang S, Cai H, Yang Q, Shi T, Pan C, Lei C, et al. Identification of novel alternative splicing transcript and expression analysis of bovine *TMEM95* gene. Gene. 2016;575:531–6.

6. Xie Y, Yang S, Cui X, Jiang L, Zhang S, Zhang Q, et al. Identification and expression pattern of two novel alternative splicing variants of *EEF1D* gene of dairy cattle. Gene. 2014;534:189–96.

7. Ma J, Yang J, Zhou L, Ren J, Liu X, Zhang H, et al. A splice mutation in the *PHKG1* gene causes high glycogen content and low meat quality in pig skeletal muscle. PLoS Genet. 2014;10:e1004710.

8. Koltes JE, Fritz-Waters E, Eisley CJ, Choi I, Bao H, Kommadath A, et al. Identification of a putative quantitative trait nucleotide in guanylate binding protein 5 for host response to PRRS virus infection. BMC Genomics. 2015;16:4

9. Cánovas A, Quintanilla R, Amills M, Pena RN. Muscle transcriptomic profiles in pigs with divergent phenotypes for fatness traits. BMC Genomics. 2010; 11:372.

10. Ayuso M, Óvilo C, Rodríguez-Bertos A, Rey AI, Daza A, Fenández A, et al. Dietary vitamin A restriction affects adipocyte differentiation and fatty acid composition of intramuscular fat in Iberian pigs. Meat Sci. 2015;108:9–16.

11. Cánovas A, Pena RN, Gallardo D, Ramírez O, Amills M, Quintanilla R, et al. Segregation of regulatory polymorphisms with effects on the *gluteus medius* transcriptome in a purebred pig population. PLoS One. 2012;7: e35583.

12. Puig-Oliveras A, Ramayo-Caldas Y, Corominas J, Estellé J, Pérez-Montarelo D, Hudson NJ, et al. Differences in muscle transcriptome among pigs phenotypically extreme for fatty acid composition. PLoS One. 2014;9:e99720.

13. Gallardo D, Pena RN, Amills M, Varona L, Ramírez O, Reixach J, et al. Mapping of quantitative trait loci for cholesterol, LDL, HDL, and triglyceride serum concentrations in pigs. Physiol Genomics. 2008;35:199–209.

14. Mach N, Devant M, Díaz I, Font-Furnols M, Oliver MA, García JA, et al. Increasing the amount of n-3 fatty acid in meat from young Holstein bulls through nutrition. J Anim Sci. 2006;84:3039–48.

15. Friedewald WT, Levy RI, Fredrickson DS. Estimation of the concentration of low-density lipoprotein cholesterol in plasma, without use of the preparative ultracentrifuge. Clin Chem. 1972;18:499–502.

16. Bolger AM, Lohse M, Usadel B. Trimmomatic: a flexible trimmer for Illumina sequence data. Bioinformatics. 2014;30:2114–20.

17. Dobin A, Davis CA, Schlesinger F, Drenkow J, Zaleski C, Jha S, et al. STAR: ultrafast universal RNA-Seq aligner. Bioinformatics. 2013;29:15–21.

18. Li B, Dewey CN. RSEM: accurate transcript quantification from RNA-Seq data with or without a reference genome. BMC Bioinformatics. 2011;12:323.

19. Love MI, Huber W, Anders S. Moderated estimation of fold change and dispersion for RNA-Seq data with DESeq2. Genome Biol. 2014;15:550.

20. Robinson MD, Smyth GK. Small-sample estimation of negative binomial dispersion, with applications to SAGE data. Biostatistics. 2008;9:321–32.

21. Zhang C, Zhang B, Lin LL, Zhao S. Evaluation and comparison of computational tools for RNA-Seq isoform quantification. BMC Genomics. 2017;18:583.

22. Alamancos GP, Pagès A, Trincado JL, Bellora N, Eyras E. Leveraging transcript quantification for fast computation of alternative splicing profiles. RNA. 2015;21:1521–31.

23. Kroll JE, Kim J, Ohno-Machado L, de Souza SJ. Splicing Express: a software suite for alternative splicing analysis using next-generation sequencing data. PeerJ. 2015;3:e1419.

24. Trapnell C, Williams BA, Pertea G, Mortazavi A, Kwan G, van Baren MJ, et al. Transcript assembly and quantification by RNA-Seq reveals unannotated transcripts and isoform switching during cell differentiation. Nat Biotechnol. 2010;28:511–5.

25. Livak KJ, Schmittgen TD. Analysis of relative gene expression data using real-time quantitative PCR and the 2^{-CT} method. Methods. 2001;25:402–8.

26. Lindholm ME, Huss M, Solnestam BW, Kjellqvist S, Lundeberg J, Sundberg CJ. The human skeletal muscle transcriptome: sex differences, alternative splicing, and tissue homogeneity assessed with RNA sequencing. FASEB J. 2014;28:4571–81.

27. Birney E, Stamatoyannopoulos JA, Dutta A, Guigo R, Gingeras TR, Margulies EH, et al. Identification and analysis of functional elements in 1% of the human genome by the ENCODE pilot project. Nature. 2007;447:799–816.

28. Taneri B, Snyder B, Novoradovsky A, Gaasterland T. Alternative splicing of mouse transcription factors affects their DNA-binding domain architecture and is tissue specific. Genome Biol. 2004;5:R75.

29. Chacko E, Ranganathan S. Genome-wide analysis of alternative splicing in cow: implications in bovine as a model for human diseases. BMC Genomics. 2009;10:S3–S11.

30. Kim N, Alekseyenko AV, Roy M, Lee C. The ASAP II database: analysis and comparative genomics of alternative splicing in 15 animal species. Nucleic Acids Res. 2007;35:D93–8.

31. Wang ET, Sandberg R, Luo S, Khrebtukova I, Zhang L, Mayr C, et al. Alternative isoform regulation in human tissue transcriptomes. Nature. 2008; 456:470–6.

32. Braunschweig U, Barbosa-Morais NL, Pan Q, Nachman EN, Alipanahi B, Gonatopoulos-Pournatzis T, et al. Widespread intron retention in mammals functionally tunes transcriptomes. Genome Res. 2014;24:1774–86.

33. Hartley SW, Mullikin JC. Detection and visualization of differential splicing in RNA-Seq data with JunctionSeq. Nucleic Acids Res. 2016;44:e127.

34. Shenker S, Miura P, Sanfilippo P, Lai EC. IsoSCM: improved and alternative 3' UTR annotation using multiple change-point inference. RNA. 2015;21:14–27.

35. Schurch NJ, Cole C, Sherstnev A, Song J, Duc C, Storey KG, et al. Improved annotation of 3′ untranslated regions and complex loci by combination of strand-specific direct RNA sequencing, RNA-Seq and ESTs. PLoS One. 2014;9: e94270.

36. Batra J, Robinson J, Soares AS, Fields AP, Radisky DC, Radisky ES. Matrix metalloproteinase-10 (MMP-10) interaction with tissue inhibitors of metalloproteinases *TIMP-1* and *TIMP-2*: binding studies and crystal structure. J Biol Chem. 2012;287:15935–46.

37. Gomis-Rüth F-X, Maskos K, Betz M, Bergner A, Huber R, et al. Mechanism of inhibition of the human matrix metalloproteinase stromelysin-1 by *TIMP-1*. Nature. 1997;389:77–81.

38. Mockenhaupt S, Makeyev EV. Non-coding functions of alternative pre-mRNA splicing in development. Semin Cell Dev Biol. 2015;47–48:32–9.

39. Roth T, Podestá F, Stepp MA, Boeri D, Lorenzi M. Integrin overexpression induced by high glucose and by human diabetes: potential pathway to cell dysfunction in diabetic microangiopathy. Proc Natl Acad Sci USA. 1993;90:9640–4.

40. Meissburger B, Stachorski L, Röder E, Rudofsky G, Wolfrum C. Tissue inhibitor of matrix metalloproteinase 1 (*TIMP1*) controls adipogenesis in obesity in mice and in humans. Diabetologia. 2011;54:1468–79.

41. Salameh A, Daquinag AC, Staquicini DI, An Z, Hajjar KA, Pasqualini R, et al. Prohibitin/annexin 2 interaction regulates fatty acid transport in adipose tissue. JCI Insight. 2016;1:e86351.

42. Ji ZZ, Dai Z, Xu YC. A new tumor necrosis factor (TNF)-α regulator, lipopolysaccharides-induced TNF-α factor, is associated with obesity and insulin resistance. Chin Med J. 2011;124:177–82.

43. Zhu H-Q, Gao F-H. The molecular mechanisms of regulation on *USP2*'s alternative splicing and the significance of its products. Int J Biol Sci. 2017; 13:1489–96.

44. Andersson L, Archibald AL, Bottema CD, Brauning R, Burgess SC, Burt DW, et al. Coordinated international action to accelerate genome-to-phenome with FAANG, the functional annotation of animal genomes project. Genome Biol. 2015;16:57.

Nutrient supply affects the mRNA expression profile of the porcine skeletal muscle.

Cardoso TF[1,2], Quintanilla R[3], Tibau J[4], Gil M[4], Mármol-Sánchez E[1], González-Rodríguez O[2], González-Prendes R[1], Amills M[5,6,a].

[1]Department of Animal Genetics, Center for Research in Agricultural Genomics (CSIC-IRTA-UAB-UB), Universitat Autònoma de Barcelona, 08193, Bellaterra, Spain. [2]CAPES Foundation, Ministry of Education of Brazil, Brasilia D. F., Zip Code 70.040-020, Brazil.[3]Animal Breeding and Genetics Program, Institute for Research and Technology in Food and Agriculture (IRTA), Torre Marimon, 08140, Caldes de Montbui, Spain.[4]IRTA-Monells, Finca Camps i Armet s/n 17121, Monells, Spain. [5]Department of Animal Genetics, Center for Research in Agricultural Genomics (CSIC-IRTA-UAB-UB), Universitat Autònoma de Barcelona, 08193, Bellaterra, Spain. marcel.amills@uab.cat.[6]Departament de Ciència Animal i dels Aliments, Facultat de Veterinària, Universitat Autònoma de Barcelona, 08193, Bellaterra, Spain. marcel.amills@uab.cat.

[a]Corresponding author: M. Amills

BMC Genomics. 2017 Aug 10;18(1):603.

doi: 10.1186/s12864-017-3986-x.

Abstract

The genetic basis of muscle fat deposition in pigs is not well known. So far, we have only identified a limited number of genes involved in the absorption, transport, storage and catabolism of lipids. Such information is crucial to interpret, from a biological perspective, the results of genome-wide association analyses for intramuscular fat content and composition traits. Herewith, we have investigated how the ingestion of food changes gene expression in the *gluteus medius* muscle of Duroc pigs. By comparing the muscle mRNA expression of fasted pigs (T0) with that of pigs sampled 5 h (T1) and 7 h (T2) after food intake, we have detected differential expression (DE) for 148 (T0-T1), 520 (T0-T2) and 135 (T1-T2) genes (q-value <0.05 and a |FC| > of 1.5). Many of these DE genes were transcription factors, suggesting that we have detected the coordinated response of the skeletal muscle to nutrient supply. We also found DE genes with a dual role in oxidative stress and angiogenesis (*THBS1, THBS2* and *TXNIP*), two biological processes that are probably activated in the post-prandial state. Finally, we have identified several loci playing a key role in the modulation of circadian rhythms (*ARNTL*, *PER1*, *PER2*, *BHLHE40*, *NR1D1*, *SIK1*, *CIART* and *CRY2*), a result that indicates that the porcine muscle circadian clock is modulated by nutrition. We have shown that hundreds of genes change their expression in the porcine skeletal muscle in response to nutrient intake. Many of these loci do not have a known metabolic role, a result that suggests that our knowledge about the genetic basis of muscle energy homeostasis is still incomplete.

Keywords: Pig, RNA-Seq, Oxidative stress, Transcription factor, Circadian rhythm, Angiogenesis

Background

Physiological genomics aims to understand the molecular basis of highly complex biological processes by applying high-throughput technologies to the large-scale analysis of genomes, transcriptomes and proteomes [1]. We have a very limited understanding of the physiological genomics of intramuscular fat (IMF) content and composition traits in

pigs. Several RNA-Seq studies comparing the muscle transcriptomes of pigs with divergent lipid profiles have been performed, demonstrating the differential expression of a number of genes related with carbohydrate and lipid metabolism [2–4]. Noteworthy, genome-wide association studies (GWAS) of blood lipid traits in humans have uncovered the existence of a large number of genes strongly associated with plasma lipid concentrations whose involvement in lipoprotein metabolism had never been reported before [5]. For instance, Teslovich et al. [6] performed a GWAS for lipid traits in 100,000 individuals and identified several associated loci (*e.g. GALNT2*, *PPP1R3B*, and *TTC39B*) whose participation in lipid metabolism had not been described previously. Similarly, the Global Lipids Genetics Consortium reported 62 novel loci displaying significant associations with blood lipid levels, and 30 of them had never been previously connected to lipid metabolism [7]. In the light of these results, we can infer that many genes contributing to muscle fat deposition remain to be identified.

The skeletal muscle compartment encompasses a substantial fraction of the body weight and accounts for ≈75% of total insulin-stimulated glucose uptake [8]. Moreover, adipose and muscle tissues absorb most of the chylomicrons generated after a meal consumption [9]. Fat deposition in the porcine muscle may depend, at least in part, on the activation of genes that regulate the uptake, transport, storage, synthesis and degradation of fatty acids (FA) and carbohydrates. As a first step to identify such genes, we have investigated how the profile of pig muscle mRNA expression changes in response to nutrient supply.

Methods

Animal material and metabolic profile

A group of 36 female piglets belonging to a commercial Duroc line were brought, after weaning (age = 3–4 weeks), to the IRTA-Pig Experimental Farm at Monells (Girona, Spain). They were fed with a transition feed for 40 days, and, at an approximate age of 2 months, they entered the fattening period. Gilts were housed individually and fed ad libitum with a commercial feeding diet (13% and 5.5% of crude protein and crude fat

respectively) until they reached an average live weight of 73 ± 1.2 kg (161 ± 1.1 days). The post-prandial time-points at which muscle gene expression should be analysed were chosen on the basis of the following experiment (experiment 1): we selected at random eight Duroc gilts (out of the 36), with an approximate age of 100 days, and blood samples were taken with citrate Vacutainer tubes before feeding and 2, 4, 6 h. after feeding. These 32 samples were submitted to the Veterinary Clinical Biochemistry Service of the Universitat Autònoma de Barcelona (http://sct.uab.cat/sbcv). The following metabolites were measured using standard protocols: plasma glucose, triglycerides, cholesterol and non-esterified fatty acids.

In experiment 2, we analysed the transcriptomic changes associated with food intake by sequencing the muscle transcriptomes of the 36 Duroc gilts mentioned in the previous paragraph. These gilts were slaughtered at the IRTA-Experimental slaughterhouse in Monells (Girona, Spain) in controlled conditions and complying all national welfare regulations. These 36 sows fasted 12 h prior slaughtering and then 12 of them were stunned, with high concentrations of CO_2 to minimize pain, and bled (T0, fasting). The remaining 24 gilts were supplied with a standard feed ad libitum, and slaughtered 5 h (T1, N = 12) and 7 h (T2, N = 12) after T0, following the same procedure reported above. Before slaughter, we took blood samples from these sows and triglyceride and plasma free FA were measured at the Veterinary Clinical Biochemistry Service of the Universitat Autònoma de Barcelona (http://sct.uab.cat/sbcv). After slaughtering, samples of the *gluteus medius* muscle were collected and submerged in RNAlater (Ambion), being stored at −80 °C until use.

RNA isolation and library construction and sequencing

Each muscle sample was individually submerged in liquid nitrogen and pulverized with a mortar and a pestle. This powder was homogenized with a polytron device in 1 mL of TRI Reagent (Thermo Fisher Scientific, Barcelona, Spain). Total RNA was extracted from *gluteus medius* muscle samples by using the acid phenol method implemented in the RiboPure kit (Ambion, Austin, TX). Total RNA concentration and purity were assessed with a Nanodrop ND-1000 spectrophotometer (Thermo Fisher Scientific, Barcelona,

Spain), while integrity was checked with a Bioanalyzer-2100 equipment (Agilent Technologies, Inc., Santa Clara, CA). Total RNA samples were submitted to the Centre Nacional d'Anàlisi Genòmica (CNAG, http://www.cnag.cat) for sequencing. Individual libraries for each one of the analysed pigs (N = 36) were prepared using the TruSeq Stranded mRNA Library Preparation Kit (Illumina Inc., CA) according to the protocols recommended by the manufacturer. This level of replication is 4-fold higher than the minimum required (3 individuals/group) in standard RNA-Seq studies. Each library was paired-end sequenced (2 × 75 bp) in a HiSeq 2000 platform (Illumina Inc., CA) by using the TruSeq SBS Kit v3-HS (Illumina Inc., CA).

Bioinformatic analyses

Quality control of sequence reads was carried out with the FASTQC software (Babraham Bioinformatics, http://www.bioinformatics.babraham.ac.uk/projects/fastqc/). We made per-sequence and per-base analyses to filter reads according to the following criteria: sequence-read distribution = 75 bp, 100% coverage in all bases, GC-content ~50%, ~25% of A, T, G and C nucleotide contributions, ambiguous base-content <0.1% and a Phred score higher than 30 (*i.e.* base-calling accuracy larger than 99.9%). Subsequently, sequences were trimmed for any remaining sequencing adapter by using Trimmomatic v.0.22 [10]. Raw reads were mapped to the pig reference genome (version 10.2) with the STAR Alignment v.2.5. software [11] by using default parameters and STAR 2-pass alignment steps. The FeatureCounts tool [12] was used to summarize counts of unambiguously mapped reads. The expression of each mRNA was estimated with DESeq2 [13]. This software builds a count matrix K_{ij} (with one row for each gene i and one column for each sample *j*) encompassing the number of sequencing reads that have been unambiguously mapped to a gene in a sample [13]. The main assumption of this method is that read counts follow a negative binomial distribution with mean μ_{ij} and dispersion α_i [13]. A second important assumption is that genes of similar average expression levels are expected to have a similar dispersion α_i value. DESeq2 calculates final dispersion values by using an empirical Bayes approach that shrinks dispersion estimates towards a set of predicted α_i values. When dealing with genes that are poorly

expressed, $\log_2$ fold-change (FC) estimates can have a high variance due to noisiness issues. To avoid this potential problem, DESeq2 shrinks $\log_2$FC estimates, with an empirical Bayes procedure [13]. Finally, a Wald test is used to infer if shrunken $\log_2$FC estimates (and their standard errors) are significantly different from zero. In the Wald test, the shrunken estimate of the $\log_2$FC is divided by its standard error, generating a z-statistic that can be compared to a standard normal distribution [13]. Correction for multiple testing is achieved by using a false discovery rate approach [14]. We considered as differentially expressed (DE) those mRNAs displaying a $|FC| > 1.5$ and a q-value <0.05.

Advaita Bio's iPathwayGuide (http://www.advaitabio.com/ipathwayguide) and the Cytoscape software [15] combined with the ReactomeFIViz app [16] were used to infer if certain gene ontology terms and pathways are enriched across the sets of DE genes as well as to build biological networks. In order to detect the GO categories that are over- or under-represented in the condition under study, Advaita Bio's iPathwayGuide uses an impact analysis method that relies on classical statistics but also takes into account other key factors such as the magnitude of each gene's expression change, their type and position in the given pathways, their interactions, etc. [17]. The ReactomeFIViz application can access the Reactome pathways database in order to do pathway enrichment analysis for a set of genes and visualize hit pathways with the aid of Cytoscape [16]. This application can also access the Reactome Functional Interaction (FI) network to construct a FI sub-network based on a set of genes [16]. In our study, the standard ReactomeFIViz "Gene Set/Mutation Analysis" application was employed to build gene functional interaction networks on the basis of a list of DE genes (q-value <0.05 and a $|FC| >$ of 1.5) and curated pathway information contained in the Reactome database. The functional enrichment analyses for pathways and GO annotations were based on a binomial test [16].

Results

In Experiment 1, measurement of the concentrations of plasma glucose, cholesterol, triglycerides and non-esterified fatty acids revealed that glycaemia and lipidemia peaks took place 2 and 4 h after the 8 Duroc gilts began to eat, a result that was very consistent across individuals (Fig. 1). Eating was also accompanied by a marked decrease of plasma

free FA (Fig. 1), a finding that agrees well with the role of these metabolites as a source of energy during fasting. We chose 5 and 7 h post-ingestion as time-points to carry out the analysis of differential expression. Our expectation was that T1 would reflect the process of lipid absorption, while T2 would correspond to a posterior phase in which lipids are stored as triglycerides or catabolized in the β-oxidation pathway to generate ATP. Nevertheless, when we measured the concentrations of triglycerides and plasma free fatty acids in the slaughtered sows forming part of Experiment 2 (Additional file 1: Figure S1), we observed that feeding is associated with an increase in the concentration of triglycerides and a decrease of circulating free FA levels, a result that matches the metabolic profile observed in Experiment 1. However, the kinetics of these two metabolites were not identical to those observed in Experiment 1 because 7 h after feeding triglyceride levels were still peaking. Despite this circumstance, our main comparison (fasting *vs* fed pigs) remains completely valid.

The RNA-Seq experiment generated an average of 45 million paired-end reads per sample and 69.8% of them were unambiguously mapped to the pig *Sscrofa*10.2 genome assembly. Analysis of the data with DESeq2 highlighted 148 (T0 *vs* T1), 520 (T0 *vs* T2) and 135 (T1 *vs* T2) differentially expressed mRNA-encoding genes (Additional file 2: Table S1). Moreover, 85 genes showed DE both in the T0-T1 and T0-T2 comparisons, a result that evidences the high consistency of our results. The analyses of pathways and signalling networks enriched in DE genes with Advaita iPathwayGuide (http://www.advaitabio.com/ ipathwayguide) revealed 18 (T0-T1), 18 (T0-T2) and 14 (T1-T2) enriched pathways (Table 1). Similarly, the ReactomeFIViz app identified 34 (T0-T1), 18 (T0-T2) and 15 (T1-T2) pathways (Additional file 3: Table S2). In both analyses, we identified pathways related with (1) T0-T1: circadian clock system, muscle contraction and signaling in cardiomyocytes; (2) T0-T2: circadian rhythm and ribosome pathway; and (3) T1-T2: oxidative phosphorylation, metabolic process and ribosome pathways. Differentially expressed mRNA-encoding genes were also grouped in gene regulatory networks with the ReactomeFIViz app. We found 6 (T0-T1), 20 (T0-T2) and 4 (T1-T2) functional interaction networks which are displayed in Figs. 2, 3 and 4. Several enriched pathways (q-value <0.05) such as Wnt signaling pathway (T0-T2), TNF signalling (T0-T1), ATF-2 transcription factor network (T0-T2) and oxidative phosphorylation (T0-T2,

T1-T2) are tightly linked to metabolism and energy homeostasis. We also found pathways related with striated muscle contraction (T0-T1) and myogenesis (T0-T2), a result that could be anticipated given the predominance of myofibrilar proteins in the muscle proteome. Other pathways of interest were circadian clock and rhythm (T0-T1, T0-T2), oxidative stress induced gene expression via Nrf2 (T0-T2) and SRP-dependent cotranslational protein targeting to membrane (T1-T2) and eukaryotic translation termination (T1-T2).

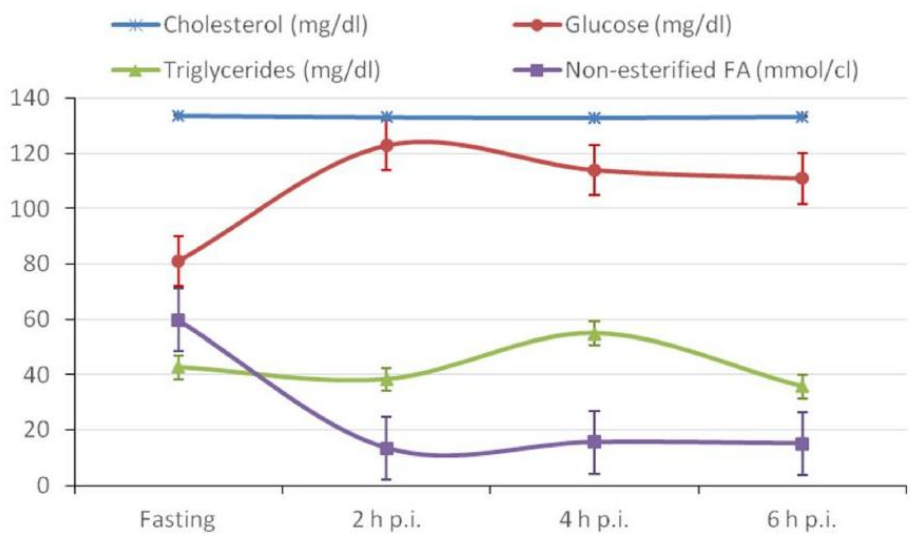

Figure 1 - Kinetics of the average concentrations of plasma glucose, cholesterol, triglycerides and non-esterified fatty acids (FA) in 8 Duroc pigs at four time points: before eating and 2, 4 and 6 h post-ingestion (p.i).

Considering gene ontology (GO) cellular component, biological process and molecular function related to network functions, the top-scoring networks were (1) T0-T1: transcription factor complex, circadian regulation of gene expression and E-box binding; (2) T0-T2: nucleo-plasm, negative regulation of transcription from RNA polymerase II promoter and structural constituent of ribosome and (3) T1-T2: cytosolic small ribosomal

subunit, translation and structural constituent of ribosome (Additional file 4: Table S3). We have an established role in metabolism, while for others evidence reported in the literature is more tenuous or even absent. For instance, the 6-phosphofructo-2-kinase/fructose-2,6-biphosphatase 3 (*PFKFB3*, T0-T1: FC = −3.01, q-value = 1.91E-07) gene can modulate glucose homeostasis by regulating the levels of fructose-2,6-biphosphate [18], and there are substantial evidences that the G0/G1 switch 2 (*G0S2*, T0-T1: FC = 1.84, q-value = 4.03E-02; T0-T2: FC = 2.06, q-value = 9.35E-04) protein is involved in the regulation of the rate-limiting lipolytic enzyme adipose triglyceride lipase [19].

Discussion

Post-prandial activation of genes with and without known roles in muscle energy homeostasis

Several of the genes that show the most significant DE between fasted and fed animals (Additional file 2: Table S1), have an established role in metabolism, while for others evidence reported in the literature is more tenuous or even absent. For instance, the 6-phosphofructo-2-kinase/fructose-2,6-biphosphatase 3 (*PFKFB3*, T0-T1: FC = −3.01, q-value = 1.91E-07) gene can modulate glucose homeostasis by regulating the levels of fructose-2,6-biphosphate [18], and there are substantial evidences that the G0/G1 switch 2 (*G0S2*, T0-T1: FC = 1.84, q-value = 4.03E-02; T0-T2: FC = 2.06, q-value = 9.35E-04) protein is involved in the regulation of the rate-limiting lipolytic enzyme adipose triglyceride lipase [19].

The analysis of Additional file 2: Table S1 also evidences the existence of DE for several genes with a plausible but poorly characterized role in metabolism. A good example is the mitoguardin 2 (*MIGA2*, T0-T1: FC = 1.62, q-value = 1.86E-02; T0-T2: FC = 2.22, q-value = 2.10E-05) gene, which shows a dramatic increase in its expression after food intake *i.e. MIGA2* is 1.62 and 2.22 times more expressed at 5 and 7 h post-ingestion, respectively. This gene encodes a protein that regulates mitochondrial [20]. Noteworthy, mitochondrial dynamics is highly inter-connected with the energy status of the cell, and it

has been demonstrated that starvation promotes an acute inhibition of mitochondrial fission [21]. Another gene of interest is syndecan 4 (*SDC4*, T0-T1: FC = −1.80, q-value = 3.88E-04; T0-T2: FC = −1.82, q-value = 9.59E-04), whose expression levels decreased at 5 h and 7 h after ingestion. In mammals, this gene has been mostly related with cell-matrix adhesion, migration, neuronal development, and inflammation, but studies performed in Drosophila have revealed that it may also have broad effects on the regulation of energy homeostasis [22]. A third example would be the cysteine- serine-rich nuclear protein 1 (*CSRNP1*, T0-T1: FC = −1.67, q-value = 5.37E-03; T0-T2: FC = −1.75, q-value = 1.07E-02), a molecule that has been mostly related with T-cell immunity and cephalic neural progenitor proliferation [24]. Interestingly, the expression of this molecule is induced by axin, which appears to promote glucose uptake by enhancing the translocation of GLUT4 [25].

Finally, there is a third category of genes, exemplified by the family with sequence similarity 212, member B (*FAM212B*, T0-T1: FC = 2.04, q-value = 3.36E-02; T0-T2: FC = 2.68, q-value = 1.13E-06), transmembrane protein 169 (*TMEM169*, T0-T2: FC = 2.83, q-value = 6.81E-07) and matrix metallopeptidase 25 (*MMP25*, T0-T2: FC = −2.41, q-value = 7.97E-04) loci, that, to the best of our knowledge, have never been reported to participate in the regulation of energy homeostasis.

The ingestion of food involves changes in the muscle expression of many transcription factors

As shown in Additional file 2: Table S1, we did not detect significant changes in the expression of several genes with a well-established role in lipid uptake (*e.g. CD36*, lipoprotein lipase), synthesis (*e.g.* acetyl-CoA carboxylase, fatty acid synthase, diacylglycerol O-acyl-transferase 1), transportation (*e.g.* FA binding proteins) and catabolism (*e.g.* genes of the β-oxidation pathway). One of the few exceptions to this general trend was the lipase G locus (*LIPG*, T0-T1: FC = −1.80, q-value = 4.10E-02), which encodes and endothelial lipase modulating lipoprotein metabolism [26]. This gene shows an important drop in its expression levels (1.8 times) 5 h after food intake, a feature that would result in an inhibition of high-density lipoprotein catabolism [26].

We observed DE for many genes encoding transcription factors (Figs. 2 and 3, Additional file 2: Table S1) *e.g.* the AT-rich interactive domain 5B (*ARID5B*, T0-T2: FC = −2.31, q-value = 5.98E-04) gene, which influences adipogenesis and also the accumulation of postnatal lipid storage [27]; Kruppel-like factor 5 (*KLF5*, T0-T2: FC = −1.96, q-value = 1.25E-02), that regulates the expression of genes involved in the β-oxidation of FA [28]; *NR4A2*, (T0-T1: FC = −2.16, q-value = 8.93E-04), a nuclear orphan receptor that controls the expression of genes related with glucose metabolism [29]; CCAAT/Enhancer Binding Protein δ (*CEBPD*, T0-T1: FC = −2.33, q-value = 6.37E-05; T0-T2: FC = −1.84, q-value = 1.71E-02) that plays an essential role in adipogenesis [30]; and forkhead box O1 (*FOXO1*, T0-T1: FC = −1.55, q-value = 2.12E-02; T0-T2: FC = −1.66, q-value = 2.7E-02), which integrates glucose utilization and lipogenesis [31]. In the T0-T2 comparison we found a similar pattern, with DE of genes encoding the nuclear receptor *NR4A3* (FC = −2.28, q-value = 1.99E-03), SRY-box 9 (*SOX9*, FC = −2.28, q-value = 6.84E-05) and BTB and CNC Homology 1, Basic Leucine Zipper (*BACH2*, FC = −2.45, q-value = 4.61E-05) transcription factors, to mention a few (Figs. 2 and 3, Additional file 2: Table S1). In the T0-T2 comparison (Fig. 3, Additional file 2: Table S1), we also detected an increase in the expression levels of the meteorin (*METRNL*, FC = 1.77, q-value = 7.33E-03) mRNA that encodes an hormone that promotes energy expenditure and glucose tolerance [32].

Feeding elicits strong changes in the expression of ribosomal protein genes

Mammalian ribosomes contain 79 different proteins, all of them being encoded by single-copy genes expressed in all tissues [33]. Interestingly, we have detected significant changes in the expression of several ribosomal protein genes (Additional file 2: Table S1). Ribosomal protein genes formed part of the Reactome functional networks shown in Figs. 3 and 4. Moreover, pathways related with ribosomal biogenesis appeared as significant in Table 1 and Additional file 3: Table S2. When nutrients are available, cells tend to activate energy-consuming anabolic pathways whilst under stress or starvation catabolic processes are predominant [33]. Ribosomal biogenesis consumes 60% of cellular energy and this is the key reason why this process is tightly coupled with nutrient supply [34]. The rapamycin (TOR) signalling pathway is deeply involved in coupling ribosome biogenesis

with the energy status of the cell by regulating the expression of ribosomal proteins and RNAs [35]. The fundamental role of ribosomal proteins in skeletal muscle metabolism has been illustrated by generating mice where the ribosomal protein S6 cannot be phosphorylated *i.e.* these mice are viable and fertile but they show muscle weakness and energy deficit [36]. According to our data, these strong changes in the expression of ribosomal protein genes are observed in the T0-T2 and T1-T2 comparisons, but not in T0-T1. Another intriguing observation of our study is that several of these DE ribosomal protein genes are consistently downregulated (*e.g. RPS6KA1,RPL35A, RPS23, RPS21*, *RPL9* and *RPL39*), a result that is counterintuitive and hard to explain.

Differential expression of genes related with angiogenesis and oxidative stress.

The thrombospondin 1 (*THBS1*, T0-T1: FC = −1.99, q-value = 8.00E-03) and 2 (*THBS2*, T0-T2: FC = 2.45, q-value = 5.18E-04) and thioredoxin interacting protein (*TXNIP*, T0-T1: FC = −1.78, q-value = 1.34E-02; T0-T2: FC = −1.79, q-value = 1.13E-02) genes showed significant DE before and after eating (Additional file 2: Table S1). Moreover, they were integrated in the Reactome functional networks depicted in Figs. 2 and 3. These loci have a dual biological role, regulating both angiogenesis and response to oxidative stress. For instance, *THBS1* and *THBS2* are negative regulators of angiogenesis [37, 38] and their expression is down- and upregulated by oxidative stress, respectively [39, 40]. This feature agrees well with our study, since we found a post-prandial (both at T1 and T2) decreased and increased expression of *THBS1* and *THBS2*, respectively. The TXNIP protein is one of the main regulators of redox homeostasis [41] and also an angiogenic factor [42]. We have observed a diminished expression of this gene after food ingestion, a finding that agrees well with its function as a promoter of oxidative stress and apoptosis [41].

Table 1 - Results of the Advaita Bio's iPathwayGuide pathway analysis based on the list of genes that are differentially expressed (q-value <0.05 and |fold-change| > 1.5) in the porcine gluteus medius muscle before (T0) *vs* 5 h (T1) and 7 h (T2) after eating. [a]the P-value corresponding to the pathway was computed using only over-representation analysis.

T0 *vs* T1		**T0 *vs* T2**		**T1 *vs* T2**	
Pathway	***P*-value**	**Pathway**	***P*-value**	**Pathway**	***P*-value**
Circadian rhythm	1.00E-03	Ribosome *	4.97E-06	Ribosome *	2.84E-13
Circadian entrainment	4.00E-03	Circadian rhythm	8.48E-04	Huntington's disease	2.84E-04
Cholinergic synapse	4.00E-03	Huntington's disease	1.00E-03	Parkinson's disease	7.33E-04
Adrenergic signaling in cardiomyocytes	4.00E-03	Legionellosis	5.00E-03	Oxidative phosphorylation *	8.74E-04
Transcriptional misregulation in cancer	7.00E-03	Parkinson's disease	6.00E-03	Alzheimer's disease	1.00E-03
TGF-beta signaling pathway	1.30E-02	Viral myocarditis	7.00E-03	Tight junction	1.30E-02
GABAergic synapse	1.50E-02	Malaria	7.00E-03	Metabolic pathways *	1.80E-02
Malaria	1.60E-02	p53 signaling pathway	1.00E-02	Herpes simplex infection	1.80E-02
Cardiac muscle contraction *	2.40E-02	Alzheimer's disease	1.10E-02	p53 signaling pathway	2.50E-02
Herpes simplex infection	2.70E-02	Mineral absorption	1.30E-02	Viral myocarditis	2.90E-02
Fructose and mannose metabolism *	3.20E-02	Toxoplasmosis	1.50E-02	Legionellosis	3.20E-02
Neuroactive ligand-receptor interaction	3.20E-02	PPAR signaling pathway	1.90E-02	Amyotrophic lateral sclerosis (ALS)	3.20E-02
Dopaminergic synapse	3.30E-02	Amyotrophic lateral sclerosis (ALS)	2.20E-02	Sulfur metabolism *	3.60E-02
Alanine, aspartate and glutamate metabolism *	3.50E-02	Sulfur metabolism *	2.40E-02	Arrhythmogenic right ventricular cardiomyopathy (ARVC)	5.00E-02
Glutamatergic synapse	3.60E-02	African trypanosomiasis	2.50E-02		
Estrogen signaling pathway	3.70E-02	Transcriptional misregulation in cancer	2.90E-02		
Bladder cancer	4.10E-02	Cardiac muscle contraction *	3.30E-02		
Dilated cardiomyopathy	4.90E-02	Tight junction	4.90E-02		

In the mitochondria, oxidative phosphorylation, by which ATP is synthesized as a source of energy, involves the generation of reactive oxygen species (*e.g.* superoxide, hydrogen peroxide, hydroxyl radical) as a byproduct [43]. This may promote a state of oxidative stress, *i.e.* an imbalance between oxidants and antioxidants, resulting in cell and tissue damage. Indeed, a single high-fat meal can temporarily impair endothelial function in healthy individuals and this effect is inhibited by antioxidants [44]. Moreover, lipid peroxidation by reactive oxygen species has been suggested as one of the main mechanisms leading to the development of mitochondrial dysfunction and insulin resistance [45]. On the other hand, it is well known that insulin, which is secreted by the pancreas in response to food ingestion, promotes vasodilation and capillary recruitment in the skeletal muscle, an effect mediated by nitric oxide [46]. These actions on the muscle vasculature are fundamental for the maintenance of glucose homeostasis [47]. As a matter of fact, oxidative stress and neovascularization are two tightly linked biological processes *i.e.* there are evidences that end products of lipid oxidation can bind the Toll-like receptor 2 promoting an angiogenic response [48]. As a whole, DE of *THBS1*, *THBS2* and *TXNIP* between pre- and post-prandial states probably reflects the combined redox and vascular response of the porcine skeletal muscle to nutrient availability.

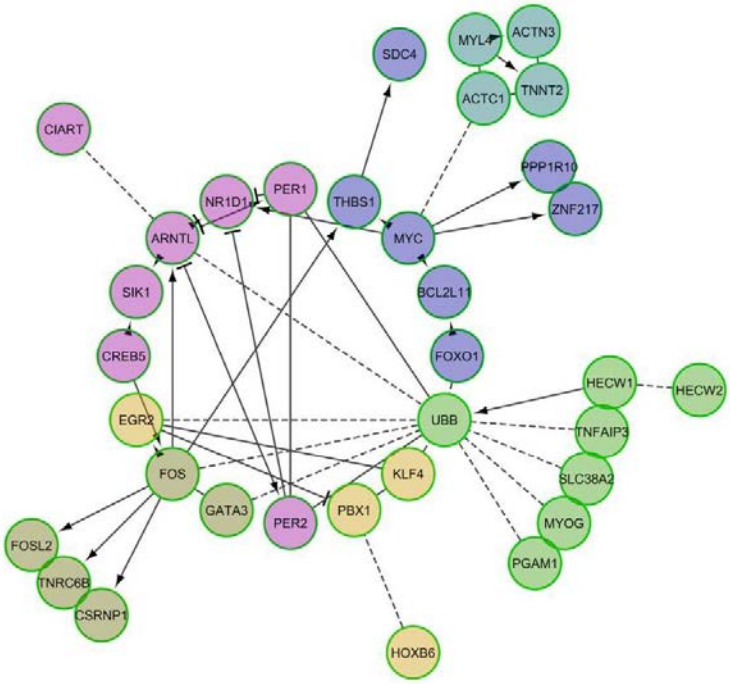

Figure 2 - Reactome functional interaction network corresponding to 148 genes that show differential expression in the T0 (fasting) vs T1 (5 h after eating) comparison. Nodes in different network modules are displayed in different colors. Letters in parentheses represent the source database as follows: R – Reactome, K – KEGG, and B – BioCarta. Enriched pathways (q-value <0.05) in each one of the individual network modules are: 1: Proteoglycans in cancer (K); 2: TNF signaling (R); 3: Circadian clock (R); 4: Bone remodeling (B); 5: Striated muscle contraction (R) and 6: Transcriptional regulation of pluripotent stem cells (R)

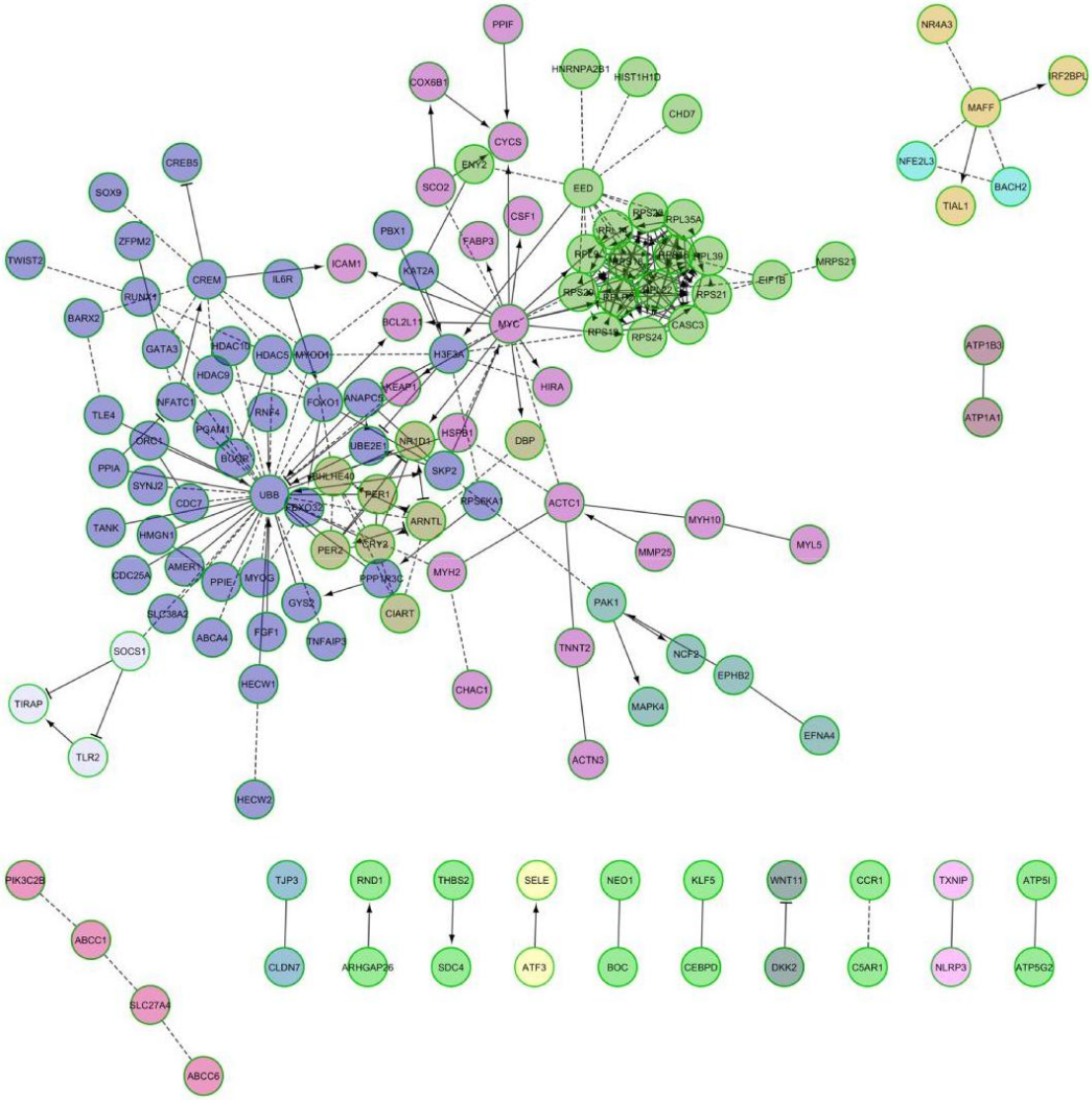

Figure 3 - Reactome functional interaction network corresponding to 520 genes showing differential expression in the T0 (fasting) vs T2 (7 h after eating) comparisons. Nodes in different network modules are displayed in different colors. Letters in parentheses represent the source database as follows: R – Reactome, K – KEGG, N – NCI PID, P - Panther, and B – BioCarta. Enriched pathways (q-value <0.05) in each one of the individual network modules are: 1: Mitotic G1-G1/S phases (R); 2: Nicotinic acetylcholine receptor signaling pathway (P); 3: SRP-dependent co-translational protein targeting to membrane (R); 4: Senescence-associated secretory phenotype (SASP) (R); 5: Signaling events mediated by HDAC Class II (N); 6: Circadian rhythm pathway (N), 7: Oxidative stress induced gene expression via Nrf2 (B); 8: ABC-family proteins mediated transport (R); 9: Toll-like receptors cascades (R); 11: Proximal tubule bicarbonate reclamation (K); 12: Wnt signaling pathway (K); 13: Nucleotide-binding domain, leucine rich repeat containing receptor (NLR) signaling pathways (R); 14: ATF-2 transcription factor network (N); 15: ECM-receptor interaction (K); 16: GPCR ligand binding (R); 17: Oxidative phosphorylation (K); 18: Integrin signalling pathway (P); 19: Myogenesis (R); 20: Transcriptional regulation of white adipocyte differentiation (R)

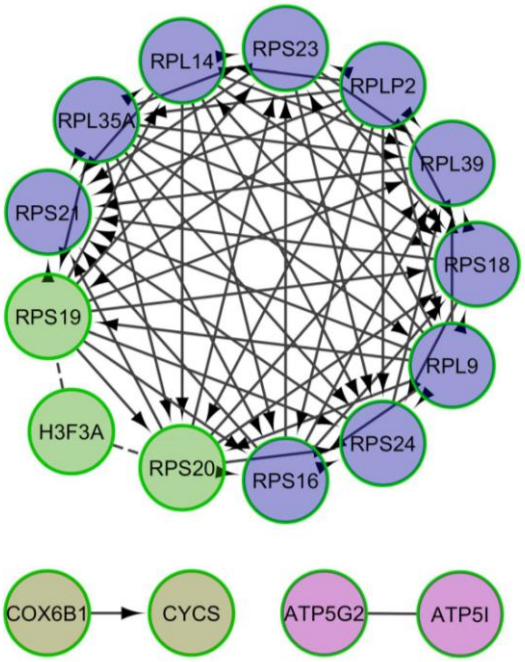

Figure 4 - Reactome functional interaction network corresponding to 135 genes showing differential expression in the T1 (5 h after eating) vs T2 (7 h after eating) comparison. Nodes in different network modules are displayed in different colors. Letters in parentheses represent the source database as follows: R – Reactome and K – KEGG. Enriched pathways (q-value <0.05) in each one of the individual network modules are: 1: SRP-dependent cotranslational protein targeting to membrane (R); 2: Eukaryotic Translation Termination (R); 3: Oxidative phosphorylation (K) and 4: Parkinson's disease (K).

A close relationship between nutritional status and the expression of genes integrated in the muscle circadian clock.

One of the main results of our experiment was the detection of DE for a set of genes that form part of the peripheral clock that determines the maintenance of circadian rhythms in the skeletal muscle (Figs. 2 and 3, and Additional file 2: Tables S1, Additional file 3: Tables S2 and Additional file 4: Tables S3). Patterns of DE in the two available comparisons (T0-T1 and T0-T2) were consistent *i.e.* there was an upregulation of *ARNTL* (T0-T1: FC = 1.87, q-value = 193E-0.4; T0-T2: FC = 2.43, q-value = 2.99E-13) and *NR1D1* (T0-T1: FC = 1.61, q-value = 8.30E-03; T0-T2: FC = 1.87, q-value = 9.52E-04), and a downregulation of *PER1* (T0-T1: FC = −2.85, q-value = 3.95E-11; T0-T2: FC = −1.83, q-value = 1.12E-0.2), *PER2* (T0-T1: FC = −1.67, q-value = 4.33E-04, T0-T2: FC = −2.48, q-value = 7.03E-14), *BHLHE40* (T0-T2: FC = −1.77, q-value = 7.87E-0.5), SIK1 (T0-T1: FC = −2.62, q-value = 1.91E-07), *CIART* (T0-T1: FC = −2.16, q-value = 5.79E-

05; T0-T2: FC = −2.35, q- value = 4.52E-06) and *CRY2* (T0-T2: FC = −1.60, q-value = 1.28E-0.2). In mammals, the circadian clock is regulated by either the CLOCK-ARNTL or the NPAS2-ARNTL heterodimers depending on the tissue under consideration [49]. These heterodimers activate the transcription of the Period (*PER1* and *PER2*) and Cryptochrome (*CRY1* and *CRY2*) genes [49]. In diurnal species, the PER and CRY complexes accumulate in the cytoplasm during daytime and they are translocated to the nucleus in the evening, thus repressing their own expression through the interaction with CLOCK/ARNTL [49]. The BHLHE40 molecule is a negative regulator of the ARNTL-CLOCK complex [50]. Other clock genes of interest are *SIK1*, that regulates the entrainment of the circadian clock [51], *CIART*, whose inactivation increases the circadian period of locomotor activity in mice [52] and *NR1D1*, a critical regulator of the circadian clock with strong effects on lipid homeostasis [53]. Our data indicate that food ingestion modulates the expression of circadian genes in the porcine skeletal muscle. It might be argued that this DE is just the obvious consequence of slaughtering pigs at different time-points (T0 = 0 h., T1 = + 5 h. and T2 = + 7 h.). However, studies performed in model species have revealed that the feeding/fasting cycle is one of the main zeitgebers (time cues) synchronizing the skeletal muscle clock [54]. Noteworthy, this clock plays a key role in muscle physiology by regulating the expression of more than one thousand genes mainly involved in metabolic processes [55]. Muscle lipid deposition in pigs could be affected by the expression of these genes because their inactivation in mouse has evidenced numerous metabolic abnormalities including ectopic fat in the muscle, reduced circulating levels of triglycerides and free fatty acids, obesity, hyperlipidemia and severe hepatic steatosis [49]. Besides, SNPs in the human clock genes have been related with abdominal obesity, increase in carbohydrate intake, higher body mass index and metabolic syndrome [56].

Conclusions

Our results indicate that the ingestion of food affects the expression of many transcription factors that are essential for coordinating the metabolic response triggered by the availability of nutrients. Amongst these, clock genes could be particularly important due to their key role in the adequate synchronization of this response as well as because of their broad effects on muscle metabolism. We have also shown that several genes without an evident link with muscle metabolism change their expression in response to nutrient

inflow, an observation that suggests that our knowledge about the genetic basis of energy homeostasis in the porcine muscle is still quite limited. Given the close physiological similarity between pigs and humans, data presented in the current study could be also of interest to understand the consequences of food intake on gene expression in this latter species.

Additional files

Additional file 1: Figure S1. Kinetics of triglyceride and non-esterified fatty acids (FA) concentrations in 36 Duroc pigs at three time points: before eating and 5 and 7 h post-ingestion.

Additional file 2: Table S1. Differentially expressed genes (q-value <0.05 and |fold-change| > 1.5) in the pig gluteus medius muscle at fasting (T0) vs 5 h (T1) vs 7 h (T2) after eating.

Additional file 3: Table S2. Pathways identified by ReactomeFIViz as enriched in differentially expressed genes (q-value <0.05 and |fold-change| > 1 .5). Three conditions were compared: fasting (T0), 5 h after eating (T1) and 7 h after eating (T2).

Additional file 4: Table S3 Gene regulatory networks identified with the ReactomeFIViz app, considering GO biological process, molecular function and cellular component (q-value<0.05).

Acknowledgements

The authors are indebted to Selección Batallé S.A. for providing the animal material. We gratefully acknowledge to J. Reixach (Selecció Batallé), J. Soler (IRTA), C. Millan (IRTA), A. Quintana (IRTA) and A. Rossell (IRTA) for their collaboration in the experimental protocols and pig management. Thanks also to the CERCA Programme of the Generalitat de Catalunya.

Funding

Part of the research presented in this publication was funded by grants AGL2013-48742-C2-1-R and AGL2013-48742-C2-2-R awarded by the Spanish Ministry of Economy and Competitivity. We also acknowledge the support of the Spanish Ministry of Economy and Competitivity for the Center of Excellence Severo Ochoa 2016-2019 (SEV-2015-0533) grant awarded to the Center for Research in Agricultural Genomics. We also acknowledge grant 2014 SGR 1528 from the Agency for Management of University and Research Grants of the Generalitat de Catalunya. Tainã F Cardoso was funded with a fellowship from the CAPES Foundation-Coordination of Improvement of Higher Education, Ministry of Education (MEC) of the Federal Government of Brazil. Emilio Mármol-Sánchez was funded with a PhD fellowship FPU15/01733 awarded by the Spanish Ministry of Education and Culture (MECD).

Availability of data and materials

Data have been submitted to the Sequence Read Archive (SRA) database (submission number: SUB2676631).

Authors' contributions

MA and RQ designed the experiment; RQ, JT and MG were responsible for the experimental protocols and generation of animal material; RGP and OG performed the kinetic study; all authors contributed to the obtaining of biological samples; TFC and EM performed RNA extractions; TFC analysed the data; MA and TFC wrote the paper; all authors read and approved the manuscript.

Ethics approval

Animal care, management procedures and blood sampling were performed following national guidelines for the Good Experimental Practices and they were approved by the Ethical Committee of the Institut de Recerca i Tecnologia Agroalimentàries (IRTA).

Consent for publication

Not applicable.

Competing interests

The authors declare that they have no competing interests.

References

1. Cowley AW. Physiological genomics: tools and concepts. J Physiol. 2004;554:3.

2. Puig-Oliveras A, Ramayo-Caldas Y, Corominas J, Estellé J, Pérez-Montarelo D, Hudson NJ, et al. Differences in muscle transcriptome among pigs phenotypically extreme for fatty acid composition. PLoS One. 2014;9:e99720.

3. Ayuso M, Fernández A, Núñez Y, Benítez R, Isabel B, Barragán C, et al. Comparative analysis of muscle transcriptome between pig genotypes identifies genes and regulatory mechanisms associated to growth, fatness and metabolism. PLoS One. 2015;10:e0145162.

4. Wang Z, Li Q, Chamba Y, Zhang B, Shang P, Zhang H, et al. Identification of genes related to growth and lipid deposition from transcriptome profiles of pig muscle tissue. PLoS One. 2015;10:e0141138.

5. Khetarpal SA, Rader DJ. Genetics of lipid traits: genome-wide approaches yield new biology and clues to causality in coronary artery disease. Biochim Biophys Acta. 2014;1842:2010–20.

6. Teslovich TM, Musunuru K, Smith AV, Edmondson AC, Stylianou IM, Koseki M, et al. Biological, clinical and population relevance of 95 loci for blood lipids. Nature. 2010;466:707–13.

7. Willer CJ, Schmidt EM, Sengupta S, Peloso GM, Gustafsson S, Kanoni S, et al. Discovery and refinement of loci associated with lipid levels. Nat Genet. 2013;45:1274–83.

8. Shulman GI, Rothman DL, Jue T, Stein P, DeFronzo RA, Shulman RG. Quantitation of muscle glycogen synthesis in normal subjects and subjects with non-insulin-Dependent diabetes by 13C nuclear magnetic resonance spectroscopy. N Engl J Med. 1990;322:223–8.

9. Frayn KN. Metabolic regulation: A Human Perspective. 3rd Edition. Wiley-Blackwell; 2010.

10. Bolger AM, Lohse M, Usadel B. Trimmomatic: a flexible trimmer for Illumina sequence data. Bioinformatics. 2014;30:2114–20.

11. Dobin A, Davis CA, Schlesinger F, Drenkow J, Zaleski C, Jha S, et al. STAR: ultrafast universal RNA-Seq aligner. Bioinformatics. 2013;29:15–21.

12. Liao Y, Smyth GK, Shi W. FeatureCounts: an efficient general purpose program for assigning sequence reads to genomic features. Bioinformatics. 2014;30:923–30.

13. Love MI, Huber W, Anders S. Moderated estimation of fold change and dispersion for RNA-Seq data with DESeq2. Genome Biol. 2014;15:550.

14. Benjamini Y, Hochberg Y. Controlling the false discovery rate: a practical and powerful approach to multiple testing. J R Stat Soc. 1995;57:289–300.

15. Shannon P, Markiel A, Ozier O, Baliga NS, Wang JT, Ramage D, et al. Cytoscape: a software environment for integrated models of biomolecular interaction networks. Genome Res. 2003;13:2498–504.

16. Wu G, Dawson E, Duong A, Haw R, Stein L. ReactomeFIViz: a Cytoscape app for pathway and network-based data analysis. F1000Res. 2014;3:146.

17. Draghici S, Khatri P, Tarca AL, Amin K, Done A, Voichita C, et al. A systems biology approach for pathway level analysis. Genome Res. 2007;17:1537–45.

18. Hue L, Rider MH. Role of fructose 2,6-bisphosphate in the control of glycolysis in mammalian tissues. Biochem J. 1987;245:313–24.

19. Heckmann BL, Zhang X, Xie X, Liu J. The G0/G1 switch gene 2 (*G0S2*): regulating metabolism and beyond. Biochim Biophys Acta. 2013;1831:276–81.

20. Zhang Y, Liu X, Bai J, Tian X, Zhao X, Liu W, et al. Mitoguardin regulates mitochondrial fusion through MitoPLD and is required for neuronal homeostasis. Mol Cell. 2016;61:111–24.

21. Liesa M, Shirihai OS. Mitochondrial dynamics in the regulation of nutrient utilization and energy expenditure. Cell Metab. 2013;17:491–506.

22. De Luca M, Klimentidis YC, Casazza K, Chambers MM, Cho R, Harbison ST, et al. A conserved role for syndecan family members in the regulation of whole-body energy metabolism. PLoS One. 2010;5:e11286.

23. Gingras RM, Warren ME, Nagengast AA, DiAngelo JR. The control of lipid metabolism by mRNA splicing in Drosophila. Biochem Biophys Res Commun. 2014;10:672–6.

24. Feijóo CG, Sarrazin AF, Allende ML, Glavic A. Cystein-serine-rich nuclear protein 1, Axud1/Csrnp1, is essential for cephalic neural progenitor proliferation and survival in zebrafish. Dev Dynam. 2009;238:2034–43.

25. Guo H-L, Zhang C, Liu Q, Li Q, Lian G, Wu D, et al. The Axin/TNKS complex interacts with KIF3A and is required for insulin-stimulated GLUT4 translocation. Cell. 2012;22:1246–57.

26. Ma K, Cilingiroglu M, Otvos JD, Ballantyne CM, Marian AJ, Chan L. Endothelial lipase is a major genetic determinant for high-density lipoprotein concentration, structure, and metabolism. Proc Natl Acad Sci U S A. 2003;100:2748–53.

27. Whitson RH, Tsark W, Huang TH, Itakura K. Neonatal mortality and leanness in mice lacking the ARID transcription factor Mrf-2. Biochem Biophys Res Commun. 2003;312:997–1004.

28. Oishi Y, Manabe I, Tobe K, Ohsugi M, Kubota T, Fujiu K, et al. SUMOylation of Krüppel-like transcription factor 5 acts as a molecular switch in transcriptional programs of lipid metabolism involving PPAR-δ. Nat Med. 2008;14:656–66.

29. Pérez-Sieira S, López M, Nogueiras R, Tovar S, Ahima RS, Flier JS, et al. Regulation of NR4A by nutritional status, gender, postnatal development and hormonal deficiency. Sci Rep. 2014;4:327–32.

30. Hishida T, Nishizuka M, Osada S, Imagawa M. The role of C/EBPδ in the early stages of adipogenesis. Biochimie. 2009;91:654–7.

31. Ido-Kitamura Y, Sasaki T, Kobayashi M, Kim HJ, Lee YS, Kikuchi O, et al. Hepatic FoxO1 integrates glucose utilization and lipid synthesis through regulation of Chrebp O-glycosylation. PLoS One. 2012;7:e47231.

32. Rao RR, Long JZ, White JP, Svensson KJ, Lou J, Lokurkar I, et al. Meteorin-like is a hormone that regulates immune-adipose interactions to increase beige fat thermogenesis. Cell. 2014;157:1279–91.

33. Mayer C, Grummt I. Ribosome biogenesis and cell growth: mTOR coordinates transcription by all three classes of nuclear RNA polymerases. Oncogene. 2006;25:6384–91.

34. Jewell JL, Guan KL. Nutrient signaling to mTOR and cell growth. Trends Biochem Sci. 2013;38:233–42.

35. Zhou X, Liao WJ, Liao JM, Liao P, Lu H. Ribosomal proteins: functions beyond the ribosome. J Mol Cell Biol. 2015;7:92–104.

36. Ruvinsky I, Katz M, Dreazen A, Gielchinsky Y, Saada A, Freedman N, et al. Mice deficient in ribosomal protein S6 phosphorylation suffer from muscle weakness that reflects a growth defect and energy deficit. PLoS One. 2009;4:e5618.

37. Bornstein P, Kyriakides TR, Yang Z, Armstrong LC, Birk DE. Thrombospondin 2 modulates collagen fibrillogenesis and angiogenesis. J Investig Dermatol Symp Proc. 2000;5:61–6.

38. Lawler J. Thrombospondin-1 as an endogenous inhibitor of angiogenesis and tumor growth. J Cell Mol Med. 2002;6:1–12.

39. Chen JK, Zhan YJ, Yang C-S, Tzeng SF. Oxidative stress-induced attenuation of thrombospondin-1 expression in primary rat astrocytes. J Cell Biochem. 2011;112:59–70.

40. Bae ON, Wang JM, Baek SH, Wang Q, Yuan H, Chen AF. Oxidative stress-mediated thrombospondin-2 upregulation impairs bone marrow-derived angiogenic cell function in diabetes mellitus. Arterioscler Thromb Vasc Biol. 2013;33:1920–7.

41. Zhou J, Chng WJ. Roles of thioredoxin binding protein (TXNIP) in oxidative stress, apoptosis and cancer. Mitochondrion. 2013;13:163–9.

42. Park SY, Shi X, Pang J, Yan C, Berk BC. Thioredoxin-interacting protein mediates sustained VEGFR2 signaling in endothelial cells required for angiogenesis. Arterioscler Thromb Vasc Biol. 2013;33:737–43.

43. Lacroix S, Rosiers CD, Tardif JC, Nigam A. The role of oxidative stress in postprandial endothelial dysfunction. Nutr Res Rev. 2012;25:288–301.

44. Sies H, Stahl W, Sevanian A. Nutritional, dietary and postprandial oxidative stress. J Nutr. 2005;135:969–72.

45. Schrauwen P, Hesselink MKC. Oxidative capacity, lipotoxicity, and mitochondrial damage in type 2 diabetes. Diabetes. 2004;53:1412–7.

46. Muniyappa R, Montagnani M, Koh KK, Quon MJ. Cardiovascular actions of insulin. Endocr Rev. 2007;28:463–91.

47. Manrique C, Sowers JR. Insulin resistance and skeletal muscle vasculature: significance, assessment and therapeutic modulators. Cardiorenal Med. 2014;4:244–56.

48. West XZ, Malinin NL, Merkulova AA, Tischenko M, Kerr BA, Borden EC, et al. Oxidative stress induces angiogenesis by activating TLR2 with novel endogenous ligands. Nature. 2010;467:972–6.

49. Gooley JJ, Chua ECP. Diurnal regulation of lipid metabolism and applications of circadian lipidomics. J Genet Genomics. 2014;41:231–50.

50. Nakashima A, Kawamoto T, Honda KK, Ueshima T, Noshiro M, Iwata T, et al. DEC1 modulates the circadian phase of clock gene expression. Mol Cell Biol. 2008;28:4080–92.

51. Jagannath A, Butler R, Godinho SIH, Couch Y, Brown LA, Vasudevan SR, et al. The CRTC1-SIK1 pathway regulates entrainment of the circadian clock. Cell. 2013;154:1100–11.

52. Goriki A, Hatanaka F, Myung J, Kim JK, Yoritaka T, Tanoue S, et al. A novel protein, CHRONO, functions as a core component of the mammalian circadian clock. PLoS Biol. 2014;12:e1001839.

53. Solt LA, Kojetin DJ, Burris TP. The REV-ERBs and RORs: molecular links between circadian rhythms and lipid homeostasis. Future Med Chem. 2011; 3:623–38.

54. Dudek M, Meng QJ. Running on time: the role of circadian clocks in the musculoskeletal system. Biochem J. 2014;463:1–8.

55. Hodge BA, Wen Y, Riley LA, Zhang X, England JH, Harfmann BD, et al. The endogenous molecular clock orchestrates the temporal separation of substrate metabolism in skeletal muscle. Skelet Muscle. 2015;5:17.

56. Ribas-Latre A, Eckel-Mahan K. Interdependence of nutrient metabolism and the circadian clock system: importance for metabolic health. Mol Metab. 2016;5:133–52.

The ingestion of food promotes changes in the expression of genes regulating circadian rhythms in four porcine tissues containing peripheral clocks

Cardoso T.F.[1,2], Quintanilla R.[3], Castelló A.[1,4], Mármol-Sánchez E.[1], Ballester M.[3], Jordana J.[4], Amills, M.[1,4,a]

[1]Department of Animal Genetics, Center for Research in Agricultural Genomics (CSIC-IRTA-UAB-UB), Campus de la Universitat Autònoma de Barcelona, Bellaterra, Spain. [2]CAPES Foundation, Ministry of Education of Brazil, Brasilia, D. F., Brazil. [3]Animal Breeding and Genetics Programme, Institute for Research and Technology in Food and Agriculture (IRTA), Torre Marimon, Caldes de Montbui, Spain. [4]Departament de Ciència Animal i dels Aliments, Universitat Autònoma de Barcelona, Bellaterra, Spain.

[a]Corresponding author: M. Amills

Submitted to Frontiers in Genetics, February 2018

Abstract

In a previous study, we demonstrated that the expression of circadian clock genes in the porcine skeletal muscle changes in response to nutrient supply. The goal of the current work was to investigate if such changes also take place in tissues containing peripheral (duodenum, dorsal fat, muscle, and liver) and central (hypothalamus) clocks. As animal material, we used 12 sows that fasted 12 h before slaughtering (T0) and 12 sows that were fed ad libitum 7 h. prior slaughtering (T2). Tissue samples were collected immediately after slaughter and total RNA was subsequently extracted. The expression of the *ARNTL, BHLHE40, CRY2, NPAS2, NR1D1, PER1, PER2* and *SIK1* genes was measured by quantitative reverse transcription PCR. Our results show that four (dorsal fat and duodenum), six (skeletal muscle) and seven (liver) genes integrated into or modulating peripheral clocks are differentially expressed before and after feeding. In contrast, none of the eight analysed genes shows a significant differential expression in hypothalamus, the tissue where the central clock resides. This result indicates that the differential expression of clock genes in the four tissues mentioned before is induced by nutrition and not by the central clock entrained by light. Moreover, we have observed that the *NPAS2* and *ARNTL* genes display positive $\log_2$(Rq) values in the five tissues under analysis, whilst the *CRY2*, *PER1* (except dorsal fat) and *PER2* (except hypothalamus) genes generally show negative $\log_2$(Rq) values. Such result might be explained by the existence of a negative feedback loop between the *ARNTL/NPAS2* and *CRY/PER* genes. Collectively, these results indicate that porcine peripheral circadian clocks are modulated by nutrition and that such regulation could be essential for coordinating the subsequent metabolic response.

Introduction

Circadian clocks are highly conserved endogenous oscillators controlling a wide repertoire of physiological events, including metabolism and behavior (Bellet & Sassone-Corsi, 2010). At the molecular level, the rhythmicity of circadian clocks is modulated by several transcriptional feedback loops composed by positive and negative regulators (Eckel-Mahan & Sassone-Corsi, 2013; Partch, Green, & Takahashi, 2014). The aryl hydrocarbon receptor nuclear translocator-like (ARNTL) transcription factor heterodimerizes with either the clock circadian regulator (CLOCK) or its paralogue, the

neuronal PAS domain protein 2 (NPAS2), thus activating the expression of the period (*PER*) and cryptochrome (*CRY*) genes. Upon reaching a critical concentration threshold, PER and CRY translocate to the nucleus where they inhibit the activity of the (CLOCK/NPAS2):ARNTL heterodimer, thus establishing a negative feedback loop (Menet et al., 2014; Peek et al., 2012). Cyclical oscillations in the expression of (CLOCK/NPAS2):ARNTL and *PER:CRY* genes modulated by this and other feedback loops promote the establishment of circadian patterns modulating the transcriptional activity of thousands of genes (Partch et al., 2014; Takahashi, 2017). This core mechanism is further refined by the action of additional genes, such as nuclear receptor subfamily 1 group D member 1 (*NR1D1*), basic helix-loop-helix family member E40 (*BHLHE40*), and salt-inducible kinase 1 (*SIK1*) which cooperate to finely tune the rhythmicity of mammalian circadian clocks (Bugge et al., 2012; Honma et al., 2002; Oike et al., 2014).

In mammals, the central circadian clock is located in the hypothalamus, and more specifically in the suprachiasmatic nucleus (Partch et al., 2014). This central clock is fundamentally entrained by the light/dark cycle (Partch et al., 2014). Circadian clocks are also present in peripheral tissues, but they are mainly entrained by feeding/fasting cycles, glucose metabolism, insulin secretion and temperature (Hastings et al., 2008; Oike et al., 2014; Richards & Gumz, 2012). Circadian clocks have a profound effect on metabolism and gene expression. For instance, a third of the genes in the mouse genome show circadian patterns of expression (Gooley & Chua, 2014). The knockout of specific circadian genes in mice is associated with a broad variety of abnormal metabolic phenotypes including obesity, hyperglycemia, hepatic steatosis, hypertriglyceridemia, hypotriglyceridemia, glucose intolerance, hypoinsulinemia and cholesterolemia (Gooley & Chua, 2014). The analysis of the murine skeletal muscle transcriptome has shown that genes related with fatty acid uptake and ß-oxidation peak in the inactive phase, whilst genes related with carbohydrate catabolism, carbohydrate storage and lipogenesis peak in the early, middle and late active phases, respectively (Hodge et al., 2015).

Whereas circadian clocks have been intensively studied in humans and mouse, little is known about the mechanisms by which these clocks respond to food intake in domestic species. Zhou et al. (2017) showed that long-chain polyunsaturated fatty acid levels in plasma and liver as well as the hepatic mRNA levels of lipid genes (*i.e. FADS1, FADS2, ELOVL2,* and *ELOVL5*) exhibit diurnal rhythms in pigs. Recently, we compared the

patterns of skeletal muscle expression of sows that fasted 12 h before slaughtering (T0) *vs* sows that were fed 5 h (T1) and 7 h (T2) before slaughtering (Cardoso et al., 2017). Our results demonstrated that nutrient supply affects the mRNA expression of circadian clock genes in the pig skeletal muscle, and such differences were particularly significant in the T0 *vs* T2 comparison (Cardoso et al., 2017). The main goal of the current work was to extend this analysis of differential expression (DE) to a broader array of tissues containing central (hypothalamus) and peripheral clocks (liver, duodenum, muscle, and dorsal fat). Our working hypothesis is that food intake promotes changes in the mRNA expression of porcine clock genes not only in the skeletal muscle but also in other tissues of metabolic importance.

Materials and Methods

RNA isolation

Sample tissues were retrieved from 12 sows that fasted 12 h before slaughtering (T0) and 12 sows that were fed *ad libitum* 7 h prior slaughtering (T2). The weight and age of the sows at slaughtering were 73 ± 1.2 kg and 161 ± 1.1 days, respectively. Additional details about how these sows were bred and fed can be found in Cardoso et al. (2017). Tissue samples (liver, dorsal fat, *gluteus medius* muscle, duodenum, and hypothalamus) were collected immediately after slaughter, submerged in RNAlater (Ambion, Austin, TX, USA), and stored at −80 °C until RNA extraction. Muscle tissue samples were individually pulverized using a pre-chilled mortar and a pestle. Powdered samples were homogenized in 1 ml TRIzol Reagent (Invitrogen Corp., Carlsbad, CA). Liver, dorsal fat, duodenum, and hypothalamus tissues were directly homogenized in TRIzol Reagent (1 ml). All samples (n = 120) were homogenized with a polytron device (IKA, Denmark). Total RNA was extracted according to the protocol recommended by Chomzynski and Sacchi (1987). In brief, homogenates were centrifuged and visible fat and cell debris were removed. Chloroform (200 μl) was added and samples were centrifuged to separate the nucleic acid and protein phases. Total RNA was precipitated using 500 μl isopropanol and washed with ethanol (75%). Finally, RNA was resuspended with RNase-free water and stored at −80 °C. RNA concentration and purity were measured using a NanoDrop ND-1000 spectrophotometer (NanoDrop Technologies, Wilmington, USA).

Synthesis of complementary DNA

Complementary DNA synthesis was carried out with the High-Capacity cDNA Reverse Transcription Kit (Applied Biosystems, Foster City, CA, USA) by using 10 µl (100 ng/µl) of total RNA as template in a final reaction volume of 20 µl. One µl of MultiScribe Reverse Transcriptase (50 U/µl), 2 µl of 10x random primers, 2 µl of 10x buffer, 0.8 µl of 25x dNTP Mix (100 mM) and 4.2 µl of water were added to the reaction. Tubes were incubated for 10 min at 25 °C, 2 h at 37 °C and 5 min at 85 °C to inactivate the reverse transcriptase according to the manufacturer instructions **(**Applied Biosystems, Foster City, CA, USA**)**. A negative control was made for each tissue with no reverse transcriptase added (−RT control). Complementary DNAs were stored at −80 °C until use.

Primer design

The eight genes included in this study were selected based on previous results obtained by Cardoso et al. (2017) as well as by performing a literature search (Gnocchi et al., 2015; Tahara & Shibata, 2013). Primers spanning exon-exon boundaries, or alternatively binding at different exons (in order to avoid the amplification of residual contaminating genomic DNA) were designed with the Primer 3 software (Untergasser et al., 2012). Primers employed in the amplification of the β-actin (*ACTB*), TATA-Box Binding Protein (*TBP*), and hypoxanthine phosphoribosyltransferase 1 (*HPRT1*) were reported by Ballester et al. (2017). Primer sequences and gene names are available in Supplementary file 1.

RT-qPCR

The quantification of mRNA expression by quantitative reverse transcription PCR (RT-qPCR) was performed by using the QuantStudio 12K Flex Real-Time PCR System (Applied Biosystems, Foster City, CA, USA). Four genes *i.e. ACTB*, *TBP*, *HPRT1*, and ß$_2$-microglobulin (*B2M*) were used as endogenous controls (Supplementary file 2). Standard curves with serial dilutions from a pool of cDNA from each tissue were made to evaluate the performance of our RT-qPCR assays. Efficiencies from 90 to 110 were obtained. In short, 3.75 µl of cDNA (1/25 diluted for samples, or 1/5-1/15,625 diluted for standard points), 7.5 µl of SYBR Select Master Mix (Applied Biosystems, Foster City, CA, USA), and 300 nM of each primer were mixed in a final volume of 15 µl. All reactions were done

in triplicate Thermal profile was 10 min at 95 °C and 40 cycles of 15 sec at 95 °C and 1 min at 60 °C. A melting curve step (95 ºC for 15 sec, 60 ºC for 1 min and a gradual increase in temperature with a ramp rate of 0.05ºC/s up to 95 ºC and a final step of 95 ºC for 15 sec) was carried out to confirm the specificity of the assays.

Data analysis

Clock gene expression data were normalized taking as a reference the mRNA levels of four reference genes (*ACTB*, *TBP*, *HPRT1*, and *B2M*), according to the stability of the gene expression for each assay. Genes selected as reference controls can be found in Supplementary file 2. Relative quantification of gene expression differences between T0 and T2 for each tissue was calculated with the $2^{-\Delta\Delta CT}$ method (Livak & Schmittgen, 2001) by using the following formulae:

$\Delta\Delta C_T = \Delta C_{T(T2)} - \Delta C_{T(T0)}$ (calibrator)

$\Delta C_{T(T2)} = (C_{T\ \text{target gene T2}} - C_{T\ \text{reference gene T2}})$ averaged across all T2 samples in each tissue

$\Delta C_{T(T0)} = (C_{T\ \text{target gene T0}} - C_{T\ \text{reference gene T0}})$ averaged across all T0 samples in each tissue

Relative quantification of gene expression differences across tissues was also calculated with the $2^{-\Delta\Delta CT}$ method. Hypothalamus samples were used as calibrator. For instance, in the case of liver samples at T0:

$\Delta\Delta C_{T(\text{liver T0})} = \Delta C_{T\ (\text{liver T0})} - \Delta C_{T(\text{hypothalamus T0})}$ (calibrator)

$\Delta C_{T(\text{liver T0})} = [C_{T(\text{target gene liver T0})} - C_{T(\text{reference genes liver T0})}]$ averaged across all T0 liver samples.

$\Delta C_{T(\text{hypothalamus})} = [C_{T(\text{target gene hypothalamus T0})} - C_{T(\text{reference genes hypothalamus T0})}]$ averaged across all T0 hypothalamus samples.

In T2, the procedure would be the same but T0 should be replaced by T2 in the above formulae.

Data were evaluated with the RT-qPCR data analysis software available in the Thermo Fisher Cloud (Thermo Fisher Scientific, Barcelona, Spain). The statistical significance of the mRNA expression differences between T0 and T2 was assessed with a Student t-test and relative quantification (Rq) was expressed in a logarithmic scale (Log_2). We considered that gene expression between T0 and T2 was significantly different when two conditions were met *i.e.* $|\log_2 Rq| > 0.58$ and q-value < 0.05. A principal component analysis (PCA) of the 120 tissue samples was carried out based on the measured ΔC_T values without correcting for any calibrator. All figures were made with the R software (https://www.r-project.org/).

Results

We have examined how the expression of eight clock genes changes in response to food ingestion across five tissues. In this study, we did not analyse the *CLOCK* gene because it was not annotated in the *Sus scrofa* genome v.10.2 (*Sscrofa 10.2* assembly; https://www.ensembl.org). In Figure 1, we have plotted a PCA of the ΔC_T values for eight genes and two timepoints (T0 and T2) of all samples from five tissues. It can be seen that in general samples cluster according to their tissue of origin (Figure 1A) rather than to the T0/T2 timepoints under consideration (Figure 1B), evidencing that tissue is the main factor that defines the patterns of clock gene expression. Moreover, the analysis of Figure 1A shows that hypothalamus and duodenum samples cluster apart from those of dorsal fat, liver, and muscle samples.

The comparison of the patterns of expression before and after feeding (T0 *vs* T2 comparison) indicates that the expression of four (dorsal fat and duodenum), six (skeletal muscle) and seven (liver) genes integrated into or modulating peripheral clocks changes in response to food ingestion (Table 1). In contrast, none of the eight analysed genes shows significant variations of expression in hypothalamus, the tissue where the central clock resides (Table 1). Another interesting observation is that in the four tissues containing peripheral clocks, the sets of genes showing a significant DE are not the same. For instance, in duodenum and muscle, there are four and six genes displaying DE between T0 and T2, but only two of them (*NPAS2* and *SIK1*) are shared by both tissues (Table 1). In contrast, the comparison of genes displaying DE in muscle (6 genes) and liver (7 genes) demonstrates the existence of a much higher level of overlap *i.e.* five genes (*BHLHE40*,

NPAS2, PER1, PER2, and *SIK1*) are shared by both tissues (Table 1). The Rq values (Table 1) do not allow comparing the magnitude of the changes in gene expression across tissues because a different calibrator sample has been used in each tissue (*e.g.* average of T0 liver samples for the liver and so on). In order to facilitate the comparison across tissues, we have made a second analysis in which the Rq of four tissues (muscle, liver, duodenum, and dorsal fat) and two timepoints (T0 and T2) are referred to a calibrator based on the average of T0 or T2 hypothalamus samples (Table 2). This analysis evidences that the mRNA levels of the eight clock genes are substantially different across tissues. Such result explains why in Figure 1 samples are clustered according to their tissue of origin whilst the timepoint (T0/T2) would have a much lower effect on sample clustering.

About the direction (positive = increased mRNA levels in T2, or negative = decreased mRNA levels in T2) of the change in expression before and after feeding, there are genes that show consistent patterns across tissues whilst others do not. For instance, the *NPAS2* and *ARNTL* genes display positive $\log_2$(Rq) values in the five tissues under analysis (Table 1), whilst *CRY2*, *PER1* (except dorsal fat) and *PER2* (except hypothalamus) generally show negative $\log_2$(Rq) values (Table 1). In contrast, the direction of the expression changes for the *BHLHE40* and *SIK1* genes is quite variable depending on the tissue under consideration. For instance, mRNA levels of the *BHLHE40* gene are decreased in liver and muscle ($\log_2$Rq = -0.94, q-value = 0.01 and $\log_2$Rq = -1.11, q-value = 0.00, respectively; Table 1), but they are increased in dorsal fat ($\log_2$Rq = 1.18, q-value = 0.02, Table 1). The expression of the Sik1 gene also presents some degree of tissue specificity, decreasing its mRNA levels in liver and muscle ($\log_2$Rq = -1.84, q-value = 0.00, and $\log_2$Rq = -2.60, q-value = 0.00, respectively; Table 1), but increasing in duodenum ($\log_2$Rq = 1.57, q-value = 0.04; Table 1).

Discussion

Clock genes play an essential role in the regulation of metabolic genes in order to coordinate their expression across tissues and organs (Jagannath et al, 2017; Patel et al., 2016; Ribas-Latre & Eckel-Mahan, 2016). We have measured the mRNA expression of eight genes that modulate circadian rhythms. The analysis of Figures 1A and 1B evidences that tissue, rather than the nutritional status, is the main factor explaining the clustering of samples. We observed that hypothalamus and duodenum samples clustered apart from

liver, muscle, and dorsal fat samples. Such groupment did not have a clear relationship with the embryonic origin of each tissue (hypothalamus: ectoderm, muscle and fat: mesoderm, liver and duodenum: endoderm) despite the fact that Ferraz et al. (2008) demonstrated, through the analysis of porcine microarray data, that tissues with similar developmental origin tend to cluster together indicating that embryonic development leaves an enduring footprint on the transcriptome. However, the importance of tissue origin in determining the mRNA levels of clock genes is also evidenced by data showing large differences in the magnitude of gene expression across tissues (Table 2).

After feeding, the expression of four (duodenum and dorsal fat) to seven (liver) clock genes changed in tissues regulated by peripheral clocks. In strong contrast, the hypothalamus, which contains the suprachiasmatic nucleus where the central clock resides, did not show any significant change in the mRNA levels of the eight analysed genes (Table 1). It is well known that food is the main entraining cue (*zeitgeber*) of peripheral clocks. Many studies suggest that feeding conditions can modify the phase of circadian gene expression in peripheral tissues while leaving the phase of cyclic gene expression in the suprachiasmatic nucleus unaffected (Damiola et al., 2000; Hirota & Fukada, 2004). Indeed, the central clock in the suprachiasmatic nucleus is entrained by the 24 h light-dark cycle and not by feeding. Importantly, the lack of mRNA expression changes in the hypothalamus that we have observed when comparing T0 and T2 sows indicates that the expression changes that we have observed in the four remaining tissues are not induced by the central clock *i.e.* they are not due to variations in the amount of light between the T0 and T2 timepoints but to nutrient supply. In order to reach a definitive conclusion, however, it would be necessary to specifically characterize the mRNA expression pattern of the suprachiasmatic nucleus because the hypothalamus is a very complex tissue containing different anatomical areas with specialized functions. In summary, our results are consistent with the notion that food intake acts as a dominant “timer” to peripheral clocks by delivering nutrients and hormonal signals, and that it does so in a suprachiasmatic nucleus-independent manner (Hirota and Fukada, 2004).

We have observed that the effects of food intake on mRNA expression patterns show marked differences across tissues *i.e.* different sets of genes display changes in their mRNA levels, and sometimes the direction of these changes varies across tissues (Table 1). These observations might be due to the fact that the timing of nutrient absorption varies

from tissue to tissue. After food ingestion, the majority of nutrients are absorbed in the intestine and the first organ that glucose and amino acids reach, through the portal system which drains blood from the gastrointestinal tract and other organs, is the liver (Frayn, 2010). Afterwards, glucose and amino acids reach the general circulation and they are absorbed in the skeletal muscle and adipose tissue (Frayn, 2010). On the other hand, the absorption and distribution of lipids are delayed, if compared with that of soluble nutrients, because they are packaged as chylomicrons in the intestine (Frayn, 2010). Thus, the expression of clock genes in distinct tissues may reflect to some extent the specific timing of nutrient absorption in each organ. Paradoxically, and despite the sequence of events outlined above, the overlap between the sets of DE genes is much higher in the liver *vs* muscle comparison than in the dorsal fat *vs* muscle comparison. This apparent contradiction might be explained by additional factors related to tissue function and environmental cues operating at a tissue-specific level. For instance, one fundamental difference between skeletal muscle and adipose depots is that the latter not only absorbs nutrients but also releases non-esterified fatty acids that are used as a source of energy during fasting (Frayn, 2010). The rhythmic release of free fatty acids and glycerol from adipocytes is locally regulated by clock genes (Shostak et al , 2013; Yoshino & Klein, 2013). In the case of the intestine, an additional key regulatory factor that modulates circadian rhythms is the microbiome. In this regard, Mukherji et al. (2013) have shown that the absence of intestinal microbiota alters drastically circadian gene expression and the cyclic production of corticosterone by the ileum, causing hyperglycemia, hypertrigliceridemia and insulin resistance (Henao-Mejia et al., 2013; Mukherji et al., 2013). Additionally, specific microbial metabolites, as *short-chain fatty acids*, may directly modulate circadian clock gene promoting diet-induced obesity by modification of the central and hepatic circadian rhythm (Leone et al., 2015). Another distinctive feature of the gastrointestinal tract is the secretion of large amounts of extrapineal melatonin, an hormone that can contribute to the synchronization of the peripheral clocks (Liu et al., 1997). Finally, the timing and phasing of clock gene expression differ across tissues because they are subject to distinct regulatory cues and, moreover, they serve distinct metabolic roles. Such organ-specific differences were recently reported in a study analysing the expression of clock genes in mouse liver and stomach and demonstrating that the acrophase of several clock genes was delayed in the stomach (Mazzoccoli et al., 2012). Storch et al. (2002) also showed that the distributions of circadian phases in the liver and

heart are substantially different and that a reduced number of genes show circadian regulation in both tissues. Importantly, Storch et al. (2002), highlighted that this specificity of circadian regulation is not explained by the tissue-specific patterns of gene expression.

When comparing the mRNA expression patterns of T0 and T2 sows, we have observed that the *NPAS2* and *ARNTL* genes display positive $\log_2$(Rq) values in the five tissues under analysis (Table 1), whilst *CRY2, PER1* (except dorsal fat) and *PER2* (except hypothalamus) generally show negative $\log_2$(Rq) values (Table 1). These observations could be explained by the existence of a negative feedback loop regulating the expression of the *NPAS2/ARNTL* and *CRY* and *PER* genes. In this way, the NPAS2/ARNTL heterodimers stimulate the transcription of *PER* and *CRY* genes. When PER and CRY reach a certain concentration threshold in the cytosol, they translocate to the nucleus and repress the expression of the *NPAS2/ARNTL* genes (Partch et al., 2014). In consequence, a certain degree of antagonism in the expression of *NPAS2/ARNTL* and *PER/CRY* genes could be anticipated. With regard to *NR1D1* (also known as REV-ERBα), it is known that this nuclear receptor binds ROR-specific response elements in the promoter of the *ARNTL* gene, thus hindering the binding of the positive transcription regulator RORα (Mazzoccoli et al., 2012; Nakashima et al., 2008). This inhibitory role of *NR1D1* on *ARNTL* mRNA expression agrees well with the fact that most of $\log_2$(Rq) values of this gene are negative (except in the skeletal muscle).

Figure 1 - Principal component analysis of the ΔC_T *values* of clock genes in five tissues (hypothalamus, liver, duodenum, muscle and dorsal fat) and two timepoints (T0 = fasting sows, T2 = fed sows). A) comparison between time-points; B) comparison between tissues. The ΔC_T values are defined as: $C_{T(targeted\ gene)} - C_{T(reference\ gene)}$.

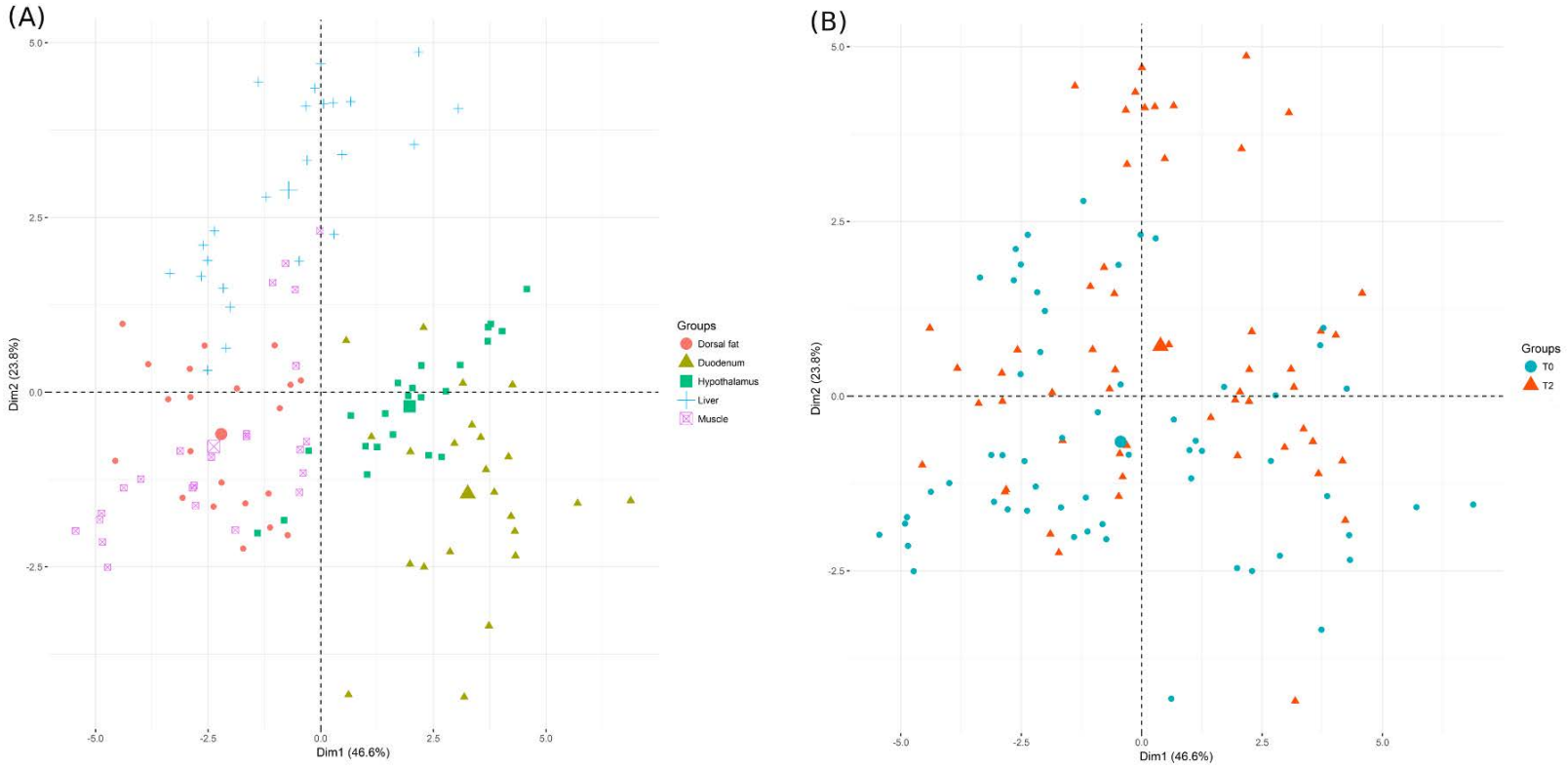

Table 1 - Differential clock gene expression at fasting (T0) and 7 h after eating (T2) in five porcine tissues[1].

	Dorsal Fat		Duodenum		Hypothalamus		Liver		Muscle	
	q-value	$\log_2$(Rq)	*q*-value	$\log_2$(Rq)	*q*-value	$\log_2$(Rq)	*q*-value	$\log_2$(Rq)	*q*-value	$\log_2$(Rq)
ARNTL	**0.00**	**2.12**	**0.02**	**1.16**	0.41	0.36	**0.00**	**1.40**	0.27	0.56
BHLHE40	**0.02**	**1.18**	1.00	0.55	0.75	-0.17	**0.01**	**-0.94**	**0.00**	**-1.11**
CRY2	0.74	-0.24	1.00	-0.41	0.72	-0.19	0.17	-0.47	**0.01**	**-1.32**
NPAS2	**0.02**	**0.68**	**0.02**	**1.05**	0.12	0.71	**0.00**	**2.07**	**0.00**	**1.02**
NR1D1	**0.02**	**-1.08**	**0.03**	**-1.48**	1.00	-0.15	**0.00**	**-1.93**	1.00	0.29
PER1	1.00	0.16	1.00	-0.05	0.50	-0.48	**0.01**	**-1.05**	**0.00**	**-1.22**
PER2	1.00	-0.14	1.00	-0.48	1.00	0.10	**0.03**	**-1.06**	**0.00**	**-1.46**
SIK1	1.00	0.00	**0.04**	**1.57**	1.00	0.10	**0.00**	**-1.84**	**0.00**	**-2.60**

[1] Genes showing a significant DE are indicated in bold. A positive $\log_2$(Rq) indicates up-regulation in the T2 timepoint and a negative $\log_2$(Rq) indicates down-regulation in the T2 timepoint.

Table 2 - Differential clock gene expression in different tissues at fasting (T0) and 7 h after eating (T2) in comparison to hypothalamus [1].

T0 timepoint								
	Dorsal Fat		Duodenum		Liver		Muscle	
	q-value	log_2(Rq)	*q*-value	log_2(Rq)	*q*-value	log_2(Rq)	*q*-value	log_2(Rq)
ARNTL	**0.03**	**-1.02**	**0.00**	**-1.93**	0.98	0.12	0.82	0.23
BHLHE40	**0.00**	**1.51**	**0.08**	**-0.93**	**0.00**	**1.50**	**0.00**	**3.58**
CRY2	0.71	0.22	0.46	0.45	**0.00**	**-1.53**	**0.00**	**2.38**
NPAS2	**0.00**	**-2.53**	**0.00**	**-1.67**	**0.00**	**-4.88**	**0.00**	**-3.66**
NR1D1	0.14	0.54	0.12	0.75	**0.03**	**-0.92**	0.56	-0.34
PER1	**0.00**	**2.37**	**0.00**	**-2.57**	**0.02**	**1.01**	**0.00**	**1.36**
PER2	**0.00**	**1.08**	**0.00**	**-2.36**	**0.00**	**1.84**	**0.00**	**2.01**
SIK1	**0.00**	**3.18**	**0.01**	**1.21**	**0.00**	**2.35**	**0.00**	**2.27**
T2 Timepoint								
	Dorsal Fat		Duodenum		Liver		Muscle	
	q-value	log_2(Rq)	*q*-value	log_2(Rq)	*q*-value	log_2(Rq)	*q*-value	log_2(Rq)
ARNTL	**0.00**	**1.38**	0.93	0.18	**0.00**	**1.34**	**0.00**	**1.09**
BHLHE40	**0.00**	**3.50**	0.36	0.51	**0.00**	**1.32**	**0.00**	**3.27**
CRY2	**0.01**	**0.75**	**0.02**	**0.90**	**0.00**	**-1.51**	**0.00**	**1.90**
NPAS2	**0.00**	**-2.04**	0.06	-0.71	**0.00**	**-3.38**	**0.00**	**-2.81**
NR1D1	0.54	0.31	0.88	-0.16	**0.00**	**-2.56**	0.10	0.89
PER1	**0.00**	**3.64**	**0.00**	**-1.43**	0.11	0.75	**0.01**	**1.27**
PER2	**0.00**	**1.49**	**0.00**	**-2.34**	**0.03**	**0.91**	**0.00**	**1.08**
SIK1	**0.00**	**3.63**	**0.00**	**2.88**	0.14	0.63	0.99	0.12

[1]Differentially expressed genes are shown in bold. A positive log2(Rq) indicates up-regulation in the targeted tissue when compared with the hypothalamus and a negative log2(Rq) indicates down-regulation in the analysed tissue in comparison to hypothalamus.

The *BHLHE40* gene displays positive $\log_2$(Rq) values in dorsal fat and duodenum, and negative values in hypothalamus, liver, and muscle (Table 1). On the other hand, the *SIK1* gene displays positive $\log_2$(Rq) values in duodenum and negative values in liver and muscle (Table 1), a pattern of expression that resembles that of *BHLHE40*. Interestingly, the functional analysis of the *SIK1* gene has shown that it is expressed in the suprachiasmatic nucleus and that it modulates the entrainment of the central circadian clock by light (Jagannath et al., 2013). Our results indicate that *SIK1* mRNA levels in liver, muscle and duodenum are also influenced by nutrition, thus suggesting that *SIK1* could also play a role in the fine tuning of peripheral clocks. The general picture that emerges from our results is that the sign of the $\log_2$(Rq) values of *BHLHE40* and *SIK1* can be positive or negative depending on the tissue under consideration (Table 1). Indeed, these genes are not only involved in the maintenance of circadian rhythms but also in many other biological processes, so their mRNA levels are determined by a multiplicity of factors and complex interactions. For instance, BHLHE40 proteins repress the NPAS2/ARNTL transactivation of the *PER1* gene promoter by competing for E-box binding and interacting with ARNTL (Honma et al. 2002). In addition, this transcription factor regulates cell proliferation and differentiation (Shen et al., 1997), adipogenesis (Ozaki et al., 2012), cytokine production by T cells (Lin et al., 2014), apoptosis (Qian et al, 2012) and cellular senescence (Yingjuan et al, 2008). Similarly, the *SIK1* gene performs a broad variety of functions related with inflammation (Lombardi et al, 2016), steroidogenesis (Hu et al, 2015), renal function (Taub et al., 2015), vascular remodeling (Bertorello et al., 2015) and glucose metabolism (Patel et al., 2014), to mention a few, so its biological role goes far beyond the modulation of circadian rhythms and this is reflected in its variable pattern of expression across porcine tissues.

In a previous work, we demonstrated, by using an RNA-Seq approach, that the expression of clock genes in the porcine skeletal muscle changes in response to food ingestion (Cardoso et al., 2017). Here, we have confirmed this result by using a RT-qPCR approach and we have also provided evidence that the expression of clock genes is affected by nutrient supply in three additional tissues regulated by peripheral clocks (duodenum, liver, and dorsal fat), but not in the hypothalamus, which contains the central master clock entrained by light. We also show that the pattern of expression of these clock genes differs across tissues, suggesting a differential modulation of circadian rhythms not only in time but also in space.

Conflict of Interest

The authors declare no conflict of interest

Author Contributions

MA, RQ, and JJ designed the experiment; RQ was responsible for the experimental protocols and generation of animal material; all authors contributed to the obtaining of biological samples; TFC and EMS performed RNA extractions; ACas designed the RT-qPCR experiments; TFC carried out the RT-qPCR experiments; TFC and ACas analysed the RT-qPCR data; MB contributed to the biological interpretation of the expression data; MA and TFC wrote the paper. All authors read and approved the manuscript.

Funding

Part of the research presented in this publication was funded by grants AGL2013-48742-C2-1-R and AGL2013-48742-C2-2-R awarded by the Spanish Ministry of Economy and Competitivity and grant 2014 SGR 1528 from the Agency for Management of University and Research Grants of the Generalitat de Catalunya. We also acknowledge the support of the Spanish Ministry of Economy and Competitivity for the *Center of Excellence Severo Ochoa 2016-2019* (SEV-2015-0533) grant awarded to the Centre for Research in Agricultural Genomics (CRAG). Tainã Figueiredo Cardoso was funded with a fellowship from the CAPES Foundation-Coordination of Improvement of Higher Education, Ministry of Education of the Federal Government of Brazil. Emilio Mármol-Sánchez was funded with an FPU Ph.D. grant from the Spanish Ministry of Education (FPU15/01733). Thanks also to the CERCA Programme of the Generalitat de Catalunya. The funders had no role in study design, data collection, and analysis, decision to publish or preparation of the manuscript.

Acknowledgments

The authors are indebted to Selección Batallé S.A. for providing the animal material. We gratefully acknowledge to J. Reixach (Selecció Batallé), J. Soler (IRTA), C. Millan

(IRTA), A. Quintana (IRTA), O. González (IRTA) and A. Rossell (IRTA) for their collaboration in the experimental protocols and pig management.

References

Ballester, M., Ramayo-Caldas, Y., Revilla, M., Corominas, J., Castelló, A., Estellé, J., et al. (2017). Integration of liver gene co-expression networks and eGWAs analyses highlighted candidate regulators implicated in lipid metabolism in pigs. Sci Rep. 7, 46539. doi: 10.1038/srep46539

Bellet, M.M., and Sassone-Corsi, P. (2010). Mammalian circadian clock and metabolism - the epigenetic link. J. Cell Sci. 123, 3837–48. doi: 10.1242/jcs.051649

Bertorello, A.M., Pires, N., Igreja, B., Pinho, M.J., Vorkapic, E., Wagsater, D. (2015). Increased arterial blood pressure and vascular remodeling in mice lacking salt-inducible kinase 1 (SIK1). Circ. Res. 116, 642–652. doi: 10.1161/CIRCRESAHA.116.304529

Bugge, A., Feng, D., Everett, L.J., Briggs, E.R., Mullican, S.E., Wang, F. (2012). Rev-erbα and Rev-erbβ coordinately protect the circadian clock and normal metabolic function. Genes Dev. 26, 657–67. doi: 10.1101/gad.186858.112

Cardoso, T.F., Quintanilla, R., Tibau, J., Gil, M., Mármol-Sánchez, E., González-Rodríguez, O. (2017). Nutrient supply affects the mRNA expression profile of the porcine skeletal muscle. BMC Genomics. 18, 603. doi: 10.1186/s12864-017-3986-x

Chomczynski, P., and Sacchi, N. (1987). Single step method of RNA isolation by acid guanidinium thiocyanate-phenol-chloroform extraction. Anal Biochem. 162, 156-159. doi: 10.1006/abio.1987.9999

Damiola, F., Le Minh, N., Preitner, N., Kornmann, B., Fleury-Olela, F., Schibler, U. (2000). Restricted feeding uncouples circadian oscillators in peripheral tissues from the central pacemaker in the suprachiasmatic nucleus. Genes Dev. 14, 2950–61. doi: 10.1101/GAD.183500

Eckel-Mahan, K., and Sassone-Corsi, P. (2013). Metabolism and the circadian clock converge. Physiol. Rev. 93, 107–35. doi: 10.1152/physrev.00016.2012

Ferraz, A.L.J., Ojeda, A., López-Béjar, M., Fernandes, L.T., Castelló, A. (2008). Transcriptome architecture across tissues in the pig. BMC Genomics. 9, 173. doi: 10.1186/1471-2164-9-173

Frayn, K.N. (2010). Metabolic regulation: A Human Perspective. Chichester, U.K.; Malden, MA: Wiley-Blackwell Pub.

Gnocchi, D., Pedrelli, M., Hurt-Camejo, E., Parini, P. (2015). Lipids around the Clock: focus on circadian rhythms and lipid metabolism. Biology. 4, 104–32. doi: 10.3390/biology4010104

Gooley, J.J., and Chua, E.C.P. (2014). Diurnal regulation of lipid metabolism and applications of circadian lipidomics. J. Genet. Genomics. doi: 10.1016/j.jgg.2014.04.001

Hastings, M.H., Maywood, E.S., Reddy, A.B. (2008). Two decades of circadian time. J. Neuroendocrinol. 20, 812–819. doi: 10.1111/j.1365-2826.2008.01715.x

Henao-Mejia, J., Strowig, T., Flavell, R.A. (2013). Microbiota keep the intestinal clock ticking. Cell. 153, 741–743. doi: 10.1016/j.cell.2013.04.043

Hirota, T., and Fukada, Y. (2004). Resetting mechanism of central and peripheral circadian clocks in mammals. Zool. Sci. 21, 359–368. doi: 10.2108/zsj.21.359

Hodge, B.A., Wen, Y., Riley, L.A., Zhang, X., England, J.H. (2015). The endogenous molecular clock orchestrates the temporal separation of substrate metabolism in skeletal muscle. Skelet. Muscle 5, 17. doi: 10.1186/s13395-015-0039-5

Honma, S., Kawamoto, T., Takagi, Y., Fujimoto, K., Sato, F., Noshiro, M. (2002). Dec1 and Dec2 are regulators of the mammalian molecular clock. Nature. 419, 841–844. doi: 10.1038/nature01123

Hu, Z., Hu, J., Shen, W.J., Kraemer, F.B., Azhar, S. (2015). A novel role of salt-inducible kinase 1 (SIK1) in the post-translational regulation of scavenger receptor class b type 1 activity. Biochem. 54, 6917–6930. doi: 10.1021/acs.biochem.5b00147

Jagannath, A., Butler, R., Godinho, S.I.H., Couch, Y., Brown, L.A., Vasudevan, S.R. (2013). The CRTC1-SIK1 pathway regulates entrainment of the circadian clock. Cell. 154, 1100–1111. doi: 10.1016/j.cell.2013.08.004

Jagannath, A., Taylor, L., Wakaf, Z., Vasudevan, S.R., Foster, R.G. (2017). The genetics of circadian rhythms, sleep and health. Hum. Mol. Genet. 26, R128–R138. doi: 0.1093/hmg/ddx240

Leone, V., Gibbons, S.M., Martinez, K., Hutchison, A.L., Huang, E.Y., Cham, C.M. (2015). Effects of diurnal variation of gut microbes and high-fat feeding on host circadian clock function and metabolism. Cell Host Microbe. 17, 681–689. doi: 10.1016/J.CHOM.2015.03.006

Lin, C.C., Bradstreet, T.R., Schwarzkopf, E.A., Sim, J., Carrero, J.A., Chou, C. (2014). Bhlhe40 controls cytokine production by T cells and is essential for pathogenicity in autoimmune neuroinflammation. Nat. Commun. 5, 3551. doi: 10.1038/ncomms4551

Liu, C., Weaver, D.R., Jin, X., Shearman, L.P., Pieschl, R.L., Gribkoff, V.K., Reppert, S.M. (1997). Molecular dissection of two distinct actions of melatonin on the suprachiasmatic circadian clock. Neuron 19, 91–102. doi: 10.1016/S0896-6273(00)80350-5

Livak, K.J., and Schmittgen, T.D. (2001). Analysis of relative gene expression data using Real-Time Quantitative PCR and the $2^{-\Delta\Delta CT}$ Method. Methods. 25, 402–408. doi: 10.1006/meth.2001.1262

Lombardi, M.S., Gilliéron, C., Dietrich, D., Gabay, C. (2016). SIK inhibition in human myeloid cells modulates TLR and IL-1R signaling and induces an anti-inflammatory phenotype. J. Leukoc. Biol. 99, 711–721. doi: 10.1189/jlb.2A0715-307R

Mazzoccoli, G., Francavilla, M., Pazienza, V., Benegiamo, G., Piepoli, A., Vinciguerra, M. (2012). Differential patterns in the periodicity and dynamics of clock gene expression in mouse liver and stomach. Chronobiol. Int. 29, 1300–1311. doi: 10.3109/07420528.2012.728662

Menet, J.S., Pescatore, S., Rosbash, M. (2014). CLOCK:BMAL1 is a pioneer-like transcription factor. Genes Dev. 28, 8–13. doi: 10.1101/gad.228536.113

Mukherji, A., Kobiita, A., Ye, T., Chambon, P. (2013). Homeostasis in intestinal epithelium is orchestrated by the circadian clock and microbiota cues transduced by TLRs. Cell. 153, 812–827. doi: 10.1016/j.cell.2013.04.020

Nakashima, A., Kawamoto, T., Honda, K.K., Ueshima, T., Noshiro, M., Iwata, T. (2008). DEC1 modulates the circadian phase of clock gene expression. Mol. Cell. Biol. 28, 4080–4092. doi: 10.1128/MCB.02168-07

Oike, H., Oishi, K., Kobori, M. (2014). Nutrients, clock genes, and chrononutrition. Curr. Nutr. Rep. 3, 204–212. doi: 10.1007/s13668-014-0082-6

Ozaki, N., Noshiro, M., Kawamoto, T., Nakashima, A., Honda, K., Fukuzaki-Dohi, U. (2012). Regulation of basic helix-loop-helix transcription factors Dec1 and Dec2 by RORα and their roles in adipogenesis. Genes Cells 17, 109–121. doi: 10.1111/j.1365-2443.2011.01574.x

Partch, C.L., Green, C.B., Takahashi, J.S. (2014). Molecular architecture of the mammalian circadian clock. Trends Cell. Biol. 24, 90–99. doi: 10.1016/j.tcb.2013.07.002

Patel, K., Foretz, M., Marion, A., Campbell, D.G., Gourlay, R., Boudaba, N. (2014). The LKB1-salt-inducible kinase pathway functions as a key gluconeogenic suppressor in the liver. Nat. Commun. 5, 4535. doi: 10.1038/ncomms5535

Patel, S.A., Velingkaar, N., Makwana, K., Chaudhari, A., Kondratov, R. (2016). Calorie restriction regulates circadian clock gene expression through BMAL1 dependent and independent mechanisms. Sci. Rep. 6, 25970. doi: 10.1038/srep25970

Peek, C.B., Ramsey, K.M., Marcheva, B., Bass, J. (2012). Nutrient sensing and the circadian clock. Trends Endocrinol. Metab. 23, 312–8. doi: 10.1016/j.tem.2012.02.003

Qian, Y., Jung, Y.-S., Chen, X. (2012). Differentiated embryo-chondrocyte expressed gene 1 regulates p53-dependent cell survival versus cell death through macrophage inhibitory cytokine-1. Proc. Natl. Acad. Sci. U.S.A. 109, 11300–11305. doi: 10.1073/pnas.1203185109

Qian, Y., Zhang, J., Yan, B., Chen, X. (2008). DEC1, a basic helix-loop-helix transcription factor and a novel target gene of the p53 family, mediates p53-dependent premature senescence. J. Biol. Chem. 283, 2896–2905. doi.org/10.1074/jbc.M708624200

Ribas-Latre, A., and Eckel-Mahan, K. (2016). Interdependence of nutrient metabolism and the circadian clock system: Importance for metabolic health. Mol. Metab. 5, 133–152. doi: 10.1016/j.molmet.2015.12.006

Richards, J., and Gumz, M.L. (2012). Advances in understanding the peripheral circadian clocks. FASEB J. 26, 3602–13. doi: 10.1096/fj.12-203554

Shen, M., Kawamoto, T., Yan, W., Nakamasu, K., Tamagami, M., Koyano, Y. (1997). Molecular characterization of the novel basic helix–loop–helix protein DEC1 expressed in differentiated human embryo chondrocytes. Biochem. Biophys. Res. Commun. 236, 294–298. doi: 10.1006/BBRC.1997.6960

Shostak, A., Meyer-Kovac, J., Oster, H. (2013). Circadian regulation of lipid mobilization in white adipose tissues. Diabetes. 62, 2195–2203. doi: 10.2337/db12-1449

Storch, K.-F., Lipan, O., Leykin, I., Viswanathan, N., Davis, F.C., Wong, W.H. (2002). Extensive and divergent circadian gene expression in liver and heart. Nature. 417, 78–83. doi: 10.1038/nature744

Tahara, Y., and Shibata, S. (2013). Chronobiology and nutrition. Neuroscience. 253, 78–88. doi: 10.1016/J.NEUROSCIENCE.2013.08.049

Takahashi, J.S. (2017). Transcriptional architecture of the mammalian circadian clock. Nat. Rev. Genet. 18, 164–179. doi: 10.1038/nrg.2016.150

Taub, M., Garimella, S., Kim, D., Rajkhowa, T., Cutuli, F. (2015). Renal proximal tubule Na,K-ATPase is controlled by CREB-regulated transcriptional coactivators as well as salt-inducible kinase 1. Cell. Signal. 27, 2568–2578. doi: 10.1016/j.cellsig.2015.09.015

Untergasser, A., Cutcutache, I., Koressaar, T., Ye, J., Faircloth, B.C., Remm, M. (2012). Primer3-- new capabilities and interfaces. Nucleic Acids Res. 40, e115. doi: 10.1093/nar/gks596

Yoshino, J., and Klein, S. (2013). A novel link between circadian clocks and adipose tissue energy metabolism. Diabetes. 62, 2175–2177. doi: 10.2337/db13-0457

Zhou, X., Wan, D., Zhang, Y., Zhang, Y., Long, C., Chen, S. (2017). Diurnal variations in polyunsaturated fatty acid contents and expression of genes involved in their *de novo* synthesis in pigs. Biochem. Biophys. Res. Commun. 483, 430–434. doi: 10.1016/J.BBRC.2016.12.126

The red and blond pigmentation of Mangalitza pigs is strongly associated with the variability of the Solute Carrier Family 45 Member 2 (*Slc45a2*) gene

Valentin A. Balteanu[1]*, Tainã F. Cardoso[2,3]*, Marcel Amills[2,4,a], István Egerszegi[5], István Anton[6], Albano Beja-Pereira[7], Attila Zsolnai[6,a]

[1]Institute of Life Sciences, Faculty of Animal Science and Biotechnologies, University of Agricultural Sciences and Veterinary Medicine, Cluj-Napoca, Romania. [2]Department of Animal Genetics, Centre for Research in Agricultural Genomics (CSIC-IRTA-UAB-UB), Campus de la Universitat Autònoma de Barcelona, Bellaterra, Spain. [3]CAPES Foundation, Ministry of Education of Brazil, Brasilia D. F., Brazil. [4]Departament de Ciència Animal i dels Aliments, Universitat Autònoma de Barcelona, Bellaterra, Spain. [5] Szent István University, Gödöllő, Hungary [6]NAIK-Research Institute for Animal Breeding, Nutrition and Food Science, Herceghalom, Hungary. [7] Centro de Investigacao em Biodiversidade e Recursos Geneticos, Universidade do Porto (CIBIO-UP), Vairao, Portugal

*V. A. Balteanu and T. F. Cardoso share the first authorship

[a]Corresponding authors: A. Zsolnai and M. Amills

Manuscript in preparation

Abstract

The Mangalitza pig breed has suffered strong demographic reductions due to competition with more productive cosmopolitan breeds. Four main varieties were created one century ago by artificial selection and admixture *i.e.* Red Mangalitza, Black Mangalitza (extinct), Blond Mangalitza and Swallow Belly Mangalitza, which has a black coat combined with yellow blond throat and underbelly. In the current work, we aimed to test two hypotheses: (1) that population recession has resulted in the contraction of the genetic diversity of Mangalitza pigs, and (2) that the red and blond colorations of Mangalitza pigs are genetically determined by one or a few loci. The analysis of BeadChip SNP60 genotypes of 45 Red (N = 20 from Hungary and N = 25 from Romania) and 37 Blond Mangalitza pigs and 191 pigs from the Hampshire, Duroc, Landrace, Large White, Piétrain breeds plus 46 wild boars from Romania and Hungary revealed that Hungarian and Romanian Red Mangalitza pigs and Romanian wild boars display an increased frequency of very long ROH (> 30 Mb), evidencing the occurrence of a recent and strong inbreeding. We also observed that Blond Mangalitza, Red Mangalitza from Hungary, wild boar from Hungary and Romania and Hampshire pigs display lower levels of heterozygosity than cosmopolitan breeds such as Landrace, Large White and Piétrain. Performance of a selection scan with hapFLK and of a GWAS for coat color in Red and Blond Mangalitza pigs highlighted the existence of one region on SSC16 (20 Mb) with potential effects on pigmentation. The analysis of the gene content of this region allowed us to detect the solute carrier family 45 member 2 (*SLC45A2*) gene, whose polymorphism has been associated with reduced levels or absence of melanin in many mammalian species. The genotyping of three missense polymorphisms in the porcine *SLC45A2* gene evidenced that c.806G>A (p.Gly269Glu) and c.956G>A (p.Arg319His) SNPs are strongly but not fully associated with the red and blond coat colors of Mangalitza pigs. Alternative genotypes were nearly fixed in Red and Mangalitza pigs illustrating the consequences of divergent directional selection for coat color in a domestic species.

Keywords: SNPs, Mangalitza, color coat, population

Introduction

Many European local pig breeds have experienced a sustained demographic recession due to indiscriminate crossbreeding, competition with more productive breeds, decline of traditional production systems, progressive abandonment of rural activities and loss of grazing land (FAO, 2015). In Europe and the Caucasus, at least 90 breeds have disappeared and many others are endangered or face extinction (FAO, 2015). One appropriate model to investigate the genetic consequences of such strong demographic contractions is the Mangalitza breed, which is distributed in Hungary and, with a much lower population census, in Romania, Germany, Austria and Switzerland (Egerszegi, Rátky, Solti, & Brüssow, 2003). In 1927-1930, there were 1,000-1,920 Mangalitza pigs in Hungary, and this number peaked to 17,691 individuals in 1955. However, this breed experienced a very serious demographic decline during the two subsequent decades, mainly due to competition with more productive breeds. Noteworthy, only 34 breeding sows were registered in the herd-book in 1975 (Egerszegi et al., 2003). Fortunately, the establishment of conservation genetic plans allowed the demographic recovery of this breed (Egerszegi et al., 2003). In Romania, the Mangalitza breed accounted for 500 individuals in 1983, but only 34 pigs remained in 1996 and nowadays this population faces extinction (Egerszegi et al., 2003) and it has a low diversity (Manunza et al., 2016). In principle, this sustained demographic decline is expected to reduce genetic variation and to increase the levels of inbreeding of Mangalitza pigs, two features that might threaten the genetic conservation of this ancient traditional breed.

The Mangalitza breed also constitutes an appropriate genetic model for investigating the inheritance of color in European pigs because several varieties with distinct pigmentation patterns have been created through artificial selection (Egerszegi et al., 2003). The Blond variety was probably obtained in the 19th century by crossing small ancient Alföldi pigs with Serbian Sumadia swine, and one of its main features is a dense and curly hair with a coloration that might go from grey-yellow to ruddy (Egerszegi et al., 2003). The Black variety, which became extinct in the 20th century, was crossed with the Blond one to yield Swallow Belly Mangalitza. These pigs have a black coat combined with yellow blond throat and underbelly (Egerszegi et al., 2003). Finally, the Red variety is the result of crossing Blond Mangalitza with Szalontai pigs and arose during the second half of the 19th century (Egerszegi et al., 2003). The hypothesis that we wanted to test in the current work were: (1) that the strong population reduction that the Mangalitza breed has

experienced during the second half of the 20th century has severely constrained the genetic diversity of this breed, and (2) that the blond *vs* red pigmentation patterns that were established in the Mangalitza breed by artificial selection one century ago are genetically determined by one or few loci.

Materials and Methods

Sample collection, DNA extraction and genotyping

Blood from Blond Mangalitza (N = 37) and Red Mangalitza from Hungary (N = 20) and Red Mangalitza from Romania (N = 25) was collected in EDTA coated vacutainer tubes. For comparative purposes, several reference populations were included in this study: Blond Mangalitza x Duroc crossed pigs (N = 48), Bazna (N = 5), Duroc (N = 56), Hampshire (N = 11), Landrace (N = 29), Large White (N = 27), Piétrain (N = 20) and wild boar from Hungary (N = 28) and Romania (N = 25). DNA was isolated from the samples using a simple protocol (Zsolnai *et al.,* 2003). In case of samples genotyped with the Illumina Infinium HD Porcine SNP60 BeadChip (Illumina, San Diego, CA) or GGP 50K Porcine SNP chip (Neogen, Scotland, UK), the service provider performed the DNA preparation from blood. A series of quality control procedures were conducted on the raw data using SVS SNP & Variation Suite 8.8.1. software (Golden Helix, Bozeman, MT, USA). Linkage disequilibrium (LD; $r^2 > 0.5$) pruning was applied to the whole dataset. Linkage disequilibrium between adjacent SNPs was calculated with the genotype correlation coefficient (r^2). In addition, monomorphic markers and unmapped SNPs, as well as those with a call rate < 95%, were eliminated from the dataset. In addition, we removed SNPs with a minor allele frequency (MAF) lower than 0.05. Duplicated samples (IBD > 0.95) and individuals with a genotype call rate < 95% were removed. After filtering steps, the final dataset included 324 animals and 30,121 SNPs (Table 1).

Population genetics analyses

The proportion of mixed ancestry and population structure were evaluated with the ADMIXTURE software v.1.3 (Alexander et al., 2009) by using default parameters. ADMIXTURE calculates maximum likelihood estimates of individual ancestries based on data provided by multiple loci. We evaluated different numbers of clusters (K-value, from

2 to 12) by considering the mixed ancestry model. The optimal K-value was determined by taking into account the estimates of the cross-validation errors (Alexander & Lange, 2011). PLINK software v1.7 (Purcell et al., 2007) was used to calculate observed (H_o) and expected (H_e) heterozygosities. This software was also used to build a multidimensional scaling (MDS) plot by using a genome-wide identity-by-state pairwise distances matrix (--mds-plot 2 and --cluster options). The analysis of runs of homozygosity (ROH) was also carried out with PLINK v1.7 (Purcell et al., 2007). We defined ROH as homozygous genomic stretches with a length of at least 1 Mb containing a minimum number of 15 SNP markers with adjusted parameters (--homozyg-density 1000, --homozyg-window-threshold 0.001, --homozyg-window-missing 5 and --homozyg-window-het 1). The inbreeding coefficient derived from ROHs (F_{ROH}) was calculated by dividing total ROH length per individual by total genome length across all 18 autosomes (2,502 Mb).

Selection scan and genome-wide association analysis

In order to investigate the genetic basis of red *vs* blond pigmentation in Mangalitza pigs, we carried out a selection scan and a genome-wide association analysis (GWAS). Selection signatures were detected with the hapFLK statistic (Fariello et al., 2013). In the hapFLK analysis, the number of haplotype clusters was set to 20 and the hapFLK statistic was calculated as the average of 30 expectation maximization iterations. Multiple testing correction was done by using a false discovery rate approach (Storey & Tibshirani, 2003).

The GWAS was performed by employing a multivariate likelihood ratio test implemented in the GEMMA software (Zhou & Stephens, 2014). Briefly, a single-SNP association analysis was performed under an additive genetic model that included the genomic kinship matrix to account for relatedness. We used the following statistical model to analyze coat color traits:

$$\boldsymbol{y} = \mathbf{W}\boldsymbol{\alpha} + \mathbf{x}\boldsymbol{\beta} + \mathbf{u} + \boldsymbol{\varepsilon},$$

where y is the vector of phenotypes (red or blond in this case) for all individuals; W is a matrix of covariates, *i.e.* country of origin (Hungary or Romania); α is a vector of the corresponding coefficients including the intercept; x is a vector of genotypes of a marker; β

is the effect size of the marker; u is a vector of random individual effects with an n-dimensional multivariate normal distribution MVN_n (0, $\lambda \tau^{-1}$ K), where τ^{-1} is the variance of the residual errors, λ is the ratio between the two variance components and K is a known relatedness matrix derived from SNPs; Z is an n × m loading matrix and ε is a vector of errors with an n-dimensional multivariate normal distribution MVNn (0, τ^{-1} I_n), where I_n is an n × n identity matrix. Correction for multiple testing was implemented with a false discovery rate approach (Benjamini & Hochberg, 1995), and SNPs with a *q*-value < 0.05 were considered as significantly associated with pigmentation.

Genotyping of the *SLC45A2* gene.

The selection of *SLC45A2* polymorphisms to be typed in our animal material was based on a set of whole-genome sequences (SRA access: SRP039012) from Mangalitza Blond and Red pigs reported by Molnár *et al.* (2014). Variant discovery procedures followed the *GATK Best Practices workflow for SNP calling on DNA-seq data* (https://gatkforums.broadinstitute.org /gatk/discussion/3238/best-practices-for-variant-discovery-in-dnaseq). Briefly, sequence reads were mapped to the porcine reference genome (*Sscrofa* 10.2, https://www.ensembl.org/) and duplicate reads were removed. Variant calling was carried out by running the HaplotypeCaller for the BAM files corresponding to each sample. The potential effects and impact of SNPs were predicted with the SnpEff software v4.3s (Cingolani et al., 2012). We used SIFT (Sorting Intolerant from Tolerant; Kumar et al., 2009) and PANTHER (Protein ANalysis THrough Evolutionary Relationships; Thomas et al., 2003) as *in silico* tools to identify the functional impact of missense mutations. SIFT prediction is based on the sequence homology and the physico-chemical properties of amino acids which are dictated by the substituted amino acid (Kumar et al., 2009). PANTHER program is a protein family and subfamily database which predicts the frequency of the occurrence of certain amino acid at a particular position in evolutionarily related protein sequences (Thomas et al., 2003). On the basis of such analyses, we selected three missense SNPs that had a differential distribution in Red and Blond Mangalitza pigs *i.e.* rs341599992 (c.806G>A, p.Gly269Glu), rs327001340 (c.829A>G, p.Ser277Gly) and rs693695020 (c.956G>A, p.Arg319His). These SNPs were typed in an independent sample of 209 pigs from the Blond Mangalitza (N = 55), Red Mangalitza (N = 65), Swallow Belly Mangalitza (N = 30), Piétrain (N = 15), Large white

(N = 15), Landrace (N = 15) and Duroc (N = 14) breeds. Genotyping tasks were carried out by the Molecular Genetics Veterinary Service from the Universitat Autonoma de Barcelona (http://sct.uab.cat/svgm/en) by using a QuantStudio 12K Flex Real-Time PCR System (ThermoFisher Scientific, Waltham, Massachusetts, USA). The association analysis between *SLC45A2* SNPs and coat color in Red and Blond Mangalitza pigs was based on a chi-square test, and the effect of *SLC45A2* gene variants was calculated as odds ratios by using the R software (https://www.r-project.org/).

Results

Autosomal diversity and population structure

To investigate the genetic relationships between Red and Blond Mangalitza and other pig and wild boar populations, we built an MDS plot based on genome-wide identity-by-state pairwise distances calculated with PLINK (Figure 1). The first principal component separated Duroc pigs from the remaining breeds (Figure 1). As expected, Blonde Mangalitza x Duroc crossed pigs occupied an intermediate position between both parental populations. In the second component, the cosmopolitan breeds Landrace, Large White and Piétrain clustered independently from Mangalitza pigs and Romanian and Hungarian wild boars. The Hampshire and Bazna pigs occupied an intermediate position between these two clusters. We also observed that Blond, Hungarian Red, and Romanian Red Mangalitza formed three different subclusters, highlighting that these populations are genetically differentiated. Moreover, we detected a close relationship between Mangalitza pigs and Romanian and Hungarian wild boars. Descriptive statistics of genetic diversity are shown in Table 1. Expected and observed heterozygosities were higher in Landrace, Large White and Piétrain pigs (H_o = 0.35-0.36, H_e = 0.35) than in Blond Mangalitza, Red Mangalitza from Hungary, wild boar from Hungary and Romania and Hampshire pigs (H_o = 0.27-0.29, H_e = 0.24-0.31). Surprisingly, the diversity of Red Mangalitza pigs from Romania (H_o = H_e = 0.35) was more similar to that of cosmopolitan breeds than to the Romanian and Hungarian domestic and wild pig populations. Finally, Blond Mangalitza x Duroc swine showed high levels of heterozygosity because of their hybrid origin (H_o = 0.40, H_e = 0.32)

The results of the Admixture analysis at K = 12 (Figure 2), the K-value with the lowest cross-validation error, provided evidence of genetic admixture for Blond Mangalitza x Duroc crossbreds, a result that was clearly expectable due to their hybrid origin, and also

for Bazna pigs. We observed that Romanian Red, Hungarian Red, and Blond Mangalitza pigs have distinct genetic backgrounds and that Hungarian wild boars share part of their genetic background with Red Mangalitza from Hungary and Blond Mangalitza (also from Hungary), but not with the four cosmopolitan breeds (Duroc, Large White, Landrace, and Piétrain). In contrast, and as previously published by Manunza *et al.* (2016), two Romanian wild boars had been clearly introgressed with cosmopolitan breeds (probably Large White). At K = 3, Duroc, the three remaining cosmopolitan breeds (Large White, Landrace, Piétrain) and Romanian and Hungarian populations formed three distinct groups (Additional file 1), and at K >= 4 we observed that Red Mangalitza from Hungary and Romania shared the same background which was different from the one displayed by Blond Mangalitza pigs (Additional file 1). From K=8 the common background of Reds of Hungary and Romania splits. Giving hints for looking at descendants of Romanian Red Mangalitza line(s) which are not present today in Hungary.

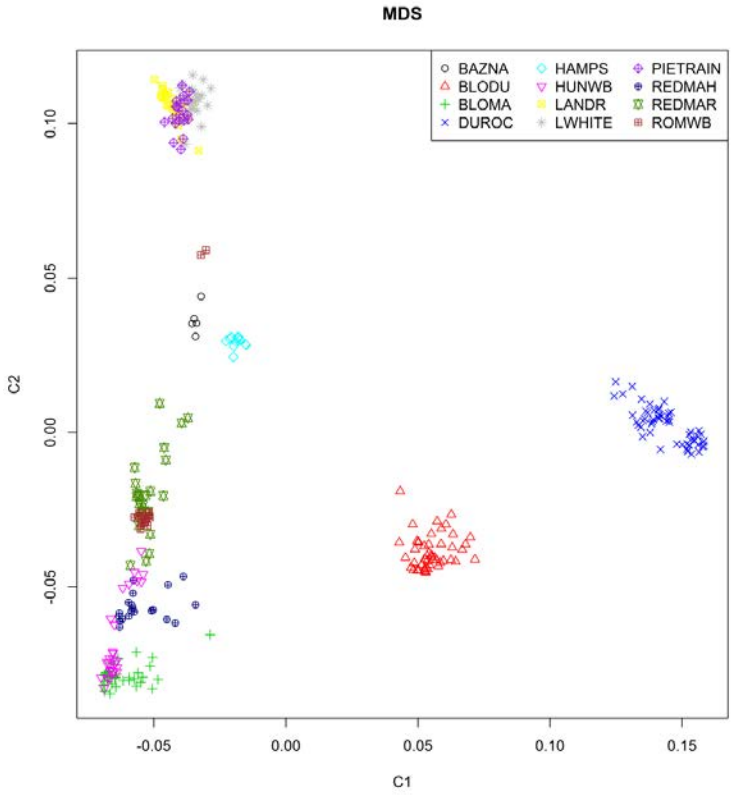

Figure 1 - Multidimensional scaling plot (MDS) depicting the relationships between Mangalitza pigs and other wild boar and pig populations. Abbreviations are defined in Table 1.

Table 1 - Summary statistics calculated over the whole set of pig populations.

Code	Breed (place of collection)	Number of animals	F_{ROH}	Observed (H_o) heterozygosities	Expected (H_e) heterozygosities
BAZNA	Bazna (Hungary)	5	-	-	-
BLODU	Blond Mangalitza x Duroc (Hungary)	48	0.01	0.40	0.32
BLOMA	Blond Mangalitza (Hungary)	37	0.13	0.28	0.28
DUROC	Duroc (Hungary)	56	0.20	0.30	0.30
HAMPS	Hampshire (Hungary)	11	0.18	0.28	0.24
HUNWB	Wild boar (Hungary)	28	0.15	0.27	0.29
LANDR	Landrace (Hungary)	29	0.11	0.35	0.35
LWHITE	Large White (Hungary)	27	0.10	0.36	0.35
PIÉTRAIN	Piétrain (Hungary)	20	0.13	0.36	0.35
REDMAH	Red Mangalitza (Hungary)	20	0.18	0.29	0.28
REDMAR	Red Mangalitza (Romania)	25	0.11	0.35	0.35
ROMWB	Wild boar (Romania)	18	0.12	0.27	0.31

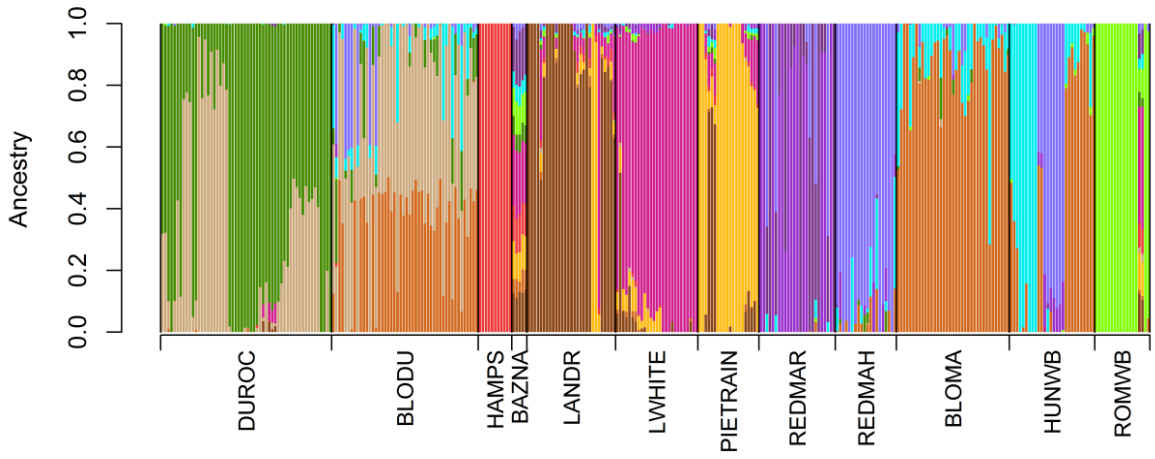

Figure 2- Admixture analysis of Mangalitza pigs and additional wild boar and pig populations for the K-value with the lowest cross-validation error (K = 12). Each individual is represented by a single column divided into K colored segments, where K is the number of assumed clusters. Populations are separated by black lines. Abbreviations are defined in Table 1.

Analysis of runs of homozygosity

We have characterized the length, distribution, and frequency of ROH in the 12 populations under analysis. In general, short and medium ROH (5-15 Mb) were much more frequent than long (15-30 Mb) or very long (> 30 Mb) ROH (Figure 3). The relatively low frequency of very short ROH (1-5 Mb) might have technical reasons *i.e.* with low-resolution SNP chips short ROH are more difficult to detect than the long ones. A comparative analysis of ROH classes revealed that Bazna, Red Mangalitza from Romania and Hungary and Romanian wild boars had the highest frequencies of very long ROH (> 30 Mb), while the levels of homozygosity in Blond Mangalitza x Duroc crossbred pigs were negligible. The number of ROH (but not the ROH coverage) was particularly high in Duroc pigs (Figure 4), while the individuals displaying the highest total ROH length (> 600 Mb) belonged to the Hungarian and Romanian wild boar, Duroc and Red Mangalitza populations (Figure 4). The F_{ROH} coefficients (Table 1) were higher in Blond Mangalitza, Red Mangalitza from Hungary, wild boar from Hungary and Romania and Hampshire pigs (F_{ROH} = 0.12-0.18) than in the Landrace, Large White and Piétrain breeds (F_{ROH} = 0.11-0.13).

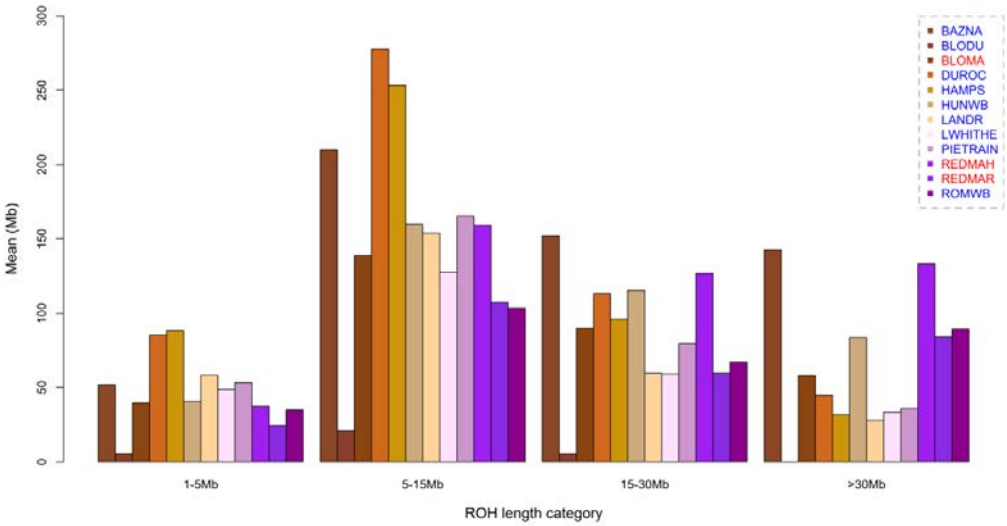

Figure 3 - Classification of the runs of homozygosity identified in Mangalitza pigs and additional wild boar and pig populations based on their size. Abbreviations are defined in Table 1.

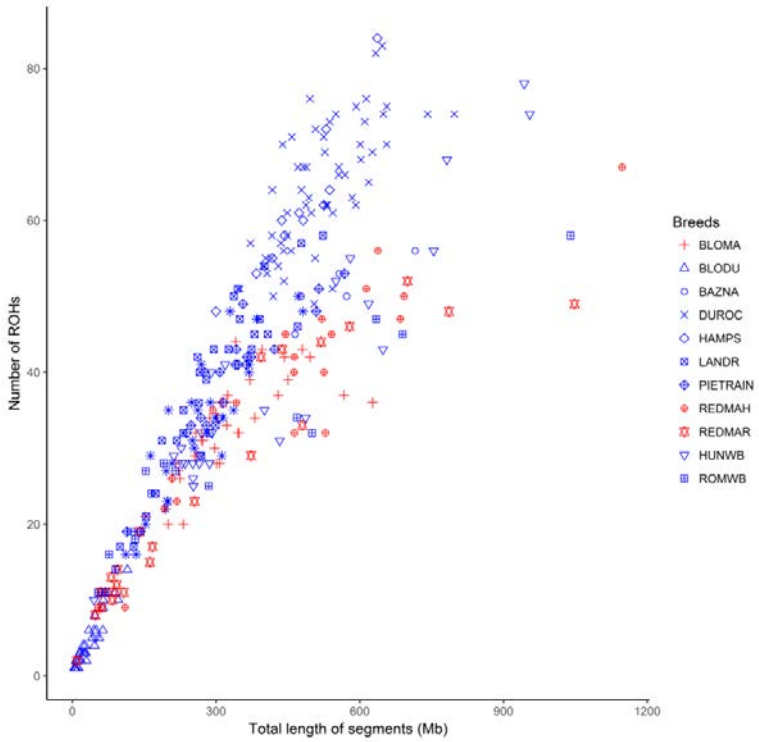

Figure 4 - Number and total length of runs of homozygosity (ROH) in Mangalitza pigs and additional wild boar and pig populations. The number of ROH estimated in each individual genome (*y-axis*) is plotted against total ROH total size (*i.e.* the number of Mb covered by ROH in each genome, *x-axis*). Abbreviations are defined in Table 1.

Selection scan and genome-wide association study for coat coloration in Mangalitza pigs

To identify the genes responsible for the coat coloration in Mangalitza pigs, we performed a selection scan by using the hapFLK software (Fariello et al., 2013). We only detected three putative selective sweeps on SSC7 (65.9-65.9 and 68.0-68.4 Mb), SSC13 (24.5-67.0 Mb) and SSC15 (129.5-133.9 Mb) that remained significant after correction for multiple testing (Figure 5 and Table 2). At the nominal level of significance (Table 2), twelve additional putative selective sweeps were detected on SSC2 (152.1-152.2 Mb), SSC3 (4.9-5.4 Mb), SSC6 (27.9-28.1 Mb), SSC7 (50.9-51.7 Mb), SSC11 (22.3-25.6 Mb), SSC12 (2.4-8.6 Mb), SSC15 (35.7-53.1 Mb), SSC16 (19.3-28.4, 35.0-52.4, 60.5-60.7 and 70.6-71.7 Mb) and SSC17 (60.5-65.8 Mb). As a complementary approach, we carried out a GWAS for red *vs* blond coloration by using the GEMMA (Xiang Zhou & Stephens, 2014) software (Additional file 2 and Table 3). This analysis indicated that the SSC16 (20 Mb) region is the one displaying the most significant associations with coat color. In addition, we found five regions on SSC11, SSC13, SSC15, and SSC16 that were associated with coat color in the GEMMA analysis and that showed evidence of containing selective sweeps in the hapFLK study (Tables 2 and 3). A detailed analysis of the gene content of regions identified by both the GWAS and the hapFLK analysis made possible to identify the *SLC45A2* gene as potential candidate locus for pigmentation. Importantly, this gene maps to the region identified in the GWAS as showing the strongest evidence of being involved in the coloration of Mangalitza pigs.

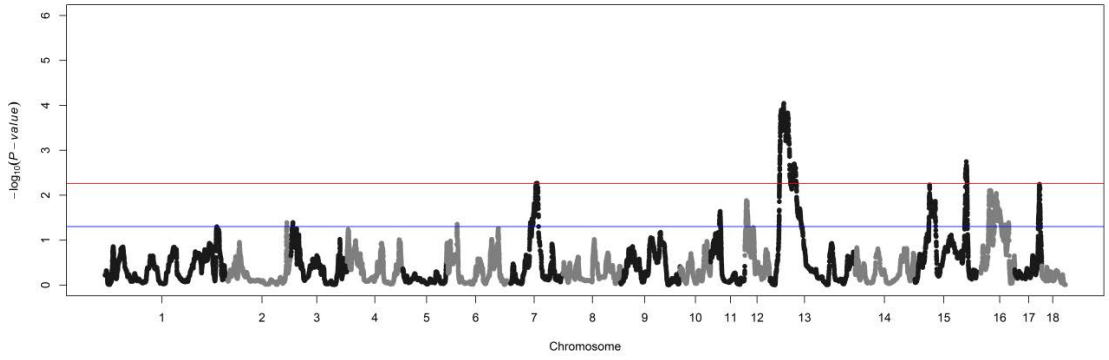

Figure 5 - Genome scan for selection in Red and Blond Mangalitza pigs using the hapFLK test. Genomic coordinates and statistical significance ($-\log_{10}$ *P*-values) are plotted in the *x*- and *y*-*axis*, respectively. Blue and red lines indicate the thresholds of significance set at 0.05 before (nominal *P*-value) and after (*q*-value) correction for multiple testing, respectively.

Table 2 - Putative selective sweeps identified in the hapFLK-based analysis.

CHR	Regions (Mb)	Flanking SNPs	Number of SNPs	Raw *P*-value	q-value
2	152.1-152.2	ASGA0012708 - ASGA0103431	2	0.041	0.285
3	4.9-5.4	ALGA0107454 - M1GA0003719	15	0.041	0.284
6	27.9-28.1	ASGA0082257 - ASGA0085552	4	0.047	0.324
7	50.9-51.7	ASGA0033485 - H3GA0021430	13	0.041	0.284
	65.9-65.9	H3GA0021970 - ALGA0042379	2	0.005	0.049
	68.0 - 68.4	INRA0026293 - ALGA0042379	1	0.005	0.048
11	**22.3-25.6**	**ALGA0116830 - ALGA0061566**	**69**	**0.023**	**0.172**
12	2.4-8.6	MARC0063986 - ALGA0064723	138	0.013	0.112
13	**24.5-67.7**	**MARC0001222 -ALGA0070577**	**475**	**0.000**	**0.001**
15	**35.7-53.1**	**ALGA0112215 - ALGA0085228**	**192**	**0.006**	**0.052**
	129.5-133.9	ALGA0112215 - ALGA0085228	68	0.002	0.013
16	**19.3-28.4**	**H3GA0053033 - ASGA0096846**	**141**	**0.008**	**0.069**
	35.0-52.4	**ASGA0099845 - ASGA0073361**	**180**	**0.009**	**0.080**
	60.5-60.7	**ASGA0073624 - ASGA0073630**	**4**	**0.046**	**0.313**
	70.6-71.7	ALGA0091290 - ALGA0091354	17	0.041	0.284
17	60.5 - 65.8	ALGA0095912 - INRA0054882	97	0.006	0.051

Those sweeps consistently found with GWAS analysis are shown in bold. **CHR** = chromosome, **Mb** = Megabase**.**

Table 3 - Markers associated with the coat pigmentation of Red *vs* Blond Mangalitza pigs.

Chr	SNP	Region (Mb)	A1	MAF	δ ± SE	*P*-value	*q*-value
1	H3GA0004085	268.57	T	0.201	1.59E-01 ± 3.81E-02	5.51E-05	4.95E-02
3	MARC0076501	13.16	T	0.463	-1.87E-01 ± 4.16E-02	1.58E-05	2.20E-02
4	ALGA0023180	11.95	C	0.305	1.77E-01 ± 3.66E-02	4.07E-06	8.10E-03
6	ALGA0104612	10.07	C	0.287	1.65E-01 ± 3.90E-02	4.18E-05	4.02E-02
	ASGA0084188	84.01	G	0.012	4.81E-01 ± 1.09E-01	2.09E-05	2.49E-02
8	ALGA0049975	141.98	A	0.378	-1.42E-01 ± 3.11E-02	1.19E-05	1.84E-02
9	ALGA0106913	152.71	C	0.259	2.04E-01 ± 4.63E-02	2.14E-05	2.49E-02
11	ALGA0061440	24.06	T	0.195	2.28E-01 ± 4.50E-02	1.52E-06	4.06E-03
12	ASGA0100764	13.47	A	0.36	-1.57E-01 ± 3.35E-02	7.73E-06	1.33E-02
	ALGA0065183	14.21	T	0.329	1.93E-01 ± 3.82E-02	1.60E-06	4.06E-03
	ASGA0083985	15.00	A	0.396	1.36E-01 ± 3.18E-02	3.70E-05	3.68E-02
	MARC0040976	15.89	G	0.037	3.58E-01 ± 7.26E-02	2.67E-06	6.21E-03
	H3GA0053469	46.59	G	0.238	2.51E-01 ± 4.86E-02	1.08E-06	4.06E-03
13	ALGA0123031	25.91	T	0.439	-1.52E-01 ± 3.51E-02	3.02E-05	3.23E-02
	ALGA0069677	40.63	G	0.061	2.23E-01 ± 5.28E-02	4.33E-05	4.02E-02
	ALGA0073466	199.92	T	0.47	-1.78E-01 ± 3.47E-02	1.27E-06	4.06E-03
14	ALGA0081626	133.51	T	0.396	-1.92E-01 ± 3.38E-02	1.17E-07	1.09E-03
15	MARC0003646	38.89	C	0.329	1.51E-01 ± 3.41E-02	1.88E-05	2.49E-02
	MARC0084849	52.27	T	0.25	1.68E-01 ± 3.28E-02	1.24E-06	4.06E-03
	ASGA0070586	133.16	T	0.366	1.35E-01 ± 3.06E-02	2.14E-05	2.49E-02
16	H3GA0053033	19.38	A	0.488	1.81E-01 ± 3.56E-02	1.44E-06	4.06E-03
	ASGA0097489	19.77	A	0.494	1.96E-01 ± 3.37E-02	6.44E-08	8.97E-04
	MARC0032767	20.30	G	0.427	-2.42E-01 ± 3.67E-02	2.00E-09	5.58E-05
	MARC0010290	20.67	A	0.494	-1.64E-01 ± 3.53E-02	8.12E-06	1.33E-02
	H3GA0046337	26.74	C	0.39	1.46E-01 ± 3.21E-02	1.33E-05	1.95E-02
	ALGA0090377	39.05	A	0.482	-1.34E-01 ± 3.09E-02	2.94E-05	3.23E-02
	ALGA0090577	48.09	T	0.439	1.65E-01 ± 3.51E-02	7.27E-06	1.33E-02
	ASGA0073624	60.52	G	0.378	1.71E-01 ± 3.53E-02	3.76E-06	8.06E-03
17	ALGA0093727	24.01	G	0.494	1.42E-01 ± 3.31E-02	3.30E-05	3.41E-02
18	ALGA0118541	0.12	G	0.262	2.62E-01 ± 5.01E-02	8.09E-07	4.06E-03

SSC: porcine chromosome, SNP: SNP displaying the significant association with the trait under study, **Region (Mb)**: region containing SNPs significantly associated with the trait under study in megabase, **A1**: minority allele, **MAF**: frequency of the minority allele, **δ**: allelic effect and its standard error (**SE**), ***P*-value**: nominal *P*-value, **q-value**: q-value calculated with a false discovery rate approach.

Analysis of the segregation of three SLC45A2 missense polymorphisms in Mangalitza pigs with distinct coat coloration.

The analysis of the gene content of the SSC16 (20 Mb) region, which was based on the annotation of the Ensembl database (https://www.ensembl.org), highlighted the solute carrier family 45 member 2 (*SLC45A2*) locus as a potential candidate gene to explain the segregation of coat color. The comparison of whole-genome sequences from one Red, one Swallow Belly and two Blond Mangalitza pigs (SRA access: SRP039012) reported by Molnar *et al.* (2014) made possible to detect 394 SNPs mapping to the *SLC45A2* gene (Additional file 3). Amongst this set of polymorphisms, we identified three missense SNPs, *i.e.* rs341599992 (c.806G>A, p.Gly269Glu, in exon 3), rs327001340 (c.829A>G, p.Ser277Gly, in exon 3) and rs693695020 (c.956G>A, p.Arg319His, in exon 4), that were genotyped in an independent sample of 209 pigs including Red, Blond and Swallow Belly Mangalitza as well as other breeds (*i.e.* these pigs were different than the ones typed with the SNP chip). We also used the Mangalitza whole genome sequences reported by Molnar *et al.* (2014) to examine the non-synonymous variability of the melanocortin receptor 1 gene (*MC1R*), which plays a key role in porcine coat color (Fang et al., 2009b). We identified two missense SNPs, *i.e.* rs45435032 (c.491T>C, Val164Ala) and rs321432333 (c.727A>G, Thr243Ala), segregating in Mangalitza pigs. This analysis showed that both Blond and Red Mangalitza pigs were homozygous for the *MC1R-0401* allele which confers a red pigmentation, *i.e.* their genotypes were TT and AA for the two above mutations.

The results of the *SLC45A2* genotyping experiment are shown in Table 4. We observed the existence of strong differences in the genotype and allele frequencies of the c.806G>A and the c.956G>A SNPs between Red and Blond Mangalitza pigs. The majority of Blond Mangalitza pigs were AA (c.806G>A) and GG (c.956G>A), while most of Red Mangalitza pigs displayed the alternative genotypes *i.e.* GG or GA (c.806G>A) and AA or GA (c.956G>A). The association between c.806G>A and c.956G>A genotypes and red and blond coloration was very high ($p = 0.001E10^{-23}$) but not complete. The Swallow Belly Mangalitza pigs, which have a black coat combined with yellow blond throat and underbelly (Egerszegi et al., 2003), had a high frequency of the A-allele of the c.806G>A SNP. This allele is relatively rare in Red Mangalitza as well as in the remaining breeds. The A-allele of the c.956G>A SNP only segregated at significant frequencies in Red Mangalitza, being very rare (Swallow Belly) or absent in the remaining populations. The

SIFT software (Kumar et al., 2009) predicted that the c.806G>A SNP is deleterious (SIFT score: 0.05), while the Panther software (Thomas et al., 2003) predicted that both c.806G>A and c.956G>A SNPs have pathogenic effects on protein function. The *c.829A>G* SNP was classified by both softwares as a non-deleterious mutation and it did not show any obvious association with coat color. Associations were much stronger for the c.806G>A (χ^2 = 88.6, p-value < 2.2E-16) and the c.956G>A SNPs (χ^2 = 78.2, p-value < 2.2E-16) than for the c.829A>G SNP (χ^2 = 5.27, *P*-value = 0.021). Our results indicate that the A-allele of the c.806G>A SNP significantly increases the chances of having a blond coat colour (OR = 14.08), while the G-allele of the c.956G>A SNP would decrease such chance (OR = 0.10). The c.829A>G SNP had an OR of 1.18, evidencing that this polymorphism is not involved in Mangalitza pigmentation.

Discussion

One of the main goals of our study was to investigate if the strong population recession experienced by Mangalitza pigs has resulted in a severe contraction of their genetic diversity. The observed and expected heterozygosities of Hungarian Red and Blond Mangalitza were lower than those estimated in cosmopolitan breeds as Large White, Landrace and Piétrain. However, this result is expectable because cosmopolitan breeds, and especially Large White swine, carry Asian alleles at high frequencies due to their introgression with Chinese sows during the 18^{th}-19^{th} centuries. In contrast, the origin of Mangalitza pigs is exclusively European (Manunza et al., 2016). Moreover, the observed and expected heterozygosities were quite high in Romanian Red Mangalitza pigs and relatively low in Hungarian and Romanian wild boars. As reported by Manunza *et al.* (2016), the low variation of East European wild boars might be due to a process of demographic reduction caused by excessive hunting, epidemic diseases, and habitat destruction. The analysis of ROH also evidenced that Bazna, Red Mangalitza from Romania and Hungary and Romanian wild boars have the highest frequencies of very long ROH (> 30 Mb), reflecting a history of strong and recent inbreeding. Similar patterns of homozygosity have been reported in Hungarian Mangalitza pigs (Yang et al., 2017). The strong reduction in population size combined with matings between related individuals might be the main cause of the high frequency of very long ROH in Hungarian Red Mangalitza. In contrast, such pattern was not obvious in Blond or Romanian Red

Mangalitza, evidencing that the three Mangalitza populations analysed in the current work underwent different demographic histories. Indeed, the MDS plot (Figure 1) and the Admixture results (Figure 2) indicated the existence of genetic differentiation between Blond and Red Mangalitza. As previously explained, Red Mangalitza was produced by crossing, approximately one century ago, Blond Mangalitza with Szalontai pigs, a high, bulky, robust and red-coated Hungarian aboriginal race devoted to produce meat (Hankó, 1940).

One of the sources of genetic variability in Mangalitza pigs could be their introgression with wild boars. Indeed, the genome-wide analysis of the diversity of Mangalitza pigs indicated the existence of a close genetic affinity between this breed and wild boars (HUNWB and ROMWB, Figure 1). In the Admixture analysis (Figure 2), Hungarian Red and Blond Mangalitza shared a common genetic background with Hungarian wild boars. Similar results have been obtained when comparing Iberian pigs and Spanish wild boars (Manunza et al., 2016), a finding that might be explained by the occurrence of ancient and recent genetic exchanges between wild and domestic pigs. Indeed, it is well known that Szalontai sows, which intervened in the formation of the Red Mangalitza variety, produce stripped piglets, a strong indication of their ancient and extensive introgression with local wild boars (Egerszegi et al., 2003). Moreover, as many as 25% pigs of the commune of Bârzava (Arad County, Romania) have been introgressed with wild boars (Matiuti et al., 2010). This high level of introgression could be due to the extensive regime of pastoral management that has been traditionally performed in certain areas of Romania, where pigs are allowed to roam free providing a window of opportunity for the occurrence of unintentional matings with wild boars (Matiuti et al., 2010). We also detected that in the MDS plot the five Bazna pigs lie at an intermediate position between Mangalitza pigs and cosmopolitan breeds and close to Hampshire pigs (Figure 1). Moreover, in the Admixture analysis (Figure 2) the Bazna pigs showed evidence of introgression with cosmopolitan breeds. This finding is consistent with the composite origin of this breed *i.e.* it was created in 1872 by crossing Mangalitza and Berkshire pigs, being subsequently introgressed with blood from Sattelschwein, Large White and Berkshire pigs (Ciobanu et al., 2001).

Table 4 - The genotype and allele frequency of *SLC45A2* polymorphisms in 209 pigs from different populations.

Breed	Number of animals	*SLC45A2*:c.829A>G					*SLC45A2*:c.806G>A					*SLC45A2*:c.956G>A				
		Genotype Frequencies			Allele Frequencies		Genotype Frequencies			Allele frequencies		Genotype frequencies			Allele frequencies	
		AA	**GA**	**GG**	**A**	**G**	**GG**	**GA**	**AA**	**G**	**A**	**GG**	**GA**	**AA**	**G**	**A**
Blond Mangalitza	55	0.96	0.04	0.00	0.98	0.02	0.00	0.04	0.96	0.02	0.98	1.00	0.00	0.00	1.00	0.00
Swallow Belly Mangalitza	30	0.63	0.30	0.07	0.78	0.22	0.13	0.23	0.63	0.25	0.75	0.93	0.07	0.00	0.97	0.03
Red Mangalitza	65	0.79	0.20	0.02	0.89	0.11	0.84	0.10	0.05	0.90	0.10	0.15	0.17	0.68	0.24	0.76
Piétrain	15	0.40	0.50	0.10	0.65	0.35	0.22	0.56	0.22	0.50	0.50	1.00	0.00	0.00	1.00	0.00
Large White	15	0.20	0.60	0.20	0.50	0.50	0.22	0.67	0.11	0.56	0.44	1.00	0.00	0.00	1.00	0.00
Landrace	15	0.00	0.07	0.93	0.03	0.97	0.88	0.13	0.00	0.94	0.06	1.00	0.00	0.00	1.00	0.00
Duroc	14	0.00	0.07	0.93	0.03	0.96	0.93	0.07	0.00	0.96	0.04	1.00	0.00	0.00	1.00	0.00

Several pigmentation loci have been identified in pigs, but the genetic basis of coat color remains to be fully elucidated. It is well known that the increase in the number of copies of the KIT proto-oncogene receptor tyrosine kinase (*KIT*) gene, which is essential for the survival, proliferation and migration of melanocytes, is the main causal factor of the white coat characteristic of certain cosmopolitan breeds such as Large White and Landrace (Giuffra et al., 2002). The polymorphism of the melanocortin receptor 1 (*MC1R*) gene is another main determinant of pig pigmentation, being associated with red, black and black spotted coat colors (Fang et al., 2009). More recently, several potential pigmentation loci, such as *TYRP1*, *MITF*, *EDNRB*, *CNTLN*, and *PINK1* have been reported in Chinese porcine breeds (Lü et al., 2016; Ren et al., 2011; Chao Wang et al., 2015; Wu et al., 2016). In the current work, we aimed to elucidate the genetic basis of the blond *vs* red color in Mangalitza pigs by using a combination of selection scan and GWAS approaches. One of the main advantages of our experimental design is that the two populations under analysis are closely related, thus minimizing the presence of regions that are highly differentiated as a consequence of drift (instead of artificial selection). The selection scan with the hapFLK software in Red *vs* Blond Mangalitza pigs revealed a very strong selective sweep on SSC13 SSC13 (24.5-67.7.0 Mb) which attained its maximum significance in the 27.1-47.2 Mb interval (q-value < 5.5E-04). Other significant selective sweeps were located on SSC2 (152.1-152.2 Mb), SSC3 (4.9-5.4 Mb), SSC6 (27.9-28.1 Mb), SSC7 (65.9-65.9, 50.9-51.7, and 68.0-68.4 Mb), SSC11 (22.3-25.6 Mb), SSC12 (2.4-8.6 Mb), SSC15 (35.7-53.1 and 129.5-133.9 Mb), SSC16 (19.3-28.4, 35.0-52.4, 60.5-60.7, and 70.6-71.7 Mb) and SSC17 (60.5-65.8 Mb). As a complementary approach, we carried out a GWAS by using the GEMMA software which confirmed that the SSC16 (20Mb) region is the one displaying the most significant association with coat color (Additional file 2 and Table 3).

We examined the gene content of this SSC16 region and we detected the presence of the *SLC45A2* gene, also known as membrane-associated transporter protein (*MATP*). Interestingly this protein is a key regulator of the melanosomal pH and tyrosinase activity (Bin et al., 2015). In humans, mutations in the *SLC45A2* gene have causal effects on oculocutaneous albinism type 4 (Tóth et al., 2017) and the variability of this gene has been associated with olive skin (Graf et al., 2005; Graf et al., 2007), blond/red hair, pale skin and freckles (Fracasso et al., 2017) and black hair (Branicki et al., 2008). The cream color of horses has also been linked to a missense substitution in the *SLC45A2* gene (Mariat et al., 2003). Moreover, there is compelling evidence that certain *SLC45A2* polymorphisms

lead to reduced levels or absence of melanin in tigers, mice, medaka fish, chicken, Japanese quails, gorillas, dogs and cattle (Rothammer et al., 2017). These evidences resulted in the selection of the *SLC45A2* locus as the most probable causal factor of the red vs blond pigmentation in Mangalitza pigs.

The genotyping of three missense mutations in the porcine *SLC45A2* locus evidenced the existence of strong associations between c.806G>A and c.956G>A SNPs and coat color (*P*-value < 2.2E-16). In contrast, the c.829A>G SNP showed a weak association with pigmentation. The A-allele of c.806G>A was almost fixed in Blond Mangalitza and nearly absent from Red Mangalitza. The A-allele was also present in Large White and Landrace pigs, two breeds that are white due to the epistatic effect of the *KIT* duplication, which suppresses any pigmentation. The A-allele of the c.956G>A SNP has a high frequency in Red Mangalitza pigs being absent from the remaining breeds. The most probable cause for the near-fixation of alternative *SLC45A2* genotypes in Blond and Red Mangalitza pigs is divergent directional selection for color. These two missense substitutions are predicted to be deleterious by Panther and they are located in a cytoplasmic domain (Uniprot: Q4LE88). According to Loganathan *et al.* (2016), the cytoplasmic domain plays a fundamental role in the transport function of the integral membrane transport protein *SLC4A11*. Although the associations between *SLC45A2* genotypes and coat color are very strong, they are not complete suggesting the existence of additional factors regulating pigmentation in Mangalitza pigs. This conclusion is supported by the simultaneous identification, with GEMMA and hapFLK, of several regions on SSC11, SSC13, SSC15 and SSC16 as associated with color and containing selective sweeps.

The knowledge about the genetic basis of pigmentation in pigs is still poorly understood. Our study adds a new gene, the *SLC45A2* locus, to the catalogue of loci with a well established or probable role in the genetic determination of porcine coat color. Further studies will be needed to finely map the causal mutation as well as to elucidate the existence of genetic interactions between *SLC45A2* and other genes. Our study also illustrates the power of dissecting the genomic basis of simple phenotypes by employing sets of closely related lines or populations and combining different statistical approaches.

Conflict of Interest

The authors declare no conflict of interest

Author Contributions

AZ, VAB and MA designed the experiments; AZ, IA and VAB were responsible for the experimental protocols and generation of animal material; ABJ, AZ, IA, IE and VAB contributed to the obtaining of biological samples; AZ performed DNA extractions; AZ and TFC carried out the diversity analyses, TFC carried out the selection scan and the GWAS; MA and TFC analysed the gene content of selected regions, TFC contributed to the genotyping of the *SLC45A2* gene; MA, TFC, AZ and VAB wrote the paper. All authors read and approved the manuscript.

Funding

Part of the research presented in this publication was funded by grant AGL2013–48742-C2–1-R awarded by the Spanish Ministry of Economy, and by projects TKISSE and TGENRE supported by the Hungarian Ministry of Agriculture. We also acknowledge the support of the Spanish Ministry of Economy and Competitivity for the *Center of Excellence Severo Ochoa 2016-2019* (SEV-2015-0533) grant awarded to the Centre for Research in Agricultural Genomics (CRAG). Tainã Figueiredo Cardoso was funded with a fellowship from the CAPES Foundation-Coordination of Improvement of Higher Education, Ministry of Education of the Federal Government of Brazil. Thanks also to the CERCA Programme of the Generalitat de CatalunyaThe funders had no role in study design, data collection, and analysis, decision to publish or preparation of the manuscript.

References

Alexander DH, Lange K (2011). Enhancements to the ADMIXTURE algorithm for individual ancestry estimation. *BMC Bioinformatics* **12**: 246.

Alexander DH, Novembre J, Lange K (2009). Fast model-based estimation of ancestry in unrelated individuals. *Genome Research* **19:** 1655–64.

Benjamini Y, Hochberg Y (1995). Controlling the false discovery rate: a practical and powerful approach to multiple testing. *Journal of the Royal Statistical Society* **57**: 289–300.

Bin B-H, Bhin J, Yang SH, Shin M, Nam Y-J, Choi D-H, et al. (2015). Membrane-associated transporter protein (MATP) regulates melanosomal ph and influences tyrosinase activity. *PLoS One* **10**: e0129273.

Branicki W, Brudnik U, Draus-Barini J, Kupiec T, Wojas-Pelc A (2008). Association of the *SLC45A2* gene with physiological human hair colour variation. *Journal of Human Genetics* **53**: 966–971.

Cingolani P, Platts A, Wang LL, Coon M, Nguyen T, Wang L, et al. (2012). A program for annotating and predicting the effects of single nucleotide polymorphisms, SnpEff. *Fly* **6**: 80–92.

Ciobanu DC, Day AE, Nagy A, Wales R, Rothschild MF, Plastow GS (2001). Genetic variation in two conserved local Romanian pig breeds using type 1 DNA markers. *Genetics, Selection, Evolution : GSE* **33**: 417–32.

Egerszegi I, Rátky J, Solti L, Brüssow K-P (2003). Mangalica: an indigenous swine breed from Hungary (Review). *Archives Animal Breeding* **46**: 245–256.

Fang M, Larson G, Soares Ribeiro H, Li N, Andersson L (2009). Contrasting mode of evolution at a coat color locus in wild and domestic pigs. *PLoS Genetics* **5**: e1000341.

FAO (2015). *The Second Report on the State of the World's Animal Genetic Resources for Food and Agriculture*. AO Commission on Genetic Resources for Food and Agriculture Assessments: Rome.

Fariello MI, Boitard S, Naya H, SanCristobal M, Servin B (2013). Detecting signatures of selection through haplotype differentiation among hierarchically structured populations. *Genetics* **193**: 929–941.

Fracasso NC de A, de Andrade ES, Wiezel CEV, Andrade CCF, Zanão LR, da Silva MS, et al. (2017). Haplotypes from the SLC45A2 gene are associated with the presence of freckles and eye, hair and skin pigmentation in Brazil. *Legal Medicine* **25**: 43–51.

Giuffra E, Törnsten A, Marklund S, Bongcam-Rudloff E, Chardon P, Kijas JMH, et al. (2002). A large duplication associated with dominant white color in pigs originated by homologous recombination between LINE elements flanking KIT. *Mammalian Genome* **13**: 569–577.

Graf J, Hodgson R, van Daal A (2005). Single nucleotide polymorphisms in the *MATP* gene are associated with normal human pigmentation variation. *Human Mutation* **25**: 278–284.

Graf J, Voisey J, Hughes I, van Daal A (2007). Promoter polymorphisms in the *MATP* (*SLC45A2*) gene are associated with normal human skin color variation. *Human Mutation* **28**: 710–717.

Hankó B (1940). *Ancient domestic animals of Hungary*. (Ősi magyar háziállataink) Debrecen Tiszántúli Mg-i Kamara.

Kumar P, Henikoff S, Ng PC (2009). Predicting the effects of coding non-synonymous variants on protein function using the SIFT algorithm. *Nature Protocols* **4**: 1073–1081.

Loganathan SK, Lukowski CM, Casey JR (2016). The cytoplasmic domain is essential for transport function of the integral membrane transport protein SLC4A11. *American Journal of Physiology-Cell Physiology* **310**: C161–C174.

Lü M-D, Han X-M, Ma Y-F, Irwin DM, Gao Y, Deng J-K, et al. (2016). Genetic variations associated with six-white-point coat pigmentation in Diannan small-ear pigs. *Scientific Reports* **6**: 27534.

Manunza A, Amills M, Noce A, Cabrera B, Zidi A, Eghbalsaied S, et al. (2016). Romanian wild boars and Mangalitza pigs have a European ancestry and harbour genetic signatures compatible with past population bottlenecks. **Scientific Reports** *6*: 29913.

Mariat D, Taourit S, Guérin G (2003). A mutation in the *MATP* gene causes the cream coat colour in the horse. *Genetics, Selection, Evolution : GSE* **35**: 119–33.

Matiuti M, Bogdan AT, Crainiceanu E, Matiuti C (2010). Research Regarding the Hybrids Resulted from the Domestic Pig and the Wild Boar. 43: 188–191.

Molnár J, Nagy T, Stéger V, Tóth G, Marincs F, Barta E (2014). Genome sequencing and analysis of Mangalica, a fatty local pig of Hungary. *BMC Genomics* **15**: 761.

Purcell S, Neale B, Todd-Brown K, Thomas L, Ferreira MAR, Bender D, et al. (2007). PLINK: a tool set for whole-genome association and population-based linkage analyses. *American journal of human genetics* **81**: 559–75.

Ren J, Mao H, Zhang Z, Xiao S, Ding N, Huang L (2011). A 6-bp deletion in the *TYRP1* gene causes the brown colouration phenotype in Chinese indigenous pigs. *Heredity* **106**: 862–8.

Rothammer S, Kunz E, Seichter D, Krebs S, Wassertheurer M, Fries R, et al. (2017). Detection of two non-synonymous SNPs in *SLC45A2* on BTA20 as candidate causal mutations for oculocutaneous albinism in Braunvieh cattle. *Genetics, Selection, Evolution : GSE* **49**: 73.

Storey JD, Tibshirani R (2003). Statistical significance for genomewide studies. *Proceedings of the National Academy of Sciences of the United States of America* **100**: 9440–5.

Thomas PD, Campbell MJ, Kejariwal A, Mi H, Karlak B, Daverman R, et al. (2003). PANTHER: A Library of Protein Families and Subfamilies Indexed by Function. *Genome Research* **13**: 2129–2141.

Tóth L, Fábos B, Farkas K, Sulák A, Tripolszki K, Széll M, et al. (2017). Identification of two novel mutations in the *SLC45A2* gene in a Hungarian pedigree affected by unusual OCA type 4. *BMC Medical Genetics* **18**: 27.

Wang C, Wang H, Zhang Y, Tang Z, Li K, Liu B (2015). Genome-wide analysis reveals artificial selection on coat colour and reproductive traits in Chinese domestic pigs. *Molecular Ecology Resources* **15**: 414–424.

Wu X, Zhang Y, Shen L, Du J, Luo J, Liu C, et al. (2016). A 6-bp deletion in exon 8 and two mutations in introns of TYRP1 are associated with blond coat color in Liangshan pigs. *Gene* **578**: 132–136.

Yang B, Cui L, Perez-Enciso M, Traspov A, Crooijmans RPMA, Zinovieva N, et al. (2017). Genome-wide SNP data unveils the globalization of domesticated pigs. *Genetics Selection Evolution*: *GSE* **49**: 71.

Zhou X, Stephens M (2014). Efficient multivariate linear mixed model algorithms for genome-wide association studies. *Nature Methods* **11**: 407–409.

Zsolnai A, Anton I, Kuhn C, Fesus L (2003). Detection of single-nucleotide polymorphisms coding for three ovine prion protein variants by primer extension assay and capillary electrophoresis. *Electrophoresis* **24**:634–638.

Zsolnai A, Szántó-Egész R, Anton I, Tóth P, Micsinai A, Rátky J (2013a). Mangalica fajták genetikai távolsága, elkülönítésük nukleotid polimorfizmust mutató DNS markerekkel [Genetic distance of Mangalica breeds, distinction by DNA markers showing nucleotide polymorphism]. *Hungarian Veterinary Journal* **135**: 303–307.

Zsolnai A, Tóth G, Molnár J, Stéger V, Marincs F, Jánosi A, et al., (2013b). Looking for breed differentiating SNP loci and for a SNP set for parentage testing in Mangalica. Archives of Animal Breeding 56: 200–207.

LEGENDS TO ADDITIONAL FILES

Additional file 1. Admixture analysis of Mangalitza pigs and additional wild boar and pig populations for a range of K-values (K = 2-11). Each individual is represented by a single column divided into K colored segments, where K is the number of assumed clusters. Populations are separated by black lines.

Additional file 2. Manhattan plot corresponding to the genome-wide association analysis performed for coat color in Red and Blond Mangalitza pigs. In the y-axis, statistical significance is expressed as a $-\log_{10}$ (*q*-value) whilst genomic coordinates are displayed in the x-axis. The red and blue lines indicate the thresholds of genome-wide significance corresponding to q-values of 0.01 and 0.05.

Additional file 3. List of *SLC45A2* SNPs identified through the comparison of whole-genome sequences corresponding to Red, Blond and Swallow Belly Mangalitza pigs and reported by Molnar et al. (2014).

General Discussion

Chapter 4

One of the main goals of this Thesis was to investigate the molecular basis of fat deposition in pigs. Such biological knowledge is necessary for understanding the functions of genes and their interactions as well as to interpret correctly the results of genome-wide association analyses. In this regard, studies performed in humans have demonstrated that many genes involved in carbohydrate and lipid metabolism remain to be identified (Khetarpal & Rader, 2014; Teslovich et al., 2010; Willer et al., 2013). For instance, 48% of novel loci displaying significant associations with blood lipid levels described by Willer et al. (2013) had never been previously connected to lipid metabolism.

To gain new insights into the genetic basis of meat quality and muscle metabolism, we have analysed skeletal muscle mRNA expression in two different biological models: (1) Two groups of pigs with distinct fatness profiles, and (2) Three groups of pigs with different nutritional status (*i.e.* fasting, and 5 h. and 7 h. after feeding). In the next sections, we will discuss the main results obtained through transcriptomics analysis of these two different models using RNA-Seq technology

4.1 Differential expression of metabolic genes in the skeletal muscle of Duroc pigs with different fatness profiles

The biological model employed in the first chapter of the Thesis consisted of 52 Duroc pigs retrieved from an experimental population denominated as *Lipgen* (Gallardo et al. 2008). These 52 pigs represented two different metabolic patterns defined by a subset of 13 fatness and growth-related traits (Figure 4.1). HIGH pigs were fatter and they had a higher IMF, SFA and MUFA contents as well as elevated serum lipid concentrations when compared to LOW pigs. In contrast, LOW pigs had a higher muscle PUFA content and were leaner than HIGH pigs.

Even though the initial analysis of RNA-Seq data made possible to identify 1,430 DE mRNAs genes when considering a significance threshold of P-value < 0.05, this list of DE genes suffered a strong reduction (96 genes) when we applied a more stringent threshold (P-value < 0.01 and FC > 1.5). Moreover, only 21 genes showed a significant DE after correcting for multiple testing (q-value < 0.05). The level of concordance between our analysis and a previous study carried out by Cánovas et al (2010) using microarray techlogy was quite modest, although the Spearman correlation between RNA-Seq and microarray expression values was 0.54. A modest overlap between microarray and RNA-

Seq data has been reported in previous studies (Trost et al., 2015; Wang et al., 2014). Moreover, the study of Cánovas et al (2010) was based on 104 individuals and the estimation of highly and lowly expressed genes with microarrays is difficult (Black et al., 2014). In addition, the gene annotation of the porcine microarray is considerably poor (Tsai et al., 2006). Seyednasrollah and coworkers (2015) performed a systematic comparison of different pipelines for detecting differential expression by using RNA-Seq data. They demonstrated that there are large differences across pipelines, and this can lead to considerable variability in the reported results.

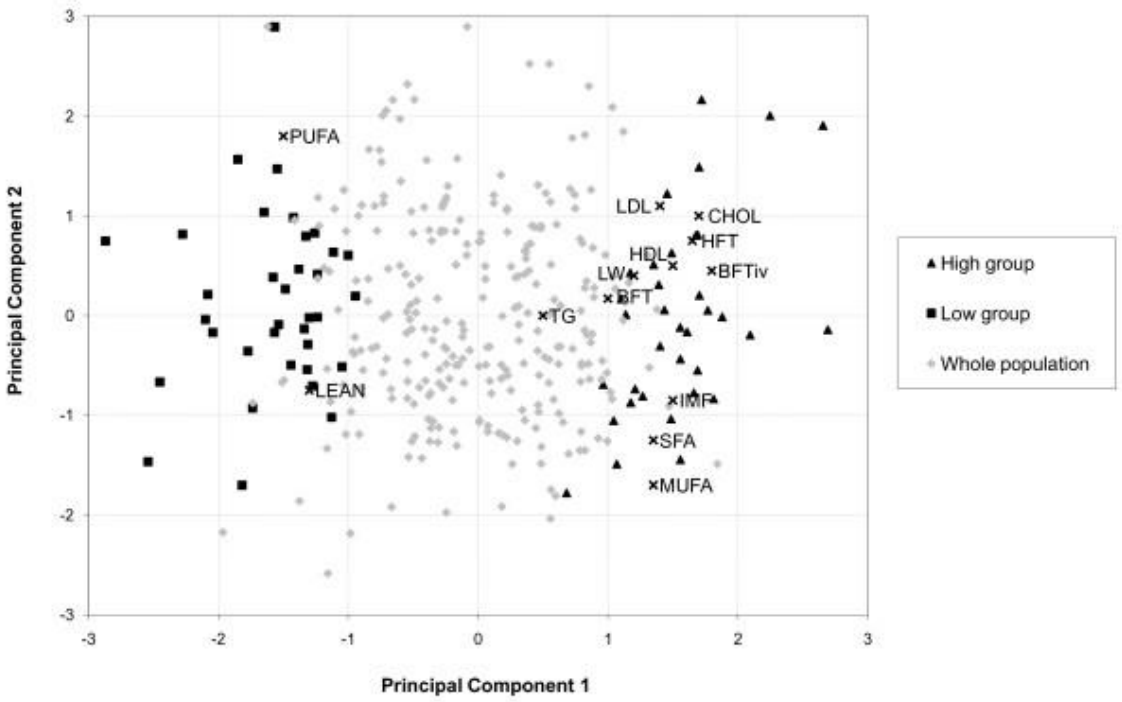

Figure 4.1 - Graphical plot of the first and second principal components summarising phenotypic variation in the Duroc population. Summary of phenotypic variation of serum lipid, growth and fatness parameters in the Duroc pig resource population. The distribution of the individuals selected as HIGh and LOW is shown in the graph. **PUFA** = % Polyunsaturated fatty acids; **LEAN** = %Lean; **TG** = Triacylglycerides (mg/dl); **LDL** = LDL-cholesterol (mg/dl); **HDL** = HDL-cholesterol (mg/dl); **CHOL** = Total cholesterol (mg/dl); **LW** = Live weight (Kg); **BFTiv** = Backfat thickness (*in vivo*) (mm); **BFT** = Backfat thickness 3^{rd}-$4t^{h}$ ribs (mm); **HFT** = Ham fat thickness (mm); **IMF** = % Intramuscular fat; **SFA** = % Saturated fatty acids; **MUFA** = % Monounsaturated fatty acids (Cánovas et al., 2010).

The functions of the most significant DE loci between HIGH and LOW pigs are quite heterogeneous. We have detected genes that have a well-known role in the development of obesity and lipid metabolism. For instance, the long-chain fatty acid transport protein 4

(*SLC27A4*) is the principal fatty acid transporter in small intestinal enterocytes and its expression is correlated with adipose differentiation and the development of insulin resistance (Yu et al., 2018). The acyl-CoA synthetase short-chain family member 1 (*ACSS1*) gene has also a key role in lipid metabolism because it converts acetate to acetyl-CoA, a lipogenic substrate (Schwer et al., 2006). Moreover, overexpression of the *SOD3* gene blocks high-fat diet-induced obesity, fatty liver, and insulin resistance (Cui et al., 2014). In an experiment of differential gene expression, it is difficult to evaluate if differential expression is the cause or the consequence of obesity. The altered expression of several genes might contribute to establishing a phenotype of increased fatness, and such phenotype might have downstream effects on the expression of other genes with heterogeneous and unrelated functions. For instance, in obesity, to avert systemic lipotoxicity from chronic overfeeding, adipocytes promote the activation of several inflammatory pathways. This activation of macrophages/immune system genes culminates in the development of insulin-resistant adipocytes that release excessive amounts of free fatty acids and cause insulin resistance and lipoapoptosis in other tissues, *e.g.* liver and muscle (Cusi, 2012)

To facilitate the interpretation of the data generated in the RNA-Seq experiment, we explored the biological pathways enriched in the set of DE genes (96 genes, *P*-value < 0.01 and a FC > 1.5) and we also built networks connecting DE genes. In this way, we identified pathways related with lipid synthesis (stearate, palmitate and γ-linolenate synthesis, FA activation, CDP-diacylglycerol biosynthesis), catabolism (triacylglycerol degradation), glucose metabolism (glucose synthesis and degradation) and hormonal response (insulin-like growth factor-1, growth hormone, and hepatocyte growth factor). Similar results were obtained by Cánovas et al. (2010), when analyzing the same population with microarrays, as well as by other authors. For instance, a higher muscle PUFA content in pigs has been related with the enrichment of pathways involved in adipocyte differentiation and lipid metabolism (LXR/RXR activation, FXR/RXR activation, and biosynthesis of retinoids) (Ayuso et al., 2016 and Puig-Oliveras et al., 2014). The overexpression of carbohydrate (*e.g.* insulin) and lipogenic-related pathways (*e.g.* PPAR signaling) in HIGH pigs has been also observed by Puig-Oliveras et al. (2014) when comparing the muscle mRNA expression of pigs with high muscle SFA and MUFA contents against those with a high PUFA content. In the case of HIGH and LOW pigs, we have detected pathways involved in acute myeloid leukemia signaling and CTLA4

signaling in cytotoxic T lymphocytes. One of the potential interpretations of this finding is that the metabolic stress, caused by lipotoxicity causes an activation of the immune system (Andersen et al., 2016). However, it is also necessary to take into account the intrinsic limitations of over-representation analyses (Simillion et al, 2017). For instance, the same gene can be present in multiple pathways confusing the biological interpretation of the results and complicating the correction for multiple testing (the assumption of independence is violated when there are overlapped genes amongst pathways). Converting long lists of genes into long lists of pathways does not contribute much to solve the original biological problem (Simillion et al., 2017) and enrichment analyses are prone to yield false positive results (Pavlidis et al, 2012). This means that over-representation analyses should be considered as an exploratory tool rather than as a conclusive analysis upon which biological inferences are made. Recently, bioinformatic tools as SetRank have been implemented to deal with the problems highlighted above (Simillion et al., 2017).

One of the genes that has often emerged in differential expression studies analysing different pig fatness conditions is *PPARG* (Puig-Oliveras et al., 2014; Ramayo-Caldas et al., 2014; Wei et al., 2017). In the experiment outlined in the first chapter of the thesis, we detected that the *PPARG* gene, one of the major players in PPAR signaling, is upregulated in HIGH pigs (*P*-value = 0.02 and FC = 1.36). In addition, *PPARG* was predicted to be a major transcriptional regulator (together with *PDGFB*) of several DE genes related with carbohydrate metabolism (*CEBPA*, *CES1*, and *CIDEC*) and the inhibition of insulin sensitivity (*CES1*, *CIDEC*, and *FASN*). This finding suggests that the DE of *PPARG* has consequences on carbohydrate metabolism since *CES1* is one of the main regulators of glucose homeostasis (Xu et al., 2014). Insulin stimulates the absorption of glucose, which is a lipogenic substrate, and PPARG also enhances triglyceride storage (Ferré 2004). The identification of PPARG as a key transcriptional regulator is relevant because genome-wide association analysis revealed a close association between SNPs mapping close to the *PPARG* locus and insulin sensitivity and obesity in pigs (Puig-Oliveras et al., 2016; Qiao et al., 2015).

In summary, our results in concordance with previues studies performed in pigs point to *PPARG* gene as a key factor determining porcine fatness. Activation of PPARG is directly linked to improving glucose tolerance by enhancing insulin sensitivity and restoring the function of β-cells in diabetic subjects (Sharma & Staels, 2007). Upregulation of PPARG increases the expression of genes involved in fatty acid metabolism and

triglyceride storage in adipose tissue (Sharma & Staels, 2007) and secondary effects can be seen in liver and muscle lipid metabolism pathways (Figure 4.2). The effects of PPARG also extend to macrophages (Figure 4.2), where this transcription factor suppresses the production of inflammatory mediators, improving the relationship between the macrophage and adipocyte that is distorted in obesity (Fuentes et al., 2013; Sharma and Staels, 2007).

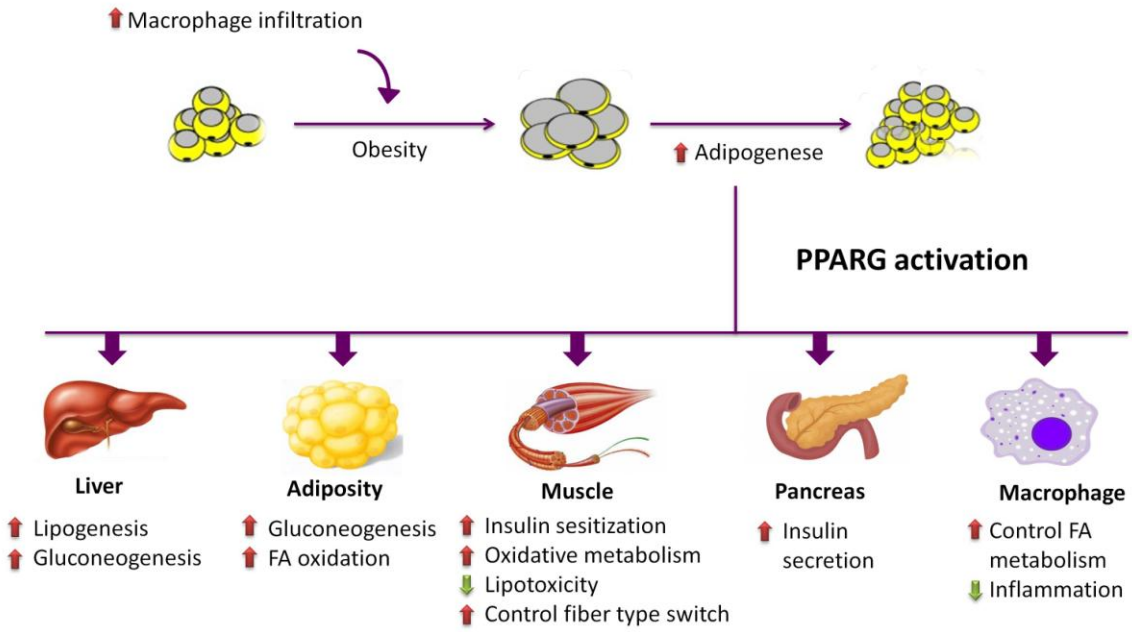

Figure 4.2- Mechanism by which PPARG activation regulates the metabolism and inflammation.

4.2 Limited contribution of the non-coding RNA transcriptome to differential expression between HIGH and LOW pigs.

In general, the majority of differential gene expression analyses in pigs have been focused on protein-encoding genes and only recently the analysis of microRNAs and lncRNAs has been undertaken (Ayuso et al., 2016; Wang et al., 2017a; Wang et al., 2015b; Zhou et al., 2014c). The general picture that emerges from the study reported in chapter 1 is that the DE of non-coding RNAs plays a minor role in the establishment of the HIGH and LOW phenotypes. In this way, we have identified a total of 1,558 muscle-expressed ncRNA transcripts, largely represented by small ncRNA. We only detected 12 ncRNAs (11 lncRNAs and 1 sncRNA) that were DE at the nominal level (*P*-value $\leq$ 0.05), while none of these ncRNAs remained significant after correction for multiple testing. Recent studies

in cattle with different IMF profiles indicate a small participation of miRNAs in the determination of this trait (Oliveira et al., 2018; Zhang et al., 2017). Cesar et al. (2015) compared the muscle expression profiles of Nellore steers displaying extreme genomic estimated breeding values for IMF and found 42 DE mRNA genes (FDR < 0.05), while Oliveira et al. (2018) using the same population found only one DE miRNA. Similarly, the gene expression analysis of the subcutaneous adipose tissue of Laiwu and Large White pigs made possible to identify 482 and 54 DE mRNAs and lncRNAs, respectively.

This apparent minor contribution of non-coding RNAs to phenotypes of economic interest in livestock may be attributed to several factors. In general, ncRNAs are expressed at lower levels than protein-coding transcripts (Palazzo & Lee, 2015). In addition, in the skeletal muscle is difficult to measure ncRNA expression accurately because myofibrillar and mitochondrial mRNA genes are highly expressed thus "masking" the expression of other genes (Mele et al., 2015). In addition, the ncRNA sequences of the porcine genome are poorly annotated. Iyer et al. (2015) performed a genome-wide lncRNA expression analysis in humans and found that 79% of genes (43,331 loci) classified as lncRNAs had not been previously annotated. This poor annotation of porcine ncRNAs becomes obvious if the current porcine Ensembl release (*Sscrofa11.1*, 3,250 ncRNAs) is compared with the 22,521 and 15,074 ncRNAs annotated in the human and mice genomes, respectively. Finally, another complicating factor is that the functions of the majority of ncRNAs are unknown (Palazzo & Lee, 2015).

There is growing evidence that lncRNAs may play a key role in the recruitment of regulatory complexes through RNA–protein interactions to influence the expression of nearby genes, and, in this way, they may act as local regulators. Engreitz et al. (2016) analysed 12 lncRNA loci in mouse embryonic stem cells and found that 5 of these loci influenced the expression of neighbouring mRNA genes in *cis*. In chapter 1, we have detected 25 mRNA-encoding genes that map near (30 kb or less) to the subset of DE ncRNA loci. Amongst these, 2 mRNAs are DE in HIGH *vs* LOW pigs (*P*-value < 0.05 and FC > 1.2) *i.e.* (1) *CU468594.8* (*P*-value = 0.003 and FC = 1.26), which is orthologous to human solute carrier family 52-riboflavin transporter, member 2 (SLC52A2), a transmembrane protein that mediates the cellular uptake of riboflavin, a cofactor of certain redox reactions (Ghisla & Massey 1989; Powers 2003); and (2) *MT-ND6* (*P*-value = 0.038 and FC = −1.21) which encodes a NADH dehydrogenase that catalyzes the oxidation of NADH by ubiquinone, an essential step in the mitochondrial electron transport chain

(Vartak et al. 2015). However, the co-localization of DE mRNA and ncRNA genes should not be considered as sufficient evidence of the latter regulating the former or vice versa. Further molecular studies would be needed to establish such relationship.

4.3 Differential expression of mRNA isoforms in the skeletal muscle of Duroc pigs with different fatness profiles

We aimed to take a further step in the analysis of gene expression differences in the skeletal muscle of HIGH and LOW pigs by studying the differential expression of mRNA isoforms generated by alternative splicing and other mechanisms. It is well established that genes undergo alternative splicing (Eswaran et al., 2013; Yao et al., 2016), and that changes in the abundance of mRNA isoforms affect metabolism regulation. For instance, Beneit et al. (2018) observed a significant relationship between insulin receptor isoforms ratios and plaque growth in early stages of atherosclerosis. Moreover, Montori-Grau et al. (2018) showed that the glycogenin-interacting protein (*GNIP*) isoform 1 is the most abundant isoform in human skeletal muscle, having a markedly glycogenic effect. An overexpression of *GNIP1* isoform decreased blood glucose levels, lactate levels and body weight (Montori-Grau et al., 2018).

In chapter 2, we describe one of the first characterizations of the mRNA isoform landscape in the skeletal muscle of pigs. The splicing landscape analysis of the porcine *gluteus medius* muscle revealed that 10.9% of the expressed protein-encoding genes generate alternative mRNA isoforms, with an average of 2.9 transcripts per gene. Exon skipping was the most prevalent AS event (41.1%) and intron retention the least favored one (12.7%). These results agree well with other studies performed in livestock species (Chacko & Ranganathan, 2009; Kim et al., 2007; Reyes & Huber, 2017). However, in humans 95% of genes can generate multiple isoforms (Barash et al., 2010). Differences in the abundance of spliced genes between humans and pigs highlights the shortcomings of pig genomic annotation, a limitation that may have a strong impact on the results of our analysis.

As the accurate quantitation of isoform mRNA abundance may vary depending on the bioinformatics pipeline employed in the analysis of the data (Hartley & Mullikin, 2016), we have used two different pipelines with the aim of minimizing the rate of false positives *i.e.* (1) STAR/RSEM/DESeq2 pipeline and (2) CLC Bio pipeline. The two differential

expression analyses made possible to identify 104 alternative transcripts and 87 genes simultaneously detected by both pipelines (*P*-value < 0.05). Moreover, 10 mRNA isoforms were categorized as differentially expressed in HIGH *vs* LOW pigs with a *P*-value < 0.01 and ± 0.6 $\log_2$FC and only five of these transcripts remained significant after correcting for multiple testing (*q*-value < 0.05 and ± 0.6 $\log_2$FC). Interestingly, if we consider the set of 10 mRNA DE isoforms (*P*-value < 0.01 and ± 0.6 $\log_2$FC) only four of these genes were identified in the global analysis of DE detailed in Chapter 1.

Upregulation of specific *ITGA5*, *TIMP1*, *ANXA2*, and *LITAF* mRNA isoforms in the skeletal muscle of HIGH group is consistent with their increased fatness and live weight and suggests that differential expression of specific mRNA isoforms might be important in the determination of lipid phenotypes. It is important to emphasize the existence of substantial differences in the isoform annotation of the *Sscrofa* genome 10.2 and 11.1 versions (Table 4.1). The *ITGA5* and *TIMP1* genes in the *Sscrofa* v. 10.2 have 4 and 5 mRNA isoforms, respectively. However, in the new updated version, only 1 isoform is described for each gene. In humans, 13 and 38 isoforms are reported for the *ITGA5* and *ANXA2* genes, respectively. While, isoform number increased on *ANXA2* gene from two mRNA isoforms (*Sscrofa* v. 10.2) to 5 mRNA isoforms using the *Sscrofa* v. 11.1. If we compare the principal isoforms discussed in this Thesis between porcine genome versions (*e.g. ITGA5* = 4445 bp, *ANXA2*= 1455 bp, version 10.2; and *ITGA5* = 9021 bp, *ANXA2* = 1618/1380 pb, version 11.1), we can see differences in length and sequence composition but they encode the same full length protein (*e.g. ITGA5* = 1057 aa, *ANXA2* = 339 aa) (Table 4.1). As shown in Table 4.1, the annotation of the pig *ITGA5, LITAF, ANXA 2* and *TIMP1* mRNA isoforms reported in *Sscrofa* v. 10.2 is more similar to that described in humans than the annotation found in *Sscrofa* v. 11.1.

Complete understanding of the functional implications of alternative splicing is still a long way off. However, Tress et al. (2007) analyzed alternatively spliced gene products annotated in the ENCODE pilot project and they found marked structural and functional differences between isoforms generated by the same gene. Importantly, they described substantial changes in relation to protein folding and activity sites.

Our results highlight the convenience of combining global and mRNA isoform analyses of gene expression (31% of genes with DE isoforms were not identified in the DE gene analysis, *P*-value < 0.05). Recently, Dapas et al. (2016) performed transcript abundance estimation on raw RNA-Seq and exon-array expression glioblastoma cancer samples using

different analysis pipelines and compared both the isoform- and gene-level expression estimates. They found that a third of genes with at least one DE isoform in the RNA-Seq or exon-array results were not likewise classified as DE in global analyses of gene expression.

4.4 The ingestion of food influences the expression of multiple transcription factors in the skeletal muscle

The second biological model that we have explored in this Thesis focuses on the effects of food ingestion on the mRNA expression patterns of the skeletal muscle. Our hypothesis was that genes that play a role in nutrient absorption and metabolism might influence the phenotypic variation of fatness and meat quality traits. The reason for choosing skeletal muscle as a target tissue is that the majority of glucose and lipid absorption after a meal consumption is featured by this tissue (Shulman et al., 1990). The postprandial kinetics of blood glucose and lipid levels in the pig had not been well characterized, so we made a pilot experiment in which we measured plasma glucose, triglycerides, cholesterol and non-esterified fatty acids in eight Duroc gilts before feeding and 2, 4, 6 h. after feeding. These results revealed that glycaemia and lipidemia peaks are reached at 2 and 4 h. after eating. We also observed a marked decrease of plasma free FA at 2 h. after feed, since nutrition abolishes the release of fatty acids by the adipose tissue.

Based on such results, the differential expression analysis comprised three different time-points: T0 (fasting), T1 (5h after eating) and T2 (7h after eating). We assumed that at 5 h after eating, lipid absorption would be at its maximum, allowing us to detect genes involved in such process, and that 7 h. after eating (*i.e.* 2 h. after absorption) the processes of triglyceride synthesis (lipid storage) and ß-oxidation of FA (lipid burning) would be also at their maxima. However, when we have analyzed triglycerides and plasma free fatty acids concentrations in T0, T1 and T2 slaughtered sows, the kinetics of these two metabolites were not identical to those observed in the pilot experiment. We found an increase in the concentration of triglycerides and a decrease of circulating free FA levels, but 7 hours after feeding triglyceride levels were still peaking. Nevertheless, our comparison between fasting and fed state remains valid (Figure 4.3).

Table 4.1 - Comparison between isoform annotation for the *Itga5, Timp1, Anxa2* and *Litaf* genes available in the *Sus scrofa* genome version 10.2 and 11.1, and the Homo sapiens genome.

	Sus scrofa 10.2			*Sus scrofa* 11.1			**Homo sapiens GRCh38.p10**		
Gene	**Number isoforms**	**Bp**	**Protein (aa)**	**Number isoforms**	**Bp**	**Protein (aa)**	**Number isoforms**	**Bp**	**Protein (aa)**
ITGA5	5	1013,766, **4445**,1255*	109,162, **1057**,93	1	9021	1057	13	4444,757,1240,1013 *	1,049,119,137,120
TIMP1	4	**931**,641, 598,173	**207**,195, 123,38	1	1061	207	5	8,921,095,626,595,340	207,136,143,165,95
ANXA2	2	**14,551,609**	**339,339**	5	2702,1618, 1380,1245, 938	322,339, 339,414, 179	38	1676,1444,1444,1435, 878,812,802,780, 777,755,744,733, 718,669,665,663, 594,580,564,561, 560,558 *	339,357,339,399, 256,176,146,142, 227,119,248,4, 176,149,139,110, 176,175,59,45, 133,119
LITAF	2	2370, **2190**	161,161	2	5396, 512	161,161	21	2632,2467,2356,2292, 1118,717,692,603, 1527,677,593,587, 579,556,554,553, 548,516,486,773,582	161,161,161,152, 161,161,152,161, 228,75,137,39, 153,33,88,136, 126,68,105,81,10

Isoforms differentially expressed found in this Thesis are shown in bold.
*Additional isoforms have been described, but they do not encode proteins.
Aa = Amino acids; **Bp** = Base pairs

The analysis of the expression data obtained by RNA-Seq highlighted 148 (T0 *vs* T1), 520 (T0 *vs* T2) and 135 (T1 *vs* T2) DE mRNA genes. Moreover, 85 genes showed DE both in the T0-T1 and T0-T2 comparisons, a result that evidences the high consistency of our results. Our data demonstrated a post-prandial activation of genes with a well-known role in energy homeostasis (*e.g. PFKFB3* and *G0S2*). Interestingly, we also detected the DE of several genes with a plausible but poorly characterized role in metabolism (*e.g. MIGA2, SDC4,* and *CSRNP1*). One of the main results of our study is that nutrition modulates the expression multiple transcription factors *e.g. ARID5B, KLF5, CEBPD,* and F*OXO1*, possibly mediating the integration of metabolic processes via PPAR (Figure 4.4). *PPARA* mRNA is induced during fasting and plays a pivotal role in the management of energy stores by enhancing hepatic fatty acid oxidation to supply substrates that can be metabolized by other tissues (Kersten et al., 1999). Recently, Liu et al. (2017) demonstrated that the knockdown of the *ARID5B* gene resulted in a reduced expression of genes involved in atherosclerosis-related inflammatory and lipid metabolism pathways. Overexpression of CCAAT/enhancer-binding protein delta (*CEBPD*) gene enhances lipid accumulation and specifically activates *PPARG* transcription in HepG2 cells (Lai et al., 2008). Armoni et al. (2006) suggested that the Forkhead box protein O1 (*FOXO1)* gene represses *PPARG* in primary rat adipocytes. In a different experiment, we have evaluated the DE of microRNAs in T0, T1, and T2 (Emilio Mármol, personal communication). Differences in the expression of microRNAs were very slight and we were unable to confirm them by quantitative PCR. The general picture that emerges from these results is that the regulation of gene expression in response to food intake is mainly featured by transcription factors.

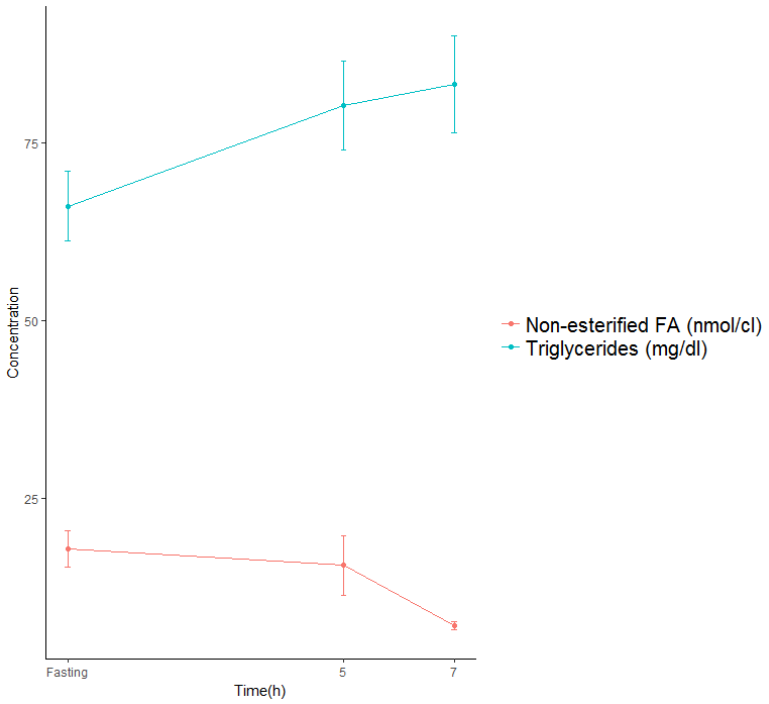

Figure 4.3 - Kinetics of the average concentrations of triglycerides and non-esterified fatty acids (FA) in 36 Duroc pigs at three-time points: before eating and 5 and 7 hours post-ingestion.

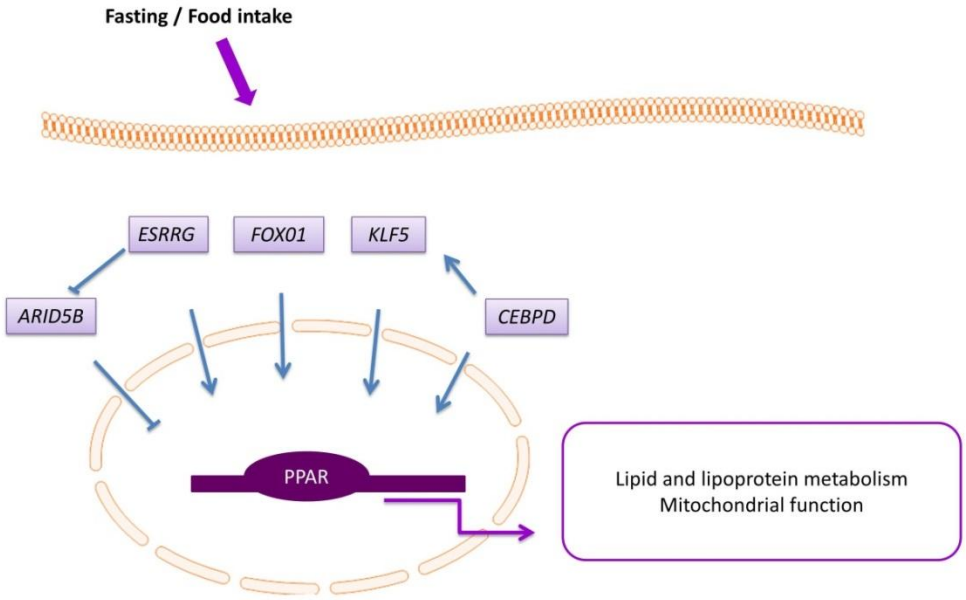

Figure 4.4 - Interaction of transcription factors modulated by nutrition with PPAR-mediated pathways.

4.5 Food intake promotes changes in the expression of genes related to oxidative stress and angiogenesis

The thrombospondin 1 (*THBS1,* T0-T1: FC = -1.99, *q*-value = 8.00E-03) and 2 (*THBS2,* T0-T2: FC = 2.45, *q*-value = 5.18E-04) and thioredoxin interacting protein (*TXNIP,* T0-T1: FC = -1.78, *q*-value = 1.34E-04; T0-T2: FC = -1.79, *q*-value = 1.13E-02) genes showed significant DE at T0-T1 and T0-T2 reflecting the combined redox and vascular response of the porcine skeletal muscle to nutrient availability. In a fed status, mitochondria produce a huge amount of free oxygen radicals as a byproduct of oxidative phosphorylation. Increased oxidative stress appears to be a determinant factor leading to insulin resistance, β-cell dysfunction, and impaired glucose tolerance, so an adequate balance between free oxygen radicals and antioxidants is necessary (Lobo et al, 2010). *THBS1* and *THBS2* are down- and upregulated by oxidative stress, respectively (Bae et al., 2013; Chen et al. 2011) and they are involved in the production of adaptive stress response factors regulating NO, H_2S, and superoxide production (Roberts et al., 2017). An upregulation of *TXNIP* has been implicated in hyperglycemia-induced β-cell dysfunction and apoptosis (Shah et al., 2013) and the thioredoxin/TXNIP system plays a major role in the regulation of redox homeostasis (Zhou & Chng, 2013). In addition, these genes have a dual biological role, also being involved in angiogenesis. Insulin, secreted by the pancreas in response to food ingestion, promotes vasodilatation and capillary recruitment in the skeletal muscle to ensure the maintenance of glucose homeostasis (Manrique & Sowers, 2014). Dunn et al. (2014) reported that overexpression of *TXNIP* mediated by high glucose levels may play a role in the pathogenesis of diabetes by impairing angiogenesis. Moreover, *THBS*1 and *THBS*2 has been shown to be powerful inhibitors of angiogenesis (Lawler & Lawler, 2012). This dual role complicates the physiological interpretation of changes in the expression of thrombospondin-related genes, To make things even more complicated, the *THBS1* and *THBS2* genes have been reported to be endogenous diet-induced weight gain and adipocyte hypertrophy repressors (Inoue et al., 2013; Shitaye et al., 2010; Soto-Pantoja et al., 2016). Inoue et al. (2013) demonstrated that *THBS1*-null mice have an insulin-sensitive phenotype. Moreover, these knockout mice display a well-controlled circadian rhythm in their energy expenditure, with higher amplitude of O_2 consumption.

4.6 Existence of a close relationship between nutritional status and the expression of genes regulating circadian rhythms.

One of the main results of our experiment was the demonstration that the nutritional status (fasting *vs* feeding) influences the expression of genes integrated into the muscle circadian clock. In the experiment reported in Chapter 3, we have observed that nutrient availability elicits an overexpression of *ARNTL* and *NR1D1* genes in the *gluteus medius* muscle, whilst *PER1, PER2, SIK1, CRY2,* and *BHLHE40* are down-regulated (Table 4.2). Mammals synchronize their circadian activity primarily under the influence of the light/dark cycles which entrain the central clock located in the suprachiasmatic nucleus of the hypothalamus (Partch et al., 2014). In addition, circadian clocks are also present in peripheral tissues, but they are mainly synchronized by nutrition, humoral signals, metabolic factors, and body temperature (Hastings et al., 2008; Oike et al., 2014; Richards & Gumz, 2012). Some of the circadian genes and the proteins they produce form a series of interacting molecular pathways that then loop back on one another (Eckel-Mahan & Sassone-Corsi, 2013; Partch et al., 2014). In this way, CLOCK/NPAS2 and ARNTL promote the transcription of *PER* and *CRY* genes which ultimately feedback and inhibit CLOCK/NPAS2 and ARNTL transcriptional activity (Figure 4.5).

Table 4.2 - Differentially expressed Clock genes (q-value < 0.05 and |fold-change| > 1.5) in the pig *gluteus medius* muscle at fasting (T0) vs 5 h (T1) and 7 h (T2) after eating.

Gene	Gene ID	T0 vs T1		T0 vs T2	
		Log_2(FC)	***q* - value**	**Log_2(FC)**	***q* - value**
ENSSSCG00000013396	*ARNTL*	0.90	1.93E-04	1.30	2.99E-13
ENSSSCG00000011534	*BHLHE40*	-	-	-0.82	7.87E-05
ENSSSCG00000013270	*CRY2*	-	-	-0.68	1.28E-02
ENSSSCG00000017481	*NR1D1*	0.69	8.30E-03	0.90	9.52E-04
ENSSSCG00000017983	*PER1*	-1.51	3.95E-11	-0.87	1.12E-02
ENSSSCG00000016338	*PER2*	-0.74	4.33E-04	-1.31	7.03E-14
ENSSSCG00000023854	*PER2*	-0.73	1.59E-03	-1.20	4.32E-10
ENSSSCG00000028137	*SIK1*	-1.39	1.91E-07	-	-

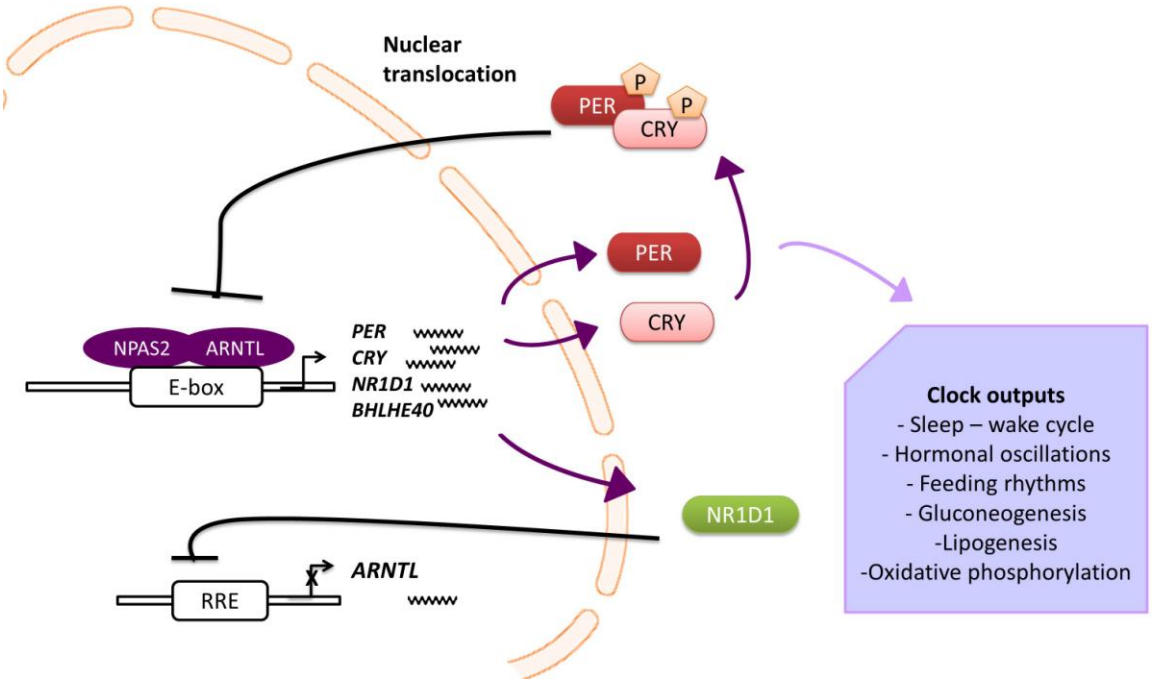

Figure 4.5 - The circadian Clock system is regulated by a self-oscillating transcriptional loop.

The demonstration that the expression of Clock genes in the porcine skeletal muscle is affected by nutrition has important metabolic implications Clock genes play a key role in muscle physiology by regulating the expression of more than one thousand genes mainly involved in metabolic processes (Hodge et al., 2015). In mice, Rudic et al. (2004) found that the absence of *ARNTL* impaired glucose metabolism and was associated with insulin hypersensitivity. *PER1* and *PER2* -deficient mice showed impaired glucose tolerance and enhanced hypoglycemia (Lamia et al., 2008) and an increased adipogenesis was also described in *PER2*$^{-/-}$ mice (Grimaldi et al., 2010). In addition, natural genetic variations in Clock genes can result in profound differences in the functioning of circadian clocks. In humans, three variants of the *CLOCK* gene have been associated with energy intake (Valladares et al., 2015). Moreover, *PER2* polymorphism has been associated with abdominal obesity (Garaulet et al., 2010). These results suggest that the altered expression of Clock genes may cause the development of metabolic disorders, such as obesity and diabetes, and influence traits related to lipid metabolism.

Given the biological relevance of the results reported in Chapter 3, we decided to extend our analysis to four additional tissues: hypothalamus (which contains the central biological clock modulated by light), liver, intestine and dorsal fat. We selected eight

Clock genes based on our previous results (Cardoso et al. 2017) as well a by performing a literature search (Gnocchi et al., 2015; Tahara & Shibata, 2013). Our goal was to analyze the effect of food intake on the mRNA expression of Clock genes in tissues with distinct metabolic roles. The results obtained in the experiment reported in Chapter 3 indicated that differences in the expression of Clock genes were particularly significant in the T0 *vs* T2 comparison (Cardoso et al., 2017). In the multissue study described in Chapter 4, we have used these two-time points to carry out the analysis of differential expression by using an RT-qPCR approach.

One of the main observations of the multissue study is that the expression of Clock genes changes in four tissues containing peripheral clocks (liver, muscle, duodenum, and dorsal fat) but not in the hypothalamus, which contains the central clock entrained by light. This observation supports the idea that the changes of expression that we observe in the four tissues mentioned before are not due to the passing of time (T0 and T2 are separated by 7 hours) but to nutrient availability. Other studies suggest that feeding conditions can modify, in a short time, the phase of circadian gene expression in peripheral tissues possibly by delivering nutrients and hormonal signals, in an SCN-independent manner (Damiola et al., 2000; Hirota & Fukada, 2004). The expression of Clock genes can have important consequences on fat deposition and composition. For instance, Paschos et al. (2012) suppressed the expression of the *ARNTL* gene in the adipose tissue of mice and observed changes in the abundance of hypothalamic peptides that regulate appetite as well as a decreased PUFA concentration in adipocytes and in the hypothalamic neurons regulating food intake.

In addition, we have observed that the patterns of differential expression of Clock genes differ across tissues *i.e.* we identified DE for four (dorsal fat and duodenum), six (skeletal muscle) and seven (liver) genes. Of the four and six genes displaying DE between T0 and T2 in duodenum and the muscle, respectively, only two of them (*NPAS2* and *SIK1*) were shared by both tissues. In contrast, muscle (6 genes) and liver (7 genes) have a higher level of overlap *i.e.* five genes (*BHLHE40, NPAS2, PER1, PER2,* and *SIK1*) are shared by both tissues. Moreover, not only the sets of DE genes vary across tissues but also there are differences in the magnitude and direction of changes in gene expression *i.e.* the mRNA levels of the *BHLHE40* gene decreased in the liver and muscle (log_2Rq = -0.94, q-value = 0.01 and log_2Rq = -1.11, q-value = 0.00, respectively), but they increased in dorsal fat (log_2Rq = 1.18, q = 0.02). Another example would be featured by the *Sik1* gene, whose

expression decreased in the liver and muscle (log_2Rq = -1.84, q-value = 0.00, and log_2Rq = -2.60, q-value = 0.00, respectively), but increased in the duodenum (log_2Rq = 1.57, q-value = 0.04). These results indicate the existence of important tisular differences in the modulation of peripheral clocks by nutrition. Activation of distinct metabolic pathways within a cell/tissue type is largely dependent on the cycling availability, sensitivity, and transport of specific substrates, as well as of released hormones such as melatonin or glucocorticoids (Gerber et al., 2013; Mühlbauer et al., 2009). In addition, differences in the circadian timing of each tissue may also be controlled by the autonomic nervous system and perhaps by other tissue clocks (Oster et al., 2006), and it could also be influenced by the function of the tissue, environmental cues (*e.g.* the microbiome in the case of the intestine) and the specific timing of nutrient availability.

4.7 The polymorphism of the SLC45A2 gene is associated with the red and blond pigmentation of Mangalitza pigs

In Chapter 5, we have analyzed the genetic diversity of Mangalitza pigs and other breeds and we have also investigated the genetic factors involved in the establishment of blond *vs* red pigmentation patterns in this breed. In general, we have found results consistent with occurrence of past population bottlenecks and recent inbreeding in Mangalitza pigs breeds and Romanian and Hungarian wild boars. Observed and expected heterozygosities were moderately high in Romanian Red Mangalitza (Ho = 0.35, He = 0.35) pigs and relatively low in Hungarian (Ho = 0.27, He = 0.29) and Romanian wild boars (Ho = 0.27, He = 0.31), while Hungarian Red (Ho = 0.29, He = 0.28) and Blond Mangalitza (Ho = 0.28, He = 0.28) displayed lower heterozygosities than those estimated in cosmopolitan breeds such as Large White, Landrace, and Piétrain (mean Ho = 0.34, He = 0.34). Admixture analysis demonstrated the existence of genetic differences between Blond Mangalitza, Hungarian Red Mangalitza, and Romanian Red Mangalitza pigs, thus evidencing that these populations underwent different demographic and/or selective histories.

Coat colour is an important phenotype in the establishment of breed standards and it was subjected to artificial selection in ancient times, dating back to about 5,000 years ago (Fang et al., 2009). Despite the broad range of coat pigmentation patterns in pigs and that several pigmentation loci have been identified (Table 4.3), the genetic basis of coat colour

remains to be fully elucidated. Red and Blond Mangalitza are closely related populations that diverged a short time ago (100-150 years), a feature that diminishes the presence of regions that are highly differentiated as a consequence of genetic drift and other neutral processes (Gregory, 2009).

We have investigated the genetic basis of the blond *vs* red coat in Mangalitza by using two approaches *i.e.* a selection scan and a GWAS. The selection scan with the hapFLK software revealed a very strong selective sweep on SSC13 (24.5-67.7.0 Mb, q-value < 5.5E-04). Other significant selective sweeps (*P*-value < 0.05) were located on SSC2 (152.1-152.2 Mb), SSC3 (4.9-5.4 Mb), SSC6 (27.9-28.1 Mb), SSC7 (65.9-65.9, 50.9-51.7, and 68.0-68.4 Mb), SSC11 (22.3-25.6 Mb), SSC12 (2.4-8.6 Mb), SSC15 (35.7-53.1 and 129.5-133.9 Mb), SSC16 (19.3-28.4, 35.0-52.4, 60.5-60.7, and 70.6-71.7 Mb) and SSC17 (60.5-65.8 Mb). These putative selective sweeps might be due to factors unrelated to pigmentation, so we carried out a GWAS with the GEMMA software. In this way, 6 regions identified in the selection scan were also identified as associated with coat color in the GWAS. We investigated the gene content of the overlapping regions identified by HapFLK and GEMMA. In doing so, we detected that the position of the *SLC45A2* gene (SSC16, 20 Mb) coincides with one of the regions (SSC16, 19-20 Mb) simultaneously identified in the selection scan and the GWAS. The *SLC45A2* gene is a key regulator of the melanosomal pH and tyrosinase activity, and mutations in *SLC45A2* are associated with changes of melanin synthesis (implying a dilution of the pigmentation) in different species, *e.g* in humans (Tóth et al., 2017), horses (Mariat et al., 2003) and cattle (Rothammer et al., 2017).

By using whole-genome sequences from one Red, one Swallow Belly and two Blond Mangalitza pigs (SRA access: SRP039012) reported by Molnar et al. (2014) we identified three missense SNPs with a differential segregation in Red and Blond Mangalitzas, *i.e.* rs341599992 (c.806G>A, p.Gly269Glu), rs327001340 (c.829A>G, p.Ser277Gly) and rs693695020 (c.956G>A, p.Arg319His) The genotyping of these three missense polymorphisms in the porcine *SLC45A2* gene in Red, Blond and Swallow Belly Mangalitza and other breeds evidenced that the c.806G>A (p.Gly269Glu) and c.956G>A (p.Arg319His) SNPs are strongly but not fully associated with the red and blond coat colours of Mangalitza pigs. Although the inheritance of pigmentation phenotypes is usually simpler than that of complex traits, such as growth and fatness, it is rarely monogenic. Recently, Crawford et al. (2017) performed a GWAS study and identified a list of genes,

which clustered in four genomic regions that together accounted for almost 30% of the phenotypic variation of pigmentation. The most significantly associated SNP were located in the *SLC24A* gene that represents a 12.8% of the variability of human skin colour. These results suggest that the genetic architecture of skin pigmentation in humans is a complex trait determined by a set of few genes of strong effect (Crawford et al., 2017). In this way, further studies will be needed to finely map the causal mutations of coat color in Mangalitza pigs as well as to elucidate the existence of genetic interactions between *SLC45A2* and other color genes.

Table 4.3 - List of genes with known associations with coat colour in pigs.

Gene	**SSC**	**Pigmentation**	**Reference**
KIT	8	White	Giuffra et al. (2002)
MITF	13	Two-end black	Wang et al. (2015a)
TYRP1	1	Blond and Brown	Wu et al. (2016) Ren et al. (2011)
MC1R	6	Black and red	Fang et al. (2009)
PINK1, and *CNTLN*	1 and 6	Two-end-black	Lü et al. (2016)
EDNRB	1	Black	Wang et al. (2015a) Lü et al. (2016)

General conclusions

Chapter 5

1. By using an RNA-Seq technology we identified a total of 18,104 mRNAs expressed in the porcine *gluteus medius* muscle of 52 Duroc pigs. The differential expression analysis of pigs with distinct growth and fatness profiles (HIGH: high backfat thickness, intramuscular fat, saturated and unsaturated fatty acid content and serum lipids *vs* LOW: opposite phenotypes), made possible to identify 1,430 mRNA transcripts that are differentially expressed at the nominal level of significance (*P*-value < 0.05). Ninety-six mRNAs were differentially expressed using more stringent parameters (*P*-value < 0.01 and fold-change > 1.5). We conclude that the differential expression of genes involved in lipid biosynthesis may explain the higher fat deposition of HIGH pigs. Moreover, in our and previus studies PPARG appears to be a key regulator of the genes differentially expressed in the skeletal muscle of pigs with distinct lipid profiles

2. We have identified a total of 1,558 non-coding RNAs (ncRNAs) expressed in the porcine *gluteus medius* muscle of HIGH and LOW pigs, however only 12 ncRNA transcripts show differential expression when considering a *P*-value < 0.05, and none when a more stringent threshold is used (*P*-value < 0.01 and fold-change > 1.5). These results indicate that the different fatness profiles of HIGH and LOW pigs might be mostly explained by the differential expression of protein-encoding genes.

3. We have found that 10.9% of genes expressed in the *gluteus medius* muscle generate alternative mRNA isoforms, with an average of 2.9 transcripts per gene. This is probably an underestimate caused by the poor annotation of the porcine mRNA isoforms. The analysis of transcriptomic data with two prediction software (SUPPA and Splicing Express) evidenced that exon skipping is the most prevalent splicing event, while intron retention is the rarest one. These results are consistent with what has been found in humans, where exon skipping has a predominant role in the generation of splicing mRNA isoforms. A total of 10 mRNA isoforms were identified by CLC Bio and DESeq2 software as differentially expressed when comparing HIGH *vs* LOW pigs (*P*-value < 0.01 and ± 0.6 $\log_2$fold-change). Five mRNA isoforms, produced by the *ITGA5*, *SEMA4D*, *LITAF*, *TIMP1* and *ANXA2* genes, remained significant after correction for multiple testing (*q*-value < 0.05 and ± 0.6 $\log_2$fold-change), being upregulated in HIGH pigs. An overexpression of *ITGA5*, *LITAF*, *TIMP1* and *ANXA2* mRNA is associated with obesity and metabolic disorders in humans. These findings indicate that fat deposition in pigs could be affected not only by global differences of

gene expression but also by the abundance of specific mRNA isoforms.

4. By comparing the muscle expression of fasted pigs (T0) vs pigs sampled 5 h (T1) and 7 h (T2) after feeding, we have detected the differential expression of 148 (T0 vs T1), 520 (T0 vs T2) and 135 (T1 vs T2) mRNA-encoding genes. We can conclude that food intake elicits changes in the expression of genes encoding transcription factors (*e.g. ARID5B, KLF5, CEBPD,* and *SOX9*) as well as of loci regulating oxidative stress and angiogenesis (*THBS1, THBS2,* and *TXNIP*) and circadian rhythms (*i.e. ARNTL, PER1, PER2, BHLHE40, NR1D1, SIK1, CIART,* and *CRY2*).

5. The analysis of the expression of eight porcine Clock genes in five tissues has shown that four (dorsal fat and duodenum), six (skeletal muscle) and seven (liver) genes integrated into or modulating peripheral clocks are differentially expressed before and after feeding. In contrast, none of the eight analysed genes shows a significant differential expression in hypothalamus, the tissue where the central clock resides. From these data, we infer that the differential expression of Clock genes in muscle, duodenum, dorsal fat and liver tissue is induced by nutrition and not by the central clock entrained by light. In addition, we have observed that the magnitude and direction of the differential expression of Clock genes differ across tissues, thus indicating that the ticking of peripheral clocks is modulated by tissue-specific factors.

6. Population analysis revealed that Blond Mangalitza, Red Mangalitza from Hungary, wild boar from Hungary and Romania and Hampshire pigs display a lower diversity than cosmopolitan breeds such as Landrace, Large White and Piétrain. In addition, Hungarian and Romanian Red Mangalitza pigs and Romanian wild boars display an increased frequency of very long ROH (> 30 Mb), evidencing the occurrence of a recent and strong inbreeding.

7. Performance of a selection scan with hapFLK and of a genome-wide association study for coat color in Red and Blond Mangalitza pigs highlighted the existence of one region on SSC16 (20 Mb) with potential effects on pigmentation. The analysis of the gene content of this region allowed us to detect the solute carrier family 45 member 2 (*SLC45A2*) gene, which has a known role in color dilution. Genotyping of three missense polymorphisms in the porcine *SLC45A2* gene evidenced that c.806G>A (p.Gly269Glu) and c.956G>A (p.Arg319His) SNPs are strongly but not fully associated with the red and blond coat colors of Mangalitza pigs. Alternative *SLC45A2* genotypes

are almost fixed in Red and Blond Mangalitza pigs, a result that is probably explained by the performance of artificial selection for coat color.

References

Chapter 6

Adzitey, F. & Nurul, H. Pale soft exudative (PSE) and dark firm dry (DFD) meats: Causes and measures to reduce these incidences - a mini review. *International Food Research Journal* **18**, 11–20 (2011).

Alekseyenko, A. V, Kim, N. & Lee, C. J. Global analysis of exon creation versus loss and the role of alternative splicing in 17 vertebrate genomes. *RNA* **13**, 661–70 (2007).

Alexandratos, N. & Bruinsma, J. The 2012 Revision World agriculture towards 2030/2050: the 2012 revision. (2012).

Allis, C. D. & Jenuwein, T. The molecular hallmarks of epigenetic control. *Nature Reviews Genetics* **17**, 487–500 (2016).

Amills, M. et al. in Encyclopedia of Life Sciences. John Wiley & Sons, Ltd (2010). doi:10.1002/9780470015902.a0022884

Anders, S. & Huber, W. Differential expression analysis for sequence count data. *Genome Biology* **11**, R106 (2010).

Anders, S., Pyl, P. T. & Huber, W. HTSeq – A Python framework to work with high-throughput sequencing data. *Bioinformatics* **15**, 166-9 (2014).

Andersen, C. J., Murphy, K. E. & Fernandez, M. L. Impact of Obesity and Metabolic Syndrome on Immunity. *Advances in Nutrition* **7**, 66–75 (2016).

Andersson, L. et al. Coordinated international action to accelerate genome-to-phenome with FAANG, the Functional Annotation of Animal Genomes project. *Genome Biology* **16**, 57 (2015).

Andrews S. FastQC A Quality Control tool for High Throughput Sequence Data. at <http://www.bioinformatics.babraham.ac.uk/projects/fastqc/> (2010).

Anthon, C. et al. Structured RNAs and synteny regions in the pig genome. *BMC Genomics* **15**, 459 (2014).

Armoni, M. et al. FOXO1 represses peroxisome proliferator-activated receptor-γ1 and -γ2 gene promoters in primary adipocytes. *Journal of Biological Chemistry* **281**, 19881–19891 (2006).

Ayuso, M. et al. Comparative analysis of muscle transcriptome between pig genotypes identifies genes and regulatory mechanisms associated to growth, fatness and metabolism. *PloS One* **10**, e0145162 (2015).

Ayuso, M. et al. Developmental stage, muscle and genetic type modify muscle transcriptome in pigs: effects on gene expression and regulatory factors involved in growth and metabolism. *PloS One* **11**, e0167858 (2016).

Bae, O.-N. et al. Oxidative stress-mediated thrombospondin-2 upregulation impairs bone marrow-derived angiogenic cell function in diabetes mellitus. *Arteriosclerosis, Thrombosis, and Vascular Biology* **33**, 1920–7 (2013).

Barak, B. et al. Opposing actions of environmental enrichment and Alzheimer's disease on the expression of hippocampal microRNAs in mouse models. *Translational psychiatry* **3**, e304 (2013).

Barash, Y. et al. Deciphering the splicing code. *Nature* **465**, 53–59 (2010).

Beltrami, C., Angelini, T. G. & Emanueli, C. Noncoding RNAs in diabetes vascular complications. *Journal of Molecular and Cellular Cardiology* **89***:* 42-50. (2014).

Beneit, N. et al. Potential role of insulin receptor isoforms and IGF receptors in plaque instability of human and experimental atherosclerosis. *Cardiovascular Diabetology* **17**, 31 (2018).

Berglund, E. C., Kiialainen, A. & Syvänen, A.-C. Next-generation sequencing technologies and applications for human genetic history and forensics. *Investigative Genetics* **2**, 23 (2011).

Black, M. B. et al. Comparison of Microarrays and RNA-Seq for gene expression analyses of dose-response experiments. *Toxicological Sciences* **137**, 385–403 (2014).

Blankenberg, D. et al. Galaxy: a web-based genome analysis tool for experimentalists. *Current Protocols in Molecular Biology* **19**: 1-21 (2010).

Borodina, T., Adjaye, J. & Sultan, M. A strand-specific library preparation protocol for RNA sequencing. *Methods in Enzymology* **500:** 79-98 (2011).

Braunschweig, M., Jagannathan, V., Gutzwiller, A. & Bee, G. Investigations on transgenerational epigenetic response down the male line in F2 pigs. *PloS One* **7**, e30583 (2012).

Bray, N. L., Pimentel, H., Melsted, P. & Pachter, L. Near-optimal probabilistic RNA-Seq quantification. *Nature Biotechnology* **34**, 525–527 (2016).

Bumgarner, R. Overview of DNA microarrays: types, applications, and their future. *Current Protocols in Molecular Biology* 22, 22.1. (2013).

Burgos-Paz, W. et al. Porcine colonization of the Americas: a 60k SNP story. *Heredity* **110**, 321–30 (2013).

Byron, S. A., Van Keuren-Jensen, K. R., Engelthaler, D. M., Carpten, J. D. & Craig, D. W. Translating RNA sequencing into clinical diagnostics: opportunities and challenges. *Nature Reviews Genetics* **17**, 257–271 (2016).

Cabling, M. M. et al. Estimation of Genetic Associations between Production and Meat Quality Traits in Duroc Pigs. *Asian-Australasian Journal of Animal Sciences* **28**, 1061–5 (2015).

Cánovas, A., Quintanilla, R., Amills, M. & Pena, R. N. Muscle transcriptomic profiles in pigs with divergent phenotypes for fatness traits. *BMC Genomics* **11**, 372 (2010).

Cardoso, T. F. et al. Nutrient supply affects the mRNA expression profile of the porcine skeletal muscle. *BMC Genomics* **18**, 603 (2017).

Carninci, P. et al. The transcriptional landscape of the mammalian genome. *Science* **309**, 1559–1563 (2005).

Cartegni, L., Chew, S. L. & Krainer, A. R. Listening to silence and understanding nonsense: exonic mutations that affect splicing. *Nature Reviews Genetics* **3**, 285–298 (2002).

Casellas, J. et al. Bayes factor analyses of heritability for serum and muscle lipid traits in Duroc pigs. *Journal of Animal Science* **88**, 2246–2254 (2010).

Cech, T. R. & Steitz, J. A. The noncoding RNA revolution-trashing old rules to forge new ones. *Cell* **157**, 77–94 (2014).

Cesar, A. S. M. et al. Putative Regulatory factors associated with intramuscular fat content. *PloS One* **10**, e0128350 (2015).

Chacko, E. & Ranganathan, S. Genome-wide analysis of alternative splicing in cow: implications in bovine as a model for human diseases. *BMC Genomics* **10** : S11 (2009).

Chen, C. et al. A global view of porcine transcriptome in three tissues from a full-sib pair with extreme phenotypes in growth and fat deposition by paired-end RNA sequencing. *BMC Genomics* **12**, 448 (2011).

Chen, J.-F. et al. microRNA-1 and microRNA-206 regulate skeletal muscle satellite cell proliferation and differentiation by repressing Pax7. *The Journal of Cell Biology* **190**, 867–879 (2010).

Chen, J.-F. et al. The role of microRNA-1 and microRNA-133 in skeletal muscle proliferation and differentiation. *Nature Genetics* **38**, 228–233 (2006).

Chen, J.-K., Zhan, Y.-J., Yang, C.-S. & Tzeng, S.-F. Oxidative stress-induced attenuation of thrombospondin-1 expression in primary rat astrocytes. *Journal of Cellular Biochemistry* **112**, 59–70 (2011).

Cheung, V. G. et al. Genetics of quantitative variation in human gene expression. *Cold Spring Harbor Symposia On Quantitative Biology* **68**, 403–7 (2003a).

Cheung, V. G. et al. Natural variation in human gene expression assessed in lymphoblastoid cells. *Nature Genetics* **33**, 422–425 (2003b).

Choi, M. et al. Genome-wide analysis of DNA methylation in pigs using reduced representation bisulfite sequencing. *DNA Research* **22**, 343–355 (2015).

Cinar, M. U. et al. Association and expression quantitative trait loci (eQTL) analysis of porcine AMBP, GC and PPP1R3B genes with meat quality traits. *Molecular Biology Reports* **39**, 4809–4821 (2012).

Ciobanu, D. C., Lonergan, S. M. & Huff-Lonergan, E. J. Genetics of meat quality and carcass traits. In The *Genetics* of the Pig. 2nd edn. (ed. Rothschild, M. F. & Ruvinsky, A.) 356 (CABI, 2011).

Clop, A. et al. A mutation creating a potential illegitimate microRNA target site in the myostatin gene affects muscularity in sheep. *Nature Genetics* **38**, 813–818 (2006).

Conesa, A. et al. A survey of best practices for RNA-Seq data analysis. *Genome Biology* **17**, 13 (2016).

Corominas, J. et al. Analysis of porcine adipose tissue transcriptome reveals differences in de novo fatty acid synthesis in pigs with divergent muscle fatty acid composition. *BMC Genomics* **14**, 843 (2013).

Crawford, N. G. et al. Loci associated with skin pigmentation identified in African populations. *Science* **358**, eaan8433 (2017).

Crist, C. G., Montarras, D. & Buckingham, M. Muscle Satellite Cells Are Primed for Myogenesis but Maintain Quiescence with Sequestration of Myf5 mRNA Targeted by microRNA-31 in mRNP Granules. *Cell Stem Cell* **11**, 118–126 (2012).

Cui, R., Gao, M., Qu, S. & Liu, D. Overexpression of superoxide dismutase 3 gene blocks high-fat diet-induced obesity, fatty liver and insulin resistance. *Gene Therapy* **21**, 840–8 (2014).

Cusi, K. Role of Obesity and Lipotoxicity in the Development of Nonalcoholic Steatohepatitis: Pathophysiology and Clinical Implications. *Gastroenterology* **142**, 711–725.e6 (2012).

Daly, T. M. et al. Precision profiling and components of variability analysis for Affymetrix microarray assays run in a clinical context. *The Journal of Molecular Diagnostics : JMD* **7**, 404–12 (2005).

Damiola, F. et al. Restricted feeding uncouples circadian oscillators in peripheral tissues from the central pacemaker in the suprachiasmatic nucleus. *Genes & Development* **14**, 2950–61. (2000).

Dapas, M., Kandpal, M., Bi, Y. & Davuluri, R. V. Comparative evaluation of isoform-level gene expression estimation algorithms for RNA-Seq and exon-array platforms. *Briefings in Bioinformatics* **18**, bbw016 (2016).

Davoli, R. & Braglia, S. Molecular approaches in pig breeding to improve meat quality. *Briefings in Functional Genomics and Proteomics* **6**, 313–321 (2008).

Day, D. A. & Tuite, M. F. Post-transcriptional gene regulatory mechanisms in eukaryotes: an overview. *The Journal of Endocrinology* **157**, 361–71 (1998).

De Smet, S. & Vossen, E. Meat: The balance between nutrition and health. A review. *Meat Science* **120**, 145–156 (2016).

Dekkers, J. C. M. Commercial application of marker-and gene-assisted selection in livestock: Strategies and lessons 1,2. *Journal Animal Science* **82**, 313–328 (2004).

DePristo, M. A. et al. A framework for variation discovery and genotyping using next-generation DNA sequencing data. *Nature Genetics* **43**, 491–8 (2011).

Derrien, T. et al. The GENCODE v7 catalog of human long noncoding RNAs: analysis of their gene structure, evolution, and expression. *Genome Research* **22**, 1775–89 (2012).

Dickenson, D. L. & Bailey, D. Meat Traceability: Are U.S. consumers willing to pay for it? *Journal of Agricultural and Resource Economics* **27***:* 348-364

Djebali, S. et al. Landscape of transcription in human cells. *Nature* **489**, 101–108 (2012).

Dobin, A. et al. STAR: ultrafast universal RNA-Seq aligner. *Bioinformatics* **29**, 15–21 (2013).

Down, T. A. et al. A Bayesian deconvolution strategy for immunoprecipitation-based DNA methylome analysis. *Nature Biotechnology* **26**, 779–785 (2008).

Duijvesteijn, N. et al. A genome-wide association study on androstenone levels in pigs reveals a cluster of candidate genes on chromosome 6. *BMC Genetics* **11**, 42 (2010).

Dunn, L. L. et al. A critical role for thioredoxin-interacting protein in diabetes-related impairment of angiogenesis. *Diabetes* **63**, 675–687 (2014).

Eckel-Mahan, K. & Sassone-Corsi, P. Metabolism and the circadian clock converge. *Physiological Reviews* **93**, 107–35 (2013).

Engreitz, J. M. et al. Local regulation of gene expression by lncRNA promoters, transcription and splicing. *Nature* **539**, 452–455 (2016).

Eswaran, J. et al. RNA sequencing of cancer reveals novel splicing alterations. *Scientific Reports* **3**, 93–97 (2013).

Fan, H. et al. Sulforaphane causes a major epigenetic repression of myostatin in porcine satellite cells. *Epigenetics* **7**, 1379–1390 (2012).

Fang, M. & Andersson, L. Mitochondrial diversity in European and Chinese pigs is consistent with population expansions that occurred prior to domestication. *Proceedings*

of the Royal Society B: Biological Sciences **273**, 1803–1810 (2006).

Fang, M., Larson, G., Soares Ribeiro, H., Li, N. & Andersson, L. Contrasting Mode of Evolution at a Coat Color Locus in Wild and Domestic Pigs. *PLoS Genetics* **5**, e1000341 (2009).

Farnham, P. J. Insights from genomic profiling of transcription factors. *Nature Reviews Genetics* **10**, 605–616 (2009).

Fernandez, X., Monin, G., Talmant, A., Mourot, J. & Lebret, B. Influence of intramuscular fat content on the quality of pig meat — 2. Consumer acceptability of m. *longissimus lumborum. Meat Science* **53**, 67–72 (1999).

Ferraz, A. L. J. et al. Transcriptome architecture across tissues in the pig. *BMC Genomics* **9**, 173 (2008).

Ferré, P. The biology of peroxisome proliferator-activated receptors: relationship with lipid metabolism and insulin sensitivity. *Diabetes* **53**, S43–50 (2004).

Freeman, T. C. et al. A gene expression atlas of the domestic pig. *BMC Biology* **10**, 90 (2012).

Fuentes, E., Guzmán-Jofre, L., Moore-Carrasco, R. & Palomo, I. Role of PPARs in inflammatory processes associated with metabolic syndrome (Review). *Molecular Medicine Reports* **8**, 1611–1616 (2013).

Gallardo, D. et al. Mapping of quantitative trait loci for cholesterol, LDL, HDL, and triglyceride serum concentrations in pigs. *Physiological Genomics* **35**, 199–209 (2008).

Garaulet, M. et al. PERIOD2 variants are associated with abdominal obesity, psycho-behavioral factors, and attrition in the dietary treatment of obesity. *Journal of the American Dietetic Association* **110**, 917–921 (2010).

García-Alcalde, F. et al. Qualimap: evaluating next-generation sequencing alignment data. *Bioinformatics* **28**, 2678–9 (2012).

Gerber, A. et al. Blood-borne circadian signal stimulates daily oscillations in actin dynamics and SRF activity. *Cell* **152**, 492–503 (2013).

Ghosh, M. et al. Evaluation of body growth and immunity-related differentially expressed genes through deep RNA sequencing in the piglets of Jeju native pig and Berkshire. *Animal Genetics* **46**, 255–264 (2015).

Ghisla, S. & Massey, V. Mechanisms of flavoprotein-catalyzed reactions. *European Journal of Biochemistry* **181**, 1–17 (1989).

Giudice, J., Loehr, J. A., Rodney, G. G. & Cooper, T. A. Alternative splicing of four trafficking genes regulates myofiber structure and skeletal muscle physiology. *Cell Reports* **17**, 1923-1933 (2016).

Giuffra, E. et al. A large duplication associated with dominant white color in pigs originated by homologous recombination between LINE elements flanking KIT. *Mammalian Genome* **13**, 569–577 (2002).

Giuffra, E. et al. The origin of the domestic pig: independent domestication and subsequent introgression. *Genetics* **154**, 1785–91 (2000).

Gnocchi, D., Pedrelli, M., Hurt-Camejo, E. & Parini, P. Lipids around the Clock: focus on circadian rhythms and lipid metabolism. *Biology* **4**, 104–32 (2015).

González-Prendes, R. et al. Joint QTL mapping and gene expression analysis identify positional candidate genes influencing pork quality traits. *Scientific Reports* **7**, 39830 (2017).

Grabherr, M. G. et al. Full-length transcriptome assembly from RNA-Seq data without a reference genome. *Nature Biotechnology* **29**, 644–652 (2011).

Gregory, T. R. Artificial selection and domestication: modern lessons from Darwin's enduring analogy. *Evolution: Education and Outreach* **2**, 5–27 (2009).

Griffith, M. et al. Alternative expression analysis by RNA sequencing. *Nature Methods* **7**, 843–847 (2010).

Grimaldi, B. et al. PER2 Controls lipid metabolism by direct regulation of PPARγ. *Cell Metabolism* **12**, 509–520 (2010).

Grundberg, E. et al. Mapping *cis*- and trans-regulatory effects across multiple tissues in twins. *Nature Genetics* **44**, 1084–9 (2012).

Haas, B. J. et al. De novo transcript sequence reconstruction from RNA-Seq using the Trinity platform for reference generation and analysis. *Nature Protocols* **8**, 1494–512 (2013).

Hartley, S. W. & Mullikin, J. C. Detection and visualization of differential splicing in RNA-Seq data with JunctionSeq. *Nucleic Acids Research* **44**, e127 (2016).

Hastings, M. H., Maywood, E. S. & Reddy, A. B. Two decades of circadian time. *Journal of Neuroendocrinology* **20**, 812–819 (2008).

Hausman, G. J. et al. Board-invited review: the biology and regulation of preadipocytes and adipocytes in meat animals. *Journal of Animal Science* **87**, 1218–46 (2009).

Hernandez-Sanchez, J. et al. Genomic architecture of heritability and genetic correlations for intramuscular and back fat contents in Duroc pigs. *Journal of Animal Science* **91**, 623–632 (2013).

Hindorff, L. A. et al. Potential etiologic and functional implications of genome-wide association loci for human diseases and traits. *Proceedings of the National Academy of Sciences* **106**, 9362–9367 (2009).

Hirota, T. & Fukada, Y. Resetting mechanism of central and peripheral circadian clocks in mammals. Zoological *Science* **21**, 359–368 (2004).

Hocquette, J. F. et al. Intramuscular fat content in meat-producing animals: development, genetic and nutritional control, and identification of putative markers. *Animal* **4**, 303–319 (2010).

Hodge, B. A. et al. The endogenous molecular clock orchestrates the temporal separation of substrate metabolism in skeletal muscle. *Skeletal Muscle* **5**, 17 (2015).

Hodkinson, B. P. & Grice, E. A. Next-Generation Sequencing: a review of technologies and tools for wound microbiome research. *Advances in Wound Care* **4**, 50–58 (2015).

Huang, D. W. et al. The DAVID Gene Functional Classification Tool: a novel biological module-centric algorithm to functionally analyze large gene lists. *Genome Biology* **8**, R183 (2007).

Huarte, M. & Marín-Béjar, O. Long noncoding RNAs: from identification to functions and mechanisms. *Advances in Genomics and Genetics* **5**, 257 (2015).

Inoue, M. et al. Thrombospondin 1 mediates high-fat diet-induced muscle fibrosis and insulin resistance in male mice. *Endocrinology* **154**, 4548–59 (2013).

Iyer, M. K. et al. The landscape of long noncoding RNAs in the human transcriptome. *Nature Genetics* **47**, 199–208 (2015).

Jia, L. et al. MiRNA-199a-3p regulates C2C12 myoblast differentiation through IGF-1/AKT/mTOR signal pathway. *International Journal of Molecular Sciences* **15**, 296–308 (2013).

Jin, B., Li, Y. & Robertson, K. D. DNA methylation: superior or subordinate in the epigenetic hierarchy? *Genes & Cancer* **2**, 607–17 (2011).

Jing, L. et al. Transcriptome analysis of mRNA and miRNA in skeletal muscle indicates an important network for differential Residual Feed Intake in pigs. *Scientific Reports* **5**, 11953 (2015).

Jones, G. F. Genetic aspects of domestication, common breeds and their origin. The genetics of the pig. In: Rothschild MF and Ruvinsky A (eds) The Genetic (1998).

Kanehisa, M. & Goto, S. KEGG: kyoto encyclopedia of genes and genomes. *Nucleic Acids Research* **28**, 27–30 (2000).

Kersten, S. et al. Peroxisome proliferator–activated receptor α mediates the adaptive response to fasting. *Journal of Clinical Investigation* **103**, 1489–1498 (1999).

Khetarpal, S. A. & Rader, D. J. Genetics of lipid traits: Genome-wide approaches yield new biology and clues to causality in coronary artery disease. *Biochimica et Biophysica Acta* **1842**, 2010–2020 (2014).

Kim, D. et al. TopHat2: accurate alignment of transcriptomes in the presence of insertions, deletions and gene fusions. *Genome Biology* **14**, R36 (2013).

Kim, N., Alekseyenko, A. V, Roy, M. & Lee, C. The ASAP II database: analysis and comparative genomics of alternative splicing in 15 animal species. Nucleic Acids Research **35**, D93-8 (2007).

Klein, R. J. et al. Complement factor H polymorphism in age-related macular degeneration. *Science* **308**, 385–9 (2005).

Koltai, H. & Weingarten-Baror, C. Specificity of DNA microarray hybridization: characterization, effectors and approaches for data correction. *Nucleic Acids Research* **36**, 2395–2405 (2008).

Korir, P. K. & Seoighe, C. Inference of Allele-Specific Expression from RNA-Seq Data. *Methods in Molecular Biology* **1112**, 49–69 (2014).

Kukurba, K. R. & Montgomery, S. B. RNA Sequencing and Analysis. *Cold Spring Harbor protocols* **2015**, 951–69 (2015).

Lai, P.-H. et al. HDAC1/HDAC3 modulates *PPARG2* transcription through the sumoylated *CEBPD* in hepatic lipogenesis. *Biochimica et Biophysica Acta (BBA) - Molecular Cell Research* **1783**, 1803–1814 (2008).

Lamia, K. A., Storch, K.-F. & Weitz, C. J. Physiological significance of a peripheral tissue circadian clock. *Proceedings of the National Academy of Sciences of the United States of America* **105**, 15172–7 (2008).

LaPlant, Q. et al. Dnmt3a regulates emotional behavior and spine plasticity in the nucleus accumbens. *Nature Neuroscience* **13**, 1137–1143 (2010).

Lappalainen, T. et al. Transcriptome and genome sequencing uncovers functional variation in humans. *Nature* **501**, 506–11 (2013).

Larson, G. et al. Ancient DNA, pig domestication, and the spread of the Neolithic into Europe. *Proceedings of the National Academy of Sciences* **104**, 15276–15281 (2007).

Larson, G. et al. Worldwide phylogeography of wild boar reveals multiple centers of pig domestication. **Science 307**, 1618–21 (2005).

Lawler, P. R. & Lawler, J. Molecular basis for the regulation of angiogenesis by thrombospondin-1 and -2. *Cold Spring Harbor Perspectives in Medicine* **2**, a006627–a006627 (2012).

Leroy, F. & Praet, I. Meat traditions. The co-evolution of humans and meat. *Appetite* **90**, 200–11 (2015).

Levy, S. E. & Myers, R. M. Advancements in Next-Generation Sequencing. *Annual Review of Genomics and Human Genetics* **17**, 95–115 (2016).

Li, A. et al. ALDB: A Domestic-Animal Long Noncoding RNA Database. *PLoS One* **10**, e0124003 (2015).

Li, B. & Dewey, C. N. RSEM: accurate transcript quantification from RNA-Seq data with or without a reference genome. *BMC Bioinformatics* **12**, 323 (2011a).

Li, B. et al. RNA-Seq analysis reveals new candidate genes for drip loss in a Piétrain × Duroc × Landrace × Yorkshire population. *Animal Genetics* **47**, 192–199 (2016a).

Li, B. et al. Identification of candidate genes associated with porcine meat color traits by genome-wide transcriptome analysis. *Scientific Reports* **6**, 35224 (2016b).

Li, H. & Durbin, R. Fast and accurate short read alignment with Burrows-Wheeler transform. *Bioinformatics* **25**, 1754–1760 (2009a).

Li, H. et al. The Sequence Alignment/Map format and SAMtools. *Bioinformatics* **25**, 2078–2079 (2009).

Li, M. et al. An atlas of DNA methylomes in porcine adipose and muscle tissues. *Nature Communications* **3**, 850 (2012).

Li, R. et al. Misregulation of alternative splicing in a mouse model of Rett Syndrome. *PLoS Genetics* **12**, e1006129 (2016).

Li, R., Li, Y., Kristiansen, K. & Wang, J. SOAP: short oligonucleotide alignment program. *Bioinformatics* **24**, 713–4 (2008).

Li, Y., Chien, J., Smith, D. I. & Ma, J. FusionHunter: identifying fusion transcripts in cancer using paired-end RNA-Seq. *Bioinformatics* **27**, 1708–1710 (2011b).

Liao, Y., Smyth, G. K. & Shi, W. featureCounts: an efficient general purpose program for assigning sequence reads to genomic features. *Bioinformatics* **30**, 923–930 (2014).

Listrat, A. et al. How Muscle Structure and composition influence meat and flesh quality. *The Scientific World Journal* **2016**, 3182746 (2016).

Liu, Y. et al. Blood monocyte transcriptome and epigenome analyses reveal loci associated with human atherosclerosis. *Nature Communications* **8**, 393 (2017).

Lobo, V., Patil, A., Phatak, A. & Chandra, N. Free radicals, antioxidants and functional foods: Impact on human health. *Pharmacognosy Reviews* **4**, 118–26 (2010).

Love, M. I., Huber, W. & Anders, S. Moderated estimation of fold change and dispersion

for RNA-Seq data with DESeq2. *Genome Biology* **15**, 550 (2014).

Lü, M.-D. et al. Genetic variations associated with six-white-point coat pigmentation in Diannan small-ear pigs. *Scientific Reports* **6**, 27534 (2016).

Lyford, C. et al. Is willingness to pay (WTP) for beef quality grades affected by consumer demographics and meat consumption preferences? *Australasian Agribusiness Review - Australasian Agribusiness Review* **18** (2010).

Ma, J. et al. A splice mutation in the *PHKG1* gene causes high glycogen content and low meat quality in pig skeletal muscle. *Plos Genetics* **10**, e1004710 (2014).

Manrique, C. & Sowers, J. R. Insulin resistance and skeletal muscle vasculature: significance, assessment and therapeutic modulators. *Cardiorenal Medicine* **4**, 244–56 (2014).

Mariat, D., Taourit, S. & Guérin, G. A mutation in the *MATP* gene causes the cream coat colour in the horse. *Genetics, Selection, Evolution : GSE* **35**, 119–33 (2003).

McPherson, A. et al. Comrad: detection of expressed rearrangements by integrated analysis of RNA-Seq and low coverage genome sequence data. *Bioinformatics* **27**, 1481–1488 (2011).

Mele, M. et al. The human transcriptome across tissues and individuals. *Science* **348**, 660–665 (2015).

Meyer, C. A. & Liu, X. S. Identifying and mitigating bias in next-generation sequencing methods for chromatin biology. *Nature Reviews Genetics* **15**, 709–721 (2014).

Miller, M. B. & Tang, Y.-W. Basic concepts of microarrays and potential applications in clinical microbiology. *Clinical Microbiology Reviews* **22**, 611–33 (2009).

Molnár J, Nagy T, Stéger V, Tóth G, Marincs F, Barta E. Genome sequencing and analysis of Mangalica, a fatty local pig of Hungary. *BMC Genomics* **15**: 761 (2014).

Montori-Grau, M. et al. GNIP1 E3 ubiquitin ligase is a novel player in regulating glycogen metabolism in skeletal muscle. *Metabolism* **18**, pii: S0026-0495(18)30044-1 (2018).

Mortazavi, A. et al. Mapping and quantifying mammalian transcriptomes by RNA-Seq. *Nature Methods* **5**, 621–628 (2008).

Mühlbauer, E., Gross, E., Labucay, K., Wolgast, S. & Peschke, E. Loss of melatonin signalling and its impact on circadian rhythms in mouse organs regulating blood glucose. *European Journal of Pharmacology* **606**, 61–71 (2009).

Neguembor, M. V., Jothi, M. & Gabellini, D. Long noncoding RNAs, emerging players in muscle differentiation and disease. *Skeletal Muscle* **4**, 8 (2014).

Nica, A. C. et al. The architecture of gene regulatory variation across multiple human tissues: the MuTHER study. *Plos Genetics* **7**, e1002003 (2011).

Nie, M., Deng, Z.-L., Liu, J. & Wang, D.-Z. Noncoding RNAs, emerging regulators of skeletal muscle development and diseases. *Biomed Research International* **2015**, 676575 (2015).

Ogłuszka, M. et al. A porcine gluteus medius muscle genome-wide transcriptome analysis: dietary effects of omega-6 and omega-3 fatty acids on biological mechanisms. *Genes & Nutrition* **12**, 4 (2017).

Oike, H., Oishi, K. & Kobori, M. Nutrients, clock genes, and chrononutrition. *Current*

Nutrition Reports **3**, 204–212 (2014).

Oliveira, G. B. et al. Integrative analysis of microRNAs and mRNAs revealed regulation of composition and metabolism in Nelore cattle. *BMC Genomics* **19**, 126 (2018).

Oster, H. et al. The circadian rhythm of glucocorticoids is regulated by a gating mechanism residing in the adrenal cortical clock. *Cell Metabolism* **4**, 163–173 (2006).

Palazzo, A. F. & Lee, E. S. Non-coding RNA: what is functional and what is junk? *Frontiers in Genetics* **6**, 2 (2015).

Partch, C. L., Green, C. B. & Takahashi, J. S. Molecular architecture of the mammalian circadian clock. *Trends in Cell Biology* **24**, 90–99 (2014).

Paschos, G. K. et al. Obesity in mice with adipocyte-specific deletion of clock component Arntl. *Nature medicine* **18**, 1768–77 (2012).

Patro, R., Duggal, G. & Kingsford, C. Salmon: accurate, versatile and ultrafast quantification from RNA-Seq data using lightweight-alignment. *bioRxiv* 21592 (2015).

Patro, R., Mount, S. M. & Kingsford, C. Sailfish enables alignment-free isoform quantification from RNA-Seq reads using lightweight algorithms. *Nature Biotechnology* **32**, 462–4 (2014).

Pavlidis, P., Jensen, J. D., Stephan, W. & Stamatakis, A. A critical assessment of storytelling: gene ontology categories and the importance of validating genomic scans. *Molecular Biology and Evolution* **29**, 3237–48 (2012).

Peek, C. B., Ramsey, K. M., Marcheva, B. & Bass, J. Nutrient sensing and the circadian clock. *Trends in endocrinology and metabolism: TEM* **23**, 312–8 (2012).

Pena, R. N. et al. Application of the microarray technology to the transcriptional analysis of muscle phenotypes in pigs. *Animal Genetics* **45**, 311–321 (2014).

Pena, R. N. et al. Transcriptional analysis of intramuscular fatty acid composition in the longissimus thoracis muscle of Iberian × Landrace back-crossed pigs. *Animal Genetics* **44**, 648–60 (2013).

Pilcher, C. M. et al. Transcript profiles in longissimus dorsi muscle and subcutaneous adipose tissue: a comparison of pigs with different postweaning growth rates. *Journal of Animal Science* **93**, 2134–2143 (2015).

Piskol, R., Ramaswami, G. & Li, J. B. Reliable identification of genomic variants from RNA-Seq data. *The American Journal of Human Genetics* **93**, 641–651 (2013).

Ponsuksili, S., Murani, E., Schwerin, M., Schellander, K. & Wimmers, K. Identification of expression QTL (eQTL) of genes expressed in porcine M. longissimus dorsi and associated with meat quality traits. *BMC Genomics* **11**, 572 (2010).

Ponsuksili, S., Murani, E., Trakooljul, N., Schwerin, M. & Wimmers, K. Discovery of candidate genes for muscle traits based on GWAS supported by eQTL-analysis. *International Journal of Biological Sciences* **10**, 327–37 (2014).

Porter, V. Pigs: A Handbook to the Breeds of the World. Mountfield: Helm Information Ltd. (1993).

Powers, H. J. Riboflavin (vitamin B-2) and health. *The American Journal of Clinical Nutrition*. **77**, 1352–60 (2003).

Przybylski, W. & Hopkins, D. Meat quality : genetic and environmental factors. CRC Press

(2015).

Puig-Oliveras, A. et al. Differences in muscle transcriptome among pigs phenotypically extreme for fatty acid composition. *PloS One* **9**, e99720 (2014).

Qiao, R. et al. Genome-wide association analyses reveal significant loci and strong candidate genes for growth and fatness traits in two pig populations. *Genetics Selection Evolution* **47**, 17 (2015).

Ramayo-Caldas, Y. et al. From SNP co-association to RNA co-expression: novel insights into gene networks for intramuscular fatty acid composition in porcine. *BMC Genomics* **15**, 232 (2014).

Ramayo-Caldas, Y. et al. Liver transcriptome profile in pigs with extreme phenotypes of intramuscular fatty acid composition. *BMC Genomics* **13**, 547 (2012).

Reane, D. et al. A MICU1 splice variant confers high sensitivity to the mitochondrial CA^{2+} uptake machinery of skeletal muscle. *Molecular Cell* **64**, 760–773 (2016).

Ren, J. et al. A 6-bp deletion in the *TYRP1* gene causes the brown colouration phenotype in Chinese indigenous pigs. *Heredity* **106**, 862–868 (2011).

Reyer, H., Ponsuksili, S., Wimmers, K. & Murani, E. Transcript variants of the porcine glucocorticoid receptor gene (*NR3C1*). *General and Comparative Endocrinology* **189**, 127–133 (2013).

Reyes, A. & Huber, W. Alternative start and termination sites of transcription drive most transcript isoform differences across human tissues. *Nucleic Acids Research* **25**, 582-592 (2017).

Richards, J. & Gumz, M. L. Advances in understanding the peripheral circadian clocks. *FASEB Journal : Official Publication of the Federation of American Societies for Experimental Biology* **26**, 3602–13 (2012).

Ritchie, M. D., Holzinger, E. R., Li, R., Pendergrass, S. A. & Kim, D. Methods of integrating data to uncover genotype–phenotype interactions. *Nature Reviews Genetics* **16**, 85–97 (2015).

Roberts, D. D., Kaur, S. & Isenberg, J. S. Regulation of cellular redox signaling by matricellular proteins in vascular biology, immunology, and cancer. *Antioxidants & Redox Signaling* **27**, 874–911 (2017).

Robertson, G. et al. Genome-wide profiles of STAT1 DNA association using chromatin immunoprecipitation and massively parallel sequencing. *Nature Methods* **4**, 651–657 (2007).

Robinson, M. D. & Oshlack, A. A scaling normalization method for differential expression analysis of RNA-Seq data. Genome Biology **11**, R25 (2010).

Robinson, M. D., McCarthy, D. J. & Smyth, G. K. edgeR: a Bioconductor package for differential expression analysis of digital gene expression data. *Bioinformatics* **26**, 139–140 (2010).

Rothammer, S. et al. Detection of two non-synonymous SNPs in *SLC45A2* on BTA20 as candidate causal mutations for oculocutaneous albinism in Braunvieh cattle. *Genetics, Selection, Evolution : GSE* **49**, 73 (2017).

Rubin, C.-J. et al. Strong signatures of selection in the domestic pig genome. *Proceedings of the National Academy of Sciences of the United States of America* **109**, 19529–36

(2012).

Rudic, R. D. et al. BMAL1 and CLOCK, two essential components of the circadian clock, are involved in glucose homeostasis. *Plos Biology* **2**, e377 (2004).

Russ, A. E. et al. Gene expression changes in the colon epithelium are similar to those of intact colon during late inflammation in interleukin-10 gene deficient mice. *Plos One* **8**, e63251 (2013).

Scandura, M. et al. Ancient vs. recent processes as factors shaping the genetic variation of the European wild boar: are the effects of the last glaciation still detectable? *Molecular Ecology* **17**, 1745–1762 (2008).

Schachtschneider, K. M. et al. Adult porcine genome-wide DNA methylation patterns support pigs as a biomedical model. *BMC Genomics* **16**, 743 (2015).

Schmidt, D. et al. Five-vertebrate chip-seq reveals the evolutionary dynamics of transcription factor binding. *Science* **328**, 1036-40 (2010).

Schurch, N. J. et al. How many biological replicates are needed in an RNA-Seq experiment and which differential expression tool should you use? *RNA* **22**, 839–51 (2016).

Schwer, B., Bunkenborg, J., Verdin, R. O., Andersen, J. S. & Verdin, E. Reversible lysine acetylation controls the activity of the mitochondrial enzyme acetyl-CoA synthetase 2. *Proceedings of the National Academy of Sciences* **103**, 10224–10229 (2006).

Seyednasrollah, F., Laiho, A. & Elo, L. L. Comparison of software packages for detecting differential expression in RNA-Seq studies. *Briefings in Bioinformatics* **16**, 59–70 (2015).

Shah, A. et al. Thioredoxin-interacting protein mediates high glucose-induced reactive oxygen species generation by mitochondria and the NADPH oxidase, Nox4, in mesangial cells. *The Journal of Biological Chemistry* **288**, 6835–48 (2013).

Shannon, P. et al. Cytoscape: a software environment for integrated models of biomolecular interaction networks. *Genome Research* **13**, 2498–504 (2003).

Sharma, A. M. & Staels, B. Peroxisome proliferator-activated receptor γ and adipose tissue—understanding obesity-related changes in regulation of lipid and glucose metabolism. *The Journal of Clinical Endocrinology & Metabolism* **92**, 386–395 (2007).

Sharma, A., Seop, J., Dang, C. G., Sudrajad, P. & Kim, H. C. Stories and challenges of genome wide association studies in livestock — A Review. *Asian-Australasian Journal of Animal Sciences* **28**, 1371–1379 (2015).

Shitaye, H. S., Terkhorn, S. P., Combs, J. A. & Hankenson, K. D. Thrombospondin-2 is an endogenous adipocyte inhibitor. *Matrix Biology : Journal of the International Society for Matrix Biology* **29**, 549–56 (2010).

Shulman, G. I. et al. Quantitation of muscle glycogen synthesis in normal subjects and subjects with non-insulin-dependent diabetes by 13C nuclear magnetic resonance spectroscopy. *The New England Journal Of Medicine* **322**, 223–8 (1990).

Simillion, C., Liechti, R., Lischer, H. E. L., Ioannidis, V. & Bruggmann, R. Avoiding the pitfalls of gene set enrichment analysis with SetRank. *BMC Bioinformatics* **18**, 151 (2017).

Smyth, G. K. Linear models and empirical bayes methods for assessing differential expression in microarray experiments. *Statistical Applications in Genetics and Molecular*

Biology **3**, 1–25 (2004).

Sodhi, S. S. et al. Comparative transcriptomic analysis by RNA-Seq to discern differential expression of genes in liver and muscle tissues of adult Berkshire and Jeju Native Pig. *Gene* **546**, 233–242 (2014).

Soto-Pantoja, D. R. et al. Dietary fat overcomes the protective activity of thrombospondin-1 signaling in the Apc Min/+ model of colon cancer. *Oncogenesis* **5**, e230–e230 (2016).

Sunwoo, H. et al. MEN epsilon/beta nuclear-retained non-coding RNAs are up-regulated upon muscle differentiation and are essential components of paraspeckles. *Genome Research 19*, 347–59 (2009).

Szklarczyk, D. et al. STRING v10: protein-protein interaction networks, integrated over the tree of life. *Nucleic Acids Research* **43**, D447–D452 (2015).

Tahara, Y. & Shibata, S. Chronobiology and nutrition. *Neuroscience* **253**, 78–88 (2013).

Tarazona, S. et al. Data quality aware analysis of differential expression in RNA-Seq with NOISeq R/Bioc package. *Nucleic Acids Research* **43**, e140 (2015).

Teslovich, T. M. et al. Biological, clinical and population relevance of 95 loci for blood lipids. *Nature* **466**, 707–13 (2010).

The ENCODE Project Consortium. An integrated encyclopedia of DNA elements in the human genome. *Nature* **489**, 57–74 (2012).

The GTEx Consortium. The Genotype-Tissue Expression (GTEx) pilot analysis: Multitissue gene regulation in humans. *Science*. **348**, 648-60 (2015).

The GTEx Consortium. The Genotype-Tissue Expression (GTEx) project. *Nature Genetics* **45**, 580–5 (2013).

Torres-Vázquez, J. A. & Spangler, M. L. Genetic parameters for docility, weaning weight, yearling weight, and intramuscular fat percentage in Hereford cattle. *Journal of Animal Science* **94**, 21 (2016).

Tóth, L. et al. Identification of two novel mutations in the *SLC45A2* gene in a Hungarian pedigree affected by unusual OCA type 4. *BMC Medical Genetics* **18**, 27 (2017).

Toyota, M. et al. CpG island methylator phenotype in colorectal cancer. *Proceedings of the National Academy of Sciences of the United States of America* **96**, 8681–6 (1999).

Trapnell, C. et al. Differential gene and transcript expression analysis of RNA-Seq experiments with TopHat and Cufflinks. *Nature Protocols* **7**, 562–578 (2012).

Trapnell, C. et al. Transcript assembly and quantification by RNA-Seq reveals unannotated transcripts and isoform switching during cell differentiation. *Nature Biotechnology* **28**, 511–5 (2010).

Trenhaile, M. D., Petersen, J. L., Kachman, S. D., Johnson, R. K. & Ciobanu, D. C. Long-term selection for litter size in swine results in shifts in allelic frequency in regions involved in reproductive processes. *Animal Genetics* **47**, 534–542 (2016).

Tress, M. L. et al. The implications of alternative splicing in the ENCODE protein complement. *Proceedings of the National Academy of Sciences of the United States of America* **104**, 5495–500 (2007).

Triantaphyllopoulos, K. A., Ikonomopoulos, I. & Bannister, A. J. Epigenetics and inheritance of phenotype variation in livestock. *Epigenetics & Chromatin* **9**, 31 (2016).

Trost, B. et al. Concordance between RNA-Sequencing data and DNA microarray data in transcriptome analysis of proliferative and quiescent fibroblasts. *Royal Society Open Science* **2**, 150402 (2015).

Tsai, S. et al. Annotation of the Affymetrix1 porcine genome microarray. *Animal Genetics* **37**, 423–424 (2006).

Vartak, R., Deng, J., Fang, H. & Bai, Y. Redefining the roles of mitochondrial DNA-encoded subunits in respiratory Complex I assembly. *Biochimica* et *Biophysica Acta* **1852**, 1531–9 (2015).

Valladares, M., Obregón, A. M. & Chaput, J.-P. Association between genetic variants of the clock gene and obesity and sleep duration. *Journal of Physiology and Biochemistry* **71**, 855–860 (2015).

van Dijk, E. L., Auger, H., Jaszczyszyn, Y. & Thermes, C. Ten years of next-generation sequencing technology. *Trends in Genetics* **30**, 418–426 (2014).

van Wijk, H. J. et al. Genetic parameters for carcass composition and pork quality estimated in a commercial production chain. *Journal of Animal Science* **83**, 324 (2005).

Vêncio, R. Z., Brentani, H., Patrão, D. F. & Pereira, C. A. Bayesian model accounting for within-class biological variability in Serial Analysis of Gene Expression (SAGE). *BMC Bioinformatic*s **5**, 119 (2004).

Vitti, J. J., Grossman, S. R. & Sabeti, P. C. Detecting natural selection in genomic data. *Annual Review of Genetics* **47**, 97–120 (2013).

Wang, C. et al. Genome-wide analysis reveals artificial selection on coat colour and reproductive traits in Chinese domestic pigs. *Molecular Ecology Resources* **15**, 414–424 (2015a).

Wang, C. et al. The concordance between RNA-Seq and microarray data depends on chemical treatment and transcript abundance. *Nature Biotechnology* **32**, 926–32 (2014).

Wang, E. T. et al. Alternative isoform regulation in human tissue transcriptomes. *Nature* **456**, 470–6 (2008).

Wang, L. et al. Alternative splicing of the porcine glycogen synthase kinase 3β (GSK-3β) gene with differential expression patterns and regulatory functions. *Plos One* **7**, e40250 (2012).

Wang, Q. et al. Differential expression profile of miRNAs in porcine muscle and adipose tissue during development. *Gene* **618**, 49–56 (2017a).

Wang, Y. et al. Dynamic transcriptome and DNA methylome analyses on longissimus dorsi to identify genes underlying intramuscular fat content in pigs. *BMC Genomics* **18**, 780 (2017b).

Wang, Z. et al. Identification of Genes Related to Growth and Lipid Deposition from Transcriptome Profiles of Pig Muscle Tissue. *Plos One* **10**, e0141138 (2015b).

Wang, Z. et al. RNA-Seq: a revolutionary tool for transcriptomics. *Nature Reviews Genetics* **10**, 57–63 (2009).

Warriss, P. D. Meat Science: An introductory text; CABI: Oxford, U.K., 2000

Watts, R., Johnsen, V. L., Shearer, J. & Hittel, D. S. Myostatin-induced inhibition of the long noncoding RNA Malat1 is associated with decreased myogenesis. *Cell Physiology* **304**, C995–C1001 (2013).

Wei, W. et al. miR-130a regulates differential lipid accumulation between intramuscular and subcutaneous adipose tissues of pigs via suppressing *PPARG* expression. *Gene* **636**, 23–29 (2017).

Willer, C. J. et al. Discovery and refinement of loci associated with lipid levels. *Nature Genetics* **45**, 1274–1283 (2013).

Wolf, J. B. W. Principles of transcriptome analysis and gene expression quantification: An RNA-Seq tutorial. *Molecular Ecology Resources* **13**, 559–572 (2013).

Wood, J. D. et al. Fat deposition, fatty acid composition and meat quality: A review. *Meat Science* **78**, 343–358 (2008).

Wu, X. et al. A 6-bp deletion in exon 8 and two mutations in introns of *TYRP1* are associated with blond coat color in Liangshan pigs. *Gene* **578**, 132–136 (2016).

Xu, J. et al. Hepatic carboxylesterase 1 is induced by glucose and regulates postprandial glucose levels. *Plos One* **9**, e109663 (2014).

Yang, B. et al. Genome-wide SNP data unveils the globalization of domesticated pigs. *Genetics Selection Evolution* **49**, 71 (2017).

Yang, I. S. & Kim, S. Analysis of Whole Transcriptome Sequencing Data: Workflow and Software. *Genomics & Informatics* **13**, 119–25 (2015).

Yao, Y. et al. Global profiling of the gene expression and alternative splicing events during hypoxia-regulated chondrogenic differentiation in human cartilage endplate-derived stem cells. *Genomics* **107**, 170–177 (2016).

Yoon, A., Tammen, S. A., Park, S., Han, S. N. & Choi, S.-W. Genome-wide hepatic DNA methylation changes in high-fat diet-induced obese mice. *Nutrition Research and Practice* **11**, 105–113 (2017).

Young, M. D., Wakefield, M. J., Smyth, G. K. & Oshlack, A. Gene ontology analysis for RNA-Seq: accounting for selection bias. *Genome Biology* **11**, R14 (2010).

Yu, H., Li, R., Huang, H., Yao, R. & Shen, S. Short-chain fatty acids enhance the lipid accumulation of 3t3-l1 cells by modulating the expression of enzymes of fatty acid metabolism. *Lipids* **53**, 77–84 (2018).

Yue, F. et al. A comparative encyclopedia of DNA elements in the mouse genome. *Nature* **515**, 355–364 (2014).

Zhang, S. et al. DNA methylation landscape of fat deposits and fatty acid composition in obese and lean pigs. *Scientific Reports* **6**, 35063 (2016).

Zhang, Y.-Y. et al. Transcriptome analysis of mRNA and microRNAs in intramuscular fat tissues of castrated and intact male Chinese Qinchuan cattle. *Plos One* **12**, e0185961 (2017).

Zhang, Z. H. et al. A Comparative Study of Techniques for Differential Expression Analysis on RNA-Seq Data. PLoS One **9**, e103207 (2014).

Zhao, Q.-Y. et al. Global histone modification profiling reveals the epigenomic dynamics during malignant transformation in a four-stage breast cancer model. *Clinical Epigenetics* **8**, 34 (2016).

Zhao, Y. et al. Dynamic transcriptome profiles of skeletal muscle tissue across 11 developmental stages for both Tongcheng and Yorkshire pigs. *BMC Genomics* **16**, 377 (2015a).

Zhou, J. & Chng, W.-J. Roles of thioredoxin binding protein (TXNIP) in oxidative stress, apoptosis and cancer. *Mitochondrion* **13**, 163–9 (2013).

Zhou, Y. et al. Integrative analysis reveals enhanced regulatory effects of human long intergenic non-coding RNAs in lung adenocarcinoma. *Journal of Genetics and Genomics* **42**, 423–36 (2015c).

Zhou, Z.-Y. et al. DNA methylation signatures of long intergenic noncoding RNAs in porcine adipose and muscle tissues. *Scientific Reports* **5**, 15435 (2015b).

Zhou, Z.-Y. et al. Genome-wide identification of long intergenic noncoding RNA genes and their potential association with domestication in pigs. *Genome Biology and Evolution* **6**, 1387–92 (2014).

Zhu, J. et al. RNA-Seq transcriptome analysis of extensor *digitorum longus* and *soleus muscles* in large white pigs. *Molecular Genetics and Genomics* **291**, 687–701 (2016).

Zhu, Y. et al. Signatures of selection and interspecies introgression in the genome of chinese domestic pigs. *Genome Biology and Evolution* **9**, 2592–2603 (2017).

Zou, C. et al. Transcriptome analysis reveals long intergenic non-coding RNAs involved in skeletal muscle growth and development in pig. *Scientific Reports* **7**, 8704 (2017).

Annexes

Chapter 7

Supplemental material Paper I: "RNA-Seq based detection of differentially expressed genes in the skeletal muscle of Duroc pigs with distinct lipid profiles"

Annex 1 - Table S1 - Differentially expressed genes in the *gluteus medius* muscle of HIGH and LOW pigs (*P*-value ≤ 0.05). (The complete table is included in the CD-Rom).

Feature ID	Gene ID	Fold Change	q- value	P-value	LOW - Means	HIGH - Means
ENSSSCG00000002041	*SLC7A7*	-1.20	1.36E-03	1.36E-07	6.02	5.03
ENSSSCG00000007705		1.26	4.28E-03	9.78E-07	2.00	2.52
ENSSSCG00000005648	*SLC27A4*	1.66	4.28E-03	1.32E-06	1.03	1.71
ENSSSCG00000027946	*MVP*	1.78	5.97E-03	2.63E-06	14.75	26.30
ENSSSCG00000010514	*RRP12*	1.25	5.97E-03	3.07E-06	9.14	11.45
ENSSSCG00000002042	*OXA1L*	-1.18	1.36E-02	1.20E-05	62.43	52.69
ENSSSCG00000001435	*AGPAT1*	1.28	1.36E-02	1.23E-05	7.15	9.19
ENSSSCG00000012914	*RAD9A*	1.35	1.36E-02	1.24E-05	0.65	0.88
ENSSSCG00000017232	*SLC9A3R1*	1.72	1.36E-02	1.26E-05	4.84	8.33
ENSSSCG00000003379	*KLHL21*	1.79	1.43E-02	1.61E-05	6.11	10.93
ENSSSCG00000024814	*MAGEB5*	-1.41	1.43E-02	1.74E-05	3.81	2.71
ENSSSCG00000005935	*AGO2*	1.59	1.43E-02	1.77E-05	3.34	5.32
ENSSSCG00000020963	*EPDR1*	-1.30	1.48E-02	1.98E-05	25.34	19.42
ENSSSCG00000011740	*SERPINI1*	-1.81	1.72E-02	2.48E-05	0.34	
ENSSSCG00000001931	*GRAMD2*	-1.58	1.76E-02	2.74E-05	2.75	1.74
ENSSSCG00000007574	*SDK1*	1.58	1.76E-02	2.97E-05		0.24
ENSSSCG00000022373	*JMJD6*	1.38	1.76E-02	3.18E-05	12.98	17.96
ENSSSCG00000011444	*NT5DC2*	1.54	1.76E-02	3.26E-05	3.12	4.81
ENSSSCG00000011398	*SEMA3F*	1.41	1.82E-02	3.56E-05	2.66	3.76
ENSSSCG00000001679		1.41	1.84E-02	3.77E-05	6.25	8.80
ENSSSCG00000007745	*SUMF2*	-1.54	1.95E-02	4.21E-05	7.38	4.80
ENSSSCG00000000293	*ITGA5*	1.72	1.96E-02	4.46E-05	4.56	7.82
ENSSSCG00000023043	*BCL2L13*	1.16	1.96E-02	4.65E-05	19.45	22.58
ENSSSCG00000007133	*ACSS1*	1.51	2.09E-02	5.18E-05	7.25	10.96
ENSSSCG00000028814	*SOD3*	1.97	2.09E-02	5.37E-05	0.89	1.75
ENSSSCG00000006277	*SPIDR*	2.04	2.19E-02	5.90E-05	6.94	14.18
ENSSSCG00000003000	*ITPKC*	1.49	2.19E-02	6.07E-05	1.41	2.10
ENSSSCG00000003267	*MBOAT7*	1.27	2.23E-02	6.44E-05	3.35	4.25
ENSSSCG00000024295	*SIAH2*	1.43	2.46E-02	7.35E-05	3.57	5.12
ENSSSCG00000026817	*ZNF646*	1.26	2.55E-02	7.91E-05	1.29	1.62
ENSSSCG00000010986		1.26	2.55E-02	8.13E-05	8.39	10.61
ENSSSCG00000003134	*GRWD1*	1.26	2.88E-02	9.84E-05	10.53	13.26
ENSSSCG00000028197	*PFKL*	1.42	2.88E-02	1.01E-04	2.96	4.22
ENSSSCG00000007554	*ZFAND2A*	2.54	2.88E-02	1.01E-04	11.81	29.98
ENSSSCG00000000431		1.24	2.91E-02	1.06E-04	2.49	3.08
ENSSSCG00000010070	*SMARCB1*	1.19	2.91E-02	1.08E-04	9.58	11.39
ENSSSCG00000003105	*SLC1A5*	1.67	3.07E-02	1.17E-04	3.21	5.37
ENSSSCG00000006635	*SEMA6C*	-1.38	3.10E-02	1.21E-04	28.68	20.80
ENSSSCG00000012655	*BCORL1*	1.44	3.11E-02	1.26E-04	0.54	0.78

ENSSSCG00000012886		1.18	3.11E-02	1.28E-04	2.65	3.12
ENSSSCG00000010529	*SFRP5*	2.03	3.11E-02	1.31E-04	1.98	4.02
ENSSSCG00000006245	*SDR16C5*	3.02	3.15E-02	1.36E-04	0.58	1.77
ENSSSCG00000001701	*HSP90AB1*	1.35	3.31E-02	1.47E-04	83.96	113.70
ENSSSCG00000013579	*CD209*	1.95	3.31E-02	1.50E-04	1.32	2.57
ENSSSCG00000004388	*ARMC2*	-1.43	3.35E-02	1.55E-04	0.30	0.21
ENSSSCG00000024235	*NPLOC4*	1.19	3.40E-02	1.63E-04	45.12	53.82
ENSSSCG00000010107	*MED15*	1.24	3.40E-02	1.65E-04	11.94	14.82
ENSSSCG00000022227	*BRD4*	1.22	3.40E-02	1.71E-04	8.56	10.45
ENSSSCG00000017882	*MYBBP1A*	1.21	3.40E-02	1.72E-04	16.87	20.36
ENSSSCG00000016207	*FAM134A*	1.16	3.46E-02	1.79E-04	18.18	21.05
ENSSSCG00000017479	*WIPF2*	1.22	3.46E-02	1.82E-04	1.97	2.40
ENSSSCG00000027689	*SRM*	1.36	3.46E-02	1.85E-04	3.33	4.52
ENSSSCG00000017774	*FAM222B*	1.20	3.46E-02	1.89E-04	2.07	2.49
ENSSSCG00000016775	*ZNF777*	1.16	3.46E-02	1.94E-04	7.80	9.04
ENSSSCG00000017835	*CLUH*	1.34	3.46E-02	1.96E-04	18.74	25.07
ENSSSCG00000008232	*RNF181*	-2.09	3.57E-02	2.05E-04	20.92	9.99
ENSSSCG00000030165	*MAFF*	1.67	3.72E-02	2.22E-04	12.50	20.89
ENSSSCG00000027779	*TMEM259*	1.17	3.72E-02	2.22E-04	28.80	33.63
ENSSSCG00000005943	*ST3GAL1*	1.42	3.75E-02	2.27E-04	2.58	3.67
ENSSSCG00000006496	*LMNA*	1.28	3.87E-02	2.39E-04	47.69	60.85
ENSSSCG00000001004	*SLC22A23*	1.42	4.30E-02	2.70E-04	4.34	6.15
ENSSSCG00000014084	*POC5*	-1.39	4.33E-02	2.76E-04	2.34	1.69
ENSSSCG00000013475	*NCLN*	1.16	4.47E-02	2.90E-04	8.75	10.19
ENSSSCG00000022528	*DAZAP1*	1.21	4.57E-02	3.03E-04	20.96	25.42
ENSSSCG00000008550	*SLC5A6*	1.47	4.57E-02	3.05E-04	7.49	11.02
ENSSSCG00000024437	*AP2M1*	1.25	4.92E-02	3.34E-04	70.29	87.59
ENSSSCG00000024577		1.23	5.05E-02	3.48E-04	427.48	523.91
ENSSSCG00000013303	*ABTB2*	1.95	5.05E-02	3.53E-04	0.38	0.74
ENSSSCG00000003138	*HSD17B14*	1.24	5.08E-02	3.62E-04	2.94	3.65
ENSSSCG00000016648		-1.45	5.08E-02	3.67E-04	1.27	0.88
ENSSSCG00000008040	*TSC2*	1.13	5.08E-02	3.71E-04	5.86	6.65
ENSSSCG00000002824		1.93	5.21E-02	3.88E-04	1.10	2.12
ENSSSCG00000023044	*FASN*	2.06	5.21E-02	3.91E-04	11.85	24.45
ENSSSCG00000005664	*LRRC8A*	1.26	5.56E-02	4.36E-04	2.87	3.61
ENSSSCG00000001398	*SLA-6*	-1.40	5.56E-02	4.46E-04	4.00	2.85
ENSSSCG00000006518	*HCN3*	1.26	5.56E-02	4.53E-04	0.75	0.94
ENSSSCG00000014859	*SERPINH1*	1.48	5.56E-02	4.53E-04	30.63	45.18
ENSSSCG00000001700	*SLC29A1*	1.21	5.56E-02	4.62E-04	10.07	12.18
ENSSSCG00000004367	*POPDC3*	1.20	5.56E-02	4.67E-04	49.18	58.92
ENSSSCG00000002826	*CES1**	2.03	5.56E-02	4.68E-04	1.14	2.31
ENSSSCG00000030182	*DEDD2*	1.42	5.56E-02	4.69E-04	3.90	5.54
ENSSSCG00000005315	*CA9*	-1.25	5.56E-02	4.71E-04	3.21	2.57
ENSSSCG00000016191		1.29	5.56E-02	4.79E-04	2.05	2.65
ENSSSCG00000009545	*COL4A2*	1.31	5.56E-02	4.81E-04	21.20	27.73
ENSSSCG00000013745	*FARSA*	1.24	5.63E-02	4.93E-04	8.33	10.33

Annex 2 - Table S2 - List of DE genes (P-value ≤ 0.05) detected simultaneously with RNA-Seq (current work) and microarrays (Cánovas et al. 2010. BMC Genomics 11, 372).

List of	Microarray		RNA-Seq	
common genes	Fold-change	*P*-value	Fold-change	*P*-value
MVP	-1.54	1.00E-07	-1.25	8.15E-04
ZFAND2A	-1.62	1.00E-06	-1.23	1.30E-03
MAFF	2.49	1.80E-06	1.90	1.49E-03
SLC5A6	3.09	2.30E-06	1.55	2.14E-02
PRKRA	2.22	2.90E-06	1.67	1.09E-02
TKT	1.92	3.00E-06	1.35	2.99E-03
PBX3	2.12	5.00E-06	1.86	1.89E-02
COL4A1	-2.54	7.30E-06	-1.42	1.68E-02
PGM3	-1.88	8.40E-06	-1.26	3.95E-03
PTX3	-1.53	1.01E-05	-1.20	1.24E-02
PPARD	2.57	3.22E-05	7.92	9.17E-04
TXNRD1	1.55	3.84E-05	1.59	2.16E-02
BAG3	1.70	5.14E-05	1.42	3.21E-02
ORAI1	1.40	5.63E-05	1.34	5.08E-03
ITIH3	1.37	5.88E-05	-1.29	3.76E-02
SNTB1	1.59	1.31E-04	1.41	1.14E-03
PPP1R3B	1.39	1.43E-04	1.25	3.26E-02
NPC2	2.33	1.47E-04	3.27	5.33E-03
SLC25A17	1.72	1.77E-04	2.54	1.01E-04
AQP3	1.69	1.86E-04	1.51	2.76E-02
SHISA2	1.43	2.15E-04	1.34	5.07E-03
CABLES2	-1.56	2.45E-04	-1.30	4.37E-02
MLF1	-1.37	3.09E-04	-1.11	3.98E-02
AVL9	1.33	3.18E-04	1.38	5.24E-03
NPC1	1.56	3.29E-04	1.46	1.27E-03
SQRDL	1.65	3.56E-04	1.42	6.32E-04
AMPD3	1.34	3.69E-04	1.45	2.60E-03
CHCHD4	1.60	3.70E-04	1.44	1.39E-02
HSPB1	2.30	4.02E-04	1.20	4.39E-03
RXRG	1.32	5.18E-04	-1.24	1.95E-02
TLR1	1.47	5.25E-04	1.66	1.04E-02
CIDEA	-1.41	5.32E-04	-1.36	6.38E-04
ANXA2	1.33	5.43E-04	1.54	1.04E-02
SFRP1	1.56	6.20E-04	1.35	5.82E-03
NQO1	1.42	6.60E-04	1.33	3.96E-02
B4GALT5	-1.49	6.76E-04	-1.34	1.90E-02
TMEM38A	-1.39	7.58E-04	-1.12	1.40E-02
SCD	1.28	7.88E-04	1.25	3.48E-02
SH3GL1	1.33	1.32E-03	1.42	4.21E-02
MS4A2	1.49	1.35E-03	1.33	1.67E-02
PPP1R15A	-1.51	1.36E-03	-1.10	2.45E-02
GMPR	-1.29	1.51E-03	-1.28	4.30E-03
AQP4	-1.30	1.59E-03	-1.14	2.91E-02
SEC31A	-1.39	1.64E-03	-1.27	8.72E-03
CHORDC1	1.64	1.68E-03	1.45	3.38E-02
HSPH1	1.67	1.73E-03	-1.45	9.34E-03
IGFBP5	-1.29	1.74E-03	1.17	3.55E-02
FAM35A	-1.50	1.74E-03	-1.26	6.03E-04
PPARG	-1.30	1.82E-03	-1.24	4.84E-02

LIPE	-1.31	2.30E-03	-1.69	1.62E-02
ACACA	1.25	2.61E-03	1.22	2.69E-02
BMP1	-1.38	2.71E-03	-1.15	4.23E-02
TBC1D20	1.27	2.73E-03	1.78	2.63E-06
YWHAH	1.38	2.76E-03	1.42	1.51E-02
GPD1	1.26	2.90E-03	1.47	3.05E-04
IGF1R	1.56	3.14E-03	1.32	2.15E-02
CCDC86	1.48	3.20E-03	1.68	3.38E-02
HSPA2	1.39	3.42E-03	1.12	1.80E-02
HOXB6	1.25	3.44E-03	1.25	2.29E-02
LRP11	-1.30	3.56E-03	-1.27	4.80E-03
RETSAT	3.17	3.88E-03	1.96	1.50E-02
TTC9	1.28	4.01E-03	1.27	7.28E-04
ICMT	-1.44	4.06E-03	1.22	4.19E-02
FAM73B	1.26	4.41E-03	1.16	2.23E-02
ADAMTS1	1.39	4.84E-03	1.29	2.61E-02
SH3PXD2A	1.37	5.24E-03	1.67	2.22E-04
UHRF1BP1	1.31	5.25E-03	1.36	2.00E-02
BMP5	-1.57	5.78E-03	-1.56	2.01E-03
GPM6B	-1.36	6.06E-03	-1.23	1.68E-02
RAMP2	-1.44	6.32E-03	-1.29	4.06E-02
ITGB3	-1.30	6.38E-03	-1.27	1.93E-03
FOXN3	1.55	8.06E-03	1.45	1.80E-02
METRNL	1.26	8.10E-03	1.61	5.95E-03
PDGFRL	-1.36	8.15E-03	-1.29	2.91E-02
MAN2A1	1.23	8.48E-03	1.30	9.21E-04
TES	1.24	9.84E-03	1.18	3.34E-02

Annex 3 - Table S3 - Differentially expressed genes in the gluteus medius muscle of HIGH and LOW pigs (*P*-value ≤ 0.01 and fold-change ≥ 1.5).

Feature ID	Gene ID	Fold Change	q- value	*P*-value	LOW - Means	HIGH - Means
ENSSSCG00000005648	*SLC27A4*	1.66	4.28E-03	1.32E-06	1.03	1.71
ENSSSCG00000027946	*MVP*	1.78	5.97E-03	2.63E-06	14.75	26.30
ENSSSCG00000017232	*SLC9A3R1*	1.72	1.36E-02	1.26E-05	4.84	8.33
ENSSSCG00000003379	*KLHL21*	1.79	1.43E-02	1.61E-05	6.11	10.93
ENSSSCG00000005935	*AGO2*	1.59	1.43E-02	1.77E-05	3.34	5.32
ENSSSCG00000011740	*SERPINI1*	-1.81	1.72E-02	2.48E-05	0.34	
ENSSSCG00000001931	*GRAMD2*	-1.58	1.76E-02	2.74E-05	2.75	1.74
ENSSSCG00000007574	*SDK1*	1.58	1.76E-02	2.97E-05		0.24
ENSSSCG00000011444	*NT5DC2*	1.54	1.76E-02	3.26E-05	3.12	4.81
ENSSSCG00000007745	*SUMF2*	-1.54	1.95E-02	4.21E-05	7.38	4.80
ENSSSCG00000000293	*ITGA5*	1.72	1.96E-02	4.46E-05	4.56	7.82
ENSSSCG00000007133	*ACSS1*	1.51	2.09E-02	5.18E-05	7.25	10.96
ENSSSCG00000028814	*SOD3*	1.97	2.09E-02	5.37E-05	0.89	1.75
ENSSSCG00000006277	*SPIDR*	2.04	2.19E-02	5.90E-05	6.94	14.18
ENSSSCG00000007554	*ZFAND2A*	2.54	2.88E-02	1.01E-04	11.81	29.98
ENSSSCG00000003105	*SLC1A5*	1.67	3.07E-02	1.17E-04	3.21	5.37

ENSSSCG00000010529	*SFRP5*	2.03	3.11E-02	1.31E-04	1.98	4.02
ENSSSCG00000006245	*SDR16C5*	3.02	3.15E-02	1.36E-04	0.58	1.77
ENSSSCG00000013579	*CD209*	1.95	3.31E-02	1.50E-04	1.32	2.57
ENSSSCG00000008232	*RNF181*	-2.09	3.57E-02	2.05E-04	20.92	9.99
ENSSSCG00000030165	*MAFF*	1.67	3.72E-02	2.22E-04	12.50	20.89
ENSSSCG00000013303	*ABTB2*	1.95	5.05E-02	3.53E-04	0.38	0.74
ENSSSCG00000002824		1.93	5.21E-02	3.88E-04	1.10	2.12
ENSSSCG00000023044	*FASN*	2.06	5.21E-02	3.91E-04	11.85	24.45
ENSSSCG00000002826	*CES1*	2.03	5.56E-02	4.68E-04	1.14	2.31
ENSSSCG00000012051	*RUNX1*	1.99	5.63E-02	5.01E-04	4.16	8.27
ENSSSCG00000027426	*BCL3*	1.74	5.63E-02	5.17E-04	1.82	3.16
ENSSSCG00000030995	*PRAF2*	1.84	5.64E-02	5.34E-04	0.93	1.71
ENSSSCG00000011557	*CIDEC*	2.46	5.77E-02	5.64E-04	3.90	9.58
ENSSSCG00000010046	*GNAZ*	1.56	5.94E-02	6.05E-04	0.22	0.35
ENSSSCG00000010253	*HK1*	1.55	5.94E-02	6.37E-04	3.07	4.75
ENSSSCG00000013637	*QTRT1*	1.53	5.94E-02	6.37E-04	1.63	2.50
ENSSSCG00000003951	*C1orf210*	-1.66	5.94E-02	6.42E-04	0.27	
ENSSSCG00000029533	*SEMA4G*	1.52	6.12E-02	6.86E-04	0.44	0.67
ENSSSCG00000002825	*CES1*	2.41	6.17E-02	6.98E-04	1.24	2.98
ENSSSCG00000017403	*STAT3*	1.62	6.25E-02	7.20E-04	21.42	34.61
ENSSSCG00000017168	*SEPT9*	1.82	6.50E-02	7.99E-04	6.10	11.08
ENSSSCG00000027969	*AHNAK*	1.61	6.50E-02	8.03E-04	30.56	49.19
ENSSSCG00000012970	*CTSW*	-1.88	6.50E-02	8.13E-04	0.88	0.47
ENSSSCG00000007208	*TRIB3*	2.86	6.71E-02	8.69E-04	0.41	1.16
ENSSSCG00000011727	*PTX3*	7.92	6.79E-02	9.17E-04	1.74	13.76
ENSSSCG00000029944	*FASN*	2.00	6.79E-02	9.21E-04	5.04	10.07
ENSSSCG00000017767	*TLCD1*	1.71	7.21E-02	1.09E-03	0.62	1.07
ENSSSCG00000013292	*PRR5L*	1.69	7.68E-02	1.27E-03	0.43	0.72
ENSSSCG00000003458	*EFHD2*	1.57	7.68E-02	1.30E-03	6.73	10.58
ENSSSCG00000008121	*GPAT2*	-1.58	7.83E-02	1.34E-03	0.22	
ENSSSCG00000011451	*ITIH3*	1.90	8.39E-02	1.49E-03	1.48	2.82
ENSSSCG00000010974	*CNTFR*	1.57	8.39E-02	1.49E-03	10.27	16.08
ENSSSCG00000001844	*PLIN1*	2.23	8.78E-02	1.61E-03	4.15	9.24
ENSSSCG00000005465	*SUSD1*	-1.76	9.27E-02	1.88E-03	1.51	0.86
ENSSSCG00000022797	*PPP1R3B*	-1.56	9.60E-02	2.01E-03	14.82	9.48
ENSSSCG00000030018	*ZNF396*	-1.54	9.89E-02	2.10E-03		
ENSSSCG00000010926	*SYT2*	1.84	1.01E-01	2.16E-03		0.29
ENSSSCG00000016381	*SNED1*	1.75	1.02E-01	2.20E-03	0.64	1.12
ENSSSCG00000000362	*RDH5*	1.83	1.03E-01	2.28E-03	0.35	0.64
ENSSSCG00000013432	*MIDN*	1.52	1.07E-01	2.40E-03	13.43	20.36
ENSSSCG00000021143	*LIPC*	-1.52	1.10E-01	2.54E-03	0.57	0.37
ENSSSCG00000024982	*LITAF*	1.61	1.10E-01	2.57E-03	3.38	5.46
ENSSSCG00000024108	*SLC43A2*	1.51	1.12E-01	2.62E-03	40.71	61.60
ENSSSCG00000014012	*GFPT2*	1.75	1.14E-01	2.74E-03	1.39	2.43
ENSSSCG00000008985	*SOWAHB*	2.01	1.15E-01	2.88E-03	0.65	1.30
ENSSSCG00000022004	*SH3BP2*	1.62	1.16E-01	2.94E-03	0.77	1.25

ENSSSCG00000015089	*JAML*	-1.52	1.16E-01	2.96E-03	0.43	0.28
ENSSSCG00000008193	*ZAP70*	-1.89	1.20E-01	3.12E-03		
ENSSSCG00000023038		-3.22	1.23E-01	3.25E-03	1.49	0.46
ENSSSCG00000026832	*CSF1*	1.61	1.25E-01	3.34E-03	0.92	1.48
ENSSSCG00000015092	*CD3E*	-1.70	1.26E-01	3.46E-03	0.53	0.31
ENSSSCG00000000672	*CLSTN3*	1.58	1.26E-01	3.53E-03		
ENSSSCG00000028056	*ZFP36*	1.81	1.26E-01	3.59E-03	44.78	80.95
ENSSSCG00000017472	*IGFBP4*	1.65	1.27E-01	3.68E-03	4.81	7.91
ENSSSCG00000003699	*GREB1L*	-1.52	1.30E-01	3.78E-03	1.28	0.84
ENSSSCG00000027684	*TRIM63*	1.61	1.42E-01	4.57E-03	454.79	730.90
ENSSSCG00000015522	*ANGPTL1*	-1.83	1.46E-01	5.07E-03	0.88	0.48
ENSSSCG00000022492	*AMPD3*	3.27	1.50E-01	5.33E-03	8.24	26.95
ENSSSCG00000028568	*HSPB1*	1.61	1.54E-01	5.65E-03	470.31	757.67
ENSSSCG00000013263	*CREB3L1*	1.50	1.56E-01	5.91E-03	1.55	2.34
ENSSSCG00000024482	*HSPB1*	1.61	1.56E-01	5.95E-03	470.75	757.42
ENSSSCG00000011286	*KLHL40*	1.86	1.58E-01	6.10E-03	154.69	288.09
ENSSSCG00000018047	*FAM83G*	1.79	1.59E-01	6.19E-03	0.79	1.41
ENSSSCG00000008217	*CD8A*	-2.03	1.61E-01	6.42E-03	0.28	
ENSSSCG00000023176	*TROAP*	-1.56	1.62E-01	6.54E-03		
ENSSSCG00000013669	*PIN1*	-1.68	1.67E-01	6.92E-03	4.52	2.68
ENSSSCG00000011934	*PLCXD2*	1.76	1.69E-01	7.13E-03	1.01	1.77
ENSSSCG00000009314	*FLT3*	-1.79	1.72E-01	7.36E-03		
ENSSSCG00000012277	*TIMP1*	5.35	1.74E-01	7.64E-03	6.29	33.63
ENSSSCG00000000641	*KLRK1*	-2.07	1.74E-01	7.65E-03	0.63	0.31
ENSSSCG00000006416	*ACKR1*	1.59	1.75E-01	7.69E-03	5.11	8.13
ENSSSCG00000012844	*SLC25A22*	1.51	1.75E-01	7.91E-03	1.58	2.38
ENSSSCG00000013735	*JUNB*	1.72	1.80E-01	8.32E-03	22.87	39.30
ENSSSCG00000013144	*MPEG1*	-1.54	1.81E-01	8.47E-03	0.95	0.61
ENSSSCG00000021651	*SCN2B*	-1.95	1.83E-01	8.67E-03		
ENSSSCG00000030369	*KIAA1522*	1.55	1.84E-01	8.87E-03	0.31	0.48
ENSSSCG00000024344	*CCR5*	-1.82	1.86E-01	9.19E-03	0.40	0.22
ENSSSCG00000004092		1.58	1.86E-01	9.19E-03	0.30	0.48
ENSSSCG00000002866	*CEBPA*	1.64	1.86E-01	9.30E-03	0.71	1.17
ENSSSCG00000010479	*RBP4*	1.69	1.86E-01	9.42E-03	0.86	1.45

Annex 4 - Table S4 - Enriched pathways identified by IPA when using the data set of 96 differentially expressed genes (*P*-value ≤ 0.01 and fold-change ≥ 1.5). Ratio: number of DE genes in a pathway divided by the number of genes comprised in the same pathway.

Ingenuity Canonical Pathways	-log(*P*-value)	Ratio	Nodes
Acute Myeloid Leukemia Signaling	3.22	4/91	*CEBPA, FLT3, RUNX1, STAT3*
Hematopoiesis from Pluripotent Stem Cells	2.98	3/47	*CD3E, CD8E, CSF1*
Primary Immunodeficiency Signaling	2.96	3/48	*CD3E, CD8E, ZAP70*
Hepatic Fibrosis / Hepatic Stellate Cell Activation	2.12	4/183	*CCR5, CSF1, IGFBP4, TIMP1*
TR/RXR Activation	2.08	3/98	*BCL3, FASN, SYT2*
Palmitate Biosynthesis I (Animals)	2.07	1/2	*FASN*
Fatty Acid Biosynthesis Initiation II	2.07	1/2	*FASN*
CTLA4 Signaling in Cytotoxic T Lymphocytes	2.07	3/99	*CD3E, CD8A, ZAP70*
Retinoate Biosynthesis I	2.04	2/34	*RDH5, SDR16C5*
Stearate Biosynthesis I (Animals)	2.02	2/35	*FASN, SLC27A4*
T Cell Receptor Signaling	1.95	1/109	*CD3E, CD8A, ZAP70*
Retinol Biosynthesis	1.9	2/40	*CES1, LIPC*
Natural Killer Cell Signaling	1.82	2/122	*KLRK1, SH3BP2, ZAP70*
IL-9 Signaling	1.81	2/45	*BCL3, STAT3*
Triacylglycerol Degradation	1.81	2/45	*CES1, LIPC*
FXR/RXR Activation	1.78	3/126	*FASN, LIPC, RBP4*
Acetate Conversion to Acetyl-CoA	1.77	1/4	*ACSS1*
Phospholipase C Signaling	1.74	4/237	*AHNAK, CD3E, ITGA5, ZAP70*
Trehalose Degradation II (Trehalase)	1.68	1/5	*HK1*
UDP-N-acetyl-D-glucosamine Biosynthesis II	1.6	1/6	*GFPT2*
CNTF Signaling	1.53	2/63	*CNTFR, STAT3*
PCP pathway	1.53	2/63	*HSPB1, JUNB*
Calcium-induced T Lymphocyte Apoptosis	1.5	2/66	*CD3E, ZAP70*
Superoxide Radicals Degradation	1.47	1/8	*SOD8*
IL-10 Signaling	1.47	2/68	*CCR5, STAT3*
CCR5 Signaling in Macrophages	1.46	2/69	*CCR5, CD3E*
Acute Phase Response Signaling	1.46	3/169	*ITIH3, RBP4, STAT3*
Tec Kinase Signaling	1.45	3/170	*GNAZ, ITGA5, STAT3*
Pathogenesis of Multiple Sclerosis	1.43	1/9	*CCR5*
GDP-glucose Biosynthesis	1.42	1/9	*HK1*
Ephrin Receptor Signaling	1.42	3/174	*GNAZ, ITGA5, STAT3*
GM-CSF Signaling	1.42	2/73	*RUNX1, STAT3*

TREM1 Signaling	1.39	2/75	*ITGA5, STAT3*
Glucose and Glucose-1-phosphate Degradation	1.38	1/10	*HK1*
Role of Macrophages, Fibroblasts and Endothelial Cells in Rheumatoid Arthritis	1.37	4/309	*CEBPA, CSFA1, SFRP5, STAT3*
Role of NFAT in Regulation of the Immune Response	1.36	3/185	*CD3E, GNAZ, ZAP70*
Regulation of IL-2 Expression in Activated and Anergic T Lymphocytes	1.35	2/79	*CD3E, ZAP70*
UDP-N-acetyl-D-galactosamine Biosynthesis II	1.34	1/11	*HK1*
Growth Hormone Signaling	1.33	2/81	*CEBPA, STAT3*
Macropinocytosis Signaling	1.33	2/81	*CSF1, ITGA5*
RAR Activation	1.33	3/190	*RBP4, RDH5, SDR16C5*
NRF2-mediated Oxidative Stress Response	1.31	3/193	*JUNB, MAFF, SOD3*
Hematopoiesis from Multipotente Stem Cells	1.3	1/12	*CSF1, ITGA5*
FLT3 Signaling in Hematopoietic Progenitor Cells	1.3	2/85	*FLT3, STAT3*

Annex 5 - Table S5 - Pathways identified by Reactome as enriched in differentially expressed genes (*P*-value ≤ 0.01 and fold-change ≥ 1.5)

GeneSet	Ratio	P-value	Q-value	Nodes
Hematopoietic cell lineage(K)	5/87	3.50E-07	5.99E-05	*CD8A, FLT3, CD3E, CSF1, ITGA5*
Acute myeloid leukemia(K)	4/57	2.79E-06	2.37E-04	*CEBPA, FLT3, STAT3, RUNX1*
Primary immunodeficiency(K)	3/36	3.43E-05	1.96E-03	*CD8A, CD3E, ZAP70*
IL6-mediated signaling events(N)	3/47	7.55E-05	3.17E-03	*JUNB, STAT3, TIMP1*
TCR signaling in naive CD8+ T cells(N)	3/54	1.14E-04	3.86E-03	*CD8A, CD3E, ZAP70*
IL12-mediated signaling events(N)	3/61	1.63E-04	4.49E-03	*CD8A, CD3E, STAT3*
Downstream signaling in naive CD8+ T cells(N)	3/64	1.87E-04	4.49E-03	*CD8A, CD3E, JUNB*
TCR signaling in naive CD4+ T cells(N)	3/67	2.14E-04	4.49E-03	*CD3E, ZAP70, SH3BP2*
CXCR4-mediated signaling events(N)	3/80	3.59E-04	6.82E-03	*GNAZ, CD3E, STAT3*
T cell receptor signaling pathway(K)	3/104	7.68E-04	0.0131	*CD8A, CD3E, ZAP70*
TNF signaling pathway(K)	3/110	9.03E-04	0.0135	*CSF1, JUNB, BCL3*
IL12 signaling mediated by STAT4(N)	2/31	1.36E-03	0.0191	*CD3E, STAT3*
Signaling events mediated by TCPTP(N)	2/35	1.73E-03	0.022	*CSF1, STAT3*
IL23-mediated signaling events(N)	2/36	1.83E-03	0.022	*CD3E, STAT3*
Transcriptional misregulation in cancer(K)	3/179	3.61E-03	0.0376	*CEBPA, FLT3, RUNX1*
Signaling events mediated by PTP1B(N)	2/52	3.76E-03	0.0376	*CSF1, STAT3*
Pathways in cancer(K)	4/397	4.51E-03	0.0451	*CEBPA, FLT3, STAT3, RUNX1*
Costimulation by the CD28 family(R)	2/63	5.45E-03	0.0491	*CD3E, TRIB3*

AP-1 transcription factor network(N)	2/70	6.68E-03	0.0601	*JUNB, TIMP1*
T cell activation(P)	2/81	8.85E-03	0.0708	*CD3E, ZAP70*
HIF-1 signaling pathway(K)	2/103	0.014	0.0974	*STAT3, TIMP1*
S1P5 pathway(N)	1/8	0.014	0.0974	*GNAZ*
Insulin resistance(K)	2/109	0.0156	0.0974	*TRIB3, STAT3*
TCR signaling(R)	2/120	0.0186	0.0974	*CD3E, ZAP70*
lck and fyn tyrosine kinases in initiation of tcr activation(B)	1/11	0.0192	0.0974	*CD3E*
Osteoclast differentiation(K)	2/131	0.022	0.0974	*CSF1, JUNB*
Measles(K)	2/134	0.0229	0.0974	*CD3E, STAT3*
Natural killer cell mediated cytotoxicity(K)	2/134	0.0229	0.0974	*ZAP70, SH3BP2*
Atypical NF-kappaB pathway(N)	1/14	0.0244	0.0974	*BCL3*
Stress induction of hsp regulation(B)	1/14	0.0244	0.0974	*HSPB1*
Oxidative stress induced gene expression via nrf2(B)	1/14	0.0244	0.0974	*MAFF*
S1P4 pathway(N)	1/14	0.0244	0.0974	*GNAZ*
Downregulated of mta-3 in er-negative breast tumors(B)	1/18	0.0313	0.0974	*HSPB1*
Mets affect on macrophage differentiation(B)	1/18	0.0313	0.0974	*CSF1*
Gata3 participate in activating the th2 cytokine genes expression(B)	1/18	0.0313	0.0974	*JUNB*
S1P1 pathway(N)	1/19	0.033	0.0974	*GNAZ*
The co-stimulatory signal during t-cell activation(B)	1/20	0.0347	0.0974	*CD3E*
Sphingosine 1-phosphate (S1P) pathway(N)	1/21	0.0364	0.0974	*GNAZ*
p38 signaling mediated by MAPKAP kinases(N)	1/21	0.0364	0.0974	*HSPB1*
Growth hormone receptor signaling(R)	1/24	0.0415	0.0974	*STAT3*
Role of mef2d in t-cell apoptosis(B)	1/25	0.0432	0.0974	*CD3E*
S1P3 pathway(N)	1/25	0.0432	0.0974	*GNAZ*
Nongenotropic Androgen signaling(N)	1/25	0.0432	0.0974	*GNAZ*
VEGFR3 signaling in lymphatic endothelium(N)	1/25	0.0432	0.0974	*ITGA5*
S1P2 pathway(N)	1/26	0.0448	0.0974	*GNAZ*
IL27-mediated signaling events(N)	1/26	0.0448	0.0974	*STAT3*
Calcium signaling in the CD4+ TCR pathway(N)	1/27	0.0465	0.0974	*JUNB*
Epstein-Barr virus infection(K)	2/200	0.0477	0.0974	*STAT3, HSPB1*
Proteoglycans in cancer(K)	2/203	0.049	0.0974	*STAT3, ITGA5*
EGF receptor (ErbB1) signaling pathway(N)	1/29	0.0499	0.0974	*STAT3*

Annex 6 - Table S6: Regulatory networks of genes that are differentially expressed (P-value ≤ 0.01 and fold-change ≥ 1.5) in HIGH and LOW pigs

Top Diseases and Functions	Molecules DE in the Network	Score	Focus Molecules
Cardiovascular Disease, Cardiovascular System Development and Function, Organismal Injury and Abnormalities	*ANGTL1, BLC3, CD209, CREB3L1, CSF1, GFPT2, HK1, ITGA5, JUNB, KLHL21, MAFF, MPEG1, MVP, PIN1, SEPT9, SL9A3R1, TIMP1, TRIB3*	36	18
Hereditary Disorder, Immunological Disease, Organismal Injury and Abnormalities	*CD3E, CD8A, CES1, CIDEC, EFHD2, FASN, GNAZ, IGFBP4, KLRC4-KLRK1/KLRK1, LIPC, LITAF, PTX3, RBP4, SH3BP2, ZAP70*	31	15
Cell-To-Cell Signaling and Interaction, Small Molecule Biochemistry, Cell Death and Survival	*ABTB2, AMPD3, CLSTN3, FAM83G, GREB1L, QTRT1, RNF181, SDK1, SEMA4G, SLC43A2, SNED1, SYT2, ZNF396*	24	13
Cellular Development, Cellular Growth and Proliferation, Hematological System Development and Function	*CCR5, CNTFR, CTSW, FLT3, HSPB1, PRAF2, PRR5L, RUNX1, SOD3, STAT3, ZFAND2A, ZFP36*	22	12
Cell Cycle, Cell-To-Cell Signaling and Interation, Cellular Growth and Proliferation	*ACKR1, ACSS1, AHNAK, ITIH3, JAML, KIAA1522, KLHL40, PP1R3B, PTX3, SCN2B, SLC25A22, SPIDR*	22	12
Tissue Development, Hematological System Development and Function, Hematopoiesis	*AGO2, CEBPA, MIDN, RDH5, SERPINI1, SFRP5, SLC27A4, TRIMP63*	13	8
Cellular Function nd Maintenance, Inflammatory Responder, Organismal Injury and Abnormalities	*NT5DC2, SLC1A5, SUMF2, SUSD1, TROAP*	7	5
Behavior, Cancer, Cardiovascular Disease	*PLCXD2*	2	1
Lipids Metabolism, Small Molecule Biochemistry, Cancer	*GPAT2*	2	1
Developmental Disorder, Hereditary Disorder, Neurogical Disease	*TLCD1*	2	1
Connective Tissue Development and Function, Lymphoid Tissue Structure and Development, Skeletal and Muscular System Development and Function	*SDR16C5*	2	1

Annex 7 - Table S7 - Non-coding transcripts expressed in the gluteus medius muscle of HIGH and LOW pigs. (The complete table is included in the CD-Rom).

Feature ID	Gene ID	Size	FC	*P*-value	LOW - Means	HIGH - Means	Transcript type
ENSSSCG00000031004	*CH242-227G20.3*	1833	-1.44	2.46E-03	1879.03	1302.25	lincRNA
ENSSSCG00000031028	*CH242-15C8.2*	1495	-1.34	0.01	1987.17	1484.83	lincRNA
ENSSSCG00000015579	*PTGS2*	3601	-1.47	0.02	36.29	24.67	processed_transcript
ENSSSCG00000030904	*CU468594.10*	1083	-1.49	0.03	1058.89	711.39	non_coding
ENSSSCG00000001227	*TMP-SLA-3*	1767	-1.31	0.03	32900.06	25085.39	processed_transcript
ENSSSCG00000030767	*TMP-SLA-5*	1147	-1.29	0.03	10275.63	7958.96	processed_transcript
ENSSSCG00000015549	*RNASEL*	2716	-1.87	0.03	21.05	11.24	processed_transcript
ENSSSCG00000018090		70	-2.05	0.04	1850.59	900.54	Mt_tRNA
ENSSSCG00000001397	*TMP-CH242-74M17.4*	1726	-1.27	0.04	11706.02	9186.74	processed_transcript
ENSSSCG00000001227	*TMP-SLA-3*	1700	-1.30	0.04	3777.12	2906.70	processed_anscript
ENSSSCG00000004334	*MAP3K7*	2818	-1.72	0.04	326.60	189.72	processed_transcript
ENSSSCG00000015897	*IFIH1*	3720	-1.60	0.05	168.63	105.27	processed_transcript
ENSSSCG00000030790	*TMP-CH242-74M17.6*	309	-1.25	0.05	25040.66	20022.19	processed_transcript
ENSSSCG00000030936	*CH242-154K8.2*	392	-1.48	0.05	531.81	360.18	processed_transcript
ENSSSCG00000031041	*CU466547.1*	347	1.34	0.06	403.45	539.30	processed_transcript
ENSSSCG00000031015	*CH242-33O21.2*	2138	-1.27	0.06	1071.44	845.32	lincRNA
ENSSSCG00000030846	*CH242-358M12.6*	474	-1.17	0.06	6460.16	5501.10	antisense
ENSSSCG00000030923	*SBAB-554F3.8*	585	-1.26	0.07	321.55	254.22	processed_transcript
ENSSSCG00000030892	*CU302278.1*	431	-1.23	0.07	1228.62	1000.86	lincRNA
ENSSSCG00000031025	*CH242-236E18.2*	541	-1.44	0.09	100.90	70.23	lincRNA
ENSSSCG00000008841	*PDGFRA*	2859	-1.31	0.10	115.17	87.69	processed_transcript
ENSSSCG00000030844	*CH242-100L3.3*	766	-1.25	0.10	7239.06	5775.51	processed_transcript
ENSSSCG00000030916	*CH242-136A20.1*	1238	-1.26	0.10	588.78	467.07	lincRNA
ENSSSCG00000001727	*TNFRSF21*	3489	-1.36	0.10	638.39	469.72	processed_transcript
ENSSSCG00000001228	*TMP-CH242-74M17.5*	1303	-1.24	0.10	3941.47	3168.52	processed_transcript
ENSSSCG00000010709	*PLEKHG2*	3630	-1.63	0.11	22.40	13.73	processed_transcript
ENSSSCG00000024809	*CLCN4*	4337	-1.87	0.11	203.81	109.18	processed_transcript
ENSSSCG00000018079		67	-1.24	0.13	70343.42	56715.47	Mt_tRNA
ENSSSCG00000030758	*DEFB-104L*	564	-1.34	0.14	314.00	233.63	processed_transcript
ENSSSCG00000001227	*TMP-SLA-3*	1733	-1.79	0.15	256.54	143.69	processed_transcript
ENSSSCG00000030773	*CH242-77E21.3*	631	-1.29	0.17	941.24	728.98	non_coding

ENSSSCG00000026838	*IFN-ALPHA-8*	901	-1.47	0.18	173.66	117.95	processed_ transcript
ENSSSCG00000030935	*CU302278.4*	778	-1.13	0.18	25168.39	22345.07	lincRNA
ENSSSCG00000004334	*MAP3K7*	1740	-1.23	0.20	1302.05	1060.49	processed_ transcript
ENSSSCG00000030939	*CH242-124P4.2*	453	-1.13	0.20	13371.03	11795.44	processed_ transcript
ENSSSCG00000007280	*ITCH*	3517	-1.32	0.21	1707.52	1290.22	processed_ transcript
ENSSSCG00000004600	*CH242-58J12.2*	997	-1.41	0.21	54.20	38.55	processed_ transcript
ENSSSCG00000004943	*MAP2K1*	1423	-1.16	0.21	8488.64	7340.93	processed_ transcript
ENSSSCG00000001396	*SLA-8*	1305	-1.30	0.21	1614.73	1237.39	processed_ transcript
ENSSSCG00000018096		64	-1.65	0.22	5814.49	3514.84	Mt_tRNA
ENSSSCG00000020977	*SH3BGRL*	627	-1.17	0.24	1747.69	1498.53	processed_ transcript
ENSSSCG00000001241	*ZFP57*	1830	-1.58	0.25	138.01	87.60	processed_ transcript
ENSSSCG00000020977	*SH3BGRL*	352	-1.74	0.26	464.66	266.61	processed_ transcript
ENSSSCG00000020462	*SCARNA13*	276	-1.36	0.28	248.38	182.28	snoRNA
ENSSSCG00000030436		96	-1.12	0.29	26464.63	23683.55	miRNA
ENSSSCG00000030729	*CU468856.1*	208	-1.04	0.30	2320.51	2230.78	lincRNA
ENSSSCG00000004600	*CH242-58J12.2*	5982	-1.15	0.31	1436.90	1246.19	processed_ transcript
ENSSSCG00000004334	*MAP3K7*	2737	-1.23	0.32	451.30	367.78	processed_ transcript
ENSSSCG00000010709	*PLEKHG2*	4268	-1.25	0.32	186.19	148.76	processed_ transcript
ENSSSCG00000026919	*snoU89*	255	1.19	0.34	351.63	418.10	snoRNA
ENSSSCG00000004334	*MAP3K7*	1821	-1.53	0.34	140.72	91.91	processed_ transcript
ENSSSCG00000003617	*TXLNA*	1367	1.45	0.34	437.52	634.85	processed_ transcript
ENSSSCG00000012298	*CACNA1F*	6038	-1.13	0.35	2486.42	2205.10	processed_ transcript
ENSSSCG00000010709	*PLEKHG2*	4062	-1.39	0.35	18.64	13.38	processed_ transcript
ENSSSCG00000030871	*CU582909.1*	1382	-1.04	0.36	91730.05	88401.20	processed_ transcript

Annex 8 - Table S8: HIGH and LOW group mean values ± standard deviation (SD) for 13 lipid-related traits

	HIGH group (N=28)		LOW group (N=28)	
	Mean	**SD**	**Mean**	**SD**
Carcass traits				
LW - Live weight (Kg)	131.21	9.45	115.5	16.63
BFTiv - Backfat thickness (in vivo) (mm)	27.05	2.41	21.07	2.98
BFT - Backfat thickness 3rd-4th ribs (mm)	46.18	12.14	35.15	10.7
HFT - Ham fat thickness (mm)	29.09	3.37	20.02	3.67
LEAN - Lean %	39.56	5.35	45.5	3.83
Meat quality traits (*gluteus medius*)				
IMF - % Intramuscular fat	7.21	1.71	3.76	0.95
SFA - % Saturated fatty acids	38.72	1.31	34.65	1.13
PUFA - % Polyunsaturated fatty acids	14.61	2.98	27.75	4.06
MUFA - % Monounsaturated fatty acids	46.67	2.66	37.61	3.97
Serum lipid levels - 190 days				
CHOL - Total cholesterol (mg/dl)	167.25	37.23	103.18	16.68
HDL - HDL-cholesterol (mg/dl)	60.43	8.55	44.12	9.12
LDL - LDL-cholesterol (mg/dl)	92.69	36.82	48.95	15.03
TG - Triacylglycerides (mg/dl	70.54	26.06	48.3	27.74

Annex 9 - Supplementary Figure S1. Venn diagram indicating the overlap between the set of differentially expressed genes (P-value ≤ 0.05) detected in the current work (RNA-Seq) and those identified by Cánovas et al.

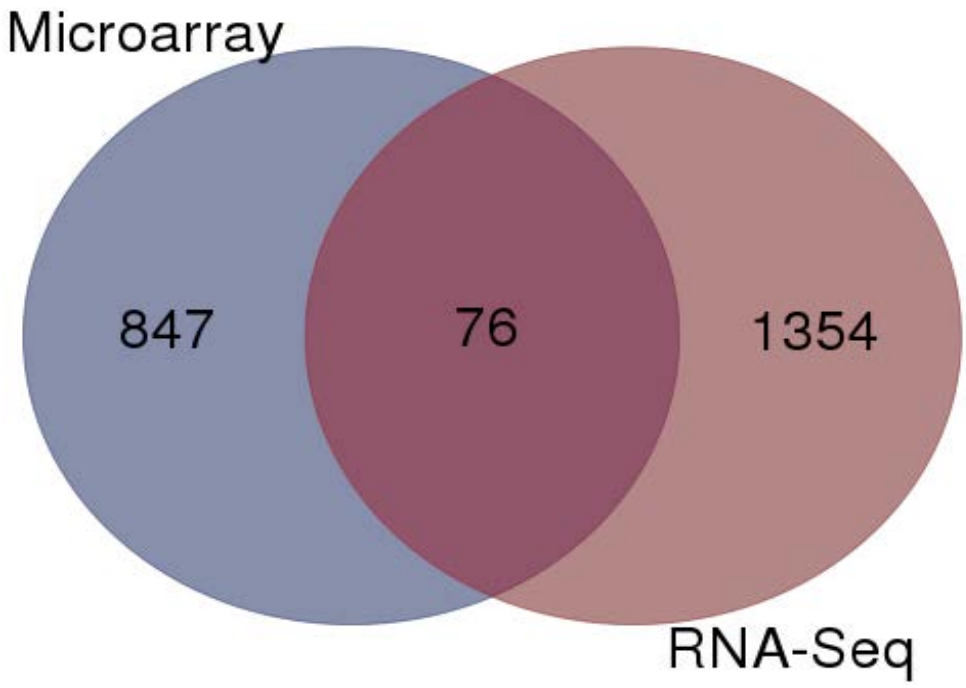

Supplemental material Paper II: "Differential expression of mRNA isoforms in the skeletal muscle of pigs with distinct growth and fatness profiles "

Annex 10 - Table S1: Distribution of the 56 animals sequenced by RNA-Seq in the 5 half-sib families reported by Gallardo et al. (2008).

Sire	Sequenced offspring - HIGH group	Sequenced offspring - LOW group
BL12441	5	8
BL12445	2	7
BR112290	14	6
BR18035	6	6
BR22311	1	1

Annex 11 - Table S2. Primers employed in the validation of four differentially expressed mRNA isoforms by RT-qPCR.

Primer	Sequence 5' to 3'
PIG_ITGA5-001_F_E22	AGTGGCCTTCGGTTCACAGT
PIG_ITGA5-001_R_E22/E23	GAGATTCTTGCTGAGGATTTGGA
PIG_MAFF-001_F_E2	CGGGAGGGCACCTTTTG
PIG_MAFF-001_R_E2/E3	GCTCGCGCTTGATCTTCAG
PIG_RXRG-002_F_E1	TGGGAAACATGCTCCTTCTGT
PIG_RXRG-002_R_E1/E2	GGTTTGATGTCCTCTGAAATGCT
PIG_SCD-001_F_E5	GCCCTTATGACAAGACTATTAGCCC
PIG_SCD-001_R_E6	AAGGTGTGGTGGTAGTTGTGGAA
PIG_TBP_F	CAGAATGATCAAACCGAGAATTGT
PIG_TBP_RV	CTGCTCTGACTTTAGCACCTGTTAA
PIG_HPRT1_F	TCATTATGCCGAGGATTTGGA
PIG_HPRT1_RV	CTCTTTCATCACATCTCGAGCAA
PIG_ACTB_F	CAAGGACCTCTACGCCAACAC
PIG_ACTB_RV	TGGAGGCGCGATGATCTT

Annex 12 - Table S3: Alternatively spliced mRNA isoforms identified in the porcine gluteus medius muscle of Duroc pigs by CLC Bio and/or STAR/RSEM/DESEq2. (The complete table is included in the CD-Rom).

Feature ID	Feature transcript ID	Gene ID	Transcript ID	Length (bp)	Relative expression CLC Bio(%)	Relative expression STAR/RSEM/DESeq2 (%)	Type
ENSSSCG00000000031	ENSSSCT00000034350	*MCAT*	*MCAT-202*	1119	2.84	0.56	Protein Coding
ENSSSCG00000000031	ENSSSCT00000035501	*MCAT*	*MCAT-203*	850	12.73	8.40	Nonsense mediated decay
ENSSSCG00000000031	ENSSSCT00000000033	*MCAT*	*MCAT-201*	1396	84.42	90.75	Protein Coding
ENSSSCG00000000031	ENSSSCT00000033405	*MCAT*	*MCAT-205*	679	-	0.29	Retained intron
ENSSSCG00000000058	ENSSSCT00000023171	*SNU13*	*SNU13-202*	1476	13.12	11.60	Protein Coding
ENSSSCG00000000058	ENSSSCT00000000064	*SNU13*	*SNU13-201*	1460	86.88	88.40	Protein Coding
ENSSSCG00000000068	ENSSSCT00000000074	*EP300*	*EP300-202*	8181	0.67	-	Protein Coding
ENSSSCG00000000068	ENSSSCT00000026332	*EP300*	*EP300-201*	8364	99.33	100.00	Protein Coding
ENSSSCG00000000076	ENSSSCT00000031184	*SGSM3*	*SGSM3-201*	2568	6.44	0.17	Protein Coding
ENSSSCG00000000076	ENSSSCT00000000082	*SGSM3*	*SGSM3-202*	2562	93.56	99.83	Protein Coding
ENSSSCG00000000087	ENSSSCT00000000093	*TAB1*	*TAB1-201*	2006	0.58	0.18	Protein Coding
ENSSSCG00000000087	ENSSSCT00000035948	*TAB1*	*TAB1-001*	2433	99.42	87.23	Protein Coding
ENSSSCG00000000087	ENSSSCT00000033099	*TAB1*	*TAB1-002*	591	-	12.59	Retained intron
ENSSSCG00000000095	ENSSSCT00000029543	*GTPBP1*	*GTPBP1-201*	3510	3.22	-	Protein Coding
ENSSSCG00000000095	ENSSSCT00000000101	*GTPBP1*	*GTPBP1-202*	3486	96.78	100.00	Protein Coding
ENSSSCG00000000107	ENSSSCT00000022980	*CSNK1E*	-	1595	7.78	12.70	Protein Coding
ENSSSCG00000000107	ENSSSCT00000000113	*CSNK1E*	-	2686	92.22	87.30	Protein Coding
ENSSSCG00000000110	ENSSSCT00000000116	*PLA2G6*	*PLA2G6-201*	2695	8.09	-	Protein Coding
ENSSSCG00000000110	ENSSSCT00000022302	*PLA2G6*	*PLA2G6-202*	2524	91.91	100.00	Protein Coding
ENSSSCG00000000137	ENSSSCT00000034941	*NCF4*	*NCF4-202*	1429	23.69	94.31	Protein Coding
ENSSSCG00000000137	ENSSSCT00000036476	*NCF4*	*NCF4-201*	1569	29.56	5.69	Protein Coding
ENSSSCG00000000137	ENSSSCT00000000143	*NCF4*	*NCF4-203*	5020	46.75	-	Protein Coding
ENSSSCG00000000138	ENSSSCT00000000144	*PVALB*	*PVALB-203*	558	0.57	5.43	Protein Coding
ENSSSCG00000000138	ENSSSCT00000032626	*PVALB*	*PVALB-202*	599	0.58	0.44	Protein Coding

ENSSSCG00000000138	ENSSSCT00000035876	*PVALB*	*PVALB-201*	585	98.85	94.13	Protein Coding
ENSSSCG00000000157	ENSSSCT00000000165	*BPIFC*	*BPIFC-202*	2004	46.45	-	Protein Coding
ENSSSCG00000000157	ENSSSCT00000036153	*BPIFC*	*BPIFC-201*	2168	53.55	-	Protein Coding
ENSSSCG00000000191	ENSSSCT00000000204	*KMT2D*	*KMT2D-202*	18097	9.44	-	Protein Coding
ENSSSCG00000000191	ENSSSCT00000031953	*KMT2D*	*KMT2D-201*	18199	90.56	100.00	Protein Coding
ENSSSCG00000000232	ENSSSCT00000000251	*ACVRL1*	*ACVRL1-203*	3787	26.21	59.75	Protein Coding
ENSSSCG00000000232	ENSSSCT00000033395	*ACVRL1*	*ACVRL1-201*	4044	73.79	19.96	Protein Coding
ENSSSCG00000000232	ENSSSCT00000036596	*ACVRL1*	*ACVRL1-202*	764	-	20.29	Processed transcript
ENSSSCG00000000242	ENSSSCT00000000261	*CH242-185F9.2*	*CH242-185F9.2-201*	346	5.77	14.19	Protein Coding
ENSSSCG00000000242	ENSSSCT00000033904	*CH242-185F9.2*	*CH242-185F9.2-001*	944	94.23	85.81	Protein Coding
ENSSSCG00000000275	ENSSSCT00000000295	*MAP3K12*	*MAP3K12-202*	2580	30.21	67.39	Protein Coding
ENSSSCG00000000275	ENSSSCT00000024918	*MAP3K12*	*MAP3K12-201*	2983	69.79	32.61	Protein Coding
ENSSSCG00000000278	ENSSSCT00000023450	*ATF7*	*ATF7-201*	1652	4.34	0.40	Protein Coding
ENSSSCG00000000278	ENSSSCT00000000299	*ATF7*	*ATF7-202*	1619	95.66	99.60	Protein Coding
ENSSSCG00000000293	ENSSSCT00000035821	*ITGA5*	*ITGA5-203*	1255	0.34	-	Nonsense mediated decay
ENSSSCG00000000293	ENSSSCT00000033141	*ITGA5*	*ITGA5-205*	766	0.59	0.36	Nonsense mediated decay
ENSSSCG00000000293	ENSSSCT00000034427	*ITGA5*	*ITGA5-204*	1013	0.71	-	Nonsense mediated decay
ENSSSCG00000000293	ENSSSCT00000000314	*ITGA5*	*ITGA5-201*	4445	98.36	99.64	Protein Coding
ENSSSCG00000000361	ENSSSCT00000032827	*CD63*	*CD63-204*	679	0.40	-	Protein Coding
ENSSSCG00000000361	ENSSSCT00000032682	*CD63*	*CD63-207*	597	0.74	21.91	Protein Coding
ENSSSCG00000000361	ENSSSCT00000035463	*CD63*	*CD63-209*	461	0.91	1.94	Protein Coding
ENSSSCG00000000361	ENSSSCT00000000383	*CD63*	*CD63-201*	901	5.36	49.05	Protein Coding
ENSSSCG00000000361	ENSSSCT00000033233	*CD63*	*CD63-202*	1370	92.60	1.61	Protein Coding
ENSSSCG00000000361	ENSSSCT00000036432	*CD63*	*CD63-211*	437	-	0.19	Retained intron
ENSSSCG00000000361	ENSSSCT00000034338	*CD63*	*CD63-203*	390	-	0.23	Retained intron
ENSSSCG00000000361	ENSSSCT00000036425	*CD63*	*CD63-205*	544	-	0.29	Retained intron

ENSSSCG00000000361	ENSSSCT00000036614	*CD63*	*CD63-206*	310	-	0.37	Retained intron
ENSSSCG00000000361	ENSSSCT00000035947	*CD63*	*CD63-208*	691	-	0.73	Retained intron
ENSSSCG00000000361	ENSSSCT00000034881	*CD63*	*CD63-210*	394	-	23.67	Processed transcript
ENSSSCG00000000403	ENSSSCT00000032195	*BAZ2A*	*BAZ2A-202*	8208	6.08	7.57	Protein Coding
ENSSSCG00000000403	ENSSSCT00000000436	*BAZ2A*	*BAZ2A-201*	8727	93.92	92.43	Protein Coding
ENSSSCG00000000405	ENSSSCT00000033906	*ATP5B*	*ATP5B-201*	1565	0.62	1.88	Protein Coding
ENSSSCG00000000405	ENSSSCT00000000438	*ATP5B*	*ATP5B-202*	1767	99.38	98.12	Protein Coding
ENSSSCG00000000444	ENSSSCT00000000464	*DCTN2*	-	1411	0.68	-	Protein Coding
ENSSSCG00000000444	ENSSSCT00000000479	*DCTN2*	-	1384	99.32	100.00	Protein Coding
ENSSSCG00000000462	ENSSSCT00000034992	*TMEM5*	*TMEM5-201*	450	2.18	6.12	Protein Coding
ENSSSCG00000000462	ENSSSCT00000000500	*TMEM5*	*TMEM5-202*	1632	97.82	93.88	Protein Coding
ENSSSCG00000000464	ENSSSCT00000000502	*C12orf56*	*C12orf56-202*	1638	44.40	-	Protein Coding
ENSSSCG00000000464	ENSSSCT00000030713	*C12orf56*	*C12orf56-201*	1644	55.60	-	Protein Coding
ENSSSCG00000000472	ENSSSCT00000000510	*LLPH*	*LLPH-202*	581	0.88	43.38	Protein Coding
ENSSSCG00000000472	ENSSSCT00000025545	*LLPH*	*LLPH-201*	1621	99.12	56.62	Protein Coding
ENSSSCG00000000475	ENSSSCT00000032082	*IRAK3*	*IRAK3-202*	490	11.10	-	Protein Coding
ENSSSCG00000000475	ENSSSCT00000031580	*IRAK3*	*IRAK3-203*	256	13.93	86.13	Protein Coding
ENSSSCG00000000475	ENSSSCT00000000513	*IRAK3*	*IRAK3-204*	948	33.53	13.87	Protein Coding
ENSSSCG00000000475	ENSSSCT00000035165	*IRAK3*	*IRAK3-201*	2155	41.45	-	Protein Coding
ENSSSCG00000000478	ENSSSCT00000033391	*GRIP1*	*GRIP1-201*	2174	44.04	-	Protein Coding
ENSSSCG00000000478	ENSSSCT00000000516	*GRIP1*	*GRIP1-202*	3408	55.96	-	Protein Coding
ENSSSCG00000000492	ENSSSCT00000033585	*LYZ*	*LYZ-003*	762	3.52	1.63	Protein Coding
ENSSSCG00000000492	ENSSSCT00000034939	*LYZ*	*LYZ-002*	858	5.33	3.16	Protein Coding
ENSSSCG00000000492	ENSSSCT00000000530	*LYZ*	*LYZ-001*	1287	91.15	95.21	Protein Coding

Annex 13 - Table S4. Classification of alternative splicing (AS) events detected in the porcine gluteus medius muscle with the SUPPA and Splicing Express softwares.

SUPPA software				
Event type	**Genes**	**Total Events**	**Events / Gene**	**% total**
Exon Skipping	3907	7651	1.96	36.75
Alternative 3' Splice Site	2692	4344	1.61	20.86
Alternative 5' Splice Site	3284	6279	1.91	30.16
Intron Retention	1490	2547	1.71	12.23
Splicing Express software				
Event type	**Genes**	**Total Events**	**Events / Gene**	**% total**
Exon Skipping	2624	14543	5.54	41.02
Alternative 3' Splice Site	2386	8656	3.63	24.41
Alternative 5' Splice Site	2286	7756	3.36	21.87
Intron Retention	1745	4502	2.58	12.70

Annex 14 - Table S5: Differentially expressed (P-value < 0.05) mRNA isoforms (HIGH vs LOW pigs) found with CLC Bio and STAR/RSEM/DESeq2 softwares (those identified by both pipelines are shown in bold). (The complete table is included in the CD-Rom).

Feature ID	Feature transcript ID	Gene ID	Transcript ID	Length (bp)	Type	CLC Bio				STAR/RSEM/DESeq2			
						log2(FC)	*P*-value	q-value	Relative expression (%)	log2 (FC)	*P*-value	q-value*	Relative expression (%)
ENSSSCG00000016893	**ENSSSCT00000018398**	***NDUFS4***	-	567	Protein Coding	-0.22	1.55E-05	2.07E-02	99.85	-0.29	9.49E-08	1.25E-04	99.51
ENSSSCG00000010313	**ENSSSCT00000011289**	***VCL***	***VCL-201***	5378	Protein Coding	-0.49	2.33E-07	1.25E-03	52.73	-0.63	1.18E-07	1.25E-04	37.61
ENSSSCG00000000293	**ENSSSCT00000000314**	***ITGA5***	***ITGA5-201***	4445	Protein Coding	0.85	2.64E-05	2.56E-02	98.36	0.85	2.54E-06	1.21E-03	99.64
ENSSSCG00000004578	**ENSSSCT00000005057**	***ANXA2***	***ANXA2-202***	1455	Protein Coding	0.70	3.32E-06	6.56E-03	98.90	0.69	4.56E-06	1.58E-03	99.82
ENSSSCG00000012440	**ENSSSCT00000032952**	***PGK1***	***PGK1-005***	401	Protein Coding	-0.24	5.55E-04	1.33E-01	12.77	-0.51	4.61E-06	1.58E-03	3.82
ENSSSCG00000006549	**ENSSSCT00000036394**	***IL6R***	***IL6R-001***	460	Protein Coding	1.25	1.89E-02	9.33E-01	71.98	1.41	6.89E-06	NA	83.85
ENSSSCG00000012440	**ENSSSCT00000034653**	***PGK1***	***PGK1-001***	1561	Protein Coding	-0.26	8.53E-03	6.29E-01	3.39	-0.30	1.78E-05	2.75E-03	89.72
ENSSSCG00000013579	**ENSSSCT00000014831**	***CD209***	***CD209-001***	1042	Protein Coding	1.03	7.84E-05	4.18E-02	93.21	1.01	2.09E-05	NA	97.00
ENSSSCG00000012448	**ENSSSCT00000033853**	***ITM2A***	***ITM2A-201***	1626	Protein Coding	-0.45	2.43E-04	8.65E-02	76.96	-0.55	3.16E-05	4.24E-03	68.73
ENSSSCG00000009584	**ENSSSCT00000034286**	***SEMA4D***	***SEMA4D-208***	487	Protein Coding	1.40	2.75E-06	6.53E-03	7.90	1.09	5.87E-05	6.59E-03	9.25
ENSSSCG00000006328	**ENSSSCT00000033501**	***RXRG***	***RXRG-202***	544	Protein Coding	-0.70	4.09E-04	1.18E-01	14.61	-0.76	9.31E-05	8.98E-03	20.75
ENSSSCG00000030970	**ENSSSCT00000035366**	***COX7B***	***COX7B-001***	439	Protein Coding	-0.23	5.46E-04	1.33E-01	87.12	-0.29	1.07E-04	9.61E-03	96.53
ENSSSCG00000024982	**ENSSSCT00000036552**	***LITAF***	***LITAF-201***	2190	Protein Coding	1.01	1.02E-04	4.38E-02	78.56	0.79	1.21E-04	1.04E-02	98.33
ENSSSCG00000010184	**ENSSSCT00000011150**	***AGT***	-	2242	Protein Coding	0.57	3.74E-04	1.09E-01	98.48	0.65	1.32E-04	1.08E-02	25.49
ENSSSCG00000013242	**ENSSSCT00000014462**	***ACP2***	***ACP2-001***	2107	Protein Coding	0.52	1.69E-03	2.56E-01	79.46	0.46	1.62E-04	1.28E-02	88.07
ENSSSCG00000012277	**ENSSSCT00000013426**	***TIMP1***	***TIMP1-001***	931	Protein Coding	2.57	4.61E-07	1.68E-03	98.97	0.79	2.01E-04	1.32E-02	96.74
ENSSSCG00000006610	**ENSSSCT00000035044**	***S100A11***	***S100A11-001***	546	Protein Coding	0.55	1.46E-03	2.36E-01	70.33	0.63	2.04E-04	1.33E-02	85.52
ENSSSCG00000015310	**ENSSSCT00000023446**	***AKAP9***	***AKAP9-202***	13006	Protein Coding	-0.34	1.77E-02	9.09E-01	55.41	-0.55	2.15E-04	1.36E-02	63.58
ENSSSCG00000026914	**ENSSSCT00000035582**	***PLA2G16***	***PLA2G16-201***	800	Protein Coding	0.36	4.57E-02	1.00E+00	63.04	0.32	3.67E-04	1.89E-02	78.13

ENSSSCG00000017983	**ENSSSCT00000032848**	***PER1***	***PER1-201***	4590	Protein Coding	0.43	2.76E-03	3.57E-01	76.76	0.42	5.13E-04	2.40E-02	77.16
ENSSSCG00000001252	**ENSSSCT00000001367**	***UBD***	***UBD-201***	1281	Protein Coding	-0.72	1.37E-03	2.29E-01	96.35	-0.83	7.73E-04	NA	55.28
ENSSSCG00000006612	**ENSSSCT00000007246**	***S100A10***	***S100A10-201***	1512	Protein Coding	0.57	1.22E-03	2.23E-01	88.28	0.51	8.47E-04	3.31E-02	26.43
ENSSSCG00000010107	**ENSSSCT00000011068**	***MED15***	***MED15-201***	2913	Protein Coding	0.37	5.83E-03	4.97E-01	98.60	0.30	1.19E-03	3.92E-02	99.89
ENSSSCG00000000657	**ENSSSCT00000034328**	***CLEC2D***	***CLEC2D-002***	1688	Protein Coding	-0.48	3.28E-02	1.00E+00	43.46	-0.70	1.24E-03	NA	51.21
ENSSSCG00000012345	**ENSSSCT00000033201**	***PFKFB1***	***PFKFB1-203***	471	Protein Coding	-0.33	3.11E-03	3.75E-01	25.63	-0.37	1.49E-03	4.47E-02	25.98
ENSSSCG00000000657	**ENSSSCT00000033596**	***CLEC2D***	***CLEC2D-001***	1673	Protein Coding	-0.57	7.04E-03	5.52E-01	56.30	-0.70	1.54E-03	NA	47.76
ENSSSCG00000014013	**ENSSSCT00000034792**	***RNF130***	-	650	Protein Coding	-0.16	2.96E-02	1.00E+00	14.03	-0.28	1.65E-03	4.79E-02	11.31
ENSSSCG00000012133	**ENSSSCT00000032369**	***ASB11***	***ASB11-001***	1464	Protein Coding	-0.14	3.98E-02	1.00E+00	81.39	-0.24	1.67E-03	4.81E-02	67.35
ENSSSCG00000011848	**ENSSSCT00000012960**	***TFRC***	***TFRC-201***	5030	Protein Coding	-0.55	1.29E-03	2.24E-01	50.32	-0.79	1.83E-03	5.02E-02	49.80
ENSSSCG00000012411	**ENSSSCT00000025272**	***PHKA1***	-	5491	Protein Coding	-0.21	2.21E-03	3.05E-01	89.03	-0.27	1.98E-03	5.28E-02	98.63
ENSSSCG00000001398	**ENSSSCT00000001327**	***SLA-6***	***SLA-6-201***	1153	Protein Coding	-0.53	1.29E-02	7.67E-01	59.78	-0.85	2.19E-03	NA	36.38
ENSSSCG00000001468	**ENSSSCT00000032605**	***PSMB9***	***PSMB9-001***	959	Protein Coding	-0.63	4.04E-02	1.00E+00	74.08	-0.91	2.25E-03	NA	86.41
ENSSSCG00000029471	**ENSSSCT00000032244**	***STAC3***	***STAC3-202***	1629	Protein Coding	-0.12	3.93E-02	1.00E+00	99.94	-0.21	2.28E-03	5.69E-02	99.94
ENSSSCG00000014920	**ENSSSCT00000033976**	***FZD4***	***FZD4-201***	6963	Protein Coding	0.38	2.98E-02	1.00E+00	99.58	0.41	2.54E-03	6.09E-02	99.68
ENSSSCG00000012653	**ENSSSCT00000013834**	***ZDHHC9***	***ZDHHC9-209***	2967	Protein Coding	0.78	3.29E-03	3.75E-01	17.33	0.77	2.56E-03	6.11E-02	18.26
ENSSSCG00000004687	**ENSSSCT00000005176**	***B2M***	-	1197	Protein Coding	-0.32	1.13E-03	2.11E-01	49.95	-0.35	2.92E-03	6.61E-02	49.59
ENSSSCG00000016186	**ENSSSCT00000026123**	***TMBIM1***	-	2030	Protein Coding	0.44	4.91E-04	1.25E-01	73.00	0.38	2.97E-03	6.65E-02	56.74
ENSSSCG00000012591	**ENSSSCT00000033097**	***AMOT***	***AMOT-201***	6928	Protein Coding	-0.15	2.38E-02	1.00E+00	73.57	-0.38	3.23E-03	7.00E-02	15.48

Annex 15 - Table S6: Relative transcript levels of a set of isoforms corresponding to five genes expressed in the gluteus medius muscle of HIGH and LOW pigs identified with the CLC Bio and STAR/RSEM/DESeq2 pipelines (those showing differential expression are indicated in bold, q-value < 0.05,|log2(fold-change)| > 0.6).

Feature transcript ID	Gene ID	Transcript ID	Length (bp)	Type	CLC Bio				STAR/RSEM/DESeq2			
					log2 (FC)	*P*-value	q-value	Relative expres-sion (%)	log2 (FC)	*P*-value	q-value*	Relative expres-sion (%)
ENSSSCT00000034155	*ANXA2*	*ANXA2-201*	1609	Protein coding	0.22	6.77E-01	1.00E+00	1.1	0.07	9.20E-01	NA	0.18
ENSSSCT00000005057	***ANXA2***	***ANXA2-202***	**1455**	**Protein coding**	0.7	**3.32E-06**	**7.23E-03**	**98.9**	0.69	4.56E-06	1.58E-03	99.82
ENSSSCT00000000314	***ITGA5***	***ITGA5-201***	**4445**	**Protein coding**	0.85	**2.64E-05**	**2.82E-02**	**98.36**	0.85	2.54E-06	1.21E-03	99.64
ENSSSCT00000035821	*ITGA5*	*ITGA5-203*	1255	Nonsense mediated decay	-0.03	9.18E-01	1.00E+00	0.34	-	-	-	0.34
ENSSSCT00000034427	*ITGA5*	*ITGA5-204*	1013	Nonsense mediated decay	-0.08	1.00E+00	1.00E+00	0.71	-	-	-	0.71
ENSSSCT00000033141	*ITGA5*	*ITGA5-205*	766	Nonsense mediated decay	-0.29	1.00E+00	1.00E+00	0.59	-0.01	9.97E-01	NA	0.36
ENSSSCT00000036552	***LITAF***	***LITAF-201***	**2190**	**Protein coding**	1.01	**1.02E-04**	**4.82E-02**	**78.56**	0.79	1.21E-04	1.04E-02	98.33
ENSSSCT00000025103	*LITAF*	*LITAF-202*	2370	Protein coding	-0.04	1.00E+00	1.00E+00	21.44	0.49	7.52E-01	NA	1.67
ENSSSCT00000033039	*SEMA4D*	*SEMA4D-201*	3625	Protein coding	0.33	3.22E-02	1.00E+00	67.7	0.24	3.94E-02	2.75E-01	58.28
ENSSSCT00000033344	*SEMA4D*	*SEMA4D-202*	2108	Protein coding	-0.29	1.00E+00	1.00E+00	0.06	-	-	-	0.06
ENSSSCT00000033105	*SEMA4D*	*SEMA4D-203*	4704	Protein coding	0.86	1.72E-02	9.86E-01	3.28	-0.21	8.34E-01	NA	0.29
ENSSSCT00000034118	*SEMA4D*	*SEMA4D-204*	594	Protein coding	0.71	1.53E-01	1.00E+00	1.7	-	-	-	1.7
ENSSSCT00000034311	*SEMA4D*	*SEMA4D-205*	823	Protein coding	0.21	2.40E-01	1.00E+00	16.3	0.24	9.34E-02	4.14E-01	23.88
ENSSSCT00000033153	*SEMA4D*	*SEMA4D-206*	794	Protein coding	0.42	8.00E-01	1.00E+00	0.3	0.77	6.15E-01	NA	0.15
ENSSSCT00000036138	*SEMA4D*	*SEMA4D-207*	1178	Protein coding	0.27	1.00E+00	1.00E+00	0.17	-0.11	9.70E-01	NA	0.02
ENSSSCT00000034286	***SEMA4D***	***SEMA4D-208***	**487**	**Protein coding**	1.4	**2.75E-06**	**7.19E-03**	**7.9**	1.09	5.87E-05	6.59E-03	9.25
ENSSSCT00000010505	*SEMA4D*	*SEMA4D-209*	4409	Protein coding	0.64	1.29E-01	1.00E+00	2.59	0.65	1.94E-03	5.25E-02	8.13
ENSSSCT00000013426	***TIMP1***	***TIMP1-001***	**931**	**Protein coding**	2.57	**4.61E-07**	**1.85E-03**	**98.97**	0.79	2.01E-04	1.32E-02	96.74
ENSSSCT00000033796	*TIMP1*	*TIMP1-002*	598	Protein coding	1.12	5.56E-01	1.00E+00	0.48	0.38	8.98E-01	NA	0.27
ENSSSCT00000034602	*TIMP1*	*TIMP1-003*	641	Protein coding	1.19	8.47E-01	1.00E+00	0.34	-0.19	7.39E-01	NA	2.81
ENSSSCT00000036308	*TIMP1*	*TIMP1-004*	173	Protein coding	3.05	4.21E-01	1.00E+00	0.21	0.18	9.52E-01	NA	0.18

Annex 16 - Figure S1. Validation by RT-qPCR of the differential expression of mRNA isoforms corresponding to the *RXRG*, *SCD*, *MAFF* and *ITGA5* genes in HIGH *vs* LOW pigs.

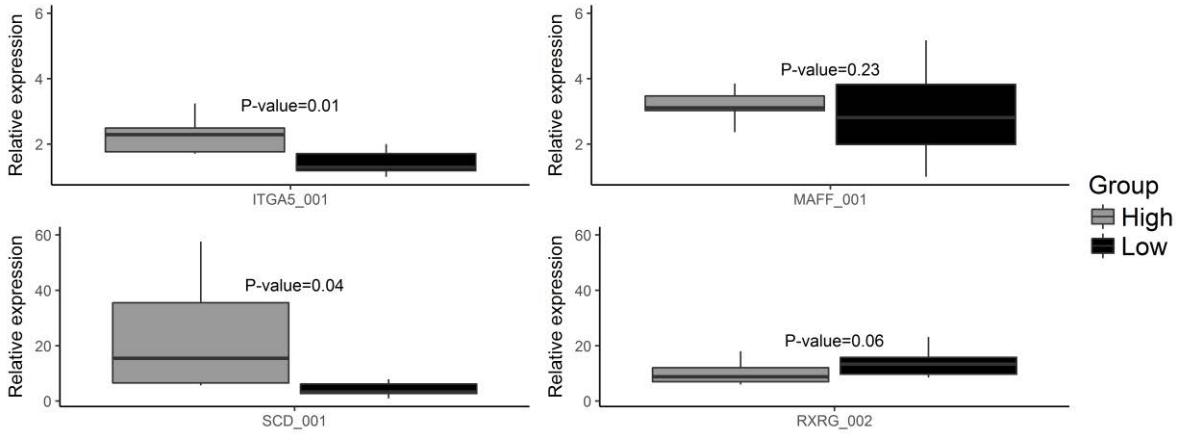

Supplemental material Paper III: "Nutrient supply affects the mRNA expression profile of the porcine skeletal muscle "

Annex 17 - Additional file 1: Figure 1 - Kinetics of the average concentrations of triglycerides and non-esterified fatty acids (FA) in 36 Duroc pigs at three time points: before eating and 5 and 7 hours post-ingestion.

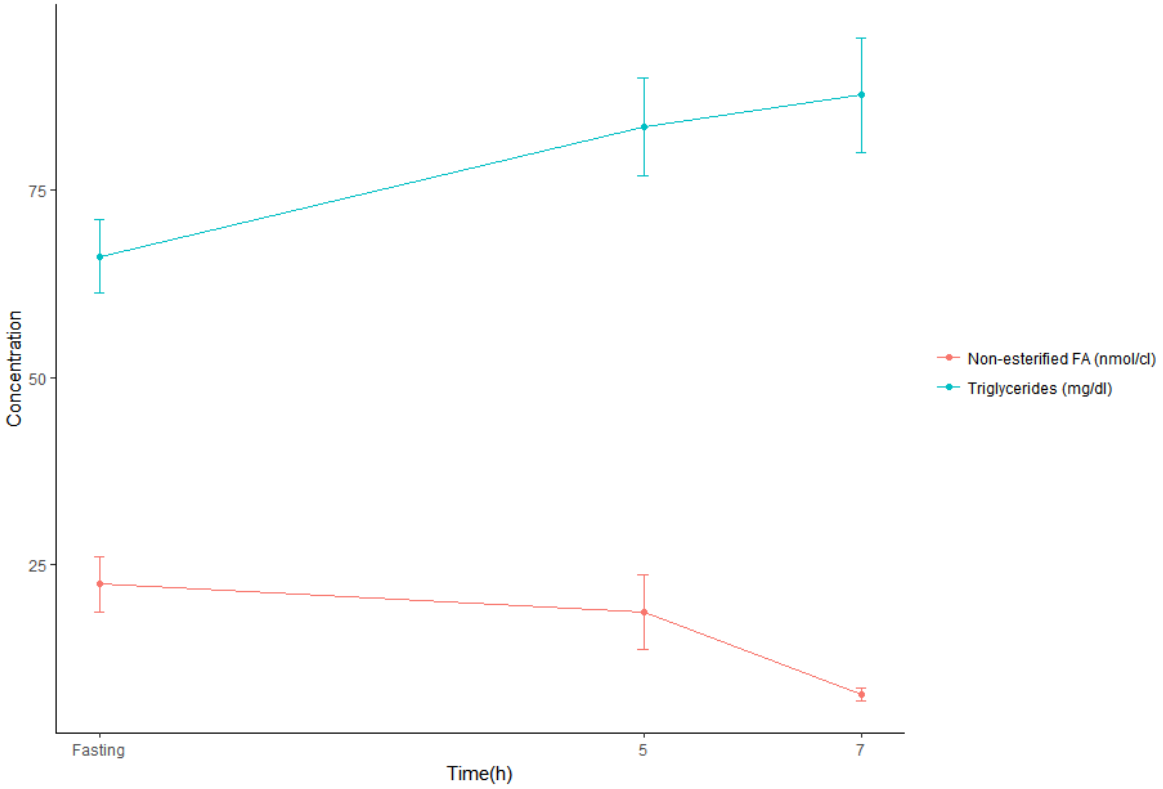

Annex 18 - Table S1. Differentially expressed genes (q-value < 0.05 and |fold-change| > 1.5) in the pig *gluteus medius* muscle at fasting (T0) vs 5 h (T1) and 7 h (T2) after eating, and 5 h (T1) vs 7 h (T2) after eating . (The complete table is included in the CD-Rom).

		T0T1				T0T2				T1T2			
Gene	**Gene ID**	**FC**	**Log2 (FC)**	***P* -value**	***q* - value**	**FC**	**Log2 (FC)**	***P* -value**	***q* - value**	**FC**	**Log2 (FC)**	***P* -value**	***q* - value**
ENSSSCG00000016386		-	-	-	-	60.97	5.93	2.12E-234	5.94E-231	46.85	5.55	7.57E-300	1.09E-295
ENSSSCG00000008767	*RPS18*	-	-	-	-	28.84	4.85	1.84E-78	8.88E-76	45.89	5.52	8.18E-261	5.91E-257
ENSSSCG00000005274		-	-	-	-	56.49	5.82	3.52E-167	4.93E-164	46.53	5.54	6.61E-248	3.18E-244
ENSSSCG00000002045		-	-	-	-	60.13	5.91	0.00E+00	0.00E+00	34.78	5.12	1.90E-244	6.85E-241
ENSSSCG00000002261		-	-	-	-	81.57	6.35	1.87E-243	6.57E-240	48.50	5.60	1.26E-240	3.64E-237
ENSSSCG00000016735		-	-	-	-	38.05	5.25	7.19E-147	9.17E-144	32.67	5.03	2.25E-216	5.41E-213
ENSSSCG00000016538		-	-	-	-	46.53	5.54	2.38E-198	5.57E-195	32.67	5.03	1.71E-210	3.54E-207
ENSSSCG00000030628	*CH242-203F13.1*	-	-	-	-	31.34	4.97	5.28E-186	1.06E-182	25.63	4.68	1.89E-202	3.41E-199
ENSSSCG00000016571	*RPS20*	-	-	-	-	19.84	4.31	4.95E-90	2.67E-87	24.93	4.64	8.34E-197	1.34E-193
ENSSSCG00000005172		-	-	-	-	54.95	5.78	1.72E-173	3.02E-170	32.90	5.04	3.04E-181	4.39E-178
ENSSSCG00000029003	*RPL14*	-	-	-	-	42.22	5.40	4.88E-267	3.42E-263	24.93	4.64	7.84E-180	1.03E-176
ENSSSCG00000014910	*RPL35A*	-	-	-	-	30.06	4.91	2.38E-255	1.11E-251	19.84	4.31	1.51E-176	1.82E-173
ENSSSCG00000024660		-	-	-	-	30.91	4.95	5.68E-112	4.69E-109	26.72	4.74	3.47E-167	3.85E-164
ENSSSCG00000025403	*RPS19*	-	-	-	-	11.63	3.54	1.09E-37	2.84E-35	28.25	4.82	4.88E-162	5.04E-159
ENSSSCG00000011910		-	-	-	-	23.26	4.54	8.54E-112	6.65E-109	20.82	4.38	6.18E-144	5.95E-141
ENSSSCG00000007500	*CH242-266P8.1*	-	-	-	-	8.94	3.16	1.83E-125	1.83E-122	8.88	3.15	3.61E-140	3.26E-137
ENSSSCG00000012578	*COPE*	-	-	-	-	58.49	5.87	2.28E-173	3.56E-170	21.86	4.45	1.04E-116	8.82E-114
ENSSSCG00000004575		-	-	-	-	9.78	3.29	5.92E-105	3.77E-102	8.82	3.14	5.45E-113	4.37E-110
ENSSSCG00000021825	*RPS21*	-	-	-	-	-14.52	-3.86	3.33E-107	2.22E-104	-12.21	-3.61	5.96E-112	4.53E-109
ENSSSCG00000011667		-	-	-	-	32.90	5.04	5.80E-129	6.78E-126	17.51	4.13	2.00E-105	1.44E-102

ENSSSCG00000030093		-	-	-	-	22.32	4.48	5.30E-100	3.10E-97	14.62	3.87	6.64E-100	4.57E-97
ENSSSCG00000016791		-	-	-	-	51.63	5.69	3.48E-120	3.26E-117	18.25	4.19	4.95E-98	3.25E-95
ENSSSCG00000002529		-	-	-	-	16.00	4.00	1.31E-52	4.36E-50	15.78	3.98	5.35E-97	3.36E-94
ENSSSCG00000000744		-	-	-	-	18.00	4.17	1.27E-79	6.36E-77	13.64	3.77	1.18E-92	7.11E-90
ENSSSCG00000027329		-	-	-	-	27.67	4.79	3.78E-91	2.12E-88	15.24	3.93	3.06E-91	1.77E-88
ENSSSCG00000009133		-	-	-	-	15.56	3.96	2.11E-126	2.28E-123	10.56	3.40	4.75E-85	2.64E-82
ENSSSCG00000016886		-	-	-	-	9.25	3.21	5.32E-33	1.26E-30	11.39	3.51	9.63E-80	5.15E-77
ENSSSCG00000009848		-	-	-	-	15.78	3.98	1.39E-71	6.07E-69	11.55	3.53	1.99E-79	1.03E-76
ENSSSCG00000026049	*CYCS*	-	-	-	-	44.32	5.47	3.87E-114	3.39E-111	13.64	3.77	8.30E-78	4.14E-75
ENSSSCG00000009677		-	-	-	-	15.56	3.96	6.10E-71	2.59E-68	11.08	3.47	1.54E-71	7.42E-69
ENSSSCG00000014974	*ENY2*	-	-	-	-	13.00	3.70	8.84E-109	6.20E-106	8.46	3.08	4.58E-68	2.13E-65
ENSSSCG00000028670		-	-	-	-	11.71	3.55	2.97E-46	8.87E-44	10.41	3.38	8.28E-66	3.74E-63
ENSSSCG00000017077		-	-	-	-	18.64	4.22	1.07E-79	5.53E-77	10.48	3.39	7.81E-65	3.42E-62
ENSSSCG00000009126		-	-	-	-	19.56	4.29	1.26E-61	4.79E-59	10.93	3.45	2.96E-63	1.26E-60
ENSSSCG00000015620	*TIAL1*	-	-	-	-	21.26	4.41	2.04E-64	8.19E-62	9.65	3.27	8.75E-59	3.61E-56
ENSSSCG00000011945		-	-	-	-	5.54	2.47	4.91E-31	1.13E-28	6.23	2.64	2.38E-56	9.54E-54
ENSSSCG00000024384	*DCAF12*	-	-	-	-	6.54	2.71	2.61E-44	7.18E-42	5.28	2.40	6.76E-54	2.64E-51
ENSSSCG00000004527		-	-	-	-	16.56	4.05	7.07E-53	2.42E-50	9.25	3.21	1.63E-53	6.21E-51
ENSSSCG00000027246	*NDUFA2*	-	-	-	-	12.04	3.59	6.11E-48	1.90E-45	8.00	3.00	3.47E-49	1.29E-46
ENSSSCG00000002850	*RPLP2*	-	-	-	-	18.51	4.21	9.38E-59	3.37E-56	8.69	3.12	5.40E-49	1.95E-46
ENSSSCG00000010221		-	-	-	-	3.61	1.85	3.27E-59	1.21E-56	3.78	1.92	6.07E-49	2.14E-46
ENSSSCG00000029019		-	-	-	-	12.64	3.66	2.01E-52	6.54E-50	7.94	2.99	1.05E-48	3.60E-46

Annex 19 - Table S2 - Pathways identified by ReactomeFIViz as enriched in differentially expressed genes (q -value < 0.05 and |fold-change| > 1 .5) between at fasting (T0) vs 5 h (T1) and 7 h (T2) after eating, and 5 h (T1)

T0 vs T1

GeneSet	P-value	*q*-value	Nodes
Circadian Clock(R)	1.53E-08	4.52E-06	*NR1D1, PER2, PER1, SIK1, ARNTL, UBB*
Circadian rhythm pathway(N)	1.20E-07	1.77E-05	*NR1D1, PER2, PER1, ARNTL*
Circadian clock system(P)	1.55E-06	1.21E-04	*PER2, PER1, ARNTL*
Circadian rhythm(K)	1.64E-06	1.21E-04	*NR1D1, PER2, PER1, ARNTL*
AP-1 transcription factor network(N)	3.96E-05	2.34E-03	*FOSL2, FOS, MYC, BCL2L11*
Regulation of nuclear SMAD2/3 signaling(N)	5.72E-05	2.80E-03	*FOXO1, FOS, GATA3, MYC*
Striated Muscle Contraction(R)	8.66E-05	3.54E-03	*MYL4, ACTN3, TNNT2*
MAPK6/MAPK4 signaling(R)	9.57E-05	3.54E-03	*FOXO1, TNRC6B, MYC, UBB*
Glucagon signaling pathway(K)	1.62E-04	5.18E-03	*PGAM1, FOXO1, SIK1, CREB5*
Calcineurin-regulated NFAT-dependent transcription in lymphocytes(N)	2.75E-04	7.62E-03	*FOS, GATA3, EGR2*
IL6-mediated signaling events(N)	2.93E-04	7.62E-03	*FOXO1, FOS, MYC*
Hepatitis B(K)	6.50E-04	1.50E-02	*FOS, MYC, EGR2, CREB5*
Adrenergic signaling in cardiomyocytes(K)	6.84E-04	1.50E-02	*MYL4, ACTC1, CREB5, TNNT2*
Oxidative Stress Induced Senescence(R)	7.17E-04	1.51E-02	*FOS, TNRC6B, UBB*
cadmium induces dna synthesis and proliferation in macrophages(B)	7.95E-04	1.51E-02	*FOS, MYC*
bone remodeling(B)	9.03E-04	1.63E-02	*FOSL2, FOS*
Cardiac muscle contraction(K)	1.27E-03	1.93E-02	*MYL4, ACTC1, TNNT2*
Glucocorticoid receptor regulatory network(N)	1.27E-03	1.93E-02	*FOS, GATA3, PBX1*
Regulation of nuclear beta catenin signaling and target gene transcription(N)	1.36E-03	1.93E-02	*MYOG, MYC, KLF4*
Transcriptional misregulation in cancer(K)	1.38E-03	1.93E-02	*FOXO1, PER2, MYC, PBX1*
Herpes simplex infection(K)	1.53E-03	2.14E-02	*FOS, PER2, PER1, ARNTL*
inhibition of cellular proliferation by gleevec(B)	2.00E-03	2.61E-02	*FOS, MYC*
Circadian entrainment(K)	2.22E-03	2.66E-02	*FOS, PER2, PER1*
CD40/CD40L signaling(N)	2.90E-03	3.35E-02	*MYC, TNFAIP3*
Oncogene Induced Senescence(R)	3.10E-03	3.35E-02	*TNRC6B, UBB*
role of egf receptor transactivation by gpcrs in cardiac hypertrophy(B)	3.30E-03	3.35E-02	*FOS, MYC*
TNF signaling pathway(K)	3.35E-03	3.35E-02	*FOS, CREB5, TNFAIP3*
Syndecan-4-mediated signaling events(N)	3.52E-03	3.52E-02	*SDC4, THBS1*
Transcriptional regulation of pluripotent stem cells(R)	4.18E-03	3.98E-02	*PBX1, KLF4*
TNF signaling(R)	4.42E-03	3.98E-02	*UBB, TNFAIP3*
Dopaminergic synapse(K)	5.21E-03	4.55E-02	*FOS, CREB5, ARNTL*
Bladder cancer(K)	5.68E-03	4.55E-02	*THBS1, MYC*
FOXM1 transcription factor network(N)	5.68E-03	4.55E-02	*FOS, MYC*
LKB1 signaling events(N)	6.23E-03	4.98E-02	*SIK1, MYC*

T0 vs T2

GeneSet	P-value	*q*-value	Nodes
Eukaryotic Translation Termination(R)	4.63E-11	1.08E-08	*RPL14, RPLP2, RPL35A, RPS18, RPS19, RPS16, RPL9, RPS20, RPS21, RPS23, RPS24, RPL39, RPL22*
Nonsense-Mediated Decay (NMD)(R)	6.29E-11	1.08E-08	*RPL14, RPLP2, RPL35A, RPS18, RPS19, RPS16, RPL9, RPS20, RPS21, RPS23, RPS24, CASC3, RPL39, RPL22*
Eukaryotic Translation Elongation(R)	7.08E-11	1.08E-08	*RPL14, RPLP2, RPL35A, RPS18, RPS19, RPS16, RPL9, RPS20, RPS21, RPS23, RPS24, RPL39, RPL22*
SRP-dependent cotranslational protein targeting to membrane(R)	6.80E-10	6.93E-08	*RPL14, RPLP2, RPL35A, RPS18, RPS19, RPS16, RPL9, RPS20, RPS21, RPS23, RPS24, RPL39, RPL22*
Selenoamino acid metabolism(R)	7.62E-10	6.93E-08	*RPL14, RPLP2, RPL35A, RPS18, RPS19, RPS16, RPL9, RPS20, RPS21, RPS23, RPS24, RPL39, RPL22*
Ribosome(K)	1.67E-09	1.18E-07	*RPL14, RPLP2, RPL35A, RPS18, RPS19, RPS16, RPL9, RPS20, RPS21, RPS23, RPS24, MRPS21, RPL39, RPL22*
Eukaryotic Translation Initiation(R)	1.81E-09	1.18E-07	*RPL14, RPLP2, RPL35A, RPS18, RPS19, RPS16, RPL9, RPS20, RPS21, RPS23, RPS24, RPL39, RPL22*
Circadian rhythm pathway(N)	5.64E-08	3.21E-06	*CRY2, ARNTL, BHLHE40, NR1D1, PER2, PER1*
Circadian Clock(R)	9.64E-07	4.82E-05	*CRY2, ARNTL, BHLHE40, UBB, NR1D1, PER2, PER1, DBP*
Circadian rhythm(K)	2.57E-06	1.16E-04	*CRY2, ARNTL, BHLHE40, NR1D1, PER2, PER1*
Circadian clock system(P)	3.28E-06	1.34E-04	*CRY2, ARNTL, PER2, PER1*
Signaling by NOTCH1(R)	9.27E-05	3.52E-03	*HDAC10, HDAC5, HDAC9, MYC, TLE4, UBB*
Myogenesis(R)	2.29E-04	8.00E-03	*MYOD1, BOC, NEO1, MYOG*
Regulation of nuclear SMAD2/3 signaling(N)	3.84E-04	1.23E-02	*MYOD1, FOXO1, GATA3, RUNX1, MYC, KAT2A*
Senescence-Associated Secretory Phenotype (SASP)(R)	4.66E-04	1.40E-02	*ANAPC5, H3F3A, UBE2E1, UBB, RPS6KA1*
p38 mapk signaling pathway(B)	5.96E-04	1.67E-02	*HMGN1, HSPB1, H3F3A, MYC*
MAPK6/MAPK4 signaling(R)	7.68E-04	2.00E-02	*FOXO1, MAPK4, HSPB1, PAK1, MYC, UBB*
Signaling events mediated by HDAC Class II(N)	1.26E-03	3.15E-02	*HDAC10, BCOR, HDAC5, HDAC9*

T1 vs T2

GeneSet	P-value	*q*-value	Nodes
Eukaryotic Translation Termination(R)	1.11E-16	1.11E-15	*RPL35A, RPL14, RPLP2, RPL39, RPS18, RPS19, RPS16, RPL9, RPS20, RPS21, RPS23, RPS24*
Eukaryotic Translation Initiation(R)	1.11E-16	1.11E-15	*RPL35A, RPL14, RPLP2, RPL39, RPS18, RPS19, RPS16, RPL9, RPS20, RPS21, RPS23, RPS24*
SRP-dependent cotranslational protein targeting to membrane(R)	1.11E-16	1.11E-15	*RPL35A, RPL14, RPLP2, RPL39, RPS18, RPS19, RPS16, RPL9, RPS20, RPS21, RPS23, RPS24*
Ribosome(K)	1.11E-16	1.11E-15	*RPL35A, RPL14, RPLP2, RPL39, RPS18, RPS19, RPS16, RPL9, RPS20, RPS21, RPS23, RPS24*
Nonsense-Mediated Decay (NMD)(R)	1.11E-16	1.11E-15	*RPL35A, RPL14, RPLP2, RPL39, RPS18, RPS19, RPS16, RPL9, RPS20, RPS21, RPS23,*

			RPS24
Eukaryotic Translation Elongation(R)	1.11E-16	1.11E-15	*RPL35A, RPL14, RPLP2, RPL39, RPS18, RPS19, RPS16, RPL9, RPS20, RPS21, RPS23, RPS24*
Selenoamino acid metabolism(R)	1.11E-16	1.11E-15	*RPL35A, RPL14, RPLP2, RPL39, RPS18, RPS19, RPS16, RPL9, RPS20, RPS21, RPS23, RPS24*
The citric acid (TCA) cycle and respiratory electron transport(R)	1.89E-04	1.70E-03	*CYCS, ATP5G2, COX6B1, ATP5I*
p38 mapk signaling pathway(B)	1.52E-03	1.22E-02	*H3F3A, HSPB1*
Oxidative phosphorylation(K)	1.83E-03	1.28E-02	*ATP5G2, COX6B1, ATP5I*
Parkinson's disease(K)	2.20E-03	1.32E-02	*CYCS, ATP5G2, COX6B1*
Alzheimer's disease(K)	3.54E-03	2.12E-02	*CYCS, ATP5G2, COX6B1*
Huntington's disease(K)	5.21E-03	2.61E-02	*CYCS, ATP5G2, COX6B1*
Aurora C signaling(N)	7.42E-03	3.71E-02	*H3F3A*
the prc2 complex sets long-term gene silencing through modification of histone tails(B)	1.11E-02	4.44E-02	*H3F3A*

Annex 20 - Table S3: Gene regulatory networks with the ReactomeFIViz app, considering GO biological process, molecular function and cellular component (q -value < 0.05). (The complete table is included in the CD-Rom).

	T0 vs T1			
	GeneSet	***P*-value**	***q*-value**	**Nodes**
Cellular component	transcription factor complex	1.32E-03	4.14E-02	*FOS, GATA3, MYOG, ARNTL*
	BIM-BCL-2 complex	2.86E-03	4.14E-02	*BCL2L11*
	BIM-BCL-xl complex	2.86E-03	4.14E-02	*BCL2L11*
Biological Process	circadian regulation of gene expression	1.89E-07	1.10E-04	*CIART, NR1D1, PER2, PER1, ARNTL*
	negative regulation of transcription. DNA-dependent	1.59E-06	4.65E-04	*CIART, FOXO1, NR1D1, GATA3, PER2, PER1, ARNTL, ZNF217, KLF4*
	circadian rhythm	2.43E-06	4.72E-04	*NR1D1, PER2, PER1, ARNTL, UBB*
Molecular function	E-box binding	5.45E-10	5.72E-08	*CIART, GATA3, PER1, MYOG, MYC, ARNTL*
	sequence-specific DNA binding transcription factor activity	1.00E-06	5.20E-05	*FOSL2, FOS, GATA3, MYOG, MYC, EGR2, CREB5, ZNF217, CSRNP1, HOXB6, PBX1, KLF4*
	transcription factor binding transcription factor activity	8.13E-06	2.85E-04	*FOXO1, PER2, PER1*
	T0 vs T2			
	GeneSet	***P*-value**	***q*-value**	**Nodes**

Cellular component	nucleoplasm	9.50E-06	1.08E-03	*HMGN1, MYOD1, HIRA, TIRAP, FOXO1, GATA3, EED, ORC1, RBFOX2, ANAPC5, HNRNPA2B1, HDAC10, SKP2, ARNTL, KEAP1, SOX9, RUNX1, KLF5, MAFF, NR4A3, HDAC5, PPIE, ATF3, RNF4, IRF2BPL, H3F3A, FBXO32, HDAC9, UBE2E1, FGF1, MYC, CDC7, TLE4, SMN1, ZFPM2, UBB, NEO1, NR1D1, PER2, MYOG, SCO2, NFATC1, KAT2A, CDC25A*
	cytosol	1.37E-05	1.08E-03	*RPL14, TIRAP, PGAM1, FOXO1, RPLP2, ORC1, RPL35A, C5AR1, ANAPC5, NCF2, CHAC1, MYH2, SOCS1, SKP2, ACTN3, TANK, BCL2L11, RPS18, RPS19, RND1, HSPB1, TNFAIP3, MYL5, AMER1, PPP1R3C, RPS20, RPS21, RPS24, CASC3, HDAC5, PPIA, FABP3, UBE2E1, HECW1, SYNJ2, FGF1, MYC, PIK3C2B, CYCS, NLRP3, SMN1, ARHGAP26, UBB, CCR1, RPL39, NFATC1, TXNIP, ACTC1, CDC25A, RPL22*
	cytosolic small ribosomal subunit	2.07E-05	1.08E-03	*RPS18, RPS19, RPS20, RPS21, RPS24*
Biological Process	negative regulation of transcription from RNA polymerase II promoter	1.11E-10	1.22E-07	*FOXO1, CRY2, GATA3, EED, TWIST2, HNRNPA2B1, HDAC10, NFE2L3, SOX9, BHLHE40, BCOR, KLF5, NR4A3, HDAC5, ATF3, IRF2BPL, HDAC9, BACH2, BARX2, MYC, HIST1H1D, TLE4, ZFPM2, UBB, NR1D1, PER2, PER1, TXNIP*
	translational termination	4.01E-09	2.22E-06	*RPL14, RPLP2, RPL35A, RPS18, RPS19, RPS20, RPS21, RPS24, RPL39, RPL22*
	nuclear-transcribed mRNA catabolic process. nonsense-mediated decay	1.19E-08	3.80E-06	*RPL14, RPLP2, RPL35A, RPS18, RPS19, RPS20, RPS21, RPS24, CASC3, RPL39, RPL22*
Molecular function	structural constituent of ribosome	2.73E-09	5.25E-07	*RPL14, RPLP2, RPL35A, RPS18, RPS19, RPS16, RPL9, RPS20, RPS21, RPS23, RPS24, MRPS21, RPL39, RPL22*
	E-box binding	4.45E-09	5.25E-07	*MYOD1, GATA3, ARNTL, CIART, BHLHE40, MYC, PER1, MYOG*
	transcription factor binding	5.52E-07	4.36E-05	*MYOD1, FOXO1, GATA3, RBFOX2, KEAP1, BCOR, HDAC5, RNF4, HDAC9, MYC, NLRP3, ZFPM2, PER1, KAT2A*
	T1 vs T2			
	GeneSet	***P*-value**	***q*-value**	**Nodes**
Cellular component	cytosolic small ribosomal subunit	9.80E-10	3.72E-08	*RPS18, RPS19, RPS20, RPS21, RPS24*
	ribosome	1.95E-08	3.71E-07	*RPS18, RPS19, RPS16, RPL9, RPS23*
	cytosolic large ribosomal subunit	7.62E-07	9.15E-06	*RPL35A, RPL14, RPLP2, RPL39*
Biological Process	translation	1.11E-16	9.99E-15	*RPL35A, RPL14, RPLP2, RPL39, RPS18, RPS19, RPS16, RPL9, RPS20, RPS21, RPS23, RPS24*
	translational termination	3.33E-16	1.50E-14	*RPL35A, RPL14, RPLP2, RPL39, RPS18, RPS19, RPS20, RPS21, RPS24*
	translational elongation	1.78E-15	5.33E-14	*RPL35A, RPL14, RPLP2, RPL39, RPS18, RPS19, RPS20, RPS21, RPS24*
Molecular function	structural constituent of ribosome	1.11E-16	3.44E-15	*RPL35A, RPL14, RPLP2, RPL39, RPS18, RPS19, RPS16, RPL9, RPS20, RPS21, RPS23, RPS24*
	hydrogen ion transmembrane transporter	3.18E-04	3.18E-03	*ATP5G2, ATP5I*

	activity			
	rRNA binding	6.53E-04	4.57E-03	*RPS18, RPL9*

Supplemental material Paper IV: "The ingestion of food promotes changes in the expression of genes regulating circadian rhythms in four porcine tissues containing peripheral clocks"

Annex 21 - Supplementary file 1. Description of primers used in the RT-qPCR analysis of gene expression.

Gene	Type	Primer sequence	
		Forward (5'> 3')	Reverse (5'> 3')
ARNT	Target	AGAGGCGTCGGGATAAGATG	GTGGCACCTCGTAACGTTTT
PER1	Target	ATCCACAGGTGACCTTCCAG	AGTCTTGGCCTTGAATGTGC
PER2	Target	GTCTCCCTGCCACCATTACT	TTCCAAGATGAGTCCACCCC
BHLHE40	Target	CAAGTGTACAAGTCGAGGCG	GCACTCGTTAATCCGGTCAC
NR1D1	Target	GGCCTCGGGTTTCCACTAT	GGTTACGATTGATGCGGACG
SIK1	Target	CTCCCTGCTCAGCTACAACT	AGGAGGTAATAGATGGCCGC
CRY2	Target	TGACGTGTTCCCAAGGCTAT	ATGCGAGTTCTCAGTCACCA
NPAS2	Target	CTCAGCTTCCAGGCCAAATG	TGTTCCCCTGCATCATCTGT
B2M	Reference	CCGAGCTCTCATTCCACCG	GGCGTGAGTAAACCTGAACC
TBP	Reference	CAGAATGATCAAACCGAGAATTGT	CTGCTCTGACTTTAGCACCTGTTAA
HPRT1	Reference	TCATTATGCCGAGGATTTGGA	CTCTTTCATCACATCTCGAGCAA
ACTB	Reference	CAAGGACCTCTACGCCAACAC	TGGAGGCGCGATGATCTT

Annex 22 - Supplementary file 2. Reference genes used as a reference in distinct RT-qPCR assays

	Reference gene			
Assay	***B2M***	***TBP***	***HPRT1***	***ACTB***
Liver (T0/T2)	X	X	X	
Duodenum (T0/T2)	X	X		X
Dorsal fat (T0/T2)	X		X	X
Muscle (T0/T2)	X		X	X
Hypothalamus (T0/T2)	X	X	X	
Different tissues in comparison to hypothalamus	X			X

[1]The selection of the reference genes in each assay was based on the stability of their expression in each specific tissue

Supplemental material Paper V: " The red and blond pigmentation of Mangalitza pigs is strongly associated with the variability of the Solute Carrier Family 45 Member 2 (Slc45a2) gene"

Annex 23 - Additional file 1. Admixture analysis of Mangalitza pigs and additional wild boar and pig populations for a range of K-values (K = 2-11). Each individual is represented by a single column divided into K colored segments, where K is the number of assumed clusters. Populations are separated by black lines.

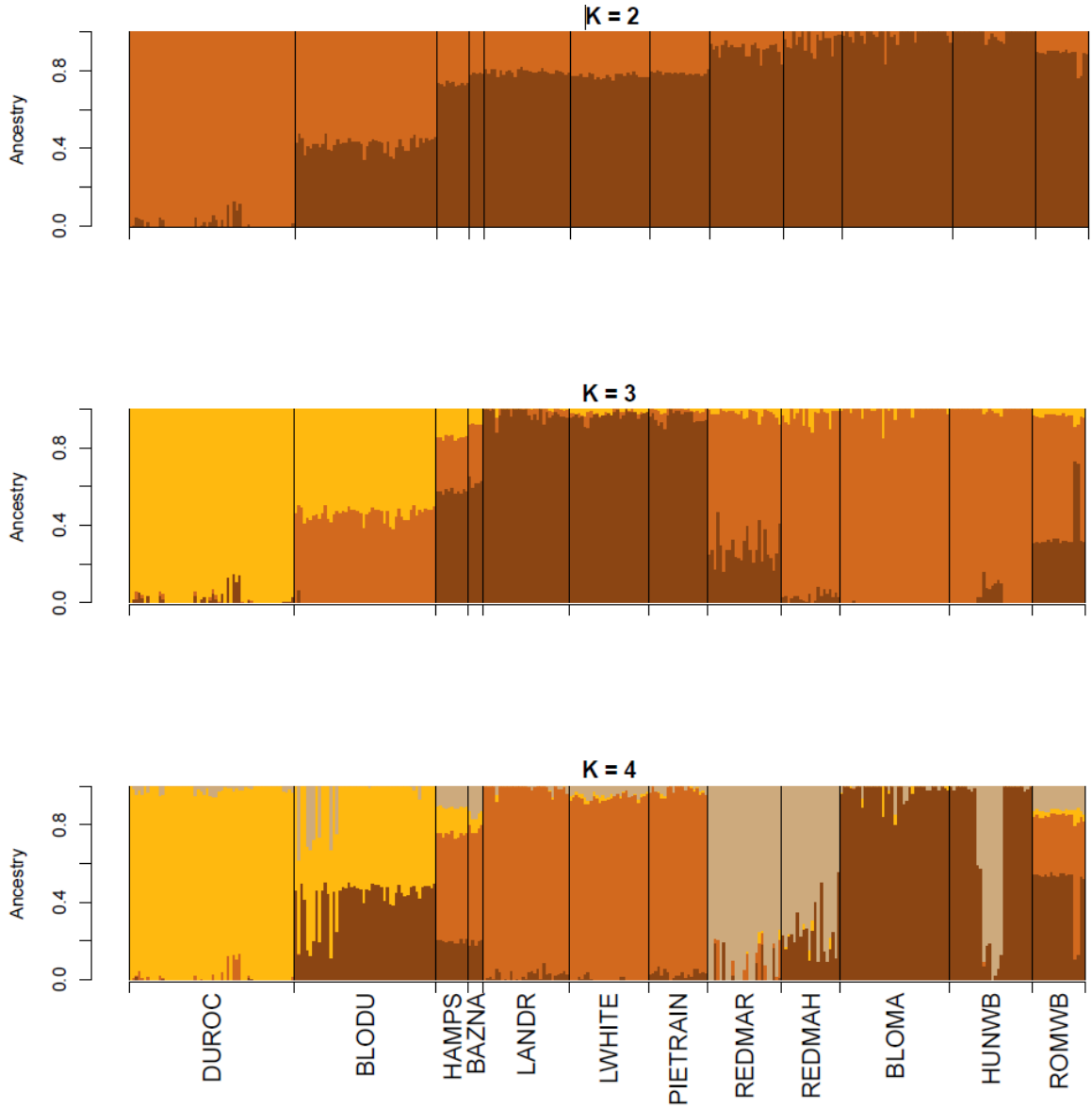

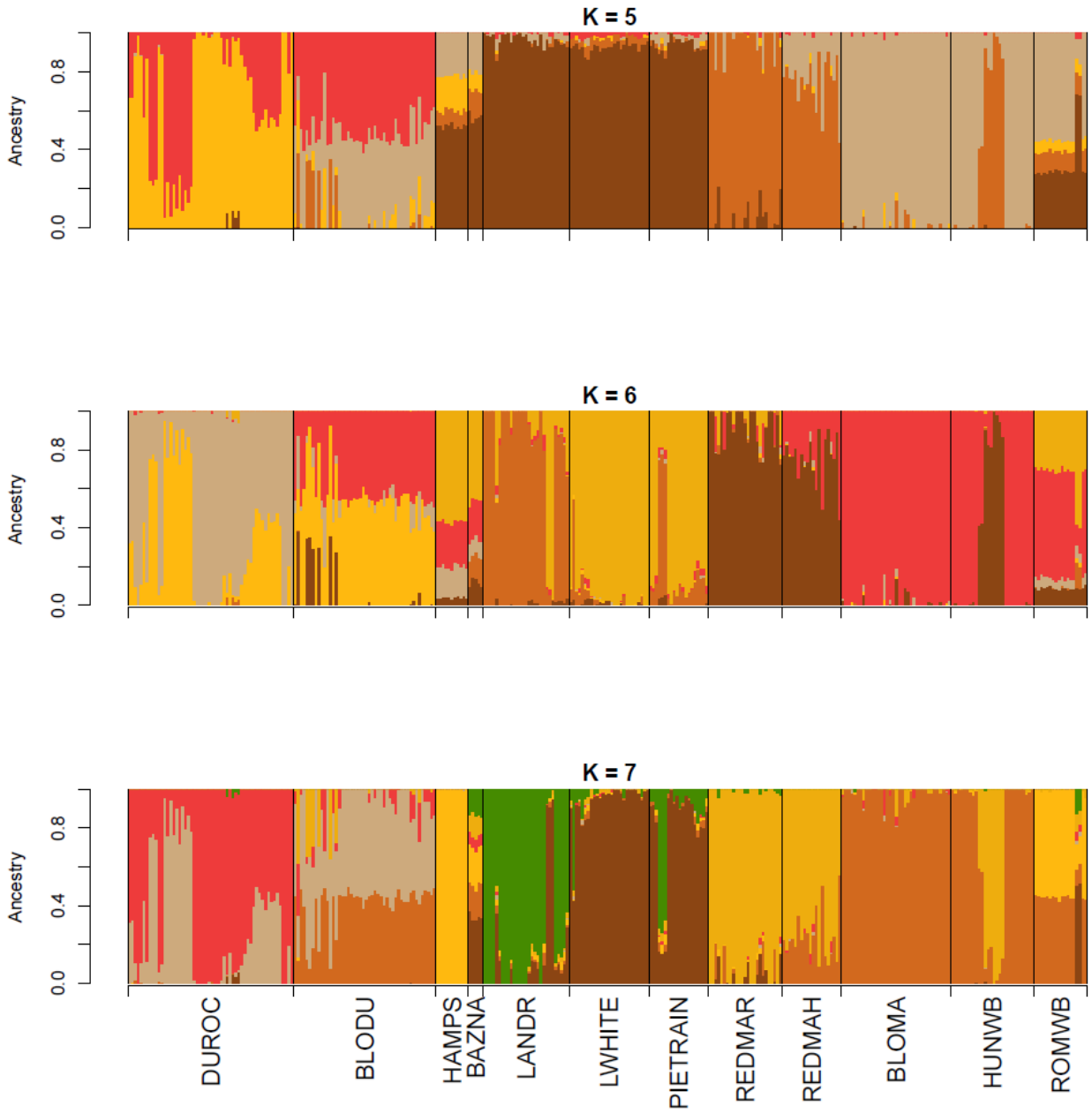
K = 5
K = 6
K = 7
Ancestry
0.0
0.4
0.8
DUROC
BLODU
HAMPS
BAZNA
LANDR
LWHITE
PIETRAIN
REDMAR
REDMAH
BLOMA
HUNWB
ROMWB

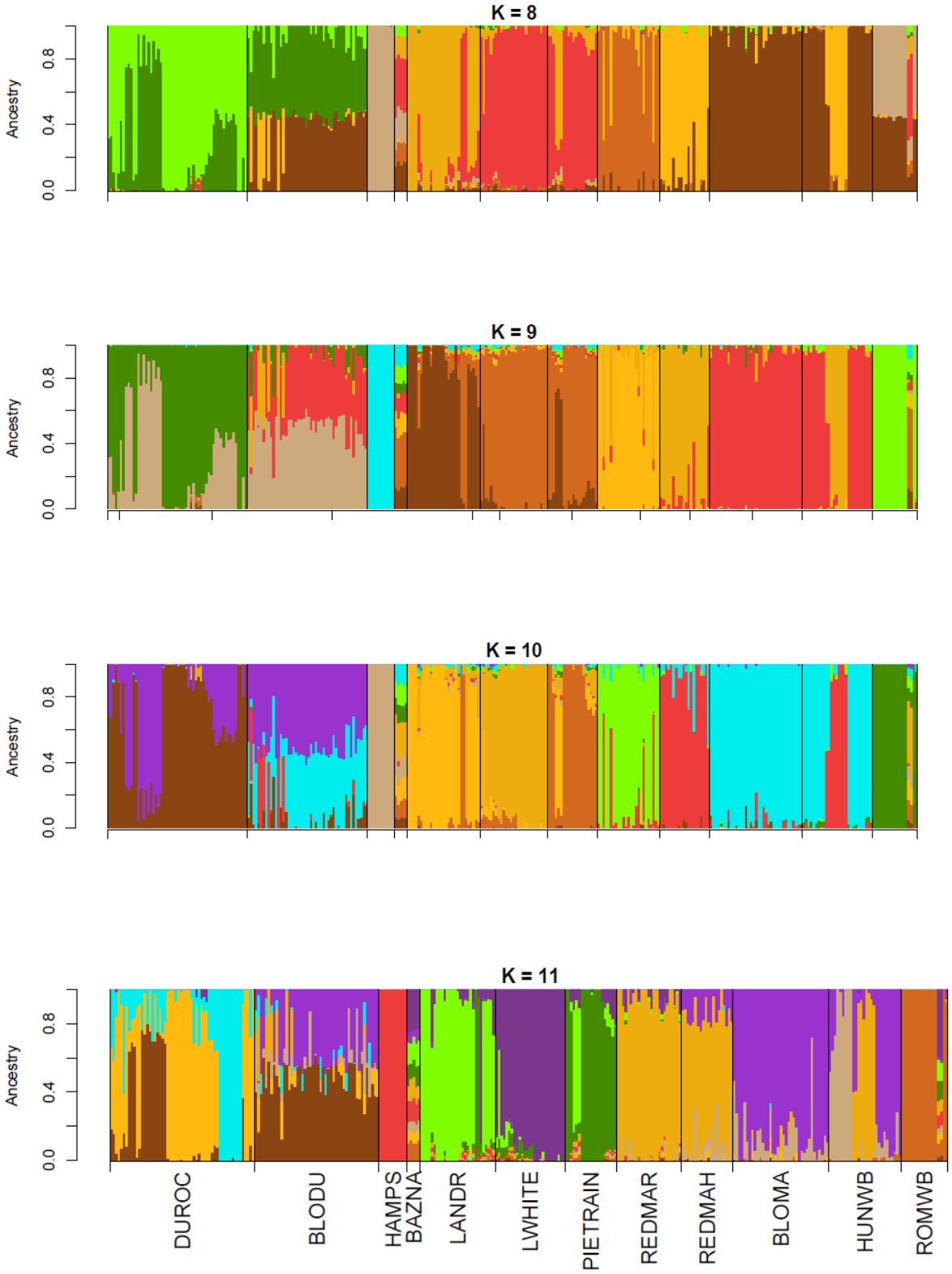
K = 8
K = 9
K = 10
K = 11
Ancestry
0.0
0.4
0.8
DUROC
BLODU
HAMPS
BAZNA
LANDR
LWHITE
PIETRAIN
REDMAR
REDMAH
BLOMA
HUNWB
ROMWB

Annex 24 - Additional file 2. Manhattan plot corresponding to the genome-wide association analysis performed for coat color in Red and Blond Mangalitza pigs. In the y-axis, statistical significance is expressed as a $-\log_{10}$(*q*-value) whilst genomic coordinates are displayed in the x-axis. The red and blue lines indicate the thresholds of genome-wide significance corresponding to q-values of 0.01 and 0.05.

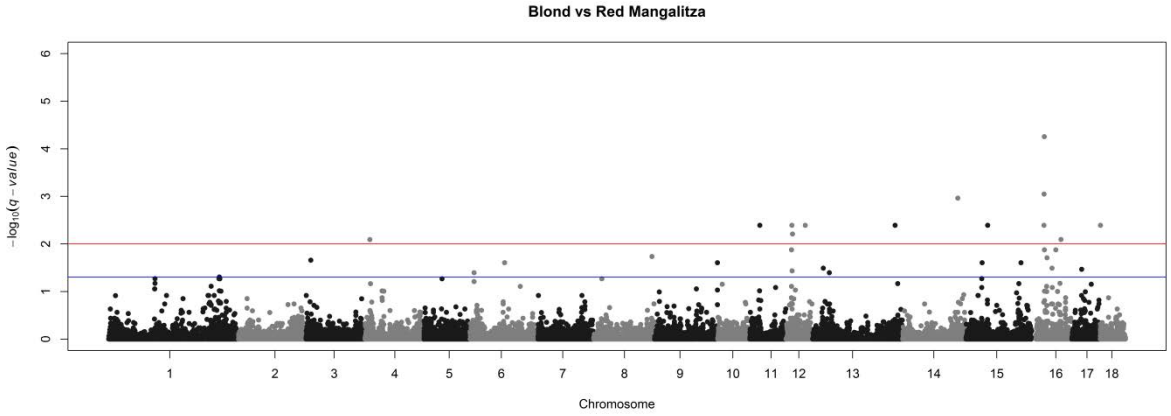

Annex 25 - Additional file 3. List of *SLC45A2* SNPs identified through the comparison of whole-genome sequences corresponding to Red, Blond and Swallow Belly Mangalitza pigs and reported by Molnar et al. (2014). (The complete table is included in the CD-Rom).

CHR	BP	SNP	REF	ALT	Swallown Belly	Blond	Blond	Red	Variant	Impact
16	20758558	.	C	G	-	-	-	0/1	synonymous_variant	LOW
16	20727710	.	A	G	-	-	-	1/1	synonymous_variant	LOW
16	20758657	.	C	T	-	-	-	0/1	synonymous_variant	LOW
16	20731696	.	C	T	1/1	1/1	1/1	-	missense_variant	MODERATE
16	20731673	.	T	C	-	-	-	0/1	missense_variant	MODERATE
16	20727744	.	C	T	-	-	-	0/1	missense_variant	MODERATE
16	20745602	.	C	A	1/1	1/1	1/1	1/1	intron_variant	MODIFIER
16	20749109	.	C	A	-	1/1	0/1	-	intron_variant	MODIFIER
16	20719572	.	G	A	-	1/1	-	-	intron_variant	MODIFIER
16	20744979	.	T	C	-	1/1	-	-	intron_variant	MODIFIER
16	20726872	.	T	C	1/1	1/1	1/1	1/1	intron_variant	MODIFIER
16	20719576	.	G	C	-	1/1	-	-	intron_variant	MODIFIER
16	20762353	.	T	C	0/1	1/1	1/1	-	upstream_gene_variant	MODIFIER
16	20745635	.	C	G	1/1	1/1	1/1	1/1	intron_variant	MODIFIER
16	20726773	.	C	G	1/1	1/1	1/1	1/1	intron_variant	MODIFIER
16	20744338	.	G	T	1/1	1/1	1/1	1/1	intron_variant	MODIFIER
16	20734564	.	G	T	1/1	1/1	1/1	-	intron_variant	MODIFIER
16	20741102	.	G	T	1/1	1/1	1/1	-	intron_variant	MODIFIER
16	20741104	.	C	T	1/1	1/1	1/1	1/1	intron_variant	MODIFIER

CHR = chromosome; **BP** = base pairs; **SNP** = Single Nucleotide Polymorphism; **REF** = reference; **ALT** = alternative

Acknowledgements

Chapter 8

“Rendam graças ao Senhor, pois ele é bom; o seu amor dura para sempre.”

1 Crônicas 16:34

Después de cuatro años, quizá este sea unos de los momentos más difíciles, no por algún pesar más por recordar de todo crecimiento personal y profesional, y de cómo la vida cambia en tan poco tiempo. Muchas personas actuaran directa o indirectamente para esto momento, y mismo que no estén citadas aquí o que mi gracias no sean tan bonitas o en un idioma indescifrable que sepan que seguramente las levare en mi corazón y que los quiero mucho.

En primer lugar, me gustaría agradecer a mi director de Tesis Dr. Marcel Amills, por ter contestado tan prontamente mi correo dando su confianza a una desconocida, además de su paciencia, amistad, ejemplo y enseñanzas durante estos años. Del mismo modo me gustaría agradecer mi directora de Tesis Dra Angela Canovas por toda ayuda y palabras de ánimos!

A mis compañeros de jornada pre-doctoral por recibirme tan cariñosamente y por acoger una brasileña (no muy típica) de una forma tan especial. Sin duda alguna una grande parte de esto trabajo y de todo que he aprovechado por aquí es debido a vosotros. A las Dra Antonia Noce, Dra Arianna Manunza, Dr Rayner Gonzales-Prendes (confeso que es un poco raro tal formalidad), Paulina Garcia, Emilio Marmól, Maria Luigi y Dailu Guan con los cuales he compartido reuniones, proyectos, ensayos y discusiones científicas (algunas ni tanto) en nuestro grupo de investigación. Gracias por todo que hemos construido juntos!!

A los otros pré-doctores del grupo de genética animal, Jordi Leno, Marta Gòdia, Lourdes Criado, Daniel Crespo, Laura Zingaretti, Lino Ramirez, Elies Ramon y a los ya doctores.. Dr Manuel Revilla y Dra Erika Bianco. Además, pero no menos importante a Dra Fabiana Quoos, Dra Ediane Paludo, Dra Sara Guiao y a Joan Rène, mi más emocionado agradecimiento. No caben palabras para describirlos. Es increíble mirar hacia atrás y ver lo cuanto hemos crecido juntos, en medio a cafés, tés, doces y ciencia!

A todos investigadores del grupo de genética animal de CRAG, Dr. Josep Maria Folch, Dr. Miguel Pérez-Enciso, Dr. Sebastián Ramos-Onsins, Dr. Alex Clop y Dr Amand Sanchez. Y todo suporte de investigación de Dra Anna Castelló, Dra Anna Mércade y Betlem Cabrera.

Así como de todo personal de la Universitat Autònoma de Barcelona (UAB), en especial a Julia Lacuesta, y todos del Centre de Recerca de Agrogènomica (CRAG), en especial a Tania Guil.

A los del programa de Genética y Mejora Animal del Institute of Agrifood Research and Technology, en especial a la Dra Raquel Quintanilla, Dra Maria Bellester y Olga González.

A todos del grupo de Animal Genetics, Bioinformatics and Breeding de la Universidad de Copenhagen por su hospitalidad durante mi estancia. En especial a Dra. Merete Fredholm, Dra Caroline Mentzel y Dra Susanna Cirera por su amizade durante los tres meses que hemos pasado juntas y por su ejemplo como persona e investigadora.

A minha família em Barcelona, com os quais tive o prazer imenso de dividir minha casa, meus dias e meu coração. Dra Nubia Caramello, Dra Francyne Elias-Piera, Dr Jackson Itikawa, Luís Fernando Gouveia, Julia Roberts, Gabriella Breda, Dra Anna Paula Machado. Além de Dr Robson Trevizan e Otavio Marçal por os momentos compartilhados.

Aos meus irmãos em Cristo: Lídia Maria, Bruna, Gustavo, Viviane, Sérgio, Roberta, Daniel, Eva, Sheila e Arthur. Por todo carinho, amizade, palavras de apoio e essa miscigenação de amor! Que Deus os abençoem!!

Em especial, a um dos maiores presentes de Barcelona e para vida. Leonardo obrigada por me ensinar o caminho, me guiar, ser meu companheiro e amigo. Te quero!

Aos meus amigos de outras décadas, com os quais já passamos tantas coisas e agora superamos a distância: Silvana; Danien, Christopher, Renata, Eduarda, e a Dra Estela. Os tenho sempre comigo.

E finalmente, aos meus pais, Jorge e Denize, que sempre colocaram meus sonhos e desejos à frente aos seus. Sei o quanto todo esse tempo longe foi difícil, mas com certeza sem o apoio de vocês essa caminhada nunca iria se realizar. A minha irmã Thais, por toda amizade, amor e por cuidar dos velhos na minha ausência. Vocês são o meu porto seguro. Os amo!!